ENHANCING PROTECTIVE IMMUNE RESPONSES ELICITED BY COMPUTATIONALLY OPTIMIZED BROADLY REACTIVE ANTIGEN (COBRA) INFLUENZA HEMAGGLUTININ AND NEURAMINIDASE VACCINES USING NOVEL ADJUVANTS

by

PEDRO LUIS SANCHEZ

(Under the Direction of Ted M. Ross)

ABSTRACT

Influenza viruses belong to the *Orthomyxoviridae* family and cause seasonal respiratory infections in humans and animals that are associated with worldwide morbidity and mortality. Current vaccines strategies are ineffective against these ever-changing viruses that undergo constant antigenic drift and shift since the vaccines that are developed every year are not always matched to the specific stains circulating for a given year. To overcome this challenge, the computationally optimized broadly reactive antigen (COBRA) methodology for designing influenza hemagglutinin (HA) and neuraminidase (NA) vaccines was employed. In this study, novel adjuvants with COBRA HA and NA vaccines were administered via different routes for enhancing the immunogenicity of these vaccines in naive mice and mice that had pre-existing immune responses to H1N1 and H3N2 historical influenza viruses. COBRA HA/NA proteins were formulated with either 1). a toll-like receptor 9 (TLR9) agonist (CpG1018), 2). a TLR4 agonist (INI 2002), 3). a TLR7/8 agonist (INI 4001), 4). a polysaccharide adjuvant derived from delta inulin

(Advax) in combination with TLR9 agonist CpG55.2 (Advax-SM™), or 5). a mast cell-activating oligopeptide, mastoparan-7 (M7-NH_2). Adjuvanting COBRA HA vaccines with INI 2002 or INI 4001 agonists in various formulation induced enhanced protective antibodies that fully protected mice from morbidity and mortality following influenza virus infection, or significantly reduced their morbidity and mortality compared to un-adjuvanted COBRA HA vaccines. Similarly, vaccinating naïve mice with Advax-SM™-adjuvanted COBRA HA vaccines induced enhance protective serum antibodies and protected mice from morbidity and mortality, following influenza virus infection. Moreover, naïve mice that were vaccinated with M7-NH_2-adjuvanted COBRA HA vaccines also had enhanced protective antibodies in their sera and in their lungs, that protected mice from H1N1 and H3N2 influenza virus infections. COBRA HA/NA mixed with CpG 1018 elicited protective antibodies in the sera and in the lungs of pre-immune mice that were vaccinated IM or IN. Furthermore, vaccinating pre-immune mice with COBRA HA and NA vaccines with CpG 1018 fully protected them from morbidity and mortality. In all, this project identified effective vaccine adjuvants that enhanced the effectiveness of parental and intranasal administration of COBRA HA and NA vaccines.

INDEX WORDS: Influenza, adjuvanted vaccine, hemagglutinin, universal, broadly reactive, HA, naïve, pre-immunity, COBRA, computationally optimized broadly reactive antigen, adjuvant, M7, Advax-SM™,

INI 2002, INI 4001, CpG 1018, novel, TLR agonist, toll-like receptor

ENHANCING PROTECTIVE IMMUNE RESPONSES ELICITED BY COMPUTATIONALLY OPTIMIZED BROADLY REACTIVE ANTIGEN (COBRA) INFLUENZA HEMAGGLUTININ AND NEURAMINIDASE VACCINES USING NOVEL ADJUVANTS

by

PEDRO LUIS SANCHEZ

BS, Barry University, 2017

A Dissertation Submitted to the Graduate Faculty of The University of Georgia in Partial Fulfillment of the Requirements for the Degree

DOCTOR OF PHILOSOPHY

ATHENS, GEORGIA

2024

ENHANCING PROTECTIVE IMMUNE RESPONSES ELICITED BY COMPUTATIONALLY OPTIMIZED BROADLY REACTIVE ANTIGEN (COBRA) INFLUENZA HEMAGGLUTININ AND NEURAMINIDASE VACCINES USING NOVEL ADJUVANTS

by

PEDRO LUIS SANCHEZ

Major Professor:	Ted M. Ross
Committee:	Jarrod Mousa
	Jeff Hogan
	Giuseppe Sautto
	Balazs Rada

Electronic Version Approved:

Ron Walcott
Vice Provost for Graduate Education and Dean of the Graduate School
The University of Georgia
August 2024

DEDICATION

I dedicate this hard work and commitment to God, my parents, both of my sisters, especially Jessica, for being there for me through the hard times that only she and I know about, and to Safa for being my rock and support during the most crucial time of my Ph.D. timeline. I would also like to dedicate this work to my nieces and nephews as a way of showing them that ANYTHING you set your minds to, is possible and attainable as long as you keep pushing.

ACKNOWLEDGEMENTS

I would like to thank Dr. Ted M. Ross for giving me the opportunity to join his lab in 2019 (during the COVID 19 pandemic) for pursuing my Ph.D. career. I would like thank Dr. Jarrod Mousa, Dr. Robert Hogan, Dr. Balazs Rada, and Dr. Giuseppe Sautto for taking on the roles of serving as my committee members, providing guidance, and for their efforts in making time for meetings and reviewing my work in a timely manner. I would also like to acknowledge Dr. James Allen and Dr. Ying Huang for training me on animal work, Michael Carlock for offering to help me troubleshoot my plaque assay in the very beginning of my training and always willing to help me when I had questions, and Spencer Pierce for the time he helped me to complete FluoroSpot assays from morning to 11pm, without hesitation.

TABLE OF CONTENTS

Page

LIST OF TABLES

Page

LIST OF FIGURES

Page

CHAPTER 1

INTRODUCTION

Influenza viruses belong to the family *Orthomyxoviridae* and are a leading cause of morbidity and mortality worldwide [1]. Influenza virus infections account for significant human respiratory infections worldwide that cause seasonal, endemic, and on occasion, pandemics. Influenza-associated symptoms during infection include fever, headache, cough, sore throat, myalgia, nasal congestion, fatigue, and loss of appetite [2]. In 1918, the Spanish Flu, was one of the worst influenza pandemics recorded in history resulting in ~50 million worldwide deaths [3]. Forty years after the Spanish Flu, the 1957 Asian Flu caused ~500,000 human infections [4]. In 1968, the Hong Kong Flu emerged and disseminated into Russia, Europe, and the Americas [4]. In a more recent occurrence, the 2009 pandemic, appeared in Mexico and in the United States from a reassorted H1N1 influenza viruses that contains human, swine, and avian influenza virus genes, and was responsible for 274,304 hospitalization and 12,469 deaths in the United Sates alone [5]. Influenza viruses have developed several mechanisms to evade the host immune response including antigenic drift and shift, where the virus particles undergo changes of their surface glycoproteins hemagglutinin (HA) and neuraminidase (NA), thus making these proteins targets for the development of influenza vaccines directed towards these viral components [6]. Influenza infection induces the production of antibodies against the HA and NA components of specific influenza stains. However, since influenza viruses are ever-changing due to

antigenic drift, existing antibodies do not recognize novel strains [7]. Therefore, a challenge in the development of influenza vaccines still remains, even though there are a variety of influenza vaccines currently available. This is because each season, wild-type influenza strains are selected for vaccine formulations and are not always matched to the strains circulating during that year, thus compromising the effectiveness of the vaccine [8]. To address the need of developing a next-generation influenza vaccines that is able to confer broad and long-lasting immunity to various influenza strains, including future emerging influenza strains, computationally optimized broadly reactive antigens (COBRA) have been developed using multiple rounds of consensus layering budling to develop H1, H3, H5, IBV, N1 and N2 rHA vaccines [9], [10], [11], [12], [13], [14]. These vaccines induce broadly reactive HA or NA-specific antibodies against drifted seasonal and pandemic viral strains and protects against morbidity and mortality. Since this COBRA vaccine strategy involves the use of rHA or rNA components, the studies in this dissertation aimed to adjuvant COBRA HA and NA vaccines with novel adjuvants that further enhanced the immunogenicity of the vaccines in a dose-sparing manner, and induce the necessary immune responses to protect vaccinated animals from morbidity and mortality. Specifically, to meet these goals, the following specific aims were addressed:

Specific Aim 1: Determine the breadth of protective antibodies elicited by COBRA HA and NA vaccines using different adjuvants in naïve mice vaccinated via different routes of administration.

The working hypothesis is that the addition of adjuvants will enhance COBRA HA and NA vaccine-induced systemic and mucosal immune responses and protect naïve mice from IAV challenge compared to unadjuvanted vaccines.

Specific Aim 2: Assess the effectiveness of COBRA HA and NA vaccines formulated with different adjuvants and administered via different routes in mice that are pre-immune to historical influenza viruses.

The working hypothesis is that the pre-immune status in mice will shape the response to vaccination and further enhanced vaccine-induced systemic and mucosal immune responses to adjuvanted COBRA HA and NA vaccines and protect mice from IAV challenge.

Specific Aim 3: Determine the elicitation of B-cell responses by adjuvants formulated with COBRA HA and NA antigens.

The working hypothesis is that naïve or pre-immune mice vaccinated with adjuvanted COBRA HA and NA vaccines will have more antibody-secreting cells in their spleens that secret a variety of antibody isotypes that are Th1 biased, Th2 biased, or balanced Th0 profiles.

CHAPTER 2

LITERATURE REVIEW

Introduction

Influenza viruses belong to the family *Orthomyxoviridae* and are enveloped viruses containing eight single segmented negative-strand RNA genome that encodes for the surface glycoproteins hemagglutinin (HA), involved in viral entry, and neuraminidase (NA), involved in the release of progeny influenza virions, and the matrix 2 (M2) ion channels which allows for the transfer of protons across the viral envelop [15]. Also encoded are the internal viral RNA polymerase acid (PA) protein (phosphoprotein that induces proteolytic degradation of co-expressed proteins), the polymerase basic 1 (PB1) protein (protein that protects the polymerase activity), the polymerase basic 2 (PB2) protein (the cap-binding protein that contains the cap-dependent endonuclease activity for initiating transcription and replication), the nucleoprotein (NP), which is critical for switching RNA synthesis from transcription to replication, the matrix 1 (M1) protein, which makes up the matrix that holds together the viral ribonucleoproteins (vRNPs), the nonstructural 1 (NS1) protein that is responsible for inhibiting type I interferon synthesis, thus allowing the virus to overcome host-immune responses to replicate efficiently, and the nuclear export protein (NEP) and the nonstructural 2 (NS2) protein that contain two nuclear export signals for transporting newly replicated vRNA across the nuclear membrane, to the plasma membrane [16], [17], [18], [19], [20], [21], [22] (Figure 2. 1). According to the

CDC, influenza A viruses are divided into different subtypes depending on their HA and NA surface proteins. Specifically, there are 18 different HA subtypes and 11 NA influenza A subtypes, but the most common ones that commonly infect humans are the A/H1N1 and A/H3N2 subtypes. These two subtypes of influenza A can also target aquatic birds, pigs, horses. Additionally, influenza B is restricted to only humans and is classified into B/Yamagata and B/Victoria lineages [23]. These viruses spread mainly by droplets made when people who have contracted influenza viruses via a sneeze or a cough [24] and they can also be transmitted from animal to human [25]. This may have occurred during one of the worst influenza pandemic, where an avian H1N1 progenitor influenza virus strain may have transmitted into a human host, causing the 1918 Spanish flu pandemic, leading to more than 40 million catastrophic influenza-associated deaths [26]. Influenza viruses also have developed mechanisms to evade the host innate and adaptive immune responses against influenza virus infections [27]. Antigenic drift is the viral alteration by which the genes of influenza A and B viruses that encode for the surface HA and NA glycoproteins undergo mutations. Consequently, these mutations change these surface glycoproteins, thus allowing the virion to evade recognition by host immune responses. Antigenic shift is the mechanism that occurs only in influenza A viruses, where two distinct influenza viruses infect the same host cell simultaneously and have the potential of undergoing gene reassortment, thus becoming a new, unrecognized strain, potentially capable of causing a pandemic [23] [28]. As a result of these mechanisms, two major events occurred that lead to the 1957 Asian flu pandemic that resulted in over 1 million deaths, worldwide, and the 1968 Hong Kong flu pandemic, which led to 1 to 4 million deaths, worldwide [29]. In a most recent event, the 2009 H1N1 pandemic was caused by a shift in an H1N1 strain where

new genes resulted from reassortment, thus becoming virulent in human [28]. According to the Centers for Disease Control and Prevention (CDC), an estimated 60.8 million cases, 274,304 hospitalizations, and 12,469 deaths were reported in the United States between April 12, 2009 and April 10, 2010 due to the emergence of the 2009 H1N1 influenza A virus pandemic. Designing effective vaccines against the ever-changing influenza A viruses (IAVs) remains a challenge. Each season, wild-type (WT) influenza strains are selected for vaccine formulation and are not necessarily matched to circulating influenza virus strains, thus compromising the effectiveness of the vaccine [8], [10]. Additionally, current influenza virus vaccines that are not adjuvanted are associated with increased influenza-associated hospitalization compared to an adjuvanted influenza vaccines [30]. For this reason, adjuvants may be needed to enhance the immunogenicity of the influenza virus vaccine components to induce long-lasting immune responses that will translate to the protection against influenza virus infection [31]. To meet the need for developing a next-generation influenza vaccine that can provide long-lasting protection against the ever-changing influenza viruses, several approaches are being explored. Furthermore, novel adjuvants that can enhance the immunogenicity of these vaccines are being studied, and both will be discussed in this review.

Viral Life Cycle

The HA glycoprotein makes up 80% of influenza virus surface proteins and interacts with sialic acid receptors linked to galactose on healthy host cells to mediate entry into the cells [32]. The NA glycoprotein makes up 17% of influenza virus surface proteins and its role is to mediate the release of newly-constructed virions from an infected host cell

[32]. To differentiate the interaction of HA according to subtype and host, sialic acid receptors are characterized into α-2,6 or α-2,3 linkages [25]. In humans, α-2,6 sialic acid is predominantly found in the upper and lower respiratory track, with lower magnitudes of α-2,3 [33]. Human influenza virus HA glycoproteins have a binding specificity to α-2,6 sialic acid [33]. In birds, a distribution of both α-2,6 and α-2,3 is found in their respiratory tract and intestines [34], [35]. Avian influenza virus HA glycoproteins have a binding specificity to α-2,3 sialic acid [35]. Pigs possess both α-2,6 and α-2,3 in their respiratory tract, thus proving the ideal vessels for mixed co-infections that can reassort and lead to a new viral strain with potential of causing a pandemic [34], [36]. During the initial influenza-host cell interaction, the HA glycoprotein plays a vital role in the success of viral infection. The HA precursor, HA0, can be divided into HA1 and HA2 subunits that are connected by disulfide bonds (Figure 2. 2). The HA1 component contains the receptor binding domain, whereas the HA2 component contains the fusion peptide [32]. Once the IAV HA binds to the attachment factors (AFs), sialic acid receptor on host cells, clathrin-mediated endocytosis occurs with the help of a signal from receptor-tyrosine kinases the to facilitate virus entry [37]. The virus-encapsulating endosome acidifies to a low pH in which HA0 undergoes a confirmational change leading to dilation of the HA1 subunit and exposing the fusion peptide located one the HA2 subunit. In turn, the HA2 subunit injects itself into the endosomal membrane, bringing the endosome and viral membranes together by fusion (Figure 2. 3). Concurrently, the acidification of the endosome opens the M2 ion channels to allow proton-exchanges that acidify the viral core for release of the internal viral ribonucleoprotein (vRNP) components into the host cell cytoplasm that will enter into the nucleus [32] (Figure 2. 4). Once in the nucleus, vRNPs undergo primary transcription

where RNA polymerase transcribes the viral negative-sense segmented RNA genome via cap-snatching to generate capped RNA fragments that act as primers for transcription of mRNA [38]. Replication of vRNAs involves a two-step process: 1). transcription of complementary RNA (cRNA) and 2). transcription of new vRNAs using the cRNA templates. To do this, the cRNAs are produced, independent of priming. Thus, this process depends on complementation of free rNTPs with the 3' end of the vRNA. In turn, the nucleotide complement complex locks the vRNA template into the polymerase active site of PB1, resulting in A–G dinucleotides where cRNA will be elongated. The cRNA then associates with NP molecules and a copy of the viral polymerase to form cRNPs [39]. The mRNAs are then directed into the cytoplasm, where they are translated into proteins that will either be transported back into the nucleus (PB2, PB1, PA, NP, M1, and NEP) via their nuclear localization signals [40] or to the plasma membrane (HA, NA, and M2) by vRNP, M1, and NEP complexes that contain two nuclear export signals (NESs) [22]. Following the re-entry of viral PB2, PB1, PA, M1, NP, and NEP proteins into the nucleus [41], the proteins will assemble with progeny vRNPs, and then are assisted by M1, NEP, and NS2 to be exported through nuclear pores on microtubules, and to the cytoplasm by NESs. Once there, M1 interacts with the vRNP, HA, NA and M2 proteins by associating with lipid rafts (membrane regions rich in sphingolipids and cholesterol) that are the site of influenza virus budding, to assist in incorporating vRNA and assembly of viral particles at the plasma membrane [42], [40], [43]. After the progeny virion has assembled, the NA glycoprotein cleaves the anchoring sialic acid from the host cell surface, releasing the virion from the infected cell, where it will go on to infect other healthy host cells [44].

Innate Immune Responses to Influenza Viruses

Understanding how the host immune system fights against influenza viruses is important when designing effective vaccines that protect against influenza. The primary innate immune response is mediated via germ-line pattern recognition receptors (PRRs) that are located on monocytes, macrophages, dendritic cells, natural killer cells, and endothelial cells [45]. Following infection with influenza viruses, the innate immune response is induced after PRRs have recognized damage-associated molecular patterns (DAMPs) inside of an infected host cell that stimulates downstream signaling pathways that lead to the production of type I interferons cytokines that are involved in host defense against IAV by damping immunopathogenic mechanisms and minimizing damage associated with infection, or pro-inflammatory cytokines that mediate local and systemic inflammation, fever, tissue damage, and modulate the adaptive immune response to IAV [46], [47], [48]. Specifically, three PRR signaling pathways that respond to influenza viruses include: 1) toll-like receptors (TLRs) that recognize intracellular influenza virus components, such as RNA from the dissociated virus in the acidified endosome that is recognized as DAMPS by TLR7 or TLR8 PRRs, [49], 2). retinoic acid-inducible gene-I (RIG-I)-like receptors (RLRs) act as antiviral proteins that directly bind to incoming IAV viral RNA in the host-cell cytoplasm or nucleus, and 3). nucleotide-binding oligomerization domain (NOD)-like receptor family pyrin domain containing 3 (NLRP3) which recognizes IAV RNA in the cytoplasm of host cells [47],[50]. In terms of TLR7 and 8 downstream stimulation, activation of the adaptor MYD88 results in the activation of nuclear factor-κB (NF-κB) and IFN-regulatory 7 (IRF7), which in turn stimulates the production of cytokines like TNF-α, IL-12, IL-α/β, IL-6, IL-8 type-I IFN-γ [51]. When a

host cell is infected with an influenza virus, RIG-I detects the 5'-triphosphate of viral ssRNA and its helicase domain binds to ATP to induce a conformational change. This allows the caspase-recruitment domains to bind mitochondrial antiviral signaling proteins. This in turns leads to NF-κB activation to produce type I IFNs and interferon stimulating genes. Moreover, the activation of NLRP3 inflammasomes results in the processing of pro-caspase 1 to produce IL-β and IL-18 [52].

Adaptive Immune Responses to Influenza

Even though the innate immune response is the first line of defense during influenza infection, an adaptive immune response that is more specific and is associated with memory for faster responses upon re-exposure to influenza viruses, is necessary for effectively clearing the infection [7]. Through the mechanisms of this second line of defense, humoral (virus-specific antibodies) and cellular responses (virus-specific- $CD4^+$ and $CD8^+$ T-cells) [7] are involved to provide broader protection against influenza infections. In concert with the innate immune response to influenza, important mediators such as B1, γδ T-cells, natural killer cells, or dendritic cells, bridge the this primary immune response with the adaptive immune response by presenting antigen to cell and inducing signals to modulate this secondary response [45] [27]. Specifically, these innate cells uptake the influenza viruses and migrate to peripheral tissues, such as lymph nodes or spleens, via CCR7 interactions with ligands CCL19 and CCL21 [27]. In these sites, APCs present peptide to naïve T-cells that become activated and differentiate into $CD4^+$ or $CD8^+$ effector T-cells and further activate naive B-cells into antibody secreting plasma cells [28]. The $CD4^+$ cells further differentiate into Th1 pro-inflammatory or Th2 anti-inflammatory

subsets that are dependent on the type of cytokines present. Th1 cells secret effector IFN-γ and IL-2, that are involved in inducing CTL responses via $CD8^+$ T-cells whereas Th2 cells secret effector IL-4, IL-5, and IL-3 that are associated with B-cell activation. Once activated, these B-cells undergo isotype switching and somatic hypermutation to strengthen the response and specificity to in influenza infections. Additionally, $CD8^+$ and $CD4^+$ subset specificity is determined by the location where viral influenza proteins are degraded within the APCs. In the event where viral proteins are degraded in the cytosol of the APC, export of the peptides into the ER will bring forth MHC I molecules to APC membrane that associate with $CD8^+$ T-cells. On the contrary, viral proteins degraded within endosomes or lysosomes associate with MHC II molecules directed to the APC membrane to associate with $CD4^+$ T-cells of the Th1 and Th2 subset [27], [7].

Influenza virus HA proteins are highly variable and undergo amino acid changes to escape immune pressure by accumulating mutations within the HA antigenic binding sites. These amino acid changes prevent antibodies from binding to these targeted sites for neutralization [53]. Specifically, the HA1 of the H1 subtypes have five sites: Sa and Sb, located on the distal end of each HA monomer, or Ca1, Ca2 and Cb, located proximally near the stalk domain [54]. HA1 of the H3 subtypes have five sites: A, B, C, D, and E located at the top the HA, around the receptor binding pocket [55]. The active sites of NA's include R118, D151, R152, R224, E276, R292, R371, and Y406 [56]. Additionally, neutralizing epitopes of HA have been identified, and include epitopes 92–105, 127–133 and 183–195 of influenza virus H3N2 [57], and 248-250, 273, 309, 338-339, 342-343, 396-397, and 456 for HXN1 influenza viruses [58].

Current Vaccines for Influenza

Current vaccines for influenza include a variety of egg-based or cell-based inactivated vaccines using different platforms [59]. All of the current types of influenza vaccines have been developed to protect against types A and B influenza viruses [60]. Live-attenuated vaccines contain living virus that has been weakened by undergoing many passages in cell or chicken eggs to the point where it loses its ability to replicate in human cells and cannot cause disease in healthy individual, while inducing strong immune responses [61]. This platform has been employed for developing many vaccines, including MMR, rotavirus, polio, influenza, shingles, adenovirus, and varicella vaccines [62]. Inactivated vaccines contain a pathogen that has been stripped of its ability to replicate by heat or chemicals, yet still maintaining its structure for inducing immune responses, however to a less extent that a live-attenuated vaccine. This platform has been employed for developing hepatitis A, influenza, polio, and rabies vaccines. Subunit vaccines contain a small part of a pathogen, such as antigen, polysaccharide, or DNA, capable of induces immune responses against that particular component. This platform is preferred for individuals with compromised immune systems where live-attenuated vaccines may be a concern and may require additional booster shots to elicit a sufficient response to the vaccines. This platform has been employed for developing several vaccines, including hepatitis B, human papillomavirus, whooping cough, and meningococcal vaccines [62].

Licensed egg-based inactivated vaccines using the split virion platform have include the Afluria® Quadrivalent vaccine, manufactured by Seqirus-Pty. Ltd, the Fluarix-quadrivalent vaccine, manufactured by Glaxo-SmithKline Biologicals, the FluLaval-quadrivalent vaccine, manufactured by ID-Biomedical, and the standard and high-dose

Fluzone® Quadrivalent vaccines, manufactured by Sanofi Pasteur, Inc. All of these vaccines have been approved in the USA for people 6 months or older in age or people 65 or older (Fluzone® High-Dose Quadrivalent).

Other licensed egg-based inactivated vaccines using the split virion platform include the FluQuadri™ and the Vaxigrip Tetra vaccines, manufactured by Sanofi-Aventis Australia, the Fluarix Quadrivalent vaccine, manufactured by Glaxo-SmithKline Biologicals, the Afluria® Quadrivalent vaccine, manufactured by Seqirus-Pty. Ltd, and the Influvac Tetra vaccine, manufactured by Mylan Health. All of these vaccines have been approved in Australia for people 6 months or older.

Licensed influenza vaccines using the recombinant technology platform include the Flublok-quadrivalent vaccines, manufactured by Sanofi-Pasteur, Inc. in the USA, and the Cadiflu-S vaccine, manufactured by CPL Biologicals Pvt Ltd. in India. Both of these influenza vaccines do not contain egg products and have been approved for people 18 years or older. Also licensed in the USA and India are the influenza vaccines using the live-attenuated platform. These include the FluMist Quadrivalent vaccine, manufactured by Med-Immune, LLC, for people between the ages of 2-49 years old in the USA, and the Nasovac S vaccine, manufactured by Serum Institute of India Ltd., for people 2 years old or older in India.

Additionally, manufactured by Seqirus, Inc., and also licensed in the USA, are the cell-based Flucelvax-quadrivalent inactivated influenza vaccine using the subunit platform, for people 6 years old or older, and the only adjuvanted influenza vaccine for people 65 years and older, Fluad-quadrivalent (egg-based) [63].

Vaccination against influenza viruses remains the most effective method for preventing influenza-associated morbidity and mortality. Although there are several influenza vaccines currently available in the market, a robust immune response that induces long-lasting immunity is not always achieved [31]. This, in part, due to influenzas ever-changing ability's, mis-matching of predicted strains to be included in the vaccines for a given year, or because of the use of partially inducing immunogens that require the help of an adjuvant in order to elicit responses that enhance the immunogenicity of vaccines components [64].

Strategies for Designing Universal Influenza Vaccines

In effort to overcome the challenge of influenzas ever-changing antigenicity and the development of yearly mismatched influenza vaccines, recent universal influenza vaccines strategies involve the targeting of conserved domains found on the HA and NA glycoproteins or on the NP and matrix protein 2 ectodomains (M2e) internal proteins [65].

The head of HA is very diverse. Strategies involving the development of universal influenza vaccines focus on the more conserved stalk region of HA, since the part of the glycoprotein is less exposed to the pressures of host-immune responses that cause influenza to drift [66]. Although the stalk region still undergoes mutations, it is at a much lower rate than the HA head [65]. Targeting the conserved stalk may help to inhibit influenza viruses from undergoing confirmational changes within the endosome that would be necessary for the virions to progress. However, the limitation to this strategies is the requirement of at least three immunizations in order to archived adequate cross-reactivity, but even with enhanced cross-reactivity, studies have shown that animals were not protected from

mortality following infection with influenza since stem-directed immunity is directed towards viral clearance and not neutralization [66].

NA is another major surface glycoprotein that is involved in cleaving sialic acid to release progeny influenza virion. A strategy used to test NA as an effective vaccine against influenza viruses involved the extraction of monoclonal antibodies from previously exposed humans that were infected with the H3N2 subtype [67]. Briefly, plasmablasts were sorted from donor blood collected 5 days after they had onset illness. Secreted monoclonal antibodies were screened and characterized prior to use for vaccination. Mice that were treated with the human anti-NA monoclonal antibodies, 2 hours after influenza infection, were protected from morbidity and mortality [67]. To date, neuraminidase inhibitors oseltamivir and zanamivir have been used against influenza infection [68]. However, several studies in human has shown influenzas increasing ability to resist the effect of these antiviral agents [69], [68].

M2 is another conserved target for development of as universal influenza vaccine [65]. This approach involves the fusion of M2e antigens to the heavy chains of a recombinant anti-C-type lectin-like (Clec9A) monoclonal antibody that is specific to type 1 conventional dendritic cells (cDC1). Because of the poor immunogenicity associated with M2e, which does not induce long-lasting effective immunity by itself, this strategy was enhanced by adjuvating the M2e vaccines with TLR9 CpG oligodeoxynucleotide agonist, or with TLR3 polyinosinic–polycytidylic acid (poly I:C) agonist. This allowed for a dose-sparing strategy that induced enhance immune responses to the vaccine, with just a single dose, in young and adult animals. However, this vaccine strategy still fail to fully protect animals from morbidity and mortality, following infection with an H1N1 virus [70].

NP is a conserved internal protein of influenza that has also been used as a strategy for the development of universal influenza vaccines [65]. The delivery of NP protein of an H5N1 influenza virus expressed on human adenoviral (HAd) type 5 (HAd5) vectors, induces CD8 T lymphocyte (CTL) and enhanced levels of antibodies when administered intranasally or intramuscularly. The vaccine-associate responses fully protected mice from H1N1 and H3N2 influenza infection, but not from H5N2, H7N9, of H9N2 influenza infection [71]. Suggesting that broad immune responses to different influenza stains was not achieved and still remains a challenge for the development of influenza vaccine.

In a more complex approach, and to confer cellular immunity against influenza virus infections, consensus sequences of highly conserved internal proteins (M1, M2, NP, PA, PB1, and PB2) of influenza viruses containing conserved T-cell epitopes of different influenza viruses was used to design influenza vaccines. Briefly, The consensus amino acids of each internal protein pertaining to many influenza virus strains was obtained and aligned to identify the consensus amino acid at each position and combining individual consensus amino acid for synthesis. The synthesized protein sequence was then cloned into vectors which are then transfected into mammalian cell line to generate adenoviruses containing the immunogens of interest that are obtained by lysis of the particles and purified [72]. When administered to animals, these vaccine approaches have been shown to elicit T-cell immunity as expected, however, mounting a humoral immune response is vital for the production of neutralizing antibodies capable of protecting animals from not just mortality, but also morbidity, following infection with influenza viruses [73]. A feature not shown to be associated using this approach [72].

Types of Consensus Sequence-based Strategies:

Consensus Hemagglutinins

One strategy for consensus HA development is through aligning multiple HA protein sequences in a given population and selecting the most common amino acids to construct consensus HA genes [66]. Briefly, 16 sequences pertaining to avian influenza viruses were downloaded and aligned and the most common amino acid at each position was chosen expressed in plasmids or on VLPs. When these vaccines were administered intramuscularly to animals using prime-boost or prime-boost-boost strategies, the vectored-vaccines provide cross-reactive cellular and humoral responses against H5N1 influenza subtypes that translated to protection following influenza challenge in mice, ferrets, and non-human primates [74].

Another approach for consensus HA development is through the combination of four micro-consensus immunogens to improve the efficacy of vaccination to multiple H3 influenza subtypes [66]. Briefly, many H3 sequences dating back from 1968 were downloaded and aligned to create four micro-consensus antigens that were expressed in DNA plasmid for vaccinations. When administered to mice in a prime-boost regime, these vector vaccines induced antigen-specific cellular cytokines, broad antibody cross-reactivity against multiple H3 influenza viruses, and protected mice from lethal infection with a couple of H3N2 influenza strains [75].

Another approach for consensus HA development is through the development of a centralized synthetic HA that is localized to the central node of the developing phylogenetic tree. This strategy aims to reduce genetic and antigenic differences of un-mated influenza virus strains [66]. Briefly, 20 full-length H1 HA sequences were selected from a larger

sequence space to represent one main branch of the H1. Specifically, the main branches of the generated H1 phylogenetic tree were selected. These sequences were then downloaded and aligned, and any ambiguities were removed. The yielding 566 amino acid consensus sequence was generated using the most common amino acids to be expressed in adenovirus vectors for vaccinations. When administered once intramuscularly to mice, these centralized consensus vaccines induced cross-reactive cellular and humoral immune responses after vaccination, but only fully protected mice from a lethal homologous influenza strain challenge [76].

COBRA-based Strategies

Computationally optimized broadly reactive antigen (COBRA) is a next-generation methodology employed to enhance the breath of protection against currently circulating and future influenza viruses using the sequences of WT influenza viruses to develop HA and NA immunogens [77]. This approach aims to confer humoral immunity against a broad range of influenza viruses, including seasonal and pandemic strains, that is targeted to a variety of influenza surface glycoproteins. Unlike conventional approaches, this strategy aims to minimize sampling or sequencing bias in a target population [66]. Briefly, multiple rounds of layered consensus building using multiple amino acids isolates pertaining to H1N1, H3N2, H5N1, or B influenza (IBV), were obtained that covered a range of years, aligned according to amino acid similarity, and separated into periods of time that represent Northern and Southern Hemisphere influenza seasons (Figure 2. 5). Multiple sequence alignments of the antigen sequence are performed to obtain clusters based on percent similarity to generate a final consensus, hence the COBRA H1, H3, IBV, N1, or N2

vaccines. This approach for developing a next-generation COBRA influenza vaccines has shown enhanced humoral responses against the ever-changing influenza virus HA and NA glycoproteins which translated to the protection against influenza virus infections in several animal models [10], [11], [12], [13], [14], [78], [79].

Adjuvants Introduction

Adjuvants are ingredients added to vaccine formulations to improve the vaccine component elicited immune responses [80]. Since the 1920's, the first adjuvant used in human vaccines was Aluminum salt (Alum) and was shown to enhance antibody production and is still used today in vaccines, including the diphtheria and tetanus toxins and pertussis (DTaP) vaccine, for hepatitis A and B [81]. Since then, advances and technology has prompted deeper exploration into the immune responses to vaccination and how adjuvants contribute to these outcomes. In doing so, knowledge of how the adjuvanticity of these vaccine helpers enhance vaccine efficacy has surfaced, but is still not fully understood [81]. During the time when new knowledge of how the immune system responds to vaccinations began to surface, it was determined that broader-immune responses that not only involved the elicitation of protective antibodies, but also involved a cell-mediated immunity, was vital. A mechanism that was no shown to be associated with the Alum adjuvant [82]. As a result, novel adjuvants have been explored in order to address this limitation to vaccine construction, with the attempt to induce antibodies, polyfunctional $CD4^+$ T cells and $CD8^+$ CTLs [83].

Adjuvant Immune Responses

To achieve these immune responses, adjuvants induce specific cell-mediated or humoral responses upon vaccination that mimic the natural responses elicited by pathogen-associated infections [84] (Figure 2. 6). A cell-mediate immune response is associated with T-helper 1 (Th1) pro-inflammatory responses that involve the secretion of interleukin (IL)-2, tumor necrosis factor (TNF)-β, and interferon (IFN)-γ cytokines, whereas a humoral response is associated with T-helper 2 (Th2) anti-inflammatory responses that involve the secretion of IL-4, IL-5, IL-10, and IL-13 [85], [84]. How these T-cell subtypes differentiate depends on how the cell is stimulated. Antigen-presenting cells (APCs) of the innate immune system, including dendritic cells (DCs) macrophages, or monocytes, express pattern recognition receptors (PRRs) on their surfaces or intracellularly, that detect pathogen-associated molecular patterns (PAMPs) or damage-associated molecular patterns (DAMPs). Upon activation of these target receptors, the APCs become highly efficient at up-taking antigens and express co-stimulatory signals and cytokines, while migrating to lymphoid tissues to bridge and initiate the adaptive immune response via T- and B- cell activation in a Th1 or Th2 biased manner [86].

Classes of Adjuvants

Adjuvants that are classified as immunostimulants because they directly activate immune cells via PAMPs or DAMPs. They include synthetic dsRNA molecule polyinosinic-polycytidylic acid (poly-IC), Monophosphoryl Lipid (MPL) TLR4 agonist, synthetic TLR7/8 Resiquimod agonist, or cytidine-phospho-guanosine (CpG) DNA TLR9 agonist [87]. Non-immunostimulants that act as delivery systems to present vaccine

components to immune cells or attract immune cells to the site of vaccination through chemotaxis [86]. They include emulsion, microparticles, iscoms, liposomes, virosomes, or virus-like particles [88]. Additionally, these classes of adjuvants can be classified as a combined adjuvant system (AS) where combinations of immunostimulants and non-immunostimulants are used together to provided synergistic adjuvant effects and elicit a variety of immune responses [89]. These adjuvant systems include lipid nanoparticle (LNP) vesicles containing internalized lipids or cholesterol, poly(lactide-co-glycolide) (PLGA) particles containing vaccine antigens, AS01 liposome-based adjuvant which contains two immunostimulants, 3-O-desacyl-4'-monophosphoryl lipid A (MPL) and saponin (QS-21), AS03 oil-in-water adjuvant consisting of squalene, alpha-tocopherol, and polysorbate-80, or AS04 adjuvant containing the TLR4 agonist MPL and aluminum salt [86], [90], [91]. Currently, there are only a few adjuvants that have been licensed for use in human vaccines (Figure 2. 7).

Current Adjuvants

Alum

The mother of all adjuvants, Alum, is a class of delivery, non-immunomodulatory vehicle adjuvant. Alum was initially formulated as precipitates containing potassium aluminum sulfate with tetanus and diphtheria toxoids proteins [92]. However, it was noted that the success of the formulation was dependent on the buffer used. Vaccine antigens are normally prepared in phosphate buffers and the buffer used in the presence of potassium aluminum sulfate can negatively impact the interaction between alum and the antigen. In order for adsorption to occur, phosphates on the surface of the antigens interact with the

hydroxyls expressed on the surface of the Alum salts [92]. As a result, Alum formulations using aluminum hydroxide or aluminum phosphate are the preferred methodology [92]. Modern Alum adjuvants formulated with vaccine antigens may provide a depot effect that involve the release of adsorbed antigen over time [93]. However, the adsorption of antigens to Alum may result in high concentrations of antigens at the site of vaccination, thus enhance uptake of the compounds by antigen presenting cells (APCs) [82]. Other proposed mechanisms of action of Alum are through direct or indirect stimulation of immune cells via complement activation, or uric acid or ATP damage-associated patterns (DAMPs) release by immune cells that in turn activated the NLRP3 inflammasome, thus inducing Th2 biased immune responses associated [82], [94]. The robust outcomes associated with Alum as an adjuvant have been tested in a variety of study models, including humans, mice, rabbits, and non-human primates, and have been safely administered with vaccines both intramuscularly or intranasally [95], [96], [97], [98], [99]. Aluminum salts induce humoral immune responses associated with B cell and $CD4^+$ Th2 cells, mediated by IL-4 and IL-5, that induce specific antibodies secretion, predominantly IgG1 [100]. However, aluminum salts do not induce cellular immune responses that are associated with Th1 or CD8 cytotoxic T cells [100]. In addition, alum increases the recruitment of monocytes and dendritic cell (DC) differentiation, as well as antigen capture by adsorption or aggregates [100], [101], [102], [103].

MF-59

MF-59 is a class of particulate formulated nanoemulsion delivery systems comprised of Squalene, a natural organic oil produced by plants, animals and can be found

in shark liver, as well as a variety of food products, such as olive oils. Squalene is also produced by the human liver as a precursor for cholesterol and is also present in human sebum. MF-59 was first developed by Novartis Vaccines and Diagnostics Inc. and licensed in 1997 for used in influenza vaccines for elderly people (Fluad®, Seqirus Inc., Holly Springs, NC, USA). This adjuvant induces pro-inflammatory cytokines, chemokines, recruitment of immune cells to the site of vaccination and robust antibody production, all while maintaining a safe profile [104]. Specifically, MF-59 adjuvant contains a mixture of polysorbate 80 (Tween 80) and sorbitan trioleate (Span 85) [105]. These two components stabilize squalene oil formulations into droplets into oil-in-water emulsions [106]. Squalene-based adjuvants have two main effects. The first one is the depot effect at the injection site [107]. Following injection, the aqueous phase disperses rapidly, which limits the formation of granulomas and abscess and the released oil droplets transport the vaccine antigens to draining lymph nodes [108]. The second effect includes targeting APCs resulting in increased secretion of cytokines, chemokines and other chemoattractant factors. This environment highly favors the recruitment of APCs to the site of vaccination to quickly and efficiently uptake more of the available antigen through phagocytosis, which protect the antigen from degradation [109]. These APCs transport the antigen to the draining lymph nodes, where there will be significant activation of T-cells, hence a stronger immune response [110], [111]. In mice, MF-59-adjuvanted influenza vaccines were associated with enhanced Th1/Th2 responses associated with IF-γ, IL-2, and IL-4, and an increase in antibody titers, including IgG1 and IgG2a. Additionally, the MF-59-adjuvanted influenza vaccines provided early protection against H7N9 influenza challenge [112], [113]. Moreover, protective antibodies were induced 21 days after the administration of

the vaccine formulated with MF-59 [114]. In elderly people, who do not have the ability to induce a strong immune response due to their exhausted immune system, the administration of influenza vaccine adjuvanted with MF-59 induced an increase in antibody titers compared to unadjuvanted vaccine [115]. In addition, the use of MF-59 in H5N1 vaccines showed a cross reactivity induced by the vaccine, hence broader protection against different strains of virus derived from the present vaccine [116].

AS01

Adjuvant system 1 (AS01) is a class of vehicle liposomal adjuvant composed of monophosphoryl lipid A (MPLA) and *Quillaja Saponaria* (QS-21) [90], [117]. AS01 has functions as an immunostimulatory and an antigen-presenter. The immunostimulatory function of AS01 is performed by MLPA that activates the innate immunity by stimulating TLR4 and inducing a Th1 response that induces the generation of cytotoxic T cells [90], [118]. QS-21 stimulates NLRP3 and promotes the production of IL-1β, IL-18 and IL-33 [119], enhances cross-presentation and promotes endosomal escape [120]. AS01 antigen-presenting function is carried out by liposomes, which have the ability to encapsulate and deliver the antigen, protecting it from degradation as a result of their phospholipid bilayer [118]. AS01 is included in licensed malaria and zoster vaccines that enhance cellular immune responses and promote antigen specific antibody production [121]. More recently, AS01 also shows promising results, safety, efficacy and prevention of tuberculosis in healthy adults, as it was used to develop a novel peptide vaccine against tuberculosis (M72/AS01E) [122], [123], [124].

AS03

The adjuvant system 3 (AS03) is a class of particulate formulated nanoemulsion delivery systems comprised of squalene, Tween 80 and alpha-tocopherol [93], [125]. AS03 has lots of indirect immunostimulatory effects on the immune system and is used in influenza vaccines against H1N1 influenza viruses (Pandemrix, TM), licensed by the European Union, and against H5N1 avian influenza viruses (GSK Biologicals), licensed by the U.S. FDA in 2013. This adjuvant allows for a broader protection spectrum of vaccines against other virus variants [126]. AS03 adjuvant is used in vaccines for its role in regulating the expression of cytokines and chemokines, enhancing antigen uptake by APCs, and increasing the number of innate cells recruitment to draining lymph nodes. Among the cytokines and chemokines regulated by AS03, IL-6, CCL2, CCL3 and CXCL1 have been some of the few mediators identified [127]. AS03 exerts its adjuvanticity through the NLRP3 and MyD88 pathways [93]. AS03 also plays a role in delivering the antigen to enhance its presentation by APCs through a depot effect [93]. This adjuvant is used in different influenza vaccines to increase titers and persistence of antibodies [128], [129]. AS03 was used in the development of COVID-19-adjuvanted vaccines with promising clinical results [130].

AS04

Adjuvant system 4 **(**AS04) is a class of combined vehicle adjuvant composed of TLR4 agonist molecule adsorbed to aluminum salts. AS04 aggregates have antigen delivery and immunostimulatory functions. The immunostimulatory function of AS04 is stronger than aluminum adjuvant due to its potent MPLA component that is derived from

LPS and can specifically activate the TLR4 on APCs. This leads to NK-κB activation and expression of pro-inflammatory cytokines such as IL-2 and IFN–γ, a profile weakly induced when alum is used alone, thus inducing a stronger Th1 response [131]. Vaccines formulated with AS04 as an adjuvant induce stronger antibody production than vaccines adjuvanted with aluminum salts alone, thereby proving the importance of TLR4 agonist functions in activating the immune system [132], [133], [134]. AS04 induces a more balanced Th1/Th2 immune response, hence the added TLR 4 component that induces Th1 biased responses and aluminum adjuvants, which are Th2 biased [135], [99]. The potential of this adjuvant is promising and has been approved for use in human papillomavirus (HPV) vaccine (Cervarix), as well as hepatitis B virus (HBV) vaccines (Fendrix) to enhance and increase antibody production and activation of antigen specific T-cells [91], [136].

Novel Adjuvants

TLRs (INI 2002 and INI 4001)

Toll was initially identified as an important gene during embryogenesis and in particularly during the establishment of the dorsoventral axis of Drosophila [137]. However, Toll plays a crucial role in pathogens recognition [138]. In response to infection, either by a bacterium or a fungus, drosophila produce a cocktail of antimicrobial peptides. A gene study of the expression of coding genes of those peptides led to the identification of the Toll pathway. This pathway is activated in response to infections and controls the expression of antifungal peptide, the drosomycin [139]. To this day, 11 TLRs are identified in human and 13 in mice [140]. These receptors are one of the most studied PRRs (Pattern-Recognition Receptors) and they are the most conserved during evolution from plates to mammals. TLRs are type I transmembrane receptors composed of 3 domains: N-terminal extracellular domain that permit ligand recognition, a transmembrane domain and a C-terminal intracellular domain that allow signal transduction. TLRs localization is variable according to the ligands they recognize and the cells in which they are expressed. TLRs are activated through pathogen-associated molecular patterns (PAMPs). APCs are capable of recognizing PAMPs via their PRRs, such as TLRs. TLRs and their ligands are numerous and can play a role of adjuvant to stimulate the innate immune response and induce an adaptive response [141]. TLR1, TLR2, TLR4, TLR5 and TLR6 are expressed on the cells surface and they mainly recognize lipoproteins, lipids and proteins coming from microbial membrane. Since TLRs are expressed on the surface of APCs and when they recognize danger signals, APCs get stimulated and they produce pro-inflammatory cytokines like IL-6, TNF-α and IL-1β orienting T cells towards a Th1 or a Th2 phenotype [87], [142]. TLRs

are also expressed in the Golgi apparatus forming a stock of TLRs. TLR4 is the receptor for lipopolysaccharides (LPS) of Gram-negative bacteria and can associate other proteins for an optimized recognition and signaling [143]. Its association with MD-2 secreted protein as well as CD14 coreceptor allow the recognition of the complex formed by the LPS and the circulating protein LBP [144]. One study set out to use a synthetic TLR4 agonist (1Z105), which is a substituted pyrimido[5,4-b]indole specific for the TLR4-MD2 complex [145]. When added to an influenza rHA vaccine and intramuscularly administered to mice, rapid and sustainable broadly protective responses were induced with Th2 biased immunity [145]. INI 2002 is a novel synthetic TLR4 agonist that induced balanced Th1 and Th2 responses while having a dose-sparing effect [146]. Specifically, mice that were vaccinated intramuscularly with a *Pseudomonas aeruginosa* (PA) coat protein (CoaB) vaccine that was adjuvanted with INI 2002 agonists induced enhanced antigen-specific serum IgG, IgG1, IgG2c that were capable of blocking the replication cycle of a phage (Pf) capable of infecting PA [146]. Additionally, INI 2002 adjuvanted vaccines induced increased levels of IFN-γ, TNF-α, IL-10, and IL-17 as detected in the spleens of the mice [146]. TLR3, TLR7, TLR8 and TLR9 are expressed in the endosomal vesicles and they recognize nucleic acids [141]. INI 4001 is a novel synthetic lapidated TLR7/8 agonist that induces potent Th1 immune responses while permitting a dose-sparing effect [147]. Specifically, mice were intramuscularly vaccinated with an anti-opioid vaccine (fentanyl-based hapten, F_1) that was adjuvanted with INI 4001 agonists [148]. This adjuvant formulation induced high serum F_1 specific IgG and IgG2a antibodies and reduced the distribution of drugs to the brains of mice after challenge with fentanyl [149]. TLR-9 recognizes bacterial DNA containing non-methylated CpG motifs [150], [151] and

synthetic oligonucleotides containing non-methylated dinucleotides CpG motifs. Some DNA viruses, such as HSV-1, HSV-2, and murine cytomegalovirus, contain genomes that are rich in CpG motifs and are capable of activating the production of cytokines and type I interferon after TLR9 stimulation [152], [153]. In humans, these agonists can be efficient in allergies, cancer or as adjuvants for vaccines [154]. In one adjuvant study, a synthetic phospholipid-conjugated TLR7 agonist (1V270) was added to a rHA influenza vaccine in mice and was effective at inducing enhanced protective antibodies and cytokines associated with Th1 cellular immunity [145]. Different signaling pathways are activated with these TLR receptors including the MyD88-TRAF6-IRF5 dependent pathway and MyD88-TRAF6-TAK1-MAPK/IKK-AP-1/NF-κB dependent pathway [155]. IRF7 can also be activated through TLR7 and TLR9 [156], but this pathway is still poorly understood.

Advax-SM™

Advax-SM™ is synthesized from a natural plant-derived polysaccharide and is formulated with TLR9 agonist CpG55.2 oligonucleotides [157]. Like other classes of non-immunomodulatory particulates, the Advax component may stimulate the recruitment of immune cells to the site of injection for enhancing the activity of presenting exogenous vaccine antigens to APCs, and in turn, cross-present the antigen to CD8 T-cells [158]. Advax is synthesized from a natural plant-derived polysaccharide, inulin, that is capable of inducing adjuvant actions when crystalized into its delta polymeric form [158]. Advax has been shown to provide promising adjuvant activity as noted by increased levels of protective antibodies and strong B and T cell responses in different animal model and through a human pre-clinical trial in which significant rise in IgM and IgG was observed

[158]. Moreover, vaccines containing Advax enhanced Th1 (IL-2, IFN-γ) and Th2 (IL-5, IL-6) cytokines [158]. Advax alone has been administered in a variety of animal models and in humans that include both intramuscular and subcutaneous injections [158], [159], [160], [161]. A combined Advax-SM™ adjuvant system was used to vaccinate mice intramuscularly resulting in Advax-SM™-adjuvanted vaccines inducing high antigen-specific neutralizing antibodies with balanced Th1/Th2 immune responses and $CD4^+$ and $CD8^+$ T-cells that further translated to the protection of mice from infection with respiratory syncytial virus (RSV) [162]. Specifically, mice had no detectable viral replication and were protected from inflammation [162]. Moreover, the administration of the combined Advax-SM™ adjuvant system was included in vaccines against severe acute respiratory syndrome (SARS) coronavirus disease and the Middle East respiratory syndrome (MERS) coronavirus disease, resulting in enhanced protection against infection in hamsters, ferrets, and non-human primates [163], [164]. This adjuvant also allowed for a dose-sparing effect of vaccines and induced both systemic and mucosal immunity in naive animals [165].

Mastoparan-7 (M7-NH_2)

M7-NH_2 is a class of soluble toll-like receptor immunomodulatory amphiphilic tetradecapeptide ligand**.** It is a 14 amino acid long cationic peptide sequence (INLKALAALAKALL-NH2) derived from the venom of *Vespula lewisii* (wasp) that has several biological activities, including mast cell degranulation [166], [167]. A unique mechanism by which M7-NH_2 activates mast cells is via its Mas-related G-protein coupled receptor member X2 (MRGPRX2) for inducing non-IgE-mediated pseudo-allergic reaction

[168], [169]. This process involves the release of inflammatory mediators [170], such as cytokines, chemokines, or histamine [171]. Mast cells circulate the blood circulation and migrate to mucosal sites, such as the respiratory or gastrointestinal tracks when activated, making them vital immune cells that are part of the innate immune response and contributors to modulating the adaptive immune response. Specifically, mast cells could potentially mediate the maturation of DCs and activation of T-cells via TNF-α and other inflammatory mediators, such as IL-1β, IL-33, and IL-18, and thereby modulate the adaptive immune response [172]. In addition to FcεRI interactions, they are capable of becoming activated through several other mechanisms, such as cross-linking of IgE receptors, viral products, immunoglobulin protein, or PRRs [173]. M7-NH_2 has been previously used in mucosal vaccines for enhancing immunity against systemic anaphylaxis caused by peanut allergic responses, as well as vaccines that were effective against cocaine challenge, in mice [174], [168], [175]. Through pre-clinical trials, M7-NH_2 enhances vaccines efficacy against HIV and influenza viruses by increased levels of IgG and IgA [173]. Additionally, M7-NH_2 enhances the efficacy of a West Nile virus subunit vaccine, administered intranasally in mice [176]. Overall, M7-NH_2-adjuvanted vaccines induces a response associated with the MyD88 (TLR adaptor) molecular pathway that is essentially for Th1 and Th2 immunity for inducing maximum M7-NH_2-adjuvanticity, independent of an allergic response [55]. Additionally, the success of this M7-NH_2 in many study models, including mice, rabbits, and non-human primates are associated with a safe profile through an intranasal route of administration [55], [166].

CpG 1018

CPG ODN 1018 is a class of immunomodulatory adjuvant that is made of a short 22-mer oligonucleotide sequence containing CpG motifs found in rodents, non-human primates, and humans [178]. These synthetic single-stranded DNA molecules have been studied extensively as TLR agonists that act as pattern recognition receptors to activate PRRs within the endosome of immune cells, including dendritic cells, B cells, and macrophages [87], [178], [179]. This adjuvant elicits an enhanced cellular immune response compared to aluminum-based adjuvants due to CpGs' ability to activate nuclear factor kappa B (NF-κB) and interferon-regulatory factor 7 (IRF7) via the myeloid differentiation factor 88 (MyD88) pathway, through TLR9 stimulation [86], [180]. The activation of MyD88 and leads to a cascade of activations resulting in the production of pro-inflammatory cytokines (IL-12) and type I interferon by APCs, hence inducing a strong Th1 biased cellular response and cytotoxic T cells production [180], [181]. When a rNA influenza vaccine was administered intramuscularly to mice in a prime-boost regimen with a CpG ODN 1018 adjuvant, the formulation induced robust anti-NA immunity and fully protected mice from influenza infection [182]. Specifically, this adjuvanted vaccine elicited enhanced cross-reactive NA-specific antibodies that were also effective following a passive transfer to other mice, and its adjuvanticity was effective with dose-sparing outcomes [182]. CPG ODN 1018 was approved for use in hepatitis B virus (HBV) vaccines and is currently being evaluated as a potential adjuvant for COVID-19 vaccines [86]. The SCB-2019 is a CPG ODN 1018 adjuvanted COVID-19 vaccine that was evaluated for emergency use amid the recent COVID-19 pandemic [183], [184].

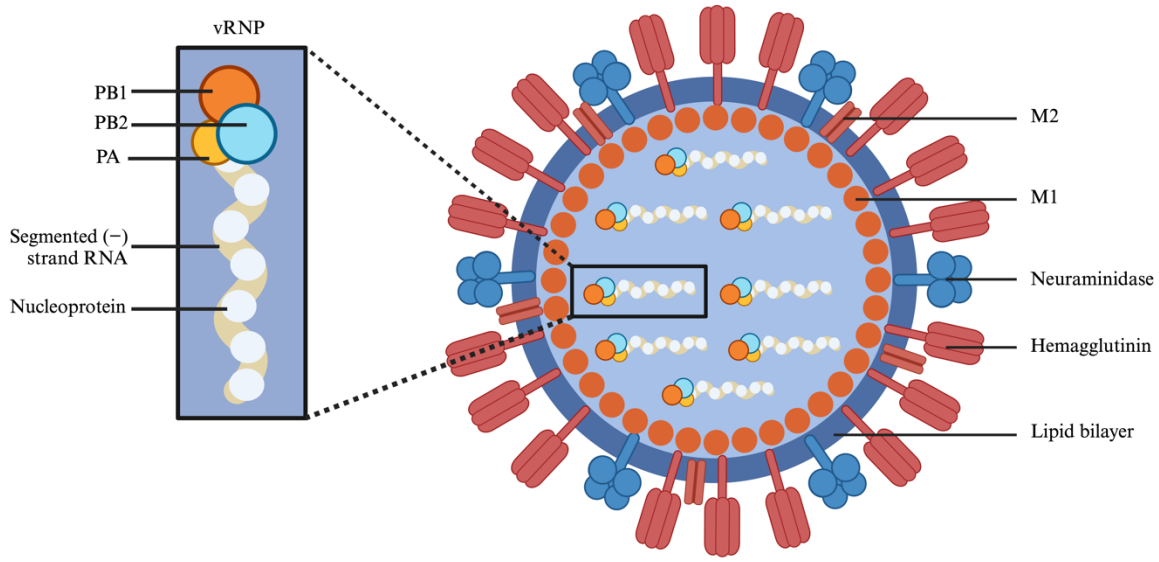

Figure 2. 1 Schematic representation of an influenza A virus.

Influenza virions contain 8 single-stranded RNA segments that encode for each viral protein. Together with the viral polymerase, they form the viral ribonucleoprotein (vRNP). The viral RNA-dependent RNA polymerase consists of the polymerase acid (PA), polymerase basic 1 (PB1), and polymerase basic 2 protein (PB2). The surface glycoproteins hemagglutinin (HA) involves entry of the virus into host cells, whereas the neuraminidase (NA) facilitates the release of progeny virions. The matrix protein (M1) forms an inner coat inside the virus envelope and the membrane protein (M2) is a proton ion channel that mediates proton exchange for acidifying the endosome, thus dissociating the entrapped virus [185]. Created with BioRender.com.

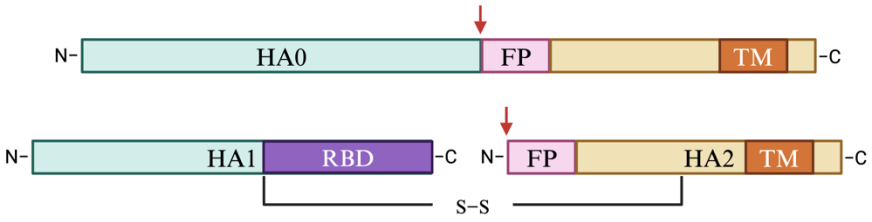

Figure 2. 2 Schematic of HA glycoprotein.

The HA precursor, HA0, can be divided into HA1 and HA2 subunits that are connected by disulfide bonds (S–S). The HA1 component contains the receptor binding domain (RBD), whereas the HA2 component contains the fusion peptide (FP) and the transmembrane domain (TM) [186]. Created with BioRender.com.

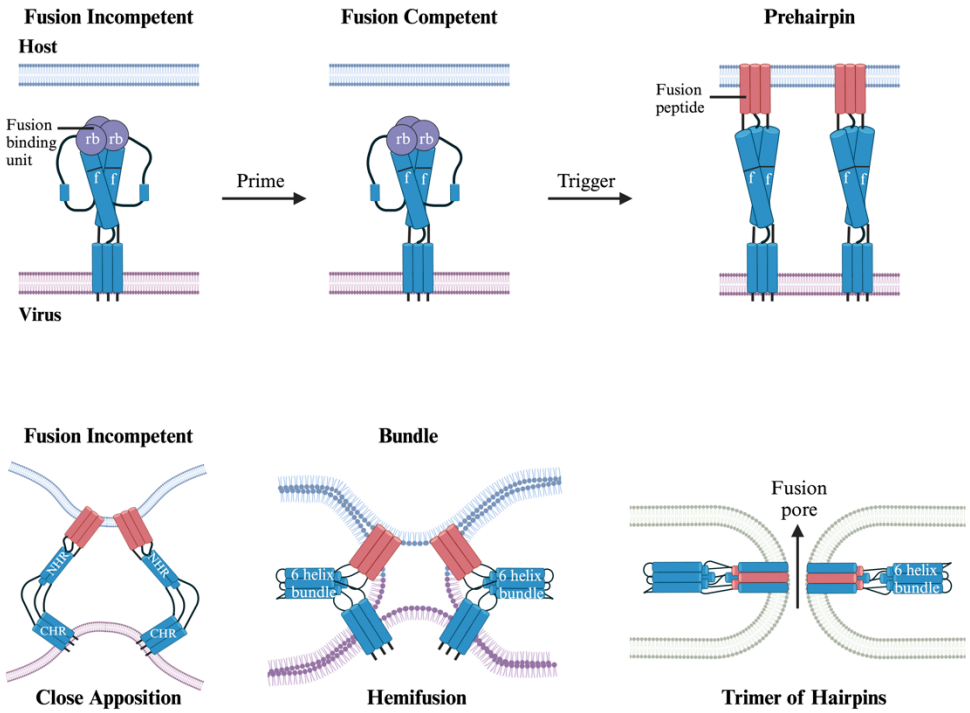

Figure 2. 3 Schematic of viral and host endosomal membrane fusion.

Within the host endosome, HA0 is in a pre-fusion, incompetent conformation with its fusion peptide intact (a). Once pH acidification (priming) occurs, HA0 becomes competent (b) and undergoes a confirmational change leading to dilation of the HA1 subunit and exposing the fusion peptide located one the HA2 subunit. In turn, the fusion peptide injects itself into the endosomal membrane (c) and pre-hairpins form and fold back causing the N- and C-α-helical heptad repeats to form a six-helix bundle (6HB) (d) bringing the endosome and viral membranes together by fusion (d). hemifusion (e) and fusion pores form, resulting in the final confirmation of trimer of hairpins (f). [187]. Created with BioRender.com.

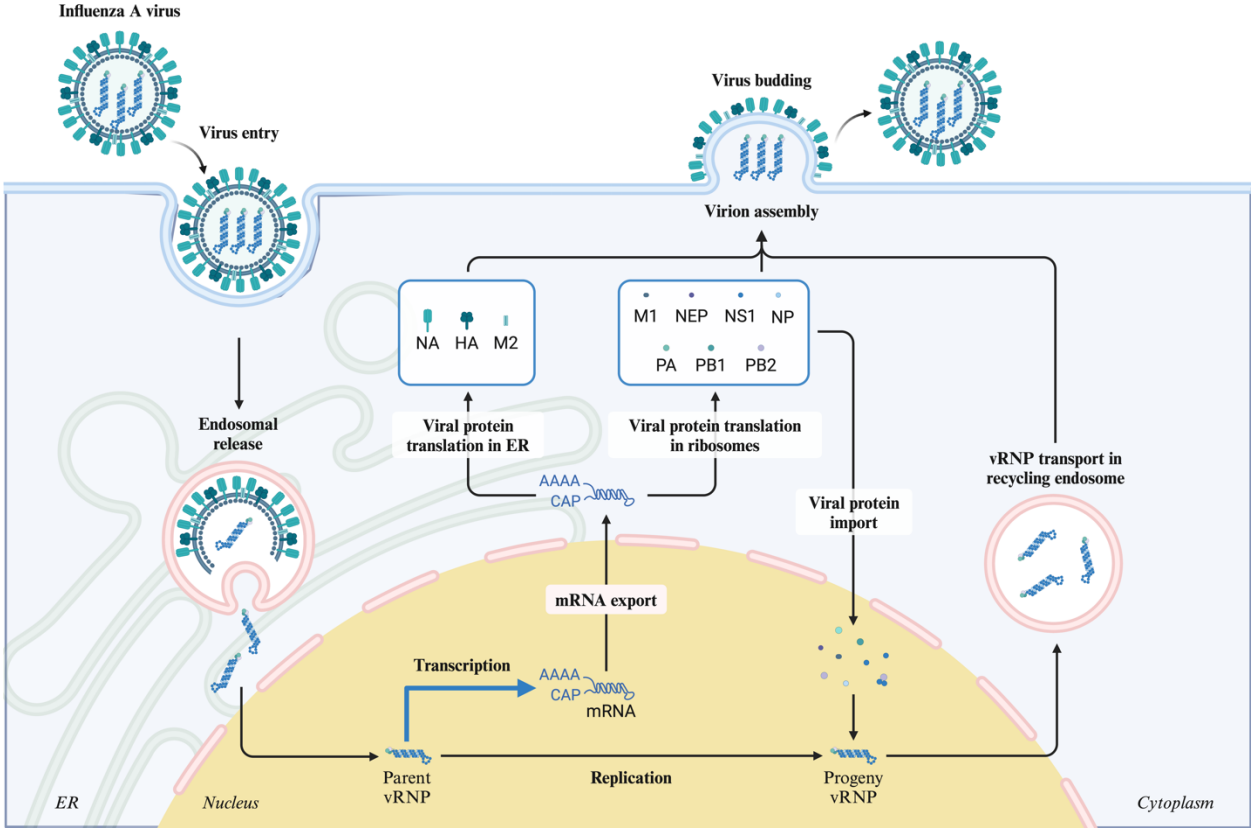

Figure 2. 4 Replication cycle of influenza A viruses.

After the HA glycoprotein of influenza binds host-cell sialic acid receptors, the virion enters via endocytosis. Upon endosome acidification, the viral ribonucleoprotein (vRNP) complexes are released into the cytoplasm and transported to the nucleus where replication and transcription take place. Messenger RNAs are exported to the cytoplasm for translation into proteins. Early viral proteins required for replication and transcription are transported back into the nucleus. The M1 and NS1 proteins facilitate the nuclear export of newly synthesized vRNPs in proximity of HA, NA, and M2 around the cell-membrane [188]. Created with BioRender.com.

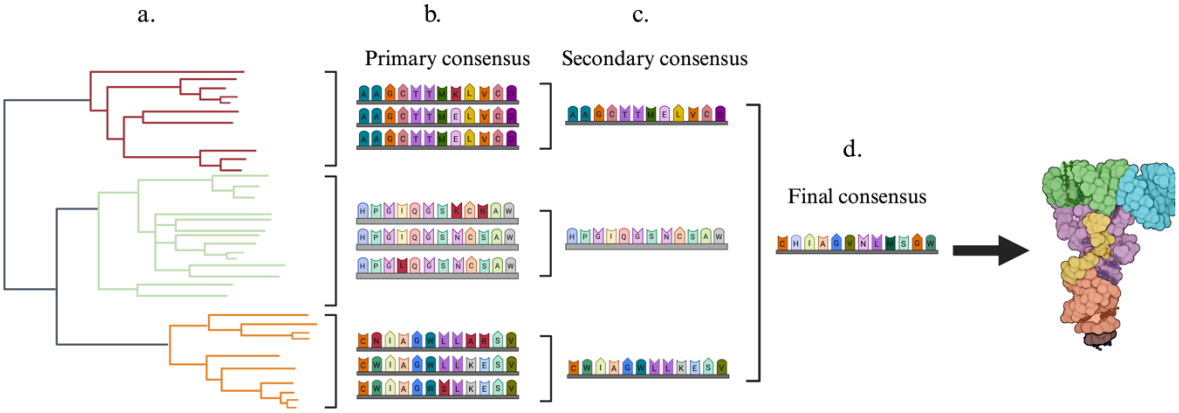

Figure 2. 5 Schematic of the COBRA-based approach.

(a.) A phylogenetic tree is extrapolated based on hemagglutinin (HA) amino acid sequences and (b.) Primary and (c.) secondary consensus sequences are generated. The secondary consensus sequences are subjected to alignment and the resulting (d.) final consensus, designated COBRA, is developed [189]. Created with BioRender.com.

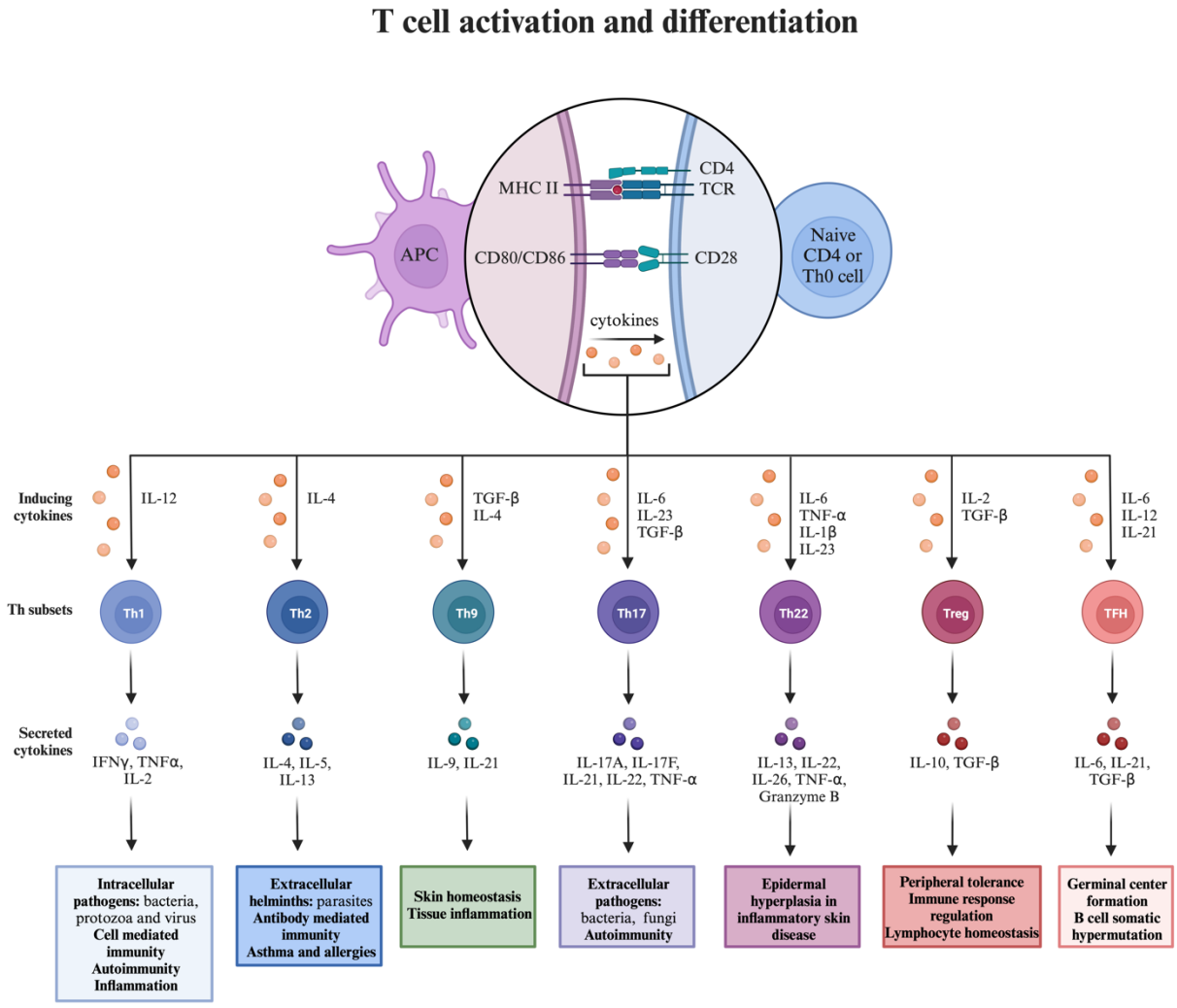

Figure 2. 6 Overview of T helper subsets.

Following encounter with foreign antigens, antigen-presenting cells (APCs,) process and present peptides to naïve $CD4^+$ T cells via major histocompatibility complex (MHC) class II molecules. During this process, inducing cytokines drive differentiation and clonal expansion of $CD4^+$ T cells into functionally distinct T helper (Th) subsets that in turn, secretes specific effector cytokines that are involved in coordinating distinct types of host immune response [190]. Created with BioRender.com.

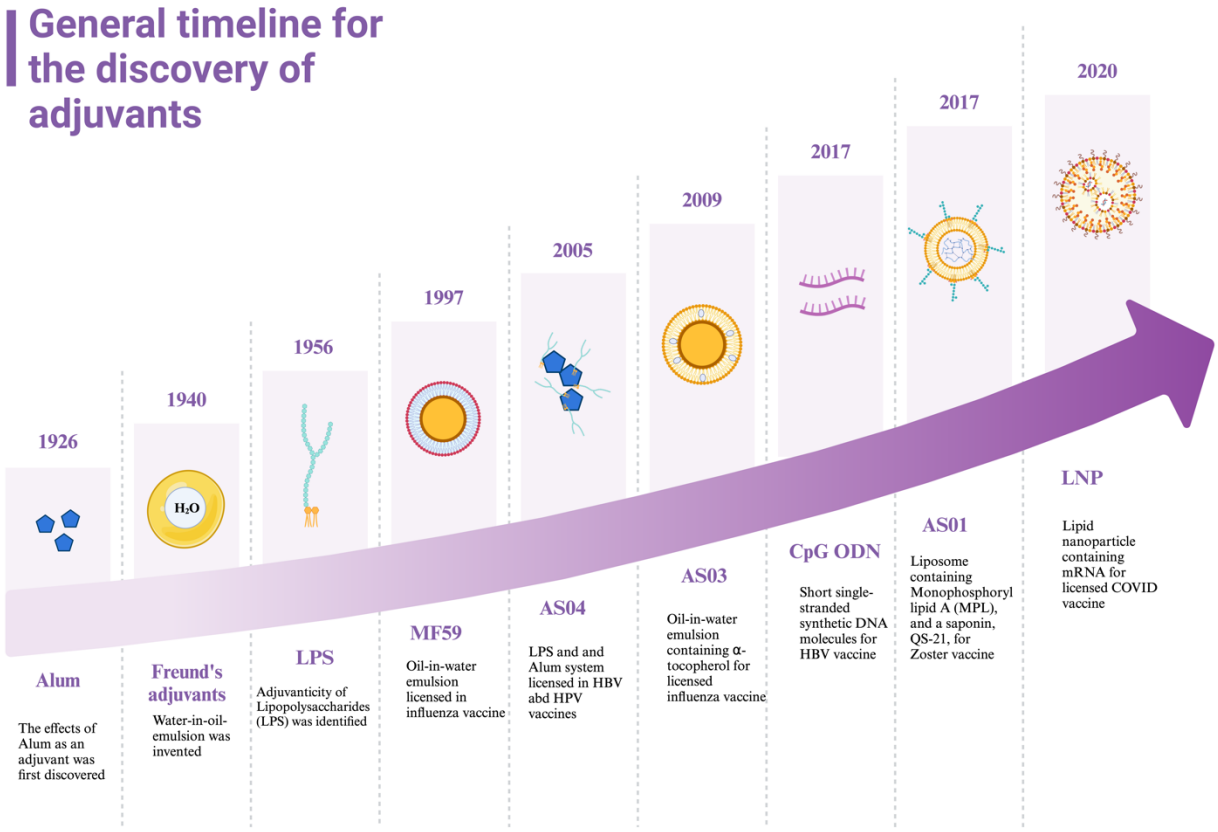

Figure 2. 7 Timeline and identification of different types of vaccine adjuvants.

[86]. Created with BioRender.com.

CHAPTER 3

ADVAX-SM™-ADJUVANTED COBRA (H1/H3) HEMAGGLUTININ INFLUENZA VACCINES[1]

[1]Sanchez, Pedro L., Greiciely Andre, Anna Antipov, Nikolai Petrovsky, and Ted M. Ross. "Advax-SM™-Adjuvanted COBRA (H1/H3) Hemagglutinin Influenza Vaccines" Vaccines 12, no. 5: 455. This is an accepted manuscript of an article published in Vaccines on April, 4, 2024, available online: doi.org/10.3390/vaccines12050455. Reprinted here with permission of publisher.

Abstract

Adjuvants enhance immune responses stimulated by vaccines. To date, many seasonal influenza virus vaccines are not formulated with an adjuvant. In this study, the adjuvant Advax-SM™ was combined with next generation, broadly-reactive influenza hemagglutinin (HA) vaccines that were designed using Computationally Optimized Broadly Reactive Antigen (COBRA) methodology. Advax-SM™ is a novel adjuvant comprising inulin polysaccharide and CpG55.2, a TLR9 agonist. COBRA HA vaccines were combined with Advax-SM™ or a comparator squalene emulsion (SE) adjuvant and administered to mice intramuscularly. Mice vaccinated with Advax-SM™ adjuvanted COBRA HA vaccines had increased serum levels of anti-influenza IgG and IgA, high hemagglutination inhibition activity against a panel of H1N1 and H3N2 influenza viruses, and increased anti-influenza antibody secreting cells isolated from spleens. COBRA HA plus Advax-SM™ immunized mice were protected against both morbidity and mortality following viral challenge and, at postmortem, had no detectable lung viral titers or lung inflammation. Overall, the Advax-SM™-adjuvanted COBRA HA formulation provided effective protection against drifted H1N1 and H3N2 influenza viruses.

Introduction

Influenza viruses are part of the family *Orthomyxoviridae* and cause annual respiratory infections that can lead to hospitalization and fatal outcomes [191], [192]. Influenza viruses can undergo antigenic drift and shift [193], [194], thus allowing these viruses to evade host immune responses directed against the viral glycoproteins hemagglutinin (HA) and neuraminidase (NA), which are located on the virion surfaces [6], [195], [196]. Designing effective vaccines against the ever-changing influenza A viruses (IAVs) is challenging. Each season, wild-type (WT) influenza strains are selected for vaccine formulation and are not necessarily matched to circulating influenza virus strains, thus compromising the effectiveness of the vaccine [10], [8]. Most commercially-available influenza vaccines are based on split-inactivated virus, recombinant hemagglutinin or live-attenuated influenza virus (LAIV) platforms that induce protective immune responses through various mechanisms, including increased serum neutralizing antibodies in the case of the non-live platforms and enhance mucosal immunity in the case of LAIV [197], [198]. Adjuvants are molecular entities that enhance immune responses when co-administered with vaccine antigens [199], [200]. Currently, the squalene oil-in-water emulsion, MF59, is the only adjuvant included in an FDA-licensed influenza vaccine which is indicated for use in the elderly [201], [202]. AddaVax (SE adjuvant) is a commercially-available squalene oil-in-water adjuvant designed to replicate MF59 [203], [204].

To rectify the need for next-generation influenza vaccines, our group has previously developed novel antigens, referred to as computationally optimized broadly reactive antigen (COBRA). This method was utilized for synthesizing rHA and rNA proteins, capable of stimulating antibodies that induce broad responses, for providing long lasting

protection against influenza virus strains that have undergone antigenic drift, [77]. COBRA HA and NA virus-like particle vaccines stimulate antibodies with protective HAI and NAI responses against influenza A and B viruses in several animal models, including rodents, ferrets, and monkeys following vaccination [10], [9], [11], [13], [205].

As adjuvants may be particularly useful to enhance vaccine immunogenicity in groups that are at higher risks, like children with untrained immune systems or the immunosenescence seen in the elderly [9], [77], [206]. In this study, the adjuvant formulation, Advax-SM™ (https://protect-us.mimecast.com/s/WtgVCrk5zWtwyoOmLT7a_P5?domain=vac.niaid.nih.gov) in combination with recombinant COBRA HA antigens, was compared to a SE adjuvant (AddaVax) to assess their relative ability to protect mice against influenza viruses. Advax-SM™ is synthesized from a natural plant-derived polysaccharide, inulin, that has immunostimulatory properties when crystalized into its delta polymeric form (delta-inulin) and formulated with TLR9 agonist CpG oligonucleotides [157]. Like other classes of non-immunomodulatory particulates, delta-inulin stimulates the recruitment of immune cells to the site of injection for enhancing the activity of presenting exogenous vaccine antigens to APCs that in turn presents antigens to $CD4^+$ and $CD8^+$ T-cells [158]. TLR9 agonist CpG oligonucleotides directly induce the activation of dendritic cells and enhance differentiation of B cells into antibody-secreting plasma cells [180], [207], [208]. Advax-SM™ adjuvant increases protective antibody titers and induces strong B and T cell responses with a significant rise in IgM and IgG levels [158]. Moreover, vaccines formulated with Advax-SM™ elicited enhanced Th1 (IL-2, IFN-γ) and Th2 (IL-5, IL-6)

cytokines [158] following either intramuscular or subcutaneous injections [158], [209], [159], [160], [161].

To enhance the immune responses elicited by COBRA HA vaccines, mice were vaccinated with COBRA HA proteins representing the H1 and H3 subtypes of influenza that were mixed with Advax-SM™ or SE adjuvant. Overall, the goal of this study was to assess how immune responses induced by vaccination with COBRA HA vaccines formulated with a novel particulate polysaccharide adjuvant containing CpG55.2 TLR9 agonist, Advax-SM™, compares to a SE adjuvant and how these responses might elicit the most protective immune responses against a diverse panel of H1N1 and H3N2 influenza viruses.

Materials and Methods

COBRA HA designs and protein synthesis

COBRA HA antigens corresponding to H1N1 and H3N2 seasonal influenza viruses (IAVs) were developed using the next-generation COBRA methodology [77]. H1 COBRA HA, Y2, was originated by extracting full length HA sequences pertaining to 6232 GISAID wild-type influenza A(H1N1) viruses. H1N1 sequences of infections collected from human isolates ranging between January 1, 2014 to December 31, 2016 were used to download the HA residues 1-566 (Methionine as the first amino acid) from online databases and organized in order of collection date [9].

H3 COBRA HA, NG2, was originated by extracting full length HA sequences pertaining to 22,144 human wild-type influenza A(H3N2) viruses. H3N2 sequences of

infections collected from human isolates ranging between January 1, 2016 to December 31, 2018 were used to download the HA residues 1-566 (Methionine as the first amino acid) from online database and organized in order of collection.

Soluble COBRA HAs were purified from cells transfected with plasmids containing a pcDNA3.1 with an incorporated truncated HA gene that was made by substituting the transmembrane domain with a T4 fold-on domain, an Avitag, and a 6× His-tag [210]. Concentrations of the soluble HA molecules were measured via the bicinchoninic acid assay (BCA). Both the full-length HA sequences used in this study and the multiple sequence alignment are indicated in Table 3. 1 (for H1N1 HAs) and Table 3. 2 (for H3N2 HAs).

Vaccination

DBA/2J female mice (n=75; 6 to 8 weeks in age) were purchased from Jackson Laboratory (Bar Harbor, ME, USA). All of the mice were contained in microisolator cages and had access to drinking water and food. USDA guidelines for laboratory animals were followed for caring for the mice and all of the procedures performed on the mice were reviewed and approved by the University of Georgia Institutional Animal Care and Use Committee (IACUC) (no. A2020 03-007-Y2-A7). Vaccinations and mouse bleeds were carried out as previously described [10]. Prior to starting the study, all of the mice were randomized and separated into different experimental groups with an n=18 per group. The remainder 3 naïve mice were used as comparers for lung pathology only, following infection. Prior to vaccination (day 0), serum samples were collected to verify that each mouse was seronegative, having no antibodies against the following viruses:

A/Texas/36/1991 (TX/91), A/Brisbane/59/2007 (Bris/07), A/California/07/2009 (Cal/09), A/Brisbane/02/2018 (Bris/18), and H3N2 viruses: A/Texas/50/2012 (TX/12), A/Switzerland/9715293/2013 (SW/13), A/Hong Kong/4801/2014 (HK/14), A/Singapore/IFNIMH/2016 (Sing/16), A/Kansas/14/2017 (KS/17), A/Switzerland/8060/2017 (SW/17), A/Hong Kong/2671/2019 (HK/19), and A/South Australia/34/2019 (SA/19). Red blood cells were isolated from sera by centrifugation at a speed of ten thousand rpm for ten minutes and the sera samples were then stored at -20°C ± 5°C. Some of the mice were vaccinated intramuscularly (IM) with 3μg of Y2 and 3μg of NG2 COBRA HA antigens, and adjuvanted with 1mg of Advax-SM™. Other mice were vaccinated with COBRA HA antigens as before and adjuvanted with SE adjuvant (AddaVax) at a 1:1 ratio. The mice pertaining to the control groups were vaccinated with no adjuvant or mock vaccinated with Advax-SM™ alone. For boost vaccinations, all of the mice were intramuscularly vaccinated at the 4^{th} and 8^{th} weeks, as before. After the last boost, each mouse was bled on days 70 and 76 and the sera was processed via centrifugation and pooled, prior to storing at -20°C ± 5°C. For challenge (day 82), the mice were anesthetized and intranasally infected with $8x10^6$ PFU of A/Bris/18 (H1N1) influenza A virus. Once the mice recovered from anesthesia, they were placed back into their cages and monitored for morbidity, mortality, and clinical signs (0-3; 0=no clinical signs; 1=weight loss 15-<20%; 2=dyspnea; 3=weight loss >20%/failure to respond to external stimulus/severe respiratory distress/neurological signs), for 14 days after. A mean clinical score 3 was considered the endpoint and the animal was humanely euthanized via carbon dioxide asphyxiation followed by secondarily cervical dislocation. At day 85, vaccinated

mice were euthanized as before and lungs were harvested from 3 mice in each group. The right lobes were snap-frozen on dry ice and stored at -80°C for determining viral lung titers.

Viral Lung Titers

The protocol used for this plaque assay was followed as previously described [9]. To determine viral lung titers, $1x10^6$ per 10 cm^2 MDCK cells were added to tissue culture plates (Fisher Scientific, Pittsburgh, PA, United States of America) and placed in a static incubator for twenty-four hours at 37 °C + 5% CO_2 until a monolayer of about ninety-five percent confluency was attained. The weights of each mouse's lungs was weighed and subjected to homogenizing in DMEM media containing 1 percent penicillin-streptomycin (P/S), in volumes of 10 times the weights of the lungs. Homogenized samples were subsequently centrifuged at one thousand five hundred rpm for ten minutes and serially diluted at 10-folds. For a positive control, Bris/18 was serial diluted as before. 100uL of the diluted homogenates were added to monolayers of MDCK cells to infect them for 60 minutes at RT, with fifteen-minute shaking interims. Some wells served as negative controls and 100μL of DMEM P/S only was added to them. Following the 60-minute incubation, the supernatants were removed from each well, laved one time with DMEM P/S media, and overlayed with 2mL of a 1:1 solution of 1.6% agarose in 2x cMEM media + TPCK-Trypsin at 1 μg/mL. The plates were then placed in a static incubator for two to five days at 37 °C + 5% CO_2. Upon confirmation of visible cytopathic effects, the agarose was detached and the monolayer of cells were fixed with ten percent formalin for ten minutes at room temperature. Subsequently, the formalin was discarded from each well and the monolayers were stained for ten to fifteen minutes at RT with one percent Crystal

Violet (Fisher Science Education, Waltham, MA, USA). Lastly, following the incubation period, the Crystal Violet was discarded from each well and the monolayers were rinsed with water. The plates were allowed to air-dry and the plaque forming units (PFUs) were determined and calculated as PFU/g of tissue.

Histopathology

At day 85, lungs were harvested from 3 mice in each group. The left lobes of each lung were inflated with 10% neutral formalin to fix the tissues for histopathology and subjected to staining with Hematoxylin and Eosin (H&E) staining on lung slices measuring 5 μm to visualize pathology in the lungs of vaccinated mice versus non-vaccinated mice.

Enzyme-linked Immunosorbent Assay (ELISA)

Total IgG in mice sera and associated binding to WT IAV HAs was assessed using in Immulon 4HBX 96-well flat bottom plates (Thermo Fisher Scientific, Waltham, MA, USA). 100μL of WT Bris/18 or Sing/16 rHAs, at 1 μg/mL in carbonate coating buffer (pH 9.4) solution was added to the well of each plate and incubated at 4°C overnight in a humidified chamber. After the incubation, the coating solutions were removed and the wells were blocked for 1.5 hours at 37°C with 200 μL of blocking buffer (BB) containing 4% FBS + 0.05% Tween. The serum samples were made at 1:100 ratio followed by serially diluting (1:3) from an initial 1:500 dilution. After blocking, 100 μL of diluted sera was added to the WT Bris/18 or Sing/16 coated plates and incubated for 1.5 hours at 37°C. After the incubation, the plates were thoroughly laved, one hundred microliters of secondary goat anti-mouse IgG HRP (Southern Biotech, Birmingham, AL, USA) antibody,

diluted 1:4000 in blocking buffer added to each well, followed by statically incubating the plates for 1.5 hours at 37°C. Subsequently, the antibody solution was discarded, each well was thoroughly laved and received one hundred microliters of 1x ABTS (VWR Corporation, Radnor, PA, USA) with static incubation for thirteen minutes at 37°C. Succeeding incubation, fifty microliters of one percent SDS was added to halt the reaction of each well. IgG titers were measured as the optical density (O.D.) of each sample at 414nm with a spectrophotometer (PowerWave XS, BioTek, Santa Clara, CA, USA) utilizing the Gen05 software (version 3.14, https://www.agilent.com/en/support/biotek-software-releases). IgG was compared to positive and negative controls within each plate. To determine IgA and the different Ig isotypes against WT rHAs, the samples were initially handled as before with subsequent static incubated with secondary goat anti-mouse IgA, IgG1, IgG2a or IgG2b antibodies and the O.D. measured as before. For these sets, sera were made at 1:100 ratio and serially diluted (1:3) from a starting 1:500 dilution for isotype determination, or prepared at 1:10 ratio for IgA, and serially diluted (1:2) from the starting 1:10.

Hemagglutination Inhibition Assay (HAI)

Neutralizing anti-HA antibodies are able to block viruses from agglutinating activity red blood cells (RBC). To determine this activity in vaccinated mice sera, the HAI assay was employed. The protocol followed the manual for laboratory diagnosis and virological surveillance of influenza published by the World Health Organization (WHO) [211]. HAI activity was tested against the H1N1 viruses shown herein: TX/36/91, Bris/02/07, Cal/07/09, Bris/02/18, and H3N2 viruses: TX/50/12, SW/9715293/13,

HK/4801/14, Sing/IFNIMH/16, KS/14/17, SW/8060/17, HK/2671/19, and SA/34/19. Specific details on how the HAI assay was completed has been described [212]. Concisely, sera from individual mice were mixed with receptor destroying enzyme (RDE) (Denka Seiken, Co., Tokyo Japan) and diluted to $1/10^{th}$ by reconstituting one hundred microliters of serum with three volumes of RDE in 1x PBS. The reconstituted samples where then incubated at 37°C overnight. After overnight incubation, the treated sera were heat inactivated in a water bath at 56°C for forty-five minutes, allowed to cooled to RT, followed by adding 6 volumes of 1x PBS. 96-well plates (v-bottoms) containing 25 µL of PBS was used to serially diluted the RDE-treated sera samples, in duplicates. 1:8 solutions of each virus to be tested was added to the plates with serially diluted sera samples and incubated at RT for twenty minutes for the H1N1 influenza viruses or thirty minutes for the H3N2 influenza viruses. After the incubation, H1N1 samples received 0.8% turkey RBC (TRBCs) and H3N2 samples received 0.8% guinea RBC (GPRBCs), were manually agitated, followed by incubated at RT for thirty minutes. Subsequently, the reciprocal dilutions of the last wells that ran (no agglutination) were reported as the titers. A 1:40 titer was the measurement of seroprotection as per the European Medicines Agency Guidelines on Influenza Vaccines [213].

FluoroSpot Assay

On day 61, spleens were collected (n=3) per study arm. Following homogenization, splenocytes were washed twice with RPMI 1640 BCM Medium (Gibco™, Grand Island, New York, USA) and centrifuged at 400G for 10 minutes, at 4°C. After the second wash, the BCM media was discarded and the cell pellets were resuspended in 4 mL of 90%

FBS/10%DMSO freezing media and aliquoted into cryotubes for storage at -80°C overnight, and then transferred to LN_2 for future use. To assess antigen-specific antibody secreting cells (ASCs), the Four Color Immunospot® kit (CTL, Shaker Heights, OH, USA) was employed. Following the manufacturer's instructions, *in vivo* pre-stimulated splenocytes were washed with BCM and filtered through 70µm MACS® SmartStrainers to removed debris. In v-bottom, 96-well plates, splenocytes were serially diluted 3-fold, in duplicates, starting at 3 x 10^5 live cells per well and transferred to pre-treated (with 70% ethanol) PVDF plates, coated with anti-Igκ/λ capture antibody, Y2, NG2, or BSA at 25 µg/mL in Diluent A, provided in the Immunospot kit. Following the addition of splenocytes to the wells, the plates were incubated in a humidified chamber with 5% CO_2 for 16-18 hours at 37°C, as per the manufacturer's instructions. Following incubation, the ASCs were removed and the plates were washed twice with 1x PBS. An anti-mouse detection solution containing IgG1/IgG2a/IgG2b was prepared and added to each well, followed by a 2h incubation in the dark, at room temperature (RT). After the incubation period, the plates were washed twice with PBS-T, follow by the addition of a prepared tertiary solution and incubated for 1h in the dark, at RT. After incubation, the plates were decanted, washed twice with distilled water, and allowed to dry overnight in a dark, running laminar flow hood, face down on paper. FluoroSpot detection was achieved upon reading the plates on the ImmunoSpot® S6 Ultimate Analyzer. Spot-forming-units (SFUs) were enumerated using the Basic Count mode of the CTL ImmunoSpot SC Studio (Version 1.6.2, Shaker Heights, OH, USA).

Statistical Analysis

The weight loss and clinical scores were statistically evaluated using two-way ANOVA by Prism 9 software (GraphPad Software, Inc., San Diego, CA, version 9.4.0, https://www.graphpad.com). p-value less than 0.05 was defined as statistically significant ($p<0.05$*, $p<0.01$**, $p<0.001$***, $p<0.0001$****). Each line represents an n=15 per group and is conveyed as the average +/- standard error of the mean (SEM).

For ELISA analysis, IgG, IgG1, IgG2a, and IgG2b titers were statistically evaluated using one-way ANOVA by Prism 9 software (GraphPad Software, Inc., San Diego, CA, version 9.4.0, https://www.graphpad.com). p-value less than 0.05 was defined as statistically significant ($p<0.05$*, $p<0.01$**, $p<0.001$***, $p<0.0001$****). Each bar corresponds to 15 individual mice according to vaccine regimens and are conveyed as the average +/- standard error of the mean (SEM).

The HAI titers were statistically evaluated using one-way ANOVA by Prism 9 software (GraphPad Software, Inc., San Diego, CA, version 9.4.0, https://www.graphpad.com). p-value less than 0.05 was defined as statistically significant ($p<0.05$*, $p<0.01$**, $p<0.001$***, $p<0.0001$****). Each column represents 15 individual mice pertaining to each vaccine regimen and are conveyed as the average +/- standard error of the mean (SEM).

For FluoroSpots analysis, ASC were statistically evaluated using one-way ANOVA by Prism 9 software (GraphPad Software, Inc., San Diego, CA, version 9.4.0, https://www.graphpad.com). p-value less than 0.05 was defined as statistically significant ($p<0.05$*, $p<0.01$**, $p<0.001$***, $p<0.0001$****). Represented is an n=3 of mice per the

indicated vaccine regimens and expressed as the average +/- standard error of the mean (SEM).

Results

Advax-SM™-adjuvanted COBRA HA vaccines protect mice against influenza virus challenge

DBA/2J mice were divided into four study arms and vaccinated intramuscularly following prime-boost-boost regimens (Figure 3. 1a-b). Control mice immunized with Advax-SM™ adjuvant alone lost an average ~20% of their original body weight by day 3 post-infection (Figure 3. 2a), with a mean clinical score of 3 (Figure 3. 2b), and all succumbed to infection by day 3 post-infection (Figure 3. 2c). All of the mice vaccinated with COBRA HA proteins formulated with either the Advax-SM™ or comparator SE adjuvant showed maximum weight loss of <5% of their original body weight at day 2 post-infection and returning to their original weight by day 4, with minimal sickness scores particularly in the Advax-SM™ group and no mortality (Figure 3. 2a-c). Mice vaccinated with COBRA HA alone lost ~11% of their original weight loss by day 3 post-infection with the survivors in this group slowly returning to their original body weight by day 8 post-infection with a mean clinical score of 2.08 and only 33% survival (Figure 3. 2a-c).

Three mice in each group were sacrificed at day 3 post-infection for assessment of lung virus titers and lung pathology. Control Advax-SM™-alone vaccinated mice had high viral lung titers as did the mice that received COBRA HA alone without adjuvant (~$1x10^6$ pfu/g of tissue) (Figure 3. 3). In contrast, none of the mice vaccinated with the COBRA

HA plus Advax-SM™ had detectable lung virus, and only one of three of the COBRA HA plus SE adjuvant immunized mice had detectable, albeit low, viral lung titers.

Advax-SM™ protects mice from developing lung pathology following influenza infection

Mice vaccinated with COBRA HA proteins plus Advax-SM™ were protected from lung injury with no inflammation (0%) observed in the upper or lower lungs following challenge with Bris/18 (Figure 3. 4c), which was similar to normal lungs of unchallenged mice (Figure 3. 4f), whereas mice vaccinated with COBRA HA alone (Figure 3. 4a) or COBRA HA plus SE adjuvant (Figure 3. 4b) had evidence of lung inflammation (~50-60%), similar to the inflammation (~60-70%) seen in Mock plus Advax-SM™ and Mock plus saline immunized mice (Figure 3. 4d-e).

Advax-SM™ adjuvant enhances serum anti-influenza IgG, IgA, and subclass switching following vaccination

To assess the anti-influenza IgG and subclasses elicited by each vaccine formulation, sera collected from mice following the last vaccine boost and were assessed for total anti-influenza IgG and IgG isotypes (Figure 3. 5). Mice vaccinated with COBRA plus Advax-SM™ had significantly higher total IgG titers against Bris/18 and Sing/16 rHAs compared to mice vaccinated with COBRA HA plus SE adjuvant or COBRA HA alone (Figure 3. 5a). Mice vaccinated with COBRA HA plus SE adjuvant had a predominance of IgG1 with only a reduced amount of IgG2a and IgG2b against Bris/18 and Sing/16 rHAs (Figure 3. 5c- d). In contrast, mice vaccinated with the same COBRA

HA with Advax-SM™ exhibited a balanced mix of IgG1, IgG2a, and IgG2b against Bris/18 and Sing/16 rHAs (Figure 3. 5c-d). COBRA only vaccinated mice had significantly less IgG1 with little to no IgG2a or IgG2b (Figure 3. 5c- d) against either WT rHA. Additionally, Mock + Advax-SM™ vaccinated mice had no detectable serum antibodies (data not shown). Only mice immunized with COBRA HA plus Advax-SM™ had measurable serum anti-influenza IgA (Figure 3. 5b).

Advax-SM™ adjuvant enhances serum hemagglutination-inhibition (HAI) titers in vaccinated mice

Vaccinated mice had sera capable of blocking panels of H1N1 and H3N2 influenza viruses from agglutinating RBCs. Mice vaccinated with Advax-SM™ adjuvanted COBRA HA antigens had elevated serum HAI titers against the H1N1 influenza viruses. However, these levels were not statistically different to mice vaccinated with SE adjuvanted COBRA HA antigens (Figure 3. 6). In contrast, only 40-50% of the mice vaccinated with the COBRA HA vaccine alone had HAI responses ≥1:40 against two influenza viruses pertaining to the H1N1 subtype (Figure 3. 6). Mice immunized with COBRA HA plus Advax-SM™ had elevated HAI responses against 7 of the 8 influenza viruses pertaining to the H3N2 subtype panel (Figure 3. 7c). Comparable findings were perceived in mice immunized with COBRA HA plus SE adjuvant (Figure 3. 7b). There were low to no HAI responses in mice immunized with unadjuvanted COBRA HA vaccines (Figure 3. 7a). and no HAI activity against any of the H3N2 viruses for the Mock vaccinated group (Figure 3. 7d). None of the mice, regardless of vaccine used, developed serum HAI titers against H1N1 TX/91 or Bris/07 (data not shown).

Advax-SM™ adjuvant drives production of IgG1 and IgG2a antibody-secreting cells

IgG1 and IgG2a antibody secreting cells (ASC) were identified in the spleens of mice vaccinated with COBRA HA proteins plus Advax-SM™. Sera of these mice had influenza-specific IgG1, IgG2a and IgG2b antibodies that bound the Y2 and NG2 HA antigens (Figure 3. 8a-c). ASC from mice vaccinated with COBRA HA proteins plus SE adjuvant secreted primarily IgG1 with little or no IgG2a (significantly lower than mice vaccinated with COBRA HA proteins plus Advax-SM™) or IgG2b (Figure 3. 8a-c). Mice vaccinated with unadjuvanted COBRA HA or adjuvant-alone control mice had little to no influenza-specific ASCs (Figure 3. 8a-c).

Discussion

The first influenza vaccines were developed in the 1930s and 1940s for the U.S. military using embryonated chicken eggs, which is a technique still used to make commercial vaccine today [60], [214], [215], [216], [217]. Other vaccine platforms have been approved for commercial seasonal influenza vaccines, including live attenuated virus (LAIV) vaccines and recombinant HA protein vaccines [197], [218], [219], [220]. The first adjuvanted influenza vaccine using MF59, a squalene oil-in-water adjuvant, was approved in 1997 and now is used in 38 countries for people 65 years and older [125], [221], [222]. Adding this adjuvant to the influenza vaccine broadens the immune responses and allows for increased protection against drift strains of influenza viruses [115], [223], [224]. Various new adjuvants may have potential to enhance the effectiveness of influenza vaccines [225], [226]. A key aim in the influenza field is to identify vaccine formulations that stimulate effective, broadly-reactive, and long-lasting protective anti-influenza

immune responses in all age groups. Newer adjuvants include toll-like-receptor (TLR) agonists such as GLA (glucopyranosyl lipid A), a TLR4 agonist, or CpG oligodeoxynucleotides which are TLR9 agonists, as well as saponin adjuvants (*e.g.* Iscomatrix or Matrix M) that act via inflammasome activation [227], [50], [228]. Falling into its own unique category, Advax-SM™, is a new particulate polysaccharide adjuvant plus CpG55.2, a TLR9 agonist. In this study, COBRA HA antigens were adjuvanted with either Advax-SM™ or a control SE adjuvant to assess potential differences in the action of these adjuvants. Advax-SM™ adjuvant appears to work via enhanced non-inflammatory recruitment of immune cells to the site of vaccination, leading to enhanced antigen presentation to influenza-specific B cells and CD4 and CD8 T cells [158], [229]. SE adjuvant works by inducing local inflammation that recruits immune cells and also helps to form an antigen depot [230], [108], [231]. Unlike some adjuvants that can be highly reactogenic, natural polysaccharides, such as delta inulin, are non-reactogenic, biodegradable and have a strong safety profile and also have good long-term, room temperature, stability [232]. Advax-SM™ adjuvant provides antigen dose-sparing and induces long-lasting T-cell and humoral immune responses, while exhibiting low local or systemic reactogenicity as compared to oil emulsion or saponin adjuvants [158].

In this study, mice vaccinated intramuscularly with the COBRA HA proteins only without adjuvant lost more than 20% body weight following influenza virus infection, exhibited severe lung inflammation, and had high mortality. These mice had high viral lung titers that were similar to adjuvant-alone vaccinated mice, which also rapidly died after infection. The same COBRA HA when formulated with Advax-SM™ or the oil-in-water adjuvant, SE adjuvant (similar to MF59), induced high serum HAI activity that translated

to complete survival with minimal weight loss, and undetectable lung virus, apart from one of three animals in the COBRA HA plus SE adjuvant group. When comparing weight loss and clinical score of mice vaccinated with COBRA HA alone to COBRA HA plus SE adjuvant or Advax-SM™, there was significant weight loss between days 3-4 post-infection and significant clinical score between days 2-6 post-infection with both adjuvanted vaccines. Mice vaccinated with COBRA HA proteins plus Advax-SM™ had ~4-fold higher HAI titers against H1N1 and most H3N2 influenza viruses when compared to mice vaccinated with COBRA HA and SE adjuvant. Notably, mice vaccinated with COBRA HA proteins plus Advax-SM™ exhibited no lung inflammation in their lungs, whereas those vaccinated with COBRA HA + SE adjuvant still exhibited significant lung inflammation similar to mice immunized with COBRA HA alone. This suggests that the two adjuvants might be working via different immune pathways. Mice vaccinated with SE adjuvant predominately generated IgG1 ASC that is indicative of a dominant T helper type 2 (Th2) $CD4^+$ T cell response and therefore resulted in a predominately IgG1 response against Bris/18 and Sing/16 rHAs, with low titers of IgG2a and IgG2b and no IgA. In contrast, mice vaccinated with COBRA HA plus Advax-SM™ had a mixed T helper response with increased IgG1 and IgG2a (IgG2a significantly higher than SE adjuvanted vaccines) ASC and higher serum IgG2a, IgG2b and IgA (IgA not significant to mice vaccinated with SE adjuvanted vaccines) antibody titers than the other study arms. The induction of T-bet and STAT-4 signaling pathways by IFN-γ activation skews immune responses towards a T helper type 1 (Th1) response, whereas STAT-6 and GATA-3 following IL-4 and IL-2 activation skews towards a Th2 responses [233], [234], [235], [236]. Hence, IFN-γ stimulates IgG isotype switching to IgG2a, a Th1 phenotype, whereas

IL-4 induces IgG1 indicative of Th2 phenotype [237], [238], [239]. While the mechanism of action of Advax-SM™ is not fully known, Advax-SM™ may function through enhanced antigen uptake by recruiting larger numbers of antigen presenting cells (APC), altered antigen processing and stimulation of different cytokine profiles than SE adjuvant oil-in-water emulsions, leading to enhanced B- and T-cell activation [158]. The induction of mixed T helper responses and a broader range of IgG isotypes and IgA by the Advax-SM™-adjuvanted COBRA HA may help explain the ability of this vaccine to reduce morbidity and mortality and, in particular, prevent lung inflammation in response to influenza virus infection compared to the SE adjuvant squalene emulsion adjuvant.

Delta inulin also activates the alternative complement pathway (ACP) resulting in the production of C3d; a degradation of the third component of complement (C3) [240]. C3d covalently couples to antigens, enhancing their immunogenicity [241]. C3d binds to the surface complement receptor 2 (CR2) of follicular dendritic cells (FDC) and B and T-cells [241]. Via FDCs, C3d stimulates antigen presentation and interacts with CR2 inducing it to co-localize with molecules such as CD19, TAPA (CD81), and Lew 13 [242]. CD19 triggers a signaling cascade that results in cell activation and proliferation that in conjunction with C3d-CR2 ligation and surface immunoglobulin (sIg) binding by the vaccine antigen, activates two signaling pathways that cross-talk and synergize to activate B cells and subsequent Ig class switching and elicitation of high titer, antigen-specific antibodies [240], [241].

Conclusions

Mice vaccinated with COBRA HA plus Advax-SM™ had increased serum IgG1, IgG2a, IgG2b, and IgG1 and IgG2a ASCs directed against H1 and H3 HA. Hence the ability of Advax-SM™ adjuvant to activate complement may contribute, at least in part, to its beneficial adjuvant effects on the COBRA HA vaccines.

Mice immunized with COBRA HA plus Advax-SM™ adjuvant had both Th1 and Th2 anti-influenza immune responses. Th1 responses and, in particular, cytotoxic CD8 T cells play a key role in clearance of IAV infection [243], [224], [245]. The ability of Advax-SM™ to induce strong Th1 responses may thereby play a key role in virus clearance. A simultaneous Th2 response induced by Advax-SM™ adjuvant may be beneficial to maximize HAI antibody levels to neutralize the virus while also helping to counteract any excessive virus-induced inflammation [246].

Overall, these findings demonstrate that Advax-SM™, as a balanced Th1 and Th2 adjuvant, was able to enhance the humoral and cellular immunogenicity and protection provided by the next-generation COBRA HA vaccines as compared to COBRA HA alone or formulated with SE adjuvant squalene emulsion adjuvant. The combination of COBRA HA with Advax-SM™ adjuvant thereby represents a promising strategy for enhancing influenza protection in immunosuppressed and high-risk human populations.

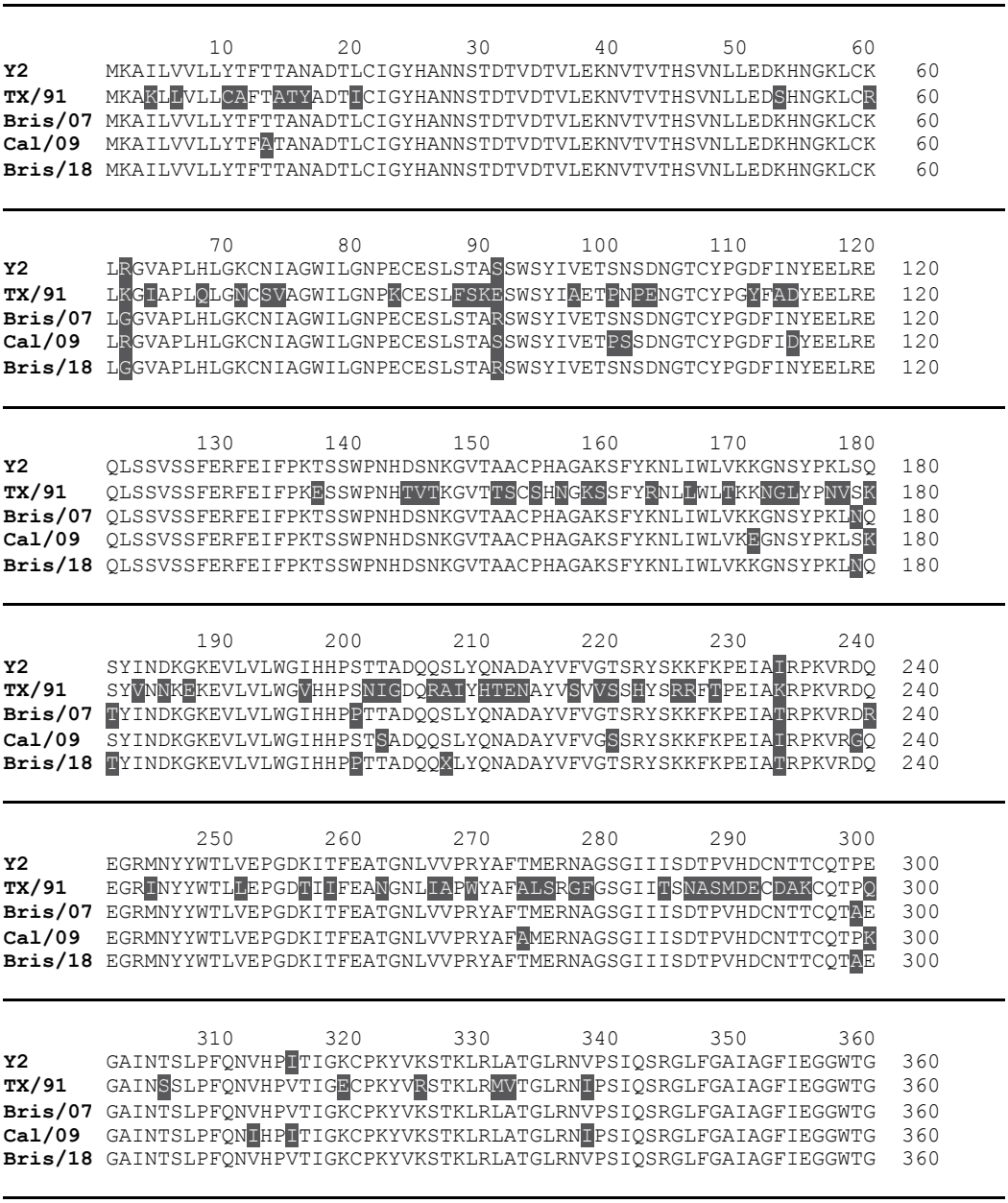
10 20 30 40 50 60
Y2 MKAILVVLLYTFTTANADTLCIGYHANNSTDTVDTVLEKNVTVTHSVNLLEDKHNGKLCK 60
TX/91 MKAKLLVLLCAFTATYADTICIGYHANNSTDTVDTVLEKNVTVTHSVNLLEDSHNGKLCR 60
Bris/07 MKAILVVLLYTFTTANADTLCIGYHANNSTDTVDTVLEKNVTVTHSVNLLEDKHNGKLCK 60
Cal/09 MKAILVVLLYTFATANADTLCIGYHANNSTDTVDTVLEKNVTVTHSVNLLEDKHNGKLCK 60
Bris/18 MKAILVVLLYTFTTANADTLCIGYHANNSTDTVDTVLEKNVTVTHSVNLLEDKHNGKLCK 60
70 80 90 100 110 120
Y2 LRGVAPLHLGKCNIAGWILGNPECESLSTASSWSYIVETSNSDNGTCYPGDFINYEELRE 120
TX/91 LKGIAPLQLGNCSVAGWILGNPKCESLFSKESWSYIAETPNPENGTCYPGYFADYEELRE 120
Bris/07 LGGVAPLHLGKCNIAGWILGNPECESLSTARSWSYIVETSNSDNGTCYPGDFINYEELRE 120
Cal/09 LRGVAPLHLGKCNIAGWILGNPECESLSTASSWSYIVETPSSDNGTCYPGDFIDYEELRE 120
Bris/18 LGGVAPLHLGKCNIAGWILGNPECESLSTARSWSYIVETSNSDNGTCYPGDFINYEELRE 120
130 140 150 160 170 180
Y2 QLSSVSSFERFEIFPKTSSWPNHDSNKGVTAACPHAGAKSFYKNLIWLVKKGNSYPKLSQ 180
TX/91 QLSSVSSFERFEIFPKESSWPNHTVTKGVTTSCSHNGKSSFYRNLLWLTKKNGLYPNVSK 180
Bris/07 QLSSVSSFERFEIFPKTSSWPNHDSNKGVTAACPHAGAKSFYKNLIWLVKKGNSYPKLNQ 180
Cal/09 QLSSVSSFERFEIFPKTSSWPNHDSNKGVTAACPHAGAKSFYKNLIWLVKEGNSYPKLSK 180
Bris/18 QLSSVSSFERFEIFPKTSSWPNHDSNKGVTAACPHAGAKSFYKNLIWLVKKGNSYPKLNQ 180
190 200 210 220 230 240
Y2 SYINDKGKEVLVLWGIHHPSTTADQQSLYQNADAYVFVGTSRYSKKFKPEIATRPKVRDQ 240
TX/91 SYVNNKEKEVLVLWGVHHPSNIGDQRAIYHTENAYVSVVSSHYSRRFTPEIAKRPKVRDQ 240
Bris/07 TYINDKGKEVLVLWGIHHPPTTADQQSLYQNADAYVFVGTSRYSKKFKPEIATRPKVRDR 240
Cal/09 SYINDKGKEVLVLWGIHHPSTSADQQSLYQNADAYVFVGSSRYSKKFKPEIAIRPKVRGQ 240
Bris/18 TYINDKGKEVLVLWGIHHPPTTADQQXLYQNADAYVFVGTSRYSKKFKPEIATRPKVRDQ 240
250 260 270 280 290 300
Y2 EGRMNYYWTLVEPGDKITFEATGNLVVPRYAFTMERNAGSGIIISDTPVHDCNTTCQTPE 300
TX/91 EGRINYYWTLLEPGDIIIFEANGNLIAPWYAFALSRGFGSGIITSNASMDECDAKCQTPQ 300
Bris/07 EGRMNYYWTLVEPGDKITFEATGNLVVPRYAFTMERNAGSGIIISDTPVHDCNTTCQTAE 300
Cal/09 EGRMNYYWTLVEPGDKITFEATGNLVVPRYAFAMERNAGSGIIISDTPVHDCNTTCQTPK 300
Bris/18 EGRMNYYWTLVEPGDKITFEATGNLVVPRYAFTMERNAGSGIIISDTPVHDCNTTCQTAE 300
310 320 330 340 350 360
Y2 GAINTSLPFQNVHPITIGKCPKYVKSTKLRLATGLRNVPSIQSRGLFGAIAGFIEGGWTG 360
TX/91 GAINSSLPFQNVHPVTIGECPKYVRSTKLRMVTGLRNIPSIQSRGLFGAIAGFIEGGWTG 360
Bris/07 GAINTSLPFQNVHPVTIGKCPKYVKSTKLRLATGLRNVPSIQSRGLFGAIAGFIEGGWTG 360
Cal/09 GAINTSLPFQNIHPITIGKCPKYVKSTKLRLATGLRNIPSIQSRGLFGAIAGFIEGGWTG 360
Bris/18 GAINTSLPFQNVHPVTIGKCPKYVKSTKLRLATGLRNVPSIQSRGLFGAIAGFIEGGWTG 360

```
                370       380       390       400       410       420
Y2       MVDGWYGYHHQNEQGSGYAADLKSTQNAIDKITNKVNSVIEKMNTQFTAVGKEFNHLEKR  420
TX/91    MIDGWYGYHHQNEQGSGYAADQKSTQNAINGITNKVNSVIEKMNTQFTAVGKEFNKLERR  420
Bris/07  MVDGWYGYHHQNEQGSGYAADLKSTQNAIDKITNKVNSVIEKMNTQFTAVGKEFNHLEKR  420
Cal/09   MVDGWYGYHHQNEQGSGYAADLKSTQNAIDEITNKVNSVIEKMNTQFTAVGKEFNHLEKR  420
Bris/18  MVDGWYGYHHQNEQGSGYAADLKSTQNAIDKITNKVNSVIEKMNTQFTAVGKEFNHLEKR  420

                430       440       450       460       470       480
Y2       IENLNKKVDDGFLDIWTYNAELLVLLENERTLDYHDSNVKNLYEKVRNQLKNNAKEIGNG  480
TX/91    MENLNKKVDDGFLDIWTYNAELLVLLENGRTLDFHDSNVKNLYEKVKSQLKNNAKEIGNG  480
Bris/07  IENLNKKVDDGFLDIWTYNAELLVLLENERTLDYHDSNVKNLYEKVRNQLKNNAKEIGNG  480
Cal/09   IENLNKKVDDGFLDIWTYNAELLVLLENERTLDYHDSNVKNLYEKVRSQLKNNAKEIGNG  480
Bris/18  IENLNKKVDDGFLDIWTYNAELLVLLENERTLDYHDSNVKNLYEKVRNQLKNNAKEIGNG  480

                490       500       510       520       530       540
Y2       CFEFYHKCDNTCMESVKNGTYDYPKYSEEAKLNREKIDGVKLESTRIYQILAIYSTVASS  540
TX/91    CFEFYHKCNNECMESVKNGTYDYPKYSEESKLNRGKIDGVKLESMGVYQILAIYSTVASS  540
Bris/07  CFEFYHKCDNTCMESVKNGTYDYPKYSEEAKLNREKIDGVKLESTRIYQILAIYSTVASS  540
Cal/09   CFEFYHKCDNTCMESVKNGTYDYPKYSEEAKLNREEIDGVKLESTRIYQILAIYSTVASS  540
Bris/18  CFEFYHKCDNTCMESVKNGTYDYPKYSEEAKLNREKIDGVKLESTRIYQILAIYSTVASS  540

                550       560
Y2       LVLVVSLGAISFWMCSNGSLQCRICI                                    566
TX/91    LVLLVSLGAISFWMCSNGSLQCRICI                                    566
Bris/07  LVLVVSLGAISFWMCSNGSLQCRICI                                    566
Cal/09   LVLVVSLGAISFWMCSNGSLQCRICI                                    566
Bris/18  LVLVVSLGAISFWMCSNGSLQCRICI                                    566
```

Table 3. 1 Multiple alignment for all full-length H1N1 HA sequences included in this study. The full length Y2 COBRA HA amino acid sequence with enumeration listed above. Four wild-type H1 HA sequences are listed viruses isolated in 1991, 2007, 2009, and 2018. Any amino acid position that has a different residue at the position than the Y2 HA sequence is highlighted in grey.

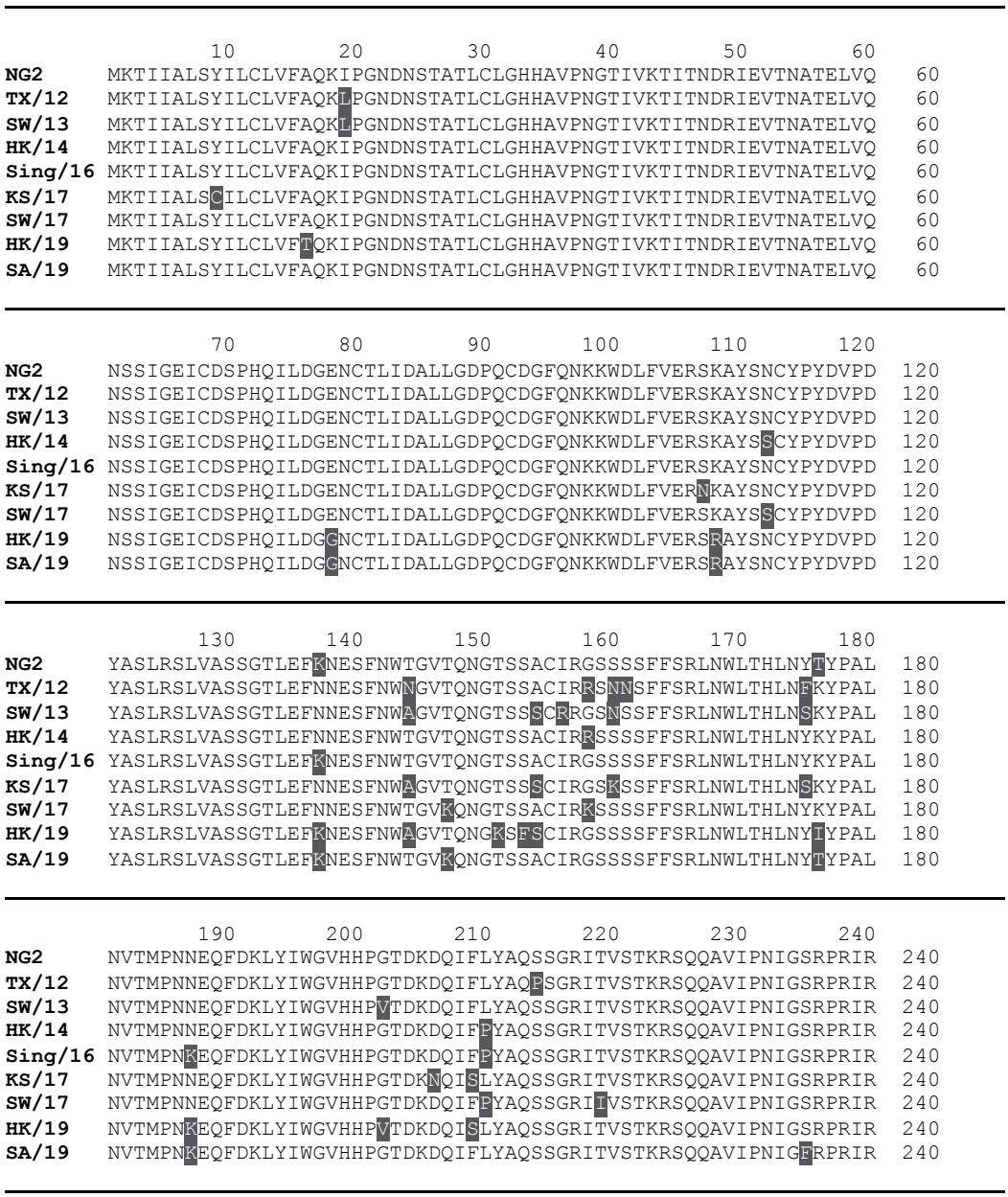
10 20 30 40 50 60
NG2 MKTIIALSYILCLVFAQKIPGNDNSTATLCLGHHAVPNGTIVKTITNDRIEVTNATELVQ 60
TX/12 MKTIIALSYILCLVFAQKLPGNDNSTATLCLGHHAVPNGTIVKTITNDRIEVTNATELVQ 60
SW/13 MKTIIALSYILCLVFAQKLPGNDNSTATLCLGHHAVPNGTIVKTITNDRIEVTNATELVQ 60
HK/14 MKTIIALSYILCLVFAQKIPGNDNSTATLCLGHHAVPNGTIVKTITNDRIEVTNATELVQ 60
Sing/16 MKTIIALSYILCLVFAQKIPGNDNSTATLCLGHHAVPNGTIVKTITNDRIEVTNATELVQ 60
KS/17 MKTIIALSCILCLVFAQKIPGNDNSTATLCLGHHAVPNGTIVKTITNDRIEVTNATELVQ 60
SW/17 MKTIIALSYILCLVFAQKIPGNDNSTATLCLGHHAVPNGTIVKTITNDRIEVTNATELVQ 60
HK/19 MKTIIALSYILCLVFTQKIPGNDNSTATLCLGHHAVPNGTIVKTITNDRIEVTNATELVQ 60
SA/19 MKTIIALSYILCLVFAQKIPGNDNSTATLCLGHHAVPNGTIVKTITNDRIEVTNATELVQ 60
70 80 90 100 110 120
NG2 NSSIGEICDSPHQILDGENCTLIDALLGDPQCDGFQNKKWDLFVERSKAYSNCYPYDVPD 120
TX/12 NSSIGEICDSPHQILDGENCTLIDALLGDPQCDGFQNKKWDLFVERSKAYSNCYPYDVPD 120
SW/13 NSSIGEICDSPHQILDGENCTLIDALLGDPQCDGFQNKKWDLFVERSKAYSNCYPYDVPD 120
HK/14 NSSIGEICDSPHQILDGENCTLIDALLGDPQCDGFQNKKWDLFVERSKAYSSCYPYDVPD 120
Sing/16 NSSIGEICDSPHQILDGENCTLIDALLGDPQCDGFQNKKWDLFVERSKAYSNCYPYDVPD 120
KS/17 NSSIGEICDSPHQILDGENCTLIDALLGDPQCDGFQNKKWDLFVERNKAYSNCYPYDVPD 120
SW/17 NSSIGEICDSPHQILDGENCTLIDALLGDPQCDGFQNKKWDLFVERSKAYSSCYPYDVPD 120
HK/19 NSSIGEICDSPHQILDGGNCTLIDALLGDPQCDGFQNKKWDLFVERSRAYSNCYPYDVPD 120
SA/19 NSSIGEICDSPHQILDGGNCTLIDALLGDPQCDGFQNKKWDLFVERSRAYSNCYPYDVPD 120
130 140 150 160 170 180
NG2 YASLRSLVASSGTLEFKNESFNWTGVTQNGTSSACIRGSSSSFFSRLNWLTHLNYTYPAL 180
TX/12 YASLRSLVASSGTLEFNNESFNWNGVTQNGTSSACIRRSNNSFFSRLNWLTHLNFKYPAL 180
SW/13 YASLRSLVASSGTLEFNNESFNWAGVTQNGTSSSCRRGSNSSFFSRLNWLTHLNSKYPAL 180
HK/14 YASLRSLVASSGTLEFNNESFNWTGVTQNGTSSACIRRSSSSFFSRLNWLTHLNYKYPAL 180
Sing/16 YASLRSLVASSGTLEFKNESFNWTGVTQNGTSSACIRGSSSSFFSRLNWLTHLNYKYPAL 180
KS/17 YASLRSLVASSGTLEFNNESFNWAGVTQNGTSSSCIRGSKSSFFSRLNWLTHLNSKYPAL 180
SW/17 YASLRSLVASSGTLEFNNESFNWTGVKQNGTSSACIRKSSSSFFSRLNWLTHLNYKYPAL 180
HK/19 YASLRSLVASSGTLEFKNESFNWAGVTQNGKSFSCIRGSSSSFFSRLNWLTHLNYIYPAL 180
SA/19 YASLRSLVASSGTLEFKNESFNWTGVKQNGTSSACIRGSSSSFFSRLNWLTHLNYTYPAL 180
190 200 210 220 230 240
NG2 NVTMPNNEQFDKLYIWGVHHPGTDKDQIFLYAQSSGRITVSTKRSQQAVIPNIGSRPRIR 240
TX/12 NVTMPNNEQFDKLYIWGVHHPGTDKDQIFLYAQPSGRITVSTKRSQQAVIPNIGSRPRIR 240
SW/13 NVTMPNNEQFDKLYIWGVHHPVTDKDQIFLYAQSSGRITVSTKRSQQAVIPNIGSRPRIR 240
HK/14 NVTMPNNEQFDKLYIWGVHHPGTDKDQIFPYAQSSGRITVSTKRSQQAVIPNIGSRPRIR 240
Sing/16 NVTMPNKEQFDKLYIWGVHHPGTDKDQIFPYAQSSGRITVSTKRSQQAVIPNIGSRPRIR 240
KS/17 NVTMPNNEQFDKLYIWGVHHPGTDKNQISLYAQSSGRITVSTKRSQQAVIPNIGSRPRIR 240
SW/17 NVTMPNNEQFDKLYIWGVHHPGTDKDQIFPYAQSSGRITVSTKRSQQAVIPNIGSRPRIR 240
HK/19 NVTMPNKEQFDKLYIWGVHHPVTDKDQISLYAQSSGRITVSTKRSQQAVIPNIGSRPRIR 240
SA/19 NVTMPNKEQFDKLYIWGVHHPGTDKDQIFLYAQSSGRITVSTKRSQQAVIPNIGFRPRIR 240

```
                250       260       270       280       290       300
NG2       DIPSRISIYWTIVKPGDILLINSTGNLIAPRGYFKIRSGKSSIMRSDAPIGKCKSECITP  300
TX/12     NIPSRISIYWTIVKPGDILLINSTGNLIAPRGYFKIRSGKSSIMRSDAPIGKCKSECITP  300
SW/13     DIPSRISIYWTIVKPGDILLINSTGNLIAPRGYFKIRSGKSSIMRSDAPIGKCKSECITP  300
HK/14     DIPSRISIYWTIVKPGDILLINSTGNLIAPRGYFKIRSGKSSIMRSDAPIGKCKSECITP  300
Sing/16   GIPSRISIYWTIVKPGDILLINSTGNLIAPRGYFKIRSGKSSIMRSDAPIGKCKSECITP  300
KS/17     DIPSRISIYWTIVKPGDILLIXSTGNLIAPRGYFKIRSGKSSIMRSDAPIGKCKSECITP  300
SW/17     DIPSRISIYWTIVKPGDILLINSTGNLIAPRGYFKIQSGKSSIMRSDAPIGKCKSECITP  300
HK/19     NIPSRISIYWTIVKPGDILLINSTGNLIAPRGYFKIRSGKSSIMRSDAPIGKCKSECITP  300
SA/19     DIPSRISIYWTIVKPGDILLINSTGNLIAPRGYFKIRSGKSSIMRSDAPIGKCKSECITP  300

                310       320       330       340       350       360
NG2       NGSIPNDKPFQNVNRITYGACPRYVKQSTLKLATGMRNVPEKQTRGIFGAIAGFIENGWE  360
TX/12     NGSIPNDKPFQNVNRITYGACPRYVKQSTLKLATGMRNVPEKQTRGIFGAIAGFIENGWE  360
SW/13     NGSIPNDKPFQNVNRITYGACPRYVKQSTLKLATGMRNVPERQTRGIFGAIAGFIENGWE  360
HK/14     NGSIPNDKPFQNVNRITYGACPRYVKHSTLKLATGMRNVPEKQTRGIFGAIAGFIENGWE  360
Sing/16   NGSIPNDKPFQNVNRITYGACPRYVKHSTLKLATGMRNVPEKQTRGIFGAIAGFIENGWE  360
KS/17     NGSIPNDKPFQNVNRITYGACPRYVKQSTLKLATGMRNVPERQTRGIFGAIAGFIENGWE  360
SW/17     NGSIPNDKPFQNVNRITYGACPRYVKHSTLKLATGMRNVPEKQTRGIFGAIAGFIENGWE  360
HK/19     NGSIPNDKPFQNVNRITYGACPRYVKQSTLKLATGMRNVPEKQTRGIFGAIAGFIENGWE  360
SA/19     NGSIPNDKPFQNVNRITYGACPRYVKQSTLKLATGMRNVPEKQTRGIFGAIAGFIENGWE  360

                370       380       390       400       410       420
NG2       GMVDGWYGFRHQNSEGRGQAADLKSTQAAIDQINGKLNRLIGKTNEKFHQIEKEFSEVEG  420
TX/12     GMVDGWYGFRHQNSEGRGQAADLKSTQAAIDQINGKLNRLIGKTNEKFHQIEKEFSEVEG  420
SW/13     GMVDGWYGFRHQNSEGRGQAADLKSTQAAIDQINGKLNRLIGKTNEKFHQIEKEFSEVEG  420
HK/14     GMVDGWYGFRHQNSEGRGQAADLKSTQAAIDQINGKLNRLIGKTNEKFHQIEKEFSEVEG  420
Sing/16   GMVDGWYGFRHQNSEGRGQAADLKSTQAAIDQINGKLNRLIGKTNEKFHQIEKEFSEVEG  420
KS/17     GMVDGWYGFRHQNSEGRGQAADLKSTQAAIDQINGKLNRLIGKTNEKFHQIEKEFSEVEG  420
SW/17     GMVDGWYGFRHQNSEGRGQAADLKSTQAAIDQINGKLNRLIGKTNEKFHQIEKEFSEVEG  420
HK/19     GMVDGWYGFRHQNSEGRGQAADLKSTQAAIDQINGKLNRLIGKTNEKFHQIEKEFSEVEG  420
SA/19     GMMDGWYGFRHQNSEGRGQAADLKSTQAAIDQINGKLNRLIGKTNEKFHQIEKEFSEVEG  420

                430       440       450       460       470       480
NG2       RIQDLEKYVEDTKIDLWSYNAELLVALENQHTIDLTDSEMNKLFEKTKKQLRENAEDMGN  480
TX/12     RIQDLEKYVEDTKIDLWSYNAELLVALENQHTIDLTDSEMNKLFEKTKKQLRENAEDMGN  480
SW/13     RIQDLEKYVEDTKIDLWSYNAELLVALENQHTIDLTDSEMNKLFEKTKKQLRENAEDMGN  480
HK/14     RIQDLEKYVEDTKIDLWSYNAELLVALENQHTIDLTDSEMNKLFEKTKKQLRENAEDMGN  480
Sing/16   RVQDLEKYVEDTKIDLWSYNAELLVALENQHTIDLTDSEMNKLFEKTKKQLRENAEDMGN  480
KS/17     RIQDLEKYVEDTKIDLWSYNAELLVALENQHTIDLTDSEMNKLFEKTKKQLRENAEDMGN  480
SW/17     RIQDLEKYVEDTKIDLWSYNAELLVALENQHTIDLTDSEMNKLFEKTKKQLRENAEDMGN  480
HK/19     RVQDLEKYVEDTKIDLWSYNAELLVALENQHTIDLTDSEMNKLFEKTKKQLRENAEDMGN  480
SA/19     RVQDLEKYVEDTKIDLWSYNAELLVALENQHTIDLTDSEMNKLFEKTKKQLRENAEDMGN  480
```

```
                490       500       510       520       530       540
NG2      GCFKIYHKCDNACIGSIRNGTYDHNVYRDEALNNRFQIKGVELKSGYKDWILWISFAISC  540
TX/12    GCFKIYHKCDNACIGSIRNGTYDHDVYRDEALNNRFQIKGVELKSGYKDWILWISFAISC  540
SW/13    GCFKIYHKCDNACIGSIRNGTYDHDVYRDEALNNRFQIKGVELKSGYKDWILWISFAISC  540
HK/14    GCFKIYHKCDNACIGSIRNGTYDHNVYRDEALNNRFQIKGVELKSGYKDWILWISFAISC  540
Sing/16  GCFKIYHKCDNACIESIRNETYDHNVYRDEALNNRFQIKGVELKSGYKDWILWISFAISC  540
KS/17    GCFKIYHKCDNACMGSIRNGTYDHNVYRDEALNNRFQIKGVELKSGYKDWILWISFAISC  540
SW/17    GCFKIYHKCDNACIGSIRNGTYDHNVYRDEALNNRFQIKGVELKSGYKDWILWISFAISC  540
HK/19    GCFKIYHKCDNACIGSIRNETYDHNVYRDEALNNRFQIKGVELKSGYKDWILWISFAISC  540
SA/19    GCFKIYHKCDNACIGSIRNETYDHNVYRDEALNNRFQIKGVELKSGYKDWILWISFAISC  540

                550       560
NG2      FLLCVALLGFIMWACQKGNIRCNICI                                    566
TX/12    FLLCVALLGFIMWACQKGNIRCNICI                                    566
SW/13    FLLCVALLGFIMWACQKGNIRCNICI                                    566
HK/14    FLLCVALLGFIMWACQKGNIRCNICI                                    566
Sing/16  FLLCVALLGFIMWACQKGNIRCNICI                                    566
KS/17    FLLCVALLGFIMWACQKGNIRCNICI                                    566
SW/17    FLLCVALLGFIMWACQKGNIRCNICI                                    566
HK/19    FLLCVALLGFIMWACQKGNIRCNICI                                    566
SA/19    FLLCIALLGFIMWACQKGNIRCNICI                                    566
```

Table 3. 2 Multiple alignment for all full-length H_3N_2 HA sequences included in this study. The full length NG2 COBRA HA amino acid sequence with enumeration listed above. Eight wild-type H3 HA sequences are listed viruses isolated in 2012, 2013, 2014, 2016, 2017, and 2019. Any amino acid position that has a different residue at the position than the NG2 HA sequence is highlighted in grey.

a.

Groups	COBRA Vaccine	Dose	Adjuvant	Challenge
1	Y2/NG2	6µg	None (Saline)	Brisbane/02/2018 H1N1
2	Y2/NG2	6µg	AddaVax (1:1)	
3	Y2/NG2	6µg	Advax-SM™ (1mg)	
4	Mock	0µg	Advax-SM™ (1mg)	

b.

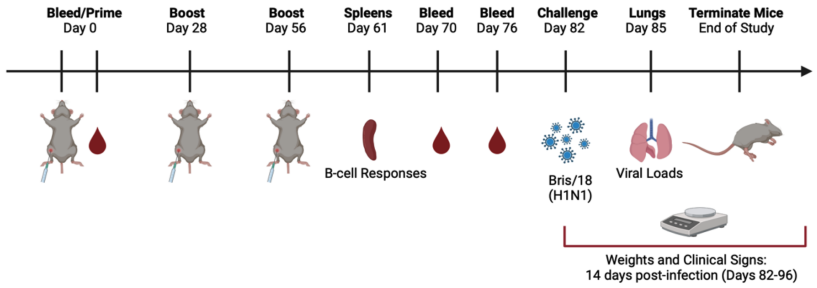

Figure 3. 1 Vaccine regimens and schematic of the study timeline.

(a) Mice were randomly divided into four groups, with n=18 mice in each group, and immunized intramuscularly (IM) with 3 µg of each COBRA HA proteins, Y2 and NG2 (total 6 µg), alone or formulated with AddaVax SE adjuvant at a 1:1 ratio or 1mg Advax-SM™. As controls, a group of mice were immunized with 1mg Advax-SM™ adjuvant only without antigen. (b) Schematic of study timeline. Mice were bled and prime-vaccinated on day 0 and boosted on days 28 and 56. On day 61, three mice from each group were sacrificed and spleens harvested for B cell FluoroSpot assays. Bleeds on remaining mice were performed on days 70 and 76, and an intranasal virus challenge was performed on day 82. Three days post-infection (day 85), lungs were harvested from three mice per group for lung viral titers and pathology, and the remaining mice were monitored for clinical illness and mortality for 14 days post infection.

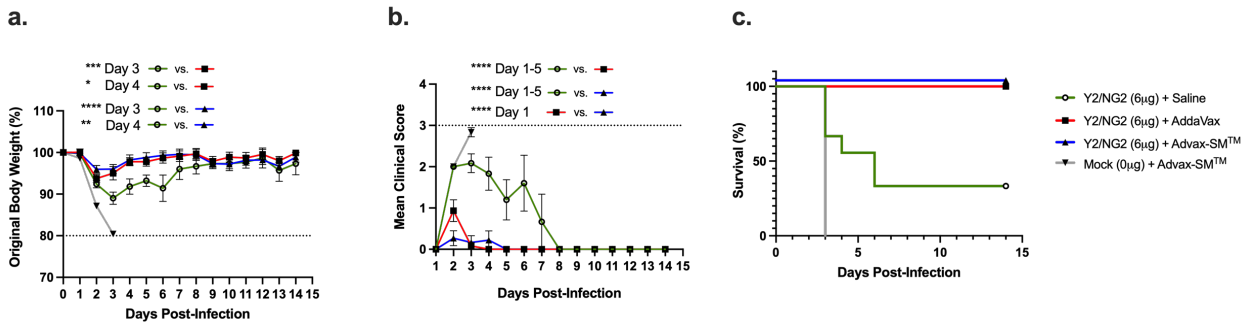

Figure 3. 2 Post-challenge weight loss, clinical signs, and survival of vaccinated mice. Mice were all challenged intranasally (IN) with the H1N1 strain, A/Brisbane/02/2018 ($8X10^6$ PFU/50μL) and observed for 14 days post-infection. (a) Percent of original body weight loss, (b) clinical scores, and (c) percent survival. The dotted line in (a) represents the 20% weight loss endpoint cutoff. The dotted line in (b) represents a mean clinical score of 3. Each line (a and b) is conveyed as the average +/- standard error of the mean (SEM).

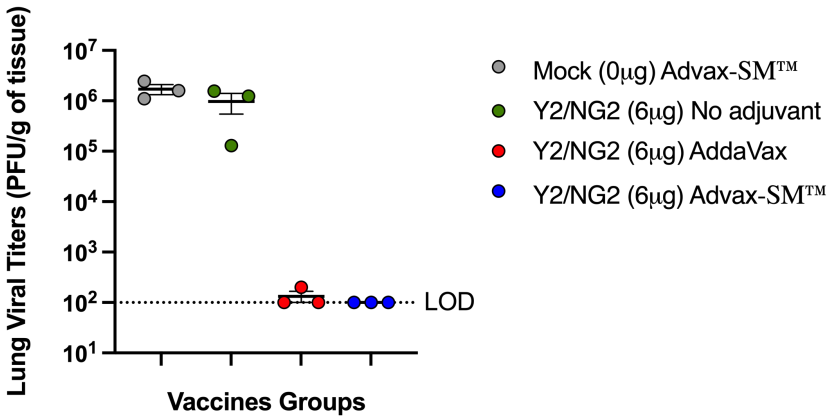

Figure 3. 3 Post-challenge viral lung titers in vaccinated mice.

Lung viral titers of mice 3 days following challenge with A/Brisbane/02/2018. The Y-axis represents the day 3 post-challenge lung viral titers (PFU/g of tissue) and the X-axis represents the vaccine groups. Advax-SM™ alone control (Grey symbols), COBRA HA alone (Green symbols), COBRA HA plus Advax-SM™ (Blue symbols), COBRA HA plus SE adjuvant (Red symbols). The dotted line represents the limit of detection (LOD).

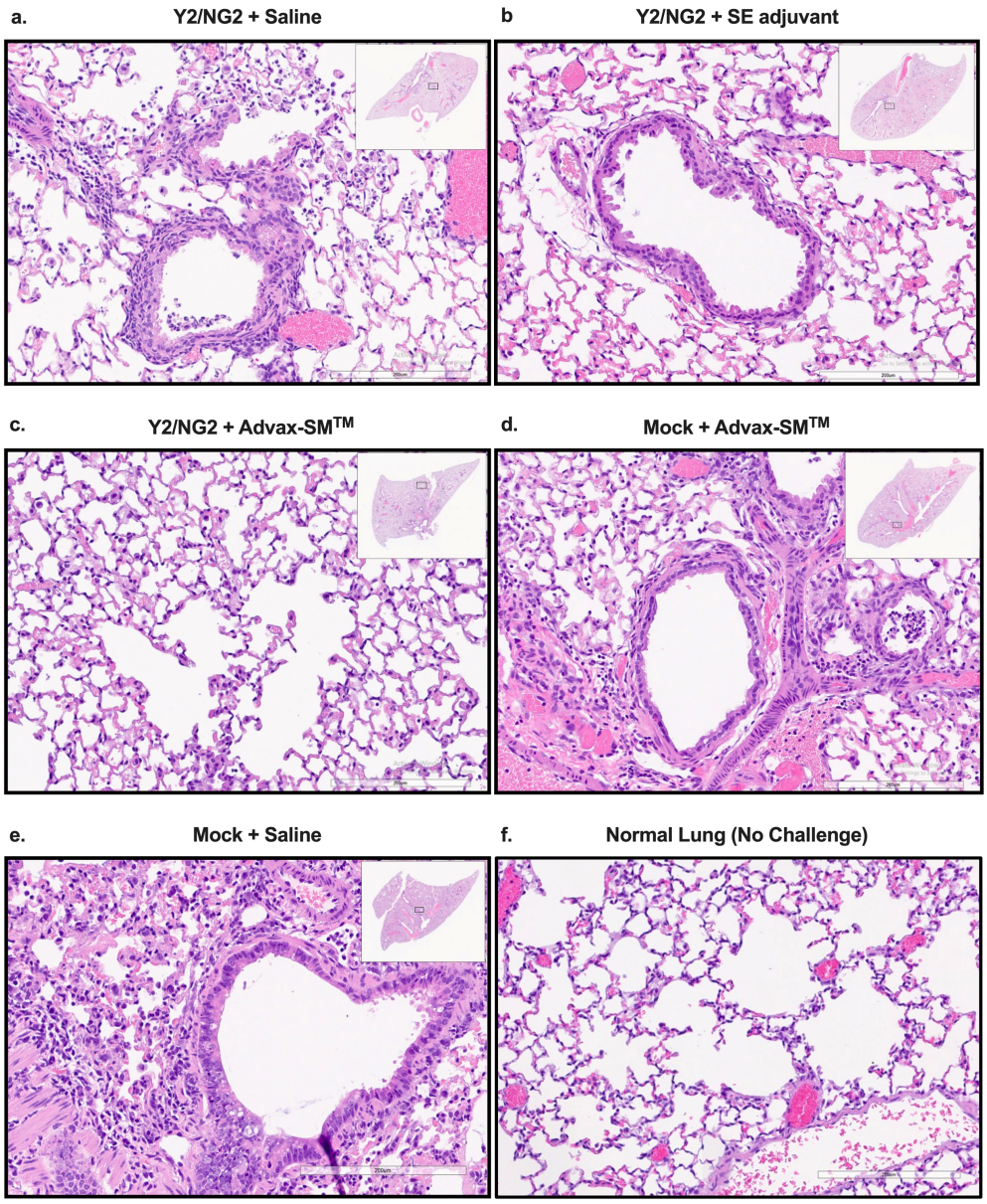

Figure 3. 4 Post-challenge lung pathology of vaccinated mice.

Histopathology of mice lung tissue harvested at 3 days post-infection with H1N1 Brisbane/02/18 influenza virus. The mice were humanely euthanized and their left lungs were infused with 10% formalin for fixing the tissue. Hematoxylin and Eosin (H&E) staining on lung slices measuring 5 µm was used to visualize pathology in the lungs. The lungs are represented at 20x magnification - the lower bar represents 200 um scale.

COBRA HA plus (a) saline, (b) SE adjuvant, or (c) Advax-SM™. Saline plus (d) Advax-SM™, Mock plus (e) saline, or (f) uninfected.

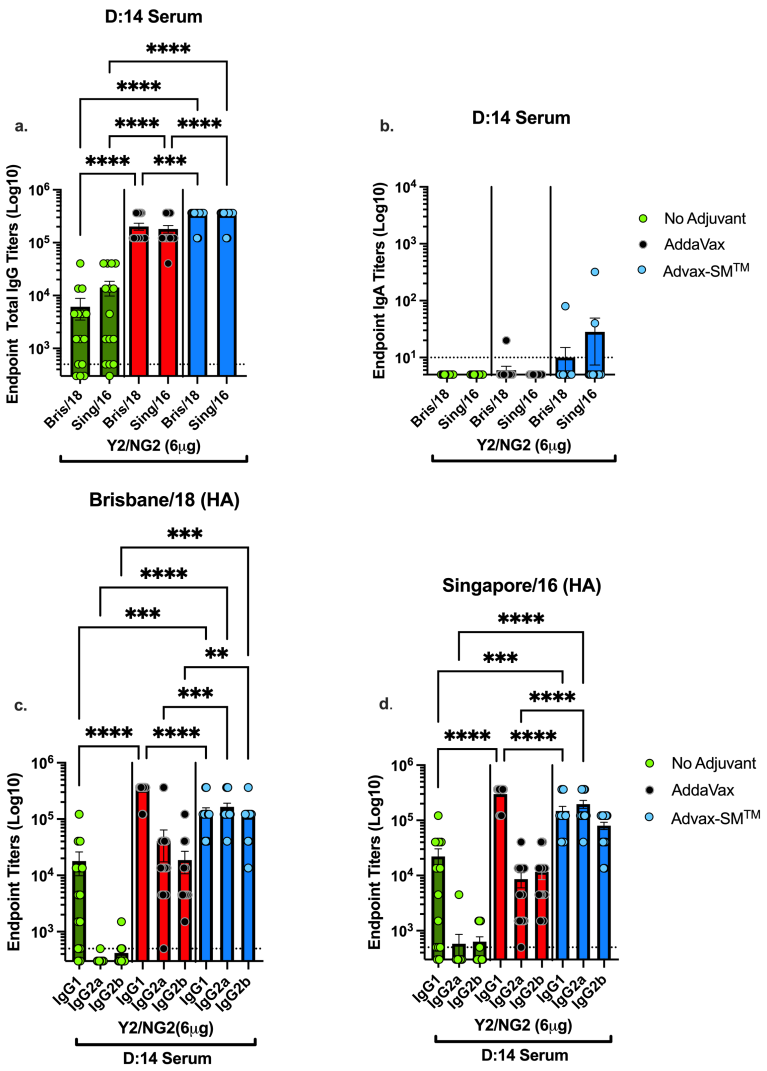

Figure 3. 5 Serum anti-influenza total IgG, IgA and IgG1, IgG2a, and IgG2b in vaccinated mice.

(a) serum anti-influenza total IgG against Bris/02/18 and Sing/16 rHA, (b) serum IgA against WT Bris/18 and Sing/16 rHA, (c) serum IgG isotype titers against WT Bris/18, and (d) serum IgG isotype titers against Sing/16 rHA. Represented on the Y-axis are the endpoint titers. Represented on the X-axis are the WT rHAs (a and b) or the Ig isotypes (c and d). Each bar corresponds to 15 individual mice according to vaccine regimens and are conveyed as the average +/- standard error of the mean (SEM).

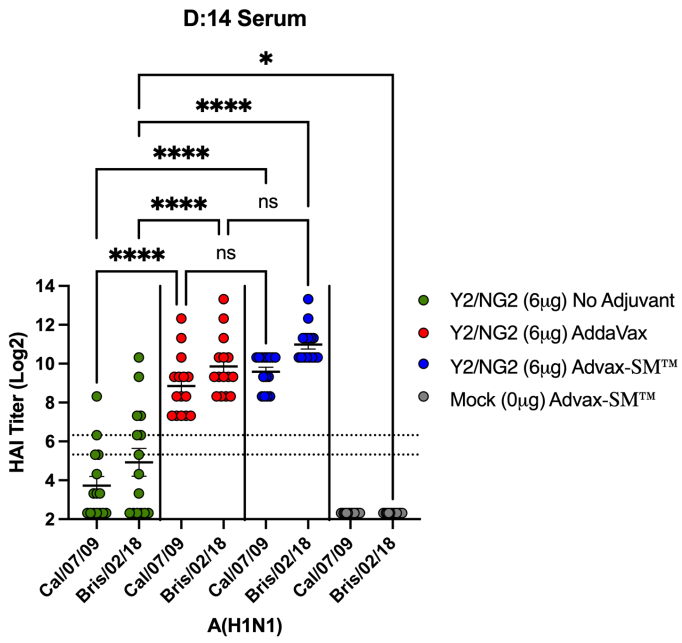

Figure 3. 6 Hemagglutination inhibition activity in mice vaccinated with COBRA HA vaccines (Y2 and NG2).

Sera collected from immunized mice at days 70 and 76 was pooled (3 weeks post the third vaccine dose) and tested for HAI activity against two H1N1 viruses, Cal/09 and Bris/18. COBRA HA alone (Green symbols), COBRA HA + SE adjuvant (1:1) (Red symbols), COBRA HA + Advax-SM™ (Blue symbols), or Mock + Advax-SM™ (Grey symbols). Represented on the Y-axis are the HAI titers on a log 2 scale. Represented on the X-axis is the panel of H1N1 influenza viruses. The top dotted line indicates a 1:80 HAI titer and the bottom dotted line indicates a 1:40 HAI titer. Each column represents 15 individual mice pertaining to each vaccine regimen and are conveyed as the average +/- standard error of the mean (SEM).

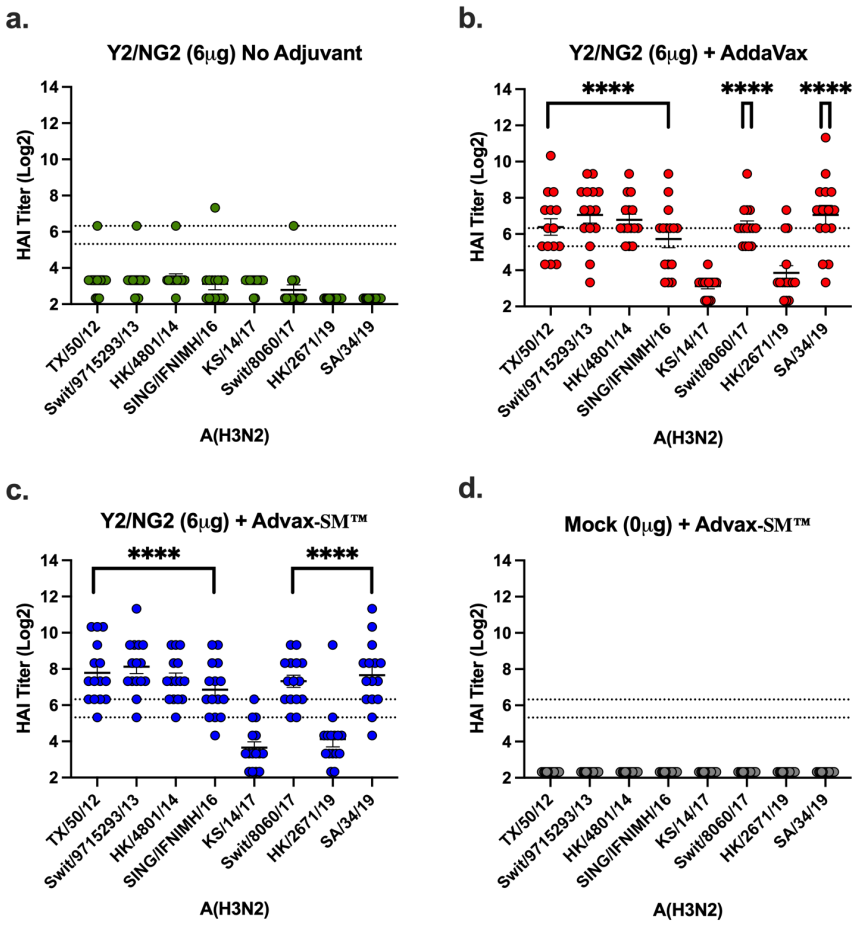

Figure 3. 7 Hemagglutinin-inhibition responses in mice immunized with COBRA HA antigens (Y2 and NG2).

(a-c) Sera collected from immunized mice at days 70 and 76 was pooled (3 weeks post the third vaccination) and tested against two H3N2 influenza viruses. (a) Advax-SM™ alone controls, (b) COBRA HA + SE adjuvant (1:1), (7c) COBRA HA + Advax-SM™, or (7d) Mock + Advax-SM™. Represented on the Y-axis are the HAI titers on a log 2 scale. Represented on the X-axis is the panel of H3N2 influenza viruses. The top dotted line indicates a 1:80 HAI titer and the bottom dotted line indicates a 1:40 HAI titer. Statistical differences shown are of group (a) compared to group (b) or (c). Each column represents 15 individual mice pertaining to each vaccine regimen and are conveyed as the average +/- standard error of the mean (SEM).

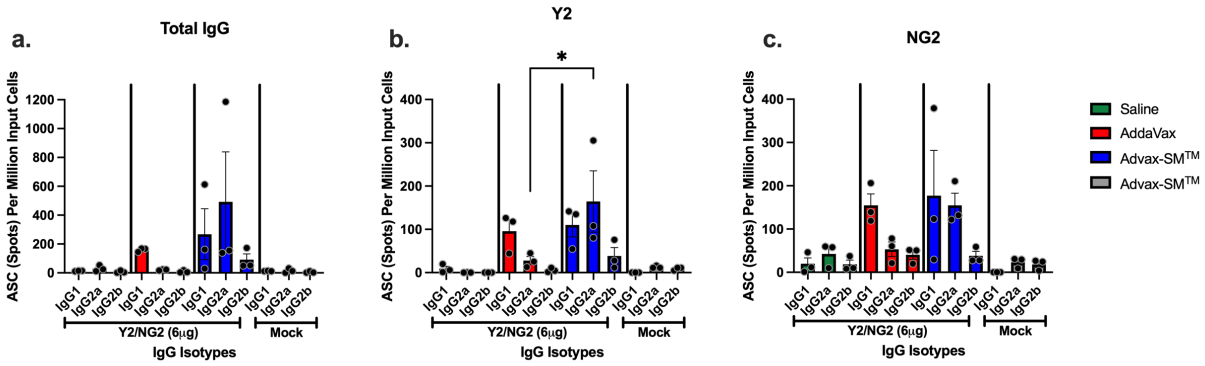

Figure 3. 8 Quantification of total IgG and antigen-specific IgG1, IgG2a, and IgG2b isotypes from antibody secreting cells (ASCs).

Spleens from DBA/2J female mice (6-8 weeks old) were harvested 5 days following the 3rd vaccination with COBRA HA+ SE adjuvant (Red), COBRA HA+ Advax-SM™ (Blue), Mock + Advax-SM™ (Grey), or COBRA HA alone (Green). Plates coated with anti-Igκ/λ (a), Y2 (b), or NG2 (c) were used to detect IgG1, IgG2a, or IgG2b ASCs. The Y-axis represents the number of ASCs (spots) per million input cells. The Ig isotypes from immunized mice are represented on the X-axis. Represented is an n=3 of mice per the indicated vaccine regimens and expressed as the average +/- standard error of the mean (SEM).

CHAPTER 4

MASTOPARAN-7 ADJUVANTED H1 AND H3 HEMAGGLUTININ INFLUENZA VACCINES[1]

[1] Sanchez, P.L., Staats, H.F., Abraham, S.N. *et al.* Mastoparan-7 adjuvanted COBRA H1 and H3 hemagglutinin influenza vaccines. *Sci Rep* **14**, 13800 (2024). This is an accepted manuscript of an article published in Scientific Reports on June, 14, 2024, available online: doi.org/10.1038/s41598-024-64351-7. Reprinted here with permission of publisher.

Abstract

Adjuvants enhance, prolong, and modulate immune responses by vaccine antigens to maximize protective immunity and enable more effective immunization in the young and elderly. Most adjuvants are formulated with injectable vaccines. However, an intranasal route of vaccination may induce mucosal and systemic immune responses for enhancing protective immunity in individuals and be easier to administer compared to injectable vaccines. In this study, a next generation of broadly-reactive influenza hemagglutinin (HA) vaccines were developed using the Computationally Optimized Broadly Reactive Antigen (COBRA) methodology. These HA vaccines were formulated with Mastoparan 7 (M7-NH2) mast cell degranulating peptide adjuvant and administered intranasally to determine vaccine-induced seroconversion of antibodies against a panel of influenza viruses and protection following infection with H1N1 and H3N2 viruses in mice. Mice vaccinated intranasally with M7-NH2-adjuvanted COBRA HA vaccines had high HAIs against a panel of H1N1 and H3N2 influenza viruses and were protected against both morbidity and mortality, with reduced viral lung titers, following challenge with an H1N1 influenza virus. Additionally, M7-NH2 adjuvanted COBRA HA vaccines induced Th2 skewed immune responses with robust IgG and isotype antibodies in the serum and mucosal lung lavages. Overall, this intranasally delivered M7-NH2 -adjuvanted COBRA HA vaccine provides effective protection against drifted H1N1 and H3N2 viruses.

Introduction

Influenza viruses belong to the family *Orthomyxoviridae* and are the cause of annual respiratory infections. Seasonal influenza virus infections can cause severe respiratory disease resulting in hospitalization and death [191]. Antigenic drift and shift allow influenza viruses to escape the host immune defenses by changing the viral surface glycoproteins hemagglutinin (HA) and neuraminidase (NA) [6]. This is important since developing an effective vaccine against ever-changing influenza A viruses (IAVs) becomes difficult since the selected wild-type (WT) strains included in each seasonal influenza vaccine are not always well matched to circulating strains in a given season, thus compromising the effectiveness of the vaccine [10]. Current commercial vaccines often use live-attenuated virus or split-inactivated virus vaccine platforms that induce high titer immune responses [197]. A few of the currently licensed vaccines have been formulated with adjuvants, such as the oil-in-water emulsion MF59 [201]. The addition of adjuvants may enhance vaccine induced immune responses in higher risk groups, such as infants with undeveloped immune systems or the elderly with impaired immune responses [125], [221].

Adjuvants serve as pharmacological or biological molecules that enhance the elicitation of specific immune responses upon co-administration with vaccine compounds [199]. To date, most influenza vaccines are administered by parenteral injections [247]. However, an intranasal route of vaccination may induce mucosal and systemic immune responses in order to enhance protective immunity in individuals with weak immune systems [248]. Intranasal vaccines are painless and easier to administer compared to the invasive methods used with injectable vaccines, thus likely improving vaccine uptake worldwide [248]. In this study, Mastoparan 7 (M7-NH_2) peptides were used as adjuvant

with hemagglutinin proteins and compared to hemagglutinin proteins with no adjuvant. The M7-NH_2 is a 14 amino acid long cationic peptide sequence (INLKALAALAKKIL-NH) derived from wasp (*Vespula lewisii*) venom and has been previously used in mucosal vaccines for enhancing immunity against systemic anaphylaxis caused by peanut allergic responses as well as vaccines that were effective against cocaine challenge, in mice [168], [174], [175]. Additionally, M7-NH_2 enhances the efficacy of a west Nile virus subunit vaccine, administered intranasally in mice [176]. M7-NH_2 activates mast cells via its Mas-related G-protein coupled receptor member X2 (MRGPRX2) [168], [169].Upon activation of mast cells by M7-NH_2, there is a release of preformed mediators, such as histamine, proteases, tumor necrosis factor (TNF-α), IL-4 and IL-5 that are degranulated at mucosal surfaces or tissues and may have different functions depending on their location [172]. Additionally, mast cells are activated by cross-linking IgE receptors or IgG Fc gamma IIIA receptors, vital for activating mast cells, and important innate components for mediating the maturation and trafficking of dendritic cells (DCs) to draining lymph nodes [249]. These dendritic cells will activate naïve T cells via TNF-α and other inflammatory mediators, such as IL-1β, IL-33, and IL-18, and thereby modulate the adaptive immune response [172]. Overall, the use of mast cell activators as adjuvants has been shown to be safe, independent of allergic responses, when tested in animal models [168].

To meet the mission for next-generation influenza vaccines, a computationally optimized broadly reactive antigen (COBRA) design methodology has been used to develop HA and NA molecules that elicit protective broadly-reactive antibodies against drifted influenza virus strains [9], [250]. In previous studies, bivalent H1 and H3 COBRA recombinant HA vaccines, B COBRA HA vaccines, H5 COBRA virus-like particle

vaccines, or N1 COBRA NA vaccines elicited antibodies with HAI and NAI activity against panels of historical and contemporary influenza A and B viruses in mice, ferrets, and non-human primates, following intramuscular injection which translated to the protection of animals against viral challenge with H1N1, H3N2, H5N1, B-Victoria, and B-Yamagata influenza lineages [9], [10], [11], [12], [13], [212]. To determine if COBRA designed vaccines were effective following intranasal delivery, mice were administered the COBRA H1 and H3 HA vaccines formulated with M7-NH_2. Intranasal delivery of these vaccines, when mixed with M7-NH_2, elicited broadly-reactive serum and mucosal antibodies and protected mice against lethal influenza virus challenge.

Materials and Methods

Antigen construction and Synthesis

COBRA hemagglutinin (HA) proteins corresponding to H1N1 and H3N2 seasonal influenza viruses (IAVs) were design based on the next-generation COBRA methodology as previously described [250]. Briefly, Y2 (H1) COBRA HA was derived from 6232 full length wild-type influenza A(H1N1) HA protein amino acid sequences, residues 1-566 (starting with Methionine as the first amino acid), from human H1N1 virus infections collected from January 1, 2014 to December, 2016 were downloaded from the EpiFlu online database and organized by their date of collection [9].

For H3 COBRA HA designated, J4 and TJ5, full length wild-type influenza A(H3N2) HA protein amino acid sequences, residues 1-566 (starting with Methionine as the first amino acid), from 54,041 human H3N2 virus infections collected from May, 1

2008 to April 2016 were downloaded from EpiFlu online database and organized by their date of collection. TJ5 was designed using the sequences between May 2008 to September 2012 and J4 was designed using the sequences between May 2013 to April 2016 [10].

Soluble HA proteins were purified from cells transiently transfected into HEK293T with plasmids expressing a truncated HA gene that was cloned into the pcDNA3.1. The truncated HA genes were generated by replacing the transmembrane domain with a T4 fold-on domain, an Avitag, and a 6× His-tag for purification [210]. The concentration of the soluble HA proteins was determined by conventional bicinchoninic acid assay (BCA) according to the manufacture's instruction (Thermo Fisher, Meridian Rd., Rockford, IL, USA).

Vaccination and Infection

DBA/2J and BALB/c female mice (n=66 and n=30, respectfully; 6-8 weeks old) were purchased from Jackson Laboratory (Bar Harbor, ME, USA) and housed in microisolator cages with access to food and water. The mice were cared for by USDA guidelines for laboratory animals and all procedures were reviewed and approved by the Institutional Animal Care and Use Committee (IACUC) (no. A2020 03-007-Y1-A0 and LRI2935) and performed in accordance with institutional and ARRIVE guidelines. Vaccinations, infections, and mouse bleeds were carried out as previously described [10]. Mice were randomly divided into six (DBA/2J) or three (BALB/c) groups, with n=11 or n=10 mice, respectfully, in each group. Prior to vaccination (day 0), all of the mice were bled via the submandibular to confirm seronegative status against seasonal H1N1 influenza viruses, including: Texas/36/1991, Solomon Islands/03/2006 (SI/06), Brisbane/59/2007

(Bris/07, California/07/2009 (Cal/09), Michigan/45/2015 (Mich/15), Brisbane/02/2018 (Bris/18), and H3N2 viruses: Texas/50/2012 (TX/12), Switzerland/9715293/2013 (Swit/13), Hong Kong/4801/2014 (HK/14), Singapore/IFNIMH/2016 (Sing/16), Kansas/14/2017 (KS/17), Switzerland/8060/2017 (Swit/17), and South Australia/34/2019 (SA/19). Mice were anesthetized with 2-3% isoflurane and prime vaccinated intranasally (IN) with 50μL of vaccine formulations containing 1, 0.1, or 0.01μg of each of the COBRA rHA proteins, Y2, J4, and TJ5, in cold 0.9% saline solution plus the addition of 28.4μg of lyophilized M7-NH_2 powder in cold 0.9% saline solution, with mixing by vortex. As controls, some mice were vaccinated with 50uL of COBRA HA vaccines without adjuvant (0.9% saline only) or mock vaccinated with 50μL of M7-NH_2 adjuvant only (0.9% saline plus M7-NH_2) vaccines (Figure 4. 1a-b). Upon recovery, all of the mice were place back into their cages and monitored. On day fourteen, all of the mice were bled and sera were separated from blood cells via centrifugation and then stored at -20°C ± 5°C (Figure 4. 1b). On day 28, the mice were boosted as before following the same vaccination regimen. Following the boost, all of the DBA/2J mice were bled on days 42 and 49, as before, and the collected sera was separated by centrifugation in microcentrifuge tubes at 10,000 rpm for 10 min, and pooled together equally and then stored at -20°C ±5°C. All of the BALB/c mice were boost-vaccinated on day 28, as before, and bled on day 42 and the collected sera was processed and stored as before (Figure 4. 2a-b). Concurrently, bronchoalveolar lavages were harvested from five BALB/c mice on day 35 post-boost-vaccination. Vaccinated mice were euthanized via carbon dioxide asphyxiation followed by secondarily cervical dislocation and lungs flushed via the trachea with 450uL of cold 1X PBS using 23G needles with 22X1 G polyethylene catheters, attached to 1mL syringes. The samples were placed

in sterile microcentrifuge tubes, on ice, followed by centrifugation at 3000 x g for 5 minutes. After centrifugation, the supernatants were transferred into fresh sterile centrifuge tubes and stored at -20°C ±5°C. At day 52, some of the DBA/2J mice were anesthetized and infected with $8x10^6$ PFU of A/Brisbane/02/2018 (H1N1) or with $7x10^5$ PFU of A/Switzerland/9715293/2013 (H3N2) influenza A viruses (IAV) via intranasal distillation. Upon recovery, the mice were returned to their cages and monitored daily for 14 days post infection for both morbidity and mortality. At day 55, following euthanasia as before, lungs were harvested from 3 DBA/2J mice in each group, snap-frozen on dry ice, and stored at -80°C for determining viral lung titers.

Hemagglutination Inhibition Assay (HAI)

The HAI assay was performed for the detection of serum antibodies that inhibit binding of influenza viruses from agglutinating red blood cells (RBCs) by preventing binding of viral surface HA to sialic acid residues on RBCs. This protocol was based on the WHO manual for laboratory diagnosis and virological surveillance of influenza [211]. This HAI assay was performed against a panel of H1N1 viruses, including: A/Solomon Island/3/2006, A/Brisbane/59/2007, A/California/07/2009, A/Michigan/45/2015, A/Brisbane/02/2018, and H3N2 viruses: A/Texas/50/2012, A/Switzerland//2013, A/Hong Kong/4801/2014, A/Singapore-IFNIMH-16-0019/2016, A/Kansas/14/2017, A/Switzerland/8060/2017, and A/South Australia/34/2019. The HAI assays were performed as previously decribed [212]. Sera from each mouse was initially treated with receptor destroying enzyme (RDE) (Denka Seiken, Co., Tokyo Japan) for eliminating non-specific inhibitors. In a deep-well, 96-well block, sera was diluted to $1/10^{th}$ final solutions

by reconsituting 100μL of serum with 3 volumes of RDE in 1x PBS, followed by overnight incubation at 37°C. The following day, the RDE-treated sera was heat inactivated in a water bath at 56°C for 45 minutes, followed by cooling to room temperature (RT) , and the addition of 6 volumes of 1x PBS. At days 35, lungs from 5 BALB/c mice were harvested and homogenized, in 1mL of cold 1X PBS, using a plunger and 70μm strainer. In a v-bottom 96-well plate, 25μL of PBS was added into each well. RDE treated sera or lung homogenate was added in duplicates and serially diluted across the plate. Following serial dilutions, each virus was prepared and tested at a 1:8 solution. The plates were incubated at RT for 20 min for H1N1 influenza viruses or 30 min for H3N2 influenza viruses. Following incubation, 0.8% turkey red blood cells (TRBCs) for H1N1 viruses or guinea pig red blood cell (GPRBCs) for H3N2 influenza viruses were added to all of the corresponding wells, mixed by agiation, and then incubated at RT for 30 min (H1N1) or 1 h (H3N2). After incubation, the titer of each serum and lung sample was reported as the reciprocal dilution of the last well without agglutination. An HAI titer of 1:40 was considered seroprotective as recommeded by the European Medicines Agency Guidelines on Influenza Vaccines [213].

Enzyme-linked Immunosorbant Assay (ELISA)

The ELISA assays were performed as previously described [78]. To assess total IgG serum antibody reactivity and specificity to COBRA HAs vaccine components or WT IAV HAs, Immulon 4HBX 96-well flat bottom plates (Thermo Fisher Scientific, Waltham, MA, USA) were coated with 100μL of Y2, J4, TJ5 COBRA or WT Bris/18, Tas/20, or Sing/16 rHAs, at 1μg/mL in carbonate coating buffer (pH 9.4) and incubated overnight in

a humidified chamber at 4°C. Following the incubation, the plates were decanted and blocked with 200µL, per well, of 4% FBS + 0.05% Tween 20 blocking buffer (BB) in 1x PBS, for 90 minutes at 37°C. During the blocking incubation, serum samples were prepared at 1:100 ratio and serially diluted (1:3) from an initial 1:500 dilution for sera, or prepared at 1:10 ratio for lung lavages, and serially diluted (1:2) from the initial 1:10. Following blocking completion, 100µL of each sera diluted sample or 50uL of each lung lavage diluted sample was added to the Y2, J4, TJ5 (for sera only) or WT Bris/18, Tas/20, Sing/16 (for sera and lung lavages) rHA coated plates and incubated for 90 min at 37°C. Plates were washed and 100µL of prepared secondary goat anti-mouse IgG HRP (Southern Biotech, Birmingham, AL, USA), diluted 1:4000 in BB, added to each well, followed by incubation for 90 min at 37°C. After incubation with secondary antibody, the plates were washed and received 100µL of 1x ABTS (VWR Corporation, Matsonford Rd Radnor, PA, USA) solution and incubated for about 13 min at 37°C. After complete colorimetric development, 50µL 1% SDS solution was added to each well to stop the colorimetric reaction. The optical density (O.D.) of the samples were immediately read at 414nm in a spectrophotometer (PowerWave XS, BioTek, Santa Clara, CA, USA) using the Gen05 software (version 3.14, https://www.agilent.com/en/support/biotek-software-releases) to measure the antibody end-point titers, and compared to positive and negative controls. To further assess IgA and specific IgG1, IgG2a, and IgG2b isotype binding antibodies, samples were processed as before on Y2 coated plates (for sera only) or WT Bris/18, Tas/20, Sing/16 rHAs (for sera and lung lavages) and incubated with secondary goat anti-mouse IgA, IgG1, IgG2a or IgG2b antibody solutions and measured as before. Both sera and lung lavages were prepared at an initial 1:10 and serially diluted (1:2) for detection of

IgA and all lung lavages were prepared at an initial 1:10 and serially diluted (1:2) for detection of IgG1, IgG2a, and IgG2b.

Lung Viral Titers

The protocol used for this plaque assay was followed as previously described [9]. MDCK cells were seeded at $1x10^6$ cells per $10cm^2$ and incubated for 24h and grown to ~95% confluency. Day 55 lungs from each DBA/2J mouse were weighed and homogenized in DMEM supplemented with 1% penicillin-streptomycin (P/S), 10 times their weights. The lung homogenates where then centrifuged at 1500 rpm for 10 min to remove debris and serially diluted, 10-fold. Additionally, a 10-fold serial dilution of Brisbane/02/2018 or A/Switzerland/9715293/2013 were used as positive controls. The diluted samples were then added to the MDCK monolayers at 100µL per well, and allowed to infect for one hour, with 15-minute shaking intervals, at RT. Moreover, negative control wells received 100µL of DMEM P/S only. After one hour of infection, the supernatant from each well was aspirated and the wells were washed once with DMEM P/S, with removal of media after the wash. Next, 2mL of a 1:1 solution of 1.6% agarose in 2x cMEM media containing TPCK-Trypsin at 1µg/mL was added to each well and allowed to solidify, followed by incubation for 2-5 days at 37 °C with 5% CO_2. Once cytopathic effects were confirmed, the agarose layers were removed from each well and the cells were fixed with 10% formalin solution for 10 minutes at RT. After the 10 min, the formalin was removed and the cells were stained with 1% Crystal Violet (Fisher Science Education, Waltham, MA, USA) at RT, for 10-15 minutes. Following completion of staining, the Crystal Violet was removed and the wells were rinsed in water. The plates were allowed to dry and the plaque forming

units (PFUs) were counted, followed by calculation of the lung viral titers as PFU/g of tissue.

Results

Antigen specific serum and lung binding antibodies

Following the second vaccination, anti-HA IgG binding antibodies to the rHA proteins used for vaccination, WT Bris/18 H1N1, WT Tas/20 H3N2, and WT Sing/16 H3N2 rHAs, was assessed (Figure 4. 3a-e). Mice vaccinated with adjuvant only or the vaccine only had no detectable IgG antibodies in their sera that bound to any of the rHA proteins. However, all mice vaccinated intranasally with the highest dose of M7-NH_2-adjuvanted HA (3μg) had high anti-HA total IgG serum titers against Y2, J4, TJ5, and all of the three WT rHAs proteins (Figure 4. 3a-e). However, ~50% of the mice vaccinated with the COBRA HA (0.3μg) vaccines plus M7-NH_2 adjuvant seroconverted and had detectable anti-HA IgG antibodies, whereas no mice seroconverted using the lowest dose of vaccine (0.03μg) formulated with the M7-NH_2 adjuvant. Mice vaccinated intranasally with the highest dose of COBRA (3μg) plus M7-NH_2 had high anti-HA total IgG titers in their lung lavages against WT Bris/18 and Sing/16 rHAs proteins and 80% of the mice had detectable IgG titers in their lung lavages against WT Tas/20 rHA (Figure 4. 3e). There were no detectable anti-HA IgA antibodies in the sera of vaccinated mice and few mice had detectable IgA antibodies in the lung lavages.

Mice vaccinated intranasally with COBRA HA (3μg) plus M7-NH_2 had predominantly IgG1 anti-HA serum antibodies with little to no IgG2a or IgG2b antibody isotypes detected (Figure 4. 4a-c). In contrast, there was significant IgG1 and IgG2b

antibodies (1:100 - 1:1000) in the lung lavages of mice vaccinated with COBRA HA plus M7-NH2 adjuvant (Figure 4. 4d-f). In comparison, mice vaccinated with COBRA HA proteins alone had no detectable IgG1, IgG2a, or IgG2b in their serum or lung lavages.

Hemagglutinin-inhibition (HAI) titers from sera and lung homogenates collected from vaccinated mice

DBA/2J mice vaccinated with 3μg of COBRA HA (Y2, J4, TJ5) vaccines formulated with M7-NH_2 had mean HAI titers between 1:80 - 1:160 against the H1N1 influenza viruses. However, all these mice had, on average, HAI titers less than 1:40 (Figure 4. 5a) against H3N2 viruses. The sera HAI titers of these DBA/2J mice is compared to mice vaccinated with 3μg of COBRA HA (Y2, J4, TJ5) alone. When these same vaccines were used to vaccinate BALB/c mice, all mice had sera with high HAI activity against the H1N1 viruses as well as 6 of 7 H3N2 influenza viruses (Figure 4. 5b). The sera HAI titers of these BALB/c mice is compared to mice vaccinated with 3μg of COBRA HA (Y2, J4, TJ5) alone. There was no detectable HAI activity against KS/17 virus in any of the groups (Figure 4. 5a-b). There was low or undetectable HAI activity in lung homogenates collected at day 35 from mice vaccinated intranasally with 3μg of COBRA HA vaccines alone or formulated with M7-NH_2. In addition, mice vaccinated with lower doses of COBRA HA vaccines (0.3μg or 0.03μg) mixed with M7-NH2, M7-NH_2 adjuvant only, or COBRA HA vaccines (0.3μg or 0.03μg) only without adjuvant had sera with no detectable HAI activity.

M7-NH_2-adjuvanted COBRA HA vaccines protected mice following influenza virus challenge

To assess protection against influenza challenge, vaccinated DBA/2J mice were infected intranasally with the H1N1 virus, Bris/18, or with the H3N2 virus, Swit/13 (Figure 4. 6). Mice vaccinated with M7-NH_2 adjuvant only or COBRA HA vaccine alone, and challenged with Bris/18 lost an average ~24% of their original body weight and succumbed to infection by day 6 post-infection with no mice surviving infection (Figure 4. 6a-b). Mice vaccinated with COBRA HA (3μg) formulated with M7-NH_2 only lost an average of ~8% (day 6) and had 100% survival (Figure 4. 6a-b). Mice vaccinated with lower doses of the COBRA HA/M7-NH_2 vaccine lost greater than 18% of their original body weight and all of mice succumbed to infection by day 6 post-infection, (Figure 4. 6a-b). Mice vaccinated with M7-NH_2 adjuvant only and challenged with Swit/13 lost an average ~26% of their original body weight and succumbed to infection by day 5 post-infection with no mice surviving infection (Figure 4. 6d-e). Mice vaccinated COBRA HA (3μg) vaccine alone and challenged with Swit/13 lost an average ~22% of their original body weight and succumbed to infection by day 6 post-infection with one mouse surviving infection (Figure 4. 6d-e). Mice vaccinated with COBRA HA (3μg) formulated with M7-NH_2 and challenged with Swit/13 only lost an average of ~5% (day 4) and had 100% survival (Figure 4. 6d-e).

At day 3 following infection with Bris/18 (day 55), mock vaccinated mice, COBRA HA vaccinated only mice, as well as mice vaccinated with the two lowest doses of COBRA HA plus M7-NH_2 adjuvant, all had high viral lung titers (~1 x 10^6 pfu/g of tissue) (Figure 4. 6c). In contrast, two of the three mice vaccinated with the highest dose of COBRA HA (3μg) plus M7-NH_2 had undetectable viral lung titers (Figure 4. 6c). One mouse (Figure 4.

6c; blue square) in the group vaccinated with 3μg of COBRA rHA plus M7-NH_2 adjuvant had viral lungs titers (6.55 x 10^5 pfu/g of tissue). While this mouse had anti-HA IgG endpoint dilution serum titer of ~1 x 10^4 against WT Bris/18 rHA, this mouse had greatly reduced HAI titers (1:20) compared to the other 2 mice in the group (Figure 4. 6c and Table 4. 1). However, this particular mouse also had little weight loss (98% of original weight at day 3 post-infection; Figure 4. 6a; Table 4. 1), following viral challenge. The other 2 mice pertaining to this vaccine regimen both had high HAI titers (1:320) and total endpoint IgG titers of 1.4x10^4 against WT Bris/18 rHA (Table 4. 1). There were also no detectable viral lung titers (Figure 4. 6c and Table 4. 1) or visible plaques at day 3 post-infection (Supplemental Figure 4. 1). Moreover, mice vaccinated IN with M7-NH_2 alone, COBRA HA (3μg) alone, or lower doses of vaccine mixed with M7-NH_2 had significant weight loss ($p<0.0001$) (Figure 4. 6a) with no mice surviving challenge (Figure 4. 6b), and high viral lung titers (~1 x 10^6 pfu/g of tissue) at day 3 post-infection (Figure 4. 6c, Table 4. 1, and Supplemental Figure 4. 1). Following challenge with Swit/13 (day 55), mice vaccinated with COBRA HA (3μg) vaccines alone had between 6.4 x 10^4 –5 x 10^5 pfu/g of tissue (Figure 4. 6f). Mice vaccinated with M7-NH_2 alone had between 9.4 x 10^4 –3 x 10^6 pfu/g of tissue (Figure 4. 6f). On the contrary, mice vaccinated with COBRA HA (3μg) plus M7-NH_2 had undetectable viral lung titers (Figure 4. 6f).

Discussion

Most seasonal influenza vaccines are not formulated with an adjuvant [251]. Although adjuvants are tolerable when administered to individuals, they may be associated with increased inflammation and reactogenicity, particularly at the injection site [221]. However, adjuvanted influenza vaccines have been approved in the U.S. and European Union (E.U.) to increase the effectiveness of vaccines for the elderly [251]. MF59 is a squalene oil-in-water adjuvant added to the split inactivated influenza vaccine (marketed under the name Fluad by Seqirus Inc., Holly Springs, NC, USA) [252]. The next-generation of adjuvants for influenza virus vaccines are currently being tested by many groups which include toll-like-receptor (TLR) agonists such as GLA (glucopyranosyl lipid A) (TLR4) and CpG oligodeoxynucleotides (TLR9), or saponins (Iscomatrix) [227]. There are many challenges when tailoring an adjuvant to a vaccine of interest in order to stimulate the necessary protective immune responses. Stimulating the innate immune system will modulate the adaptive immune response and is an efficient mechanism for eliciting protective immunity against viral infection [253]. Eliciting specific immune responses depends on the type of adjuvant used since some adjuvants induce T-bet and STAT-4 signaling pathways that lead to polarized responses that are skewed towards a pro-inflammatory Th1 response and other adjuvants result in induction of STAT-6 and GATA-3 signaling pathways that drive responses towards an anti-inflammatory Th2 response [235], [254]. Additionally, adjuvant physicochemical properties and formulations play important roles for how an adjuvant interacts with vaccine components. To date, most adjuvants are formulated with injectable vaccines and administered intramuscularly [173]. An intranasal route of vaccination may induce mucosal and systemic immune responses in

order to enhance protective immunity in individuals with weak immune systems, and may be easier to administer compared to invasive injectable vaccines since they do not require needles [173].

In this study, M7-NH_2 was administered intranasally with COBRA HA proteins in a dose-dependent approach. Vaccinated mice had high titers of blocking antibodies in their sera after two vaccinations against panels of H1N1 and H3N2 influenza viruses. Following vaccination, influenza virus-specific IgG antibodies are induced after memory B-cell activation in the spleen that further differentiate into serum IgG isotypes [255]. In the presences of T helper (Th) type 1 cytokines, such as IFN-γ, isotype class switching results in IgG2a secreted antibodies [238]. In contrast, in the presence of Th2 cytokines, such as IL-4 or IL-5, IgG isotype switching results in IgG1 secreted antibodies [176], [237]. Although Th1 pro-inflammatory immune responses are ideal for clearance or prevention of influenza virus infection, a simultaneous Th2 anti-inflammatory response may be beneficial for counteracting and depolarizing detrimental local and systemic outcomes caused by increased levels of inflammation. Mice vaccinated with COBRA HA proteins plus M7-NH_2 had high titer IgG1 serum antibodies against three WT H1N1 and H3N2 IAV HAs, with some level of detectable IgG2b antibodies, but little to no IgG2a. These finding are in agreement with previous studies demonstrating comparable enhancement of IgG1 with minimal IgG2a, in mice vaccinated with M7-NH_2-adjuvanted subunit vaccines, thus indicating a Th2 polarized response induced by M7-NH_2 [176].

Notably, mice vaccinated intranasally with COBRA HA antigens plus M7-NH_2 had total serum anti-HA IgG titers ~10^4-10^5 (primarily IgG1) compared to mice vaccinated intranasally with M7-NH_2 alone or the COBRA HA vaccine alone. Vaccinating

intranasally using M7-NH_2 has the potential to induce protective antibodies in both the nasal mucosal cavity (local) and in sera (systemic). In the sera, vaccine elicited anti-HA serum IgG, IgG1, and IgG2a antibody titers were similar to the levels of anti-HA antibody titers in the lung lavages of mice, with little to no IgA antibodies. These finding are in contrast to the intramuscularly administered AddaVax, an MF59-like adjuvant, which does not induce measurable mucosal responses in young or old mice vaccinated mice [256].

Serum HAI titers $\geq$1:40 in people following vaccination with commercial seasonal influenza vaccines are seroprotective in at least 50% of the vaccinated population and are used as a standard of an effective influenza vaccine in people [213]. Sera and lung lavages collected from mice vaccinated with COBRA HA antigens (3μg) plus M7-NH_2 had seroprotective antibody titers against a panel of H1N1 viruses isolated from 2009-2018. These same serum samples had a lower average of HAI activity against H3N2 viruses isolated between 2012 and 2019 in DBA/2J mice but still elevated in BALB/c mice. However, there were mice with low HAI titers that still survived viral challenge without significant weight loss. The dominating epitopes on the head region of HA of the wild-type and COBRA H1 subtypes lead to the recognition and binding by antibodies directed toward the HA head. COBRA HA proteins could potentially elicit antibodies directed towards the conserved stem region, and thus could contribute toward protection, independent of HAI activity [257]. Additionally, some HAI activity against three H3N2 IAVs was observed in lung homogenates of mice vaccinated with COBRA vaccines, suggesting that protective antibodies could also be retained within mucosal tissue. However, IN administration of COBRA HA proteins with M7-NH_2 did elicit HAI titers against both H1N1 and H3N2 influenza viruses, systemically and in the nasal respiratory tract. Mice vaccinated IN with

COBRA HA antigens (3μg), adjuvanted with M7-NH_2, survived Bris/18 (H1N1) virus challenge, with only about ~8% weight loss at day 6 post-infection that may correlate with the slightly lower HAI titers against the challenge strain in mouse number 2. HAI titers could potentially be enhanced following an additional vaccine boost. Additionally, mice vaccinated IN with COBRA HA antigens (3μg), adjuvanted with M7-NH_2, survived Swit/13 (H3N2) virus challenge, with only about ~4% weight loss at day 4 post-infection.

While other adjuvants such as aluminum salts, MF59, adjuvant system 03 (AS03), or an alternative adjuvant system of AS03 (AF03) may be compatible with intramuscularly administered influenza vaccines, many gaps remain in terms of their mechanism of action. To date no intranasal adjuvants have been approved for use with influenza virus vaccines. This in turn poses limitations and challenges in terms of inducing the necessary immune responses in mucosal compartments that are exposed to the external environment, where respiratory pathogens, such as influenza viruses, invade the host.

In general, rHA COBRA HA vaccines alone administered intranasally in mucosal compartments without M7-NH_2 adjuvant provide little to no immunogenicity. In this study, even with very low doses of vaccines, using the same amount of M7-NH_2 adjuvant failed to be immunogenic. To address this challenge, and to tailor this specific adjuvant to the COBRA HA vaccines for comparing to unadjuvanted COBRA HA vaccines, and explore the adjuvant-enhanced effect on vaccine efficacy, this dose-response study allowed for identifying the optimal dose of COBRA HA (3μg) vaccines required for formulating with M7-NH_2 and successfully enhance the immunogenicity of the antigens, when administered intranasally.

The findings in this study demonstrated that M7-NH_2 mast cell degranulating peptide adjuvant, was able to successfully enhance the immunogenicity following intranasal COBRA (H1/H3) HA vaccination in mice and reduce morbidity and mortality following challenge with H1N1 and H3N2 influenza viruses. Herein, M7-NH_2 peptides have potential as an intranasal adjuvant that induces mucosal and systemic immune responses to enhance protective immunity in individuals with weak immune systems, such as young kids and older adults, and provide for easier administration compared to injectable vaccines. Moreover, adjuvanting COBRA HA vaccines with M7-NH_2 peptides could potentially enhance the immune responses in humans, thus allowing for assessment of seroconversion in sera collected from participants in future human clinical trials.

a.

Groups	COBRA Vaccine	Dose	Adjuvant	Challenge
1	Y2/J4/TJ5	3µg	None (PBS)	**A/Brisbane/02/2018 H1N1 or A/Switzerland/9715293/2013 H3N2**
2	Y2/J4/TJ5	3µg	M7-NH2 (28.436µg)	
3	Y2/J4/TJ5	0.3µg	M7-NH2 (28.436µg)	
4	Y2/J4/TJ5	0.03µg	M7-NH2 (28.436µg)	
5	Mock	0µg	M7-NH2 (28.436µg)	
6	Mock	0µg	None (PBS)	

b.

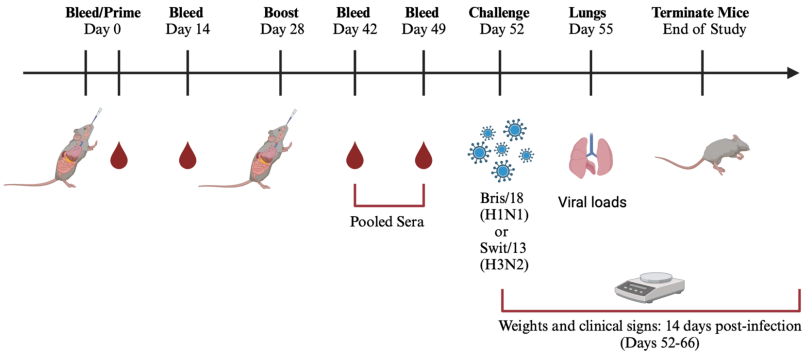

Figure 4. 1 Vaccine regimens and schematic of the study timeline of DBA/2J mice.

(a) DBA/2J (6-8 weeks old) female mice were randomly divided into six groups, with n=11 mice in each group, and vaccinated intranasally (IN) with 3, 0.3, or 0.03µg of COBRA HA proteins (Y2, J4, and TJ5) plus the addition of 28.436µg of the adjuvant, M7-NH_2 (mast cell degranulating peptide), at a 1:1 ratio. As controls, some mice were vaccinated with COBRA HAs (3µg) with 0.9% saline, with adjuvant only (0.9% saline plus M7-NH2) or without adjuvant (0.9% saline only). (b) Schematic of Study Timeline. DBA/2J mice were bled and prime vaccinated on day 0 follow by blood collection on days 14 and boost-vaccinated on day 28. On days 42 and 49, the mice were bled, followed by intranasal challenge on day 52 with A/Bris/02/2018 or with A/Swit/9715293/2013 viruses. Three days post-infections, lungs were harvested from 3 mice from each group and the remainder mice were monitored for 14 days post infection. Created with BioRender.com.

a.

Groups	COBRA Vaccine	Dose	Adjuvant
1	Y2/J4/TJ5	3µg	None (PBS)
2	Y2/J4/TJ5	3µg	M7-NH2 (28.436µg)
3	Mock	0µg	M7-NH2 (28.436µg)

b.

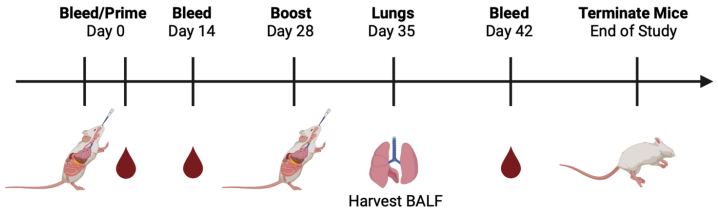

Figure 4. 2 Vaccine regimens and the study timeline of BALB/c mice.

(a) BALB/c (6-8 weeks old) female mice were randomly divided into three groups, with n=10 mice in each group, and vaccinated intranasally (IN) with 3 µg of COBRA HA proteins (Y2, J4, and TJ5) plus the addition of 28.436 µg of the adjuvant, M7-NH_2 (mast cell degranulating peptide), at a 1:1 ratio. As controls, some mice were vaccinated with COBRA HAs (3 µg) with 0.9% saline, or with adjuvant only (0.9% saline plus M7-NH_2). (b) Schematic of Study Timeline. BALB/c mice were bled and prime vaccinated (IN) on day 0 follow by blood collection on days 14 and 42. On day 28, all of the mice were boost-vaccinated as before. Seven days post-vaccinations (day 35), lungs were harvested from each mouse. Created with BioRender.com.

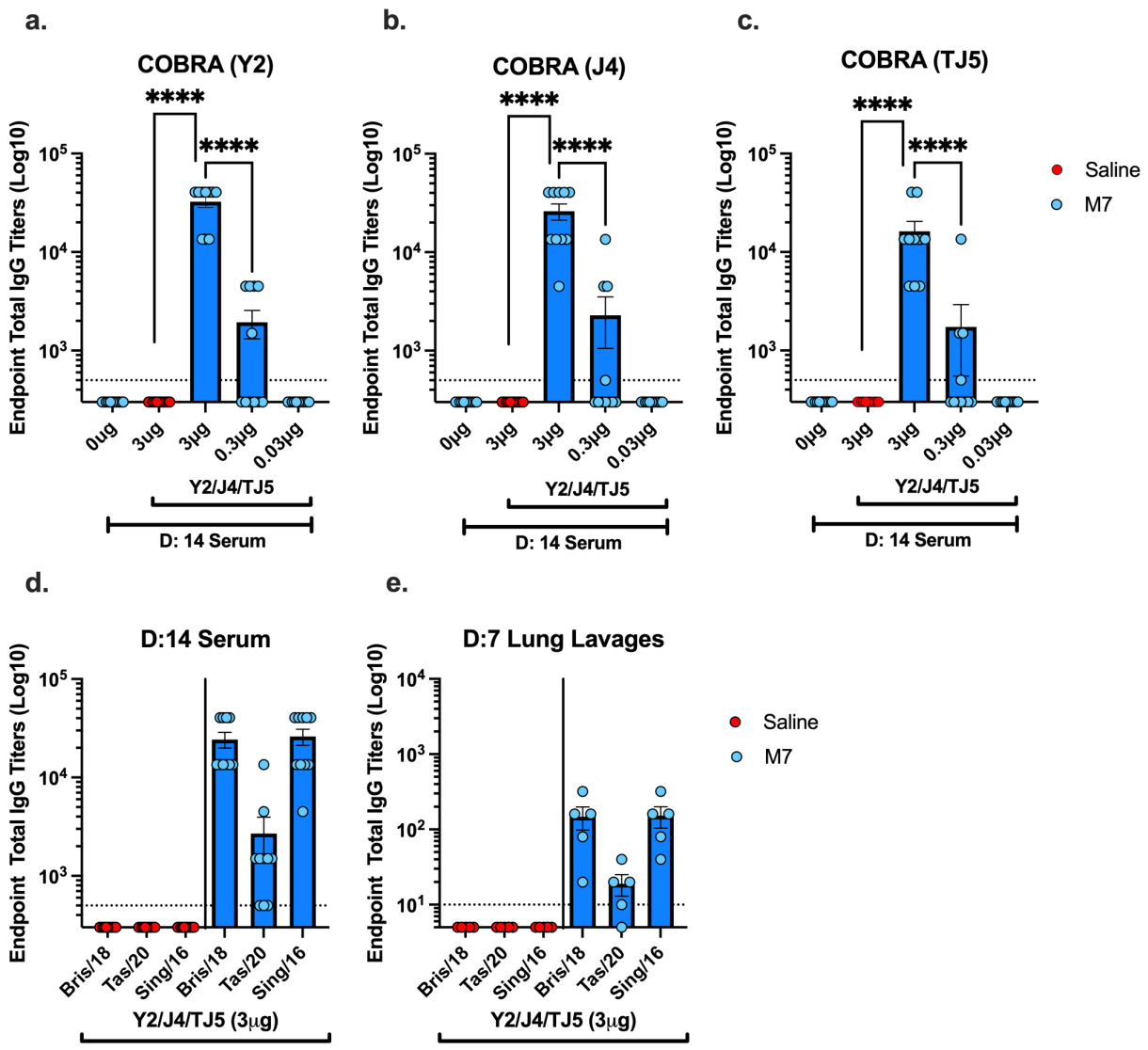

Figure 4. 3 Quantification of total IgG in DBA/2J mice serum and lung lavages.

Sera collected 14 days post-boost (Days 42 and 49) were pooled, and the lung lavages of BALB/c mice were harvested 7 days (Day 35), post two vaccinations. Mice were IN vaccinated with (Red dots) COBRA HAs (3 µg) with 0.9% saline or IN with (Blue dots) M7-NH_2 (28.436 µg) in the following formulations: with 0.9% saline only, or COBRA HAs (3, 0.3, or 0.03 µg). Antibody responses were measure against plates coated with (a) Y2, (b) J4, or (c) TJ5 COBRA HAs for DBA/2J mice day 42/49 sera, or WT IAV (d and

e) Bris/18 H1N1, Tas/20 H3N2, or Sing/16 H3N2 HAs for (d) DBA/2J sera and (e) BALB/c mice lung lavages. The Y-axis represents the endpoint total IgG titers on a log 10 scale. The X-axis represents the different (a-c) COBRA HA vaccine formulations (3 to 0.03 μg) or no COBRA HAs, and (d and e) WT Bris/18, Tas/20, or Sing/16 HAs. Each column represents dots of 10, 11 or 5 mice per vaccine group and are expressed as the average +/- standard error of the mean (SEM). IgG titers were statistically analyzed using nonparametric one-way analysis of variance (ANOVA) by Prism 9 software (GraphPad Software, Inc., San Diego, CA, version 9.4.0, https://www.graphpad.com). A *P* value of less than 0.05 was defined as statistically significant (*, P<0.05; **, P<0.01; ***, P<0.001;****, P<0.0001).

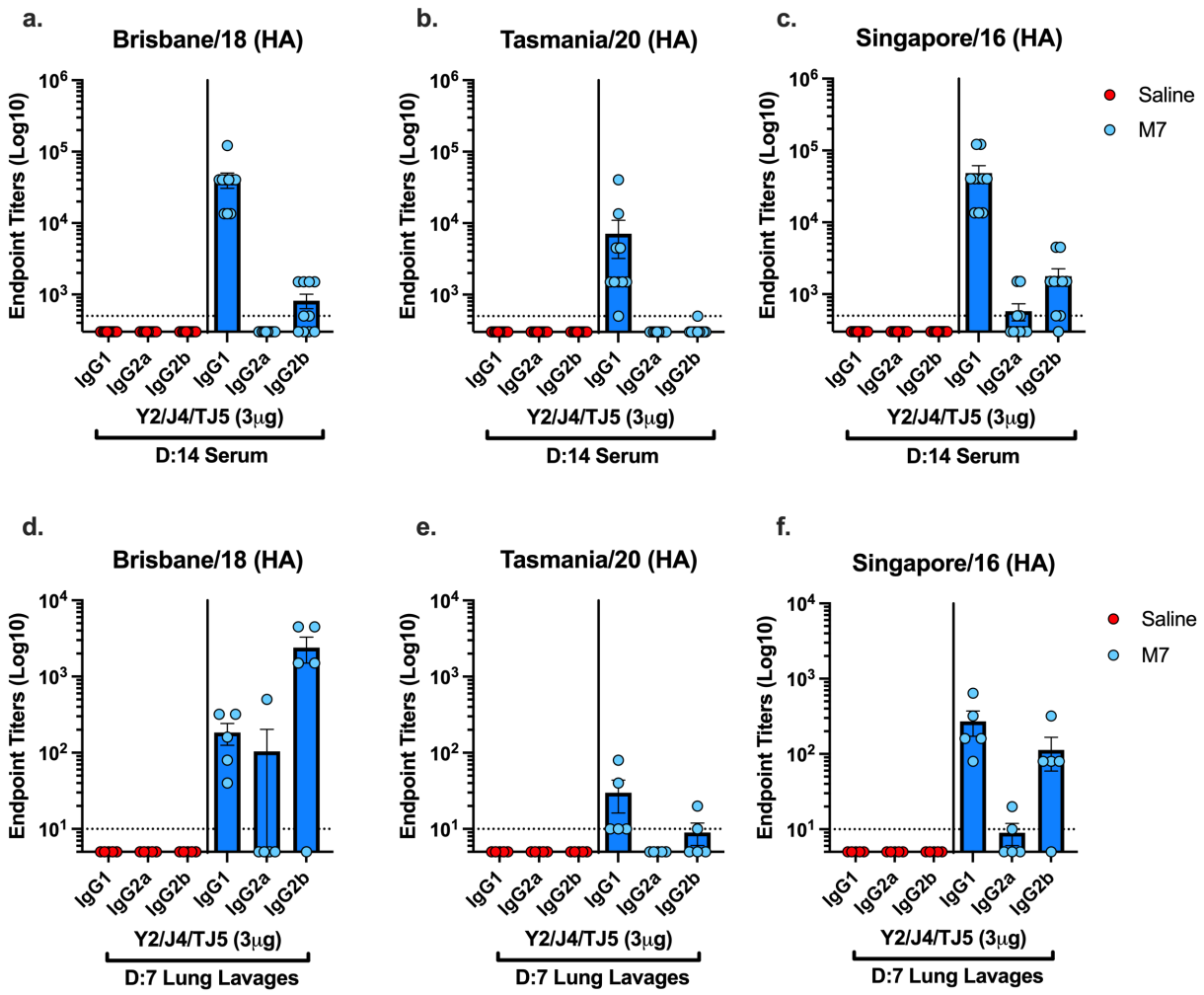

Figure 4. 4 Quantification of IgG1, IgG2a, and IgG2b isotypes in mice serum and lung lavages.

Sera was collected 14 days post-boost (Days 42 and 49), and lung lavages were harvested 7 days (Day 35) post two vaccinations. Mice were vaccinated IN with (Blue dots) M7-NH_2-Adjuvanted (28.436 μg) COBRA (3 μg) vaccines or (Red dots) COBRA (3 μg) plus 0.9% saline. Antibody responses were measure against plates coated with (A-F) WT Bris/18 H1N1, Tas/20 H3N2, or Sing/16 H3N2 HAs. The Y-axis represents the endpoint titers and the X-axis represents the different isotypes. Each column represents dots of 10, 11, or 5 mice per vaccine group and are expressed as the average +/- standard error of the mean (SEM).

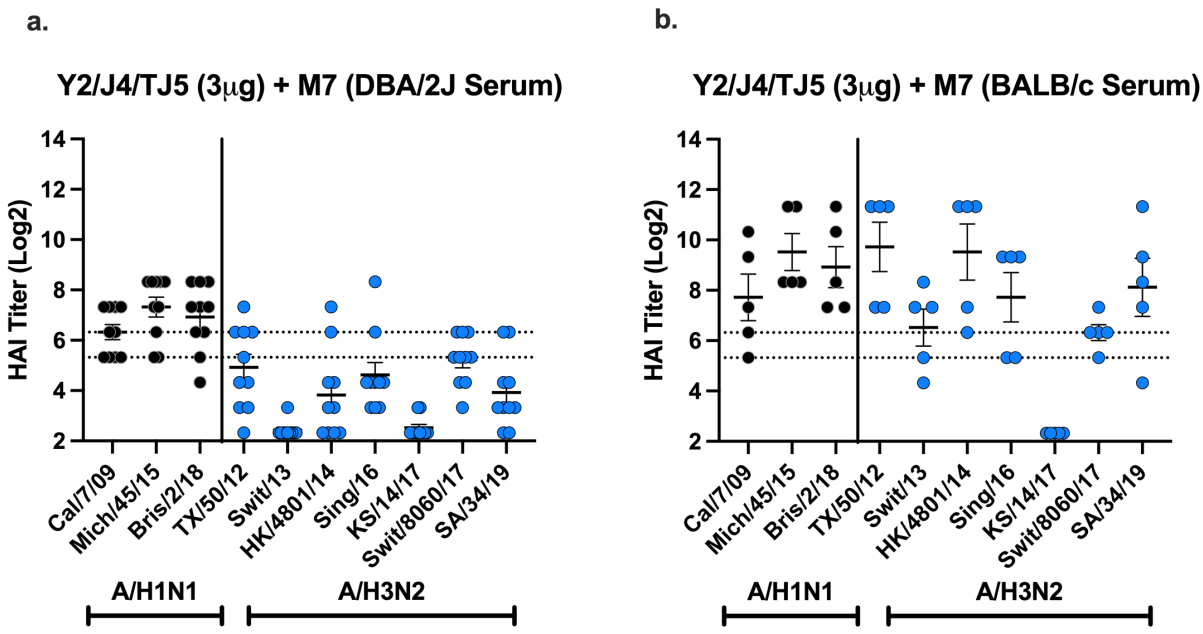

Figure 4. 5 Hemagglutinin-inhibition activity in mice vaccinated with M7-adjuvanted COBRA HA vaccines (Y2, J4, and TJ5).

(a) Sera collected from individual mice vaccinated with COBRA (3 μg) + M7-NH_2 (28.436 μg) at days 42 and 49 (DBA/2J) post-boost, was pooled, or (b) sera collected at day 42 (BALB/c) post-boost, was tested against a panel of H1N1 (Left) and H3N2 (Right) IAVs. HAI titers (Y-axis) are displayed on a log 2 scale and the panel of H1N1 and H3N2 IAVs are displayed on the X-axis. The two dotted lines represent HAI titers of 1:40 (bottom) and 1:80 (top). Each column represents dots of 10, 11, or 5 mice per vaccine group and are expressed as the average +/- standard error of the mean (SEM).

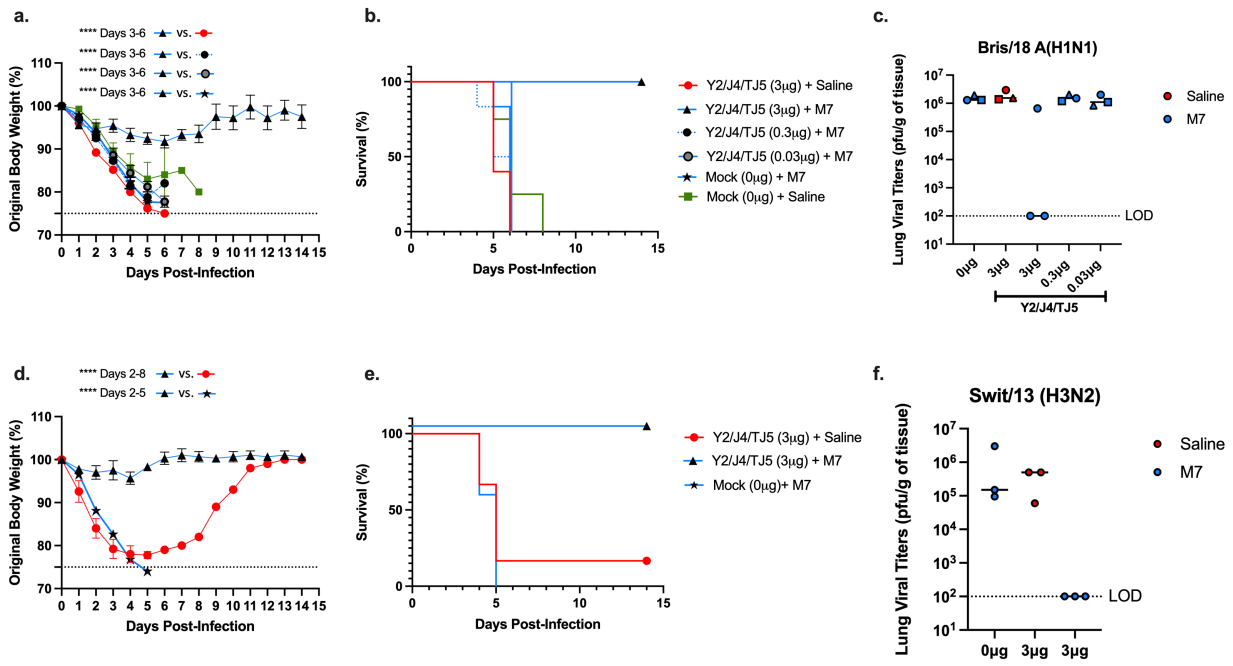

Figure 4. 6 Post-challenge weight loss, clinical signs, survival, and viral lung titers of DBA/2J mice.

Weight loss, survival, and viral lung titers of DBA/2J mice vaccinated IN with M7-NH_2. Mice were challenged IN with (a-c) A/Bris/02/2018 (8 x 10^6 PFU/50µL) or with (d-f) A/Swit/9715293/2013 (7 x 10^5 PFU/50µL) and observed for 14 days post-infection. (a and d) Percent of original body weight, (b and e) percent survival, and (c and f) day 55 viral lung titers. The dotted line in panel a represents a 25% weight loss cutoff from the original body weights. The Y-axis in (a) represents the original body weights, (b) percent survival, and (c) the day 3 post-challenge lung viral titers (PFU/g of tissue). The X-axis represents (a, b, d, and e) the days post-infection and (c and f) the vaccines with (3-0.03µg) or without (0µg) COBRA HAs, adjuvanted with (Blue) M7-NH_2 (28.436µg) or (Red) 0.9% saline only. The dotted lines in panels c and f are representative of the limit of detection (LOD). In panel c, the circles represent distinct mice identified as number one in each group, squares represent distinct mice identified as number 2, and triangles represent distinct mice

identified as number 3. Viral lung titers were statistically analyzed using nonparametric one-way analysis of variance (ANOVA) by Prism 9 software (GraphPad Software, Inc., San Diego, CA, version 9.4.0, https://www.graphpad.com). A *P* value of less than 0.05 was defined as statistically significant (*, P<0.05; **, P<0.01; ***, P<0.001; ****, P<0.0001).

Y2/J4/TJ5

Bris/18 HAI titers

Mouse ID	Mock + M7	3µg +Saline	3µg + M7	0.3µg + M7	0.03µg + M7	Mock + Saline
1	1:5	1:5	1:320	1:5	1:5	1:5
2	1:5	1:5	1:20	1:5	1:5	1:5
3	1:5	1:5	1:320	1:5	1:5	1:5

End-point total IgG titers in serum against WT Bris/18 rHA

1	0	0	$1.4x10^4$	0	0	0
2	0	0	$1.4x10^4$	0	0	0
3	0	0	$1.4x10^4$	0	0	0

% weight loss at day 3 post-infection

1	10	17	0	14	16	13
2	13	17	2	10	15	16
3	14	16	1	7	15	13

Viral lung titers (PFU/g of tissue)

1	$1.29x10^6$	$2.95x10^6$	0	$1.50x10^6$	$2.00x10^6$	$1.35x10^6$
2	$1.31x10^6$	$1.39x10^6$	$6.55x10^5$	$1.19x10^6$	$1.10x10^6$	$4.25x10^6$
3	$1.94x10^6$	$1.54x10^6$	0	$2.06x10^6$	$8.35x10^5$	$1.12x10^6$

1= ● 2= ■ 3=▲

Table 4. 1 Correlation of immunology and pathology pre-and post-Bris.18 IAV infection in DBA/2J mice.

Comparison of HAI titers against H1N1 Bris/18 IAV and endpoint of total IgG against Bris/18 IAV in DBA/2J mice sera after boost vaccination, and prior to influenza infections. Also represented are percent weight loss and viral lung titers of the corresponding mice from each vaccination group, post-infection with Bris/18. The data points represent mouse 1 (circles), mouse 2 (squares), and mouse 3 (triangles) from each vaccine group. The shapes are identifiers for Fig. 4.6c.

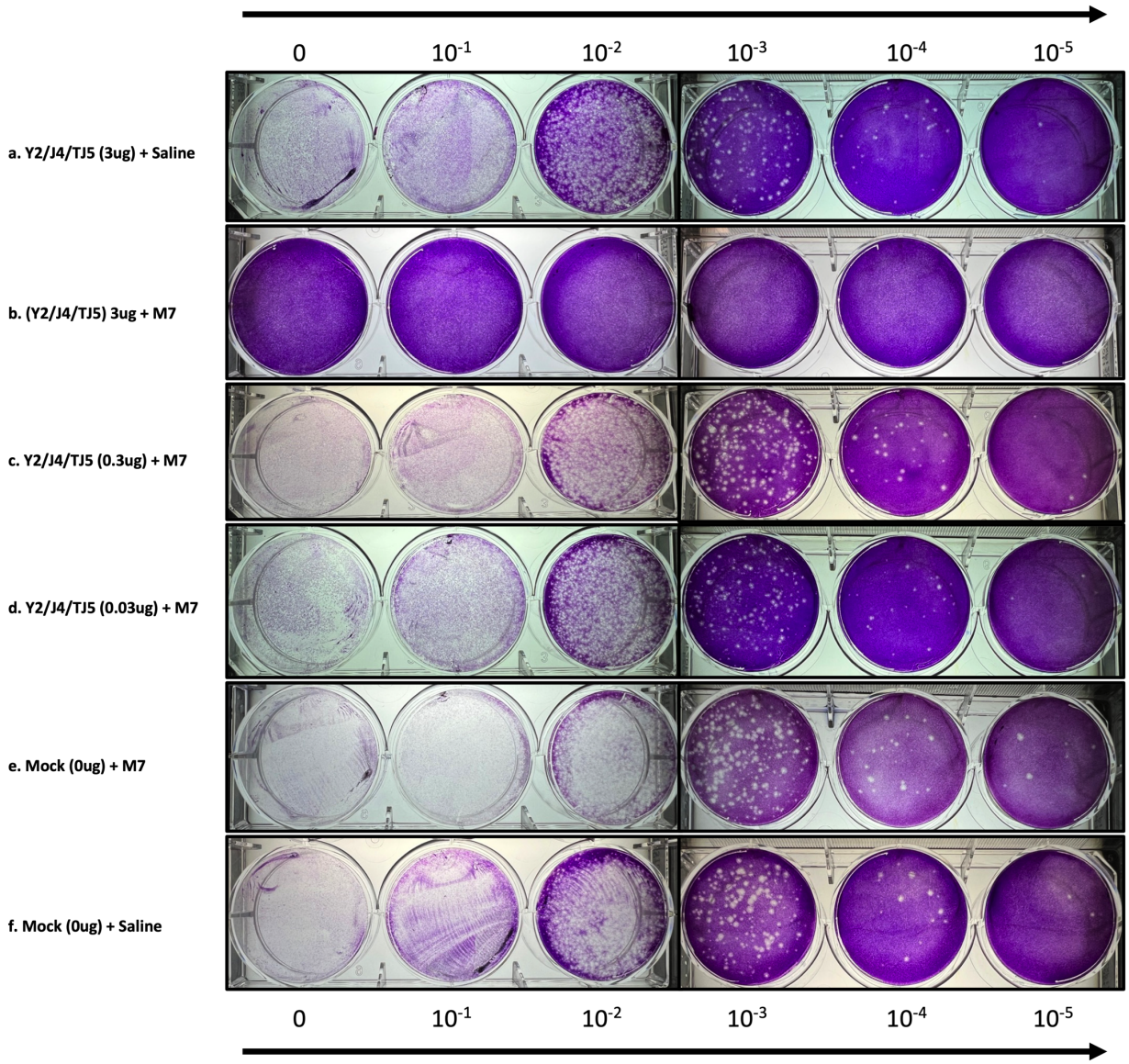

Supplemental Figure 4. 1 Qualitative analysis of viral plaques in vaccinated mice lungs. Bris/18 challenge plaque forming units (PFUs) of day 55 viral lung titer from homogenized lungs of DBA/2J mice vaccinated with (a) COBRA (3 µg) + saline, (b) COBRA (3 µg) + M7-NH_2 (28.436 µg), (c) COBRA (0.3 µg) + M7-NH_2 (28.436 µg), (d) COBRA (0.03 µg) + M7-NH_2 (28.436 µg), (E) Saline + M7-NH_2 (28.436 µg), or (F) Saline only, on the Y-axis. On the top and bottom X-axis, the dilution factors are represented from lowest to

highest in the direction of the black arrows (Left to right). The data is represented as counted spots multiplied by the dilution factor and divided by 0.1mL of lung homogenates.

CHAPTER 5

COBRA (H1) HEMAGGLUTININ INFLUENZA VACCINES ADJUVANTED WITH TLR4 OR TLR7/8 AGONISTS[1]

[1]Sanchez, Pedro L. and Ross, Ted M. "COBRA (H1) Hemagglutinin Influenza Vaccines Adjuvanted with TLR4 or TLR7/8 Agonists". To be submitted to a peer-reviewed journal.

Abstract

Adjuvants enhance, prolong, and modulate immune responses by vaccine antigens to maximize protective immunity and enable more effective immunization in the young and elderly. The goal is to enhanced immunogenicity and allow for antigen dose-sparing through the reduction of viral proteins used for vaccination. Limiting the reactogenicity associated with adjuvants and reducing the number of boosters remain concerns in vaccine development. In this study, a next-generation of broadly-reactive or universal influenza hemagglutinin (HA) vaccines were developed using the Computationally Optimized Broadly Reactive Antigen (COBRA) methodology. These HA vaccines were formulated with different toll-like receptor agonists (TLR4/7/8) to determine the protective efficacy against a panel of influenza viruses and the elicited immune responses were compared to COBRA alone or Mock. The synthetic TLR4 (INI 2001) and TLR7/8 (INI 4001) agonists were delivered in emulsion, liposomal, or aqueous formulations. It was hypothesized that INI 2001 or INI 4001 agonists would enhance COBRA HA vaccine efficiency, regardless of formulation used, compared to unadjuvanted vaccines or mock-vaccinations. Mice were vaccinated with each COBRA HA-adjuvant formulation and both immune responses and protection against viral challenge were assessed. Vaccinated mice had antibodies with high HAI activity against H1N1 influenza viruses. Regardless of INI 2001 or INI 4001 agonist formulations used, mice were protected against morbidity, including lung inflammation, and mortality following challenge with an H1N1 influenza virus. These mice also had significantly reduced or undetectable viral lung titers. Adjuvanted-vaccines induced Th1 or Th2 skewed or Th0 immune responses with robust IgG antibodies in the sera. In

conclusion, TLR INI 2001 and INI 4001 agonists enhanced the immunogenicity of COBRA HA vaccines and protected against H1N1 influenza virus infection.

Introduction

Influenza viruses are part of the family *Orthomyxoviridae* and cause annual respiratory infections that can lead to hospitalization and fatal outcomes [191], [192]. Influenza viruses can undergo antigenic drift and shift [193], [194], thus allowing these viruses to evade host immune responses directed against the viral glycoproteins hemagglutinin (HA) and neuraminidase (NA), which are located on the virion surfaces [6], [195], [196]. Since influenza A viruses (IAVs) are ever-changing, designing effective vaccines against influenza remains a challenge in the field of vaccine development. Each season, wild-type (WT) influenza strains are selected for vaccine formulation and are not necessarily matched to circulating influenza virus strains, thus compromising the effectiveness of the vaccine [10], [8]. Most commercially-available influenza vaccines are based on split-inactivated virus, recombinant hemagglutinin or live-attenuated influenza virus (LAIV) platforms that induce protective immune responses through various mechanisms, including increased serum neutralizing antibodies in the case of the non-live platforms and enhance mucosal immunity in the case of LAIV [197], [198]. Adjuvants are molecular entities that enhance immune responses when co-administered with vaccine antigens [199], [200]. Currently, the squalene oil-in-water emulsion, MF59, is the only adjuvant included in an FDA-licensed influenza vaccine which is indicated for use in the elderly [201], [202]. AddaVax (SE adjuvant) is a commercially-available squalene oil-in-water adjuvant designed to replicate MF59 [203], [204]. Although squalene-oil-in-water adjuvant are effective at recruiting immune cells to the site of vaccination for enhancing vaccine-induced responses, the use of TLR agonists that directly activate innate immune

cells for bridging and modulating the adaptive immune response has been explored extensively. [50], [227], [228].

To meet the need for a next-generation influenza vaccines, our group has previously developed novel antigens, referred to as computationally optimized broadly reactive antigen (COBRA). This method was utilized for synthesizing rHA and rNA proteins, capable of stimulating antibodies that induce broad responses, for providing long lasting protection against influenza virus strains that have undergone antigenic drift [77]. COBRA HA and NA virus-like particle vaccines stimulate antibodies with protective HAI and NAI responses against influenza A and B viruses in several animal models, including rodents, ferrets, and monkeys following vaccination [10], [9], [11], [13], [205]. Adjuvants may be particularly useful to enhance vaccine immunogenicity in groups that are at higher risks, such as children with untrained immune systems or the immunosenescence as observed in the elderly [9], [77], [206]. This study aimed to enhance the immune responses elicited by COBRA HA antigens by adjuvanting the vaccines with Toll-like receptor (TLR) 4 agonist (INI 2002) which is a synthetic monophosphoryl Lipid A (MPL) or TLR 7/8 agonist (INI 4001), which is an oxoadenine organic molecule lapidated with a palmitoyl lipid tail [147], [149], [258]. To determine the best strategy for delivering these adjuvants and for achieving optimal responses with COBRA HA vaccines, these adjuvants were formulated in aqueous, liposome, or emulsion formulations. INI-2002 (TLR4) and INI-4001 (TLR7/8) are synthetic TLR agonists that enhances cell-mediated and humoral immune responses in mice [146], [149]. Similar to conventional TLR4 and TLR7/8 agonists, these synthetic TLR agonists signal through the TIR domain–containing adapter–inducing interferon-β (TRIF) and myeloid differentiation factor 88 (MyD88) pathways for inducing Th1 TNF-α-

associated and Th2 IL-6-associated immune responses [149], [259]. Different formulations of INI-2002 or INI-4001 were combined with low doses of recombinant COBRA HA and compared to unadjuvanted COBRA HA vaccines to assess how immune responses induced by HA vaccination and formulated with novel TLR agonists in various formulations elicit the protective anti-influenza immune responses.

Materials and Methods

COBRA HA designs and protein synthesis

COBRA HA antigens corresponding to H1N1 seasonal influenza viruses (IAVs) were developed using the next-generation COBRA methodology [77]. H1 COBRA HA, Y2, was originated by extracting full length HA sequences pertaining to 6232 GISAID wild-type influenza A(H1N1) viruses. H1N1 sequences of infections collected from human isolates ranging between January 1, 2014 to December 31, 2016 were used to download the HA residues 1-566 (Methionine as the first amino acid) from online databases and organized in order of collection date [9]. Soluble COBRA HAs were purified from cells transfected with pcDNA3.1 plasmids expressing a truncated HA gene that was made by substituting the transmembrane domain with a T4 fold-on domain, an Avitag, and a 6× His-tag [210]. Concentrations of the soluble HA molecules were measured via the bicinchoninic acid assay (BCA).

Using amino acids 1 to 521, the HA nucleotide sequence was cloned into a T4 fibritin fold-on domain sequence. Towards the C-terminus of the truncated HA sequence, an Avitag (Avidity LLC, Orlando, FL, USA) and a 6X histidine (HIS) were inserted. Using the ExpiFectamine 293 Transfection Kit (Thermo Fisher Scientific, Waltham, MA, USA),

EXPI239T cells (3 x 10^6 cells/mL) were transfected with purified plasmids. Following the transfections (48-72 hours after), the expressed rHA was confirmed in supernatants and collected 7 days later. The collected rHA containing the HIS-tagged proteins were captured via purification through an immobilized Ni affinity chromatography. The samples were washed with ta buffer (containing 25 mM imidazole, 20 mM $NaPO_4$, 0.5 M NaCl) and then eluted off then column with 5x volumes of buffer containing 250 mM imidazole, 20 mM $NaPO_4$, 0.5 M NaCl. To measure the concentrations of the purified rHA proteins, a bicinchoninic acid assay (BCA) (Thermo Fisher, Waltham, MA, USA) was employed. Additionally, bovine serum albumin (BSA) (Thermo Fisher, Waltham, MA, USA) was used as a standard. To confirm the rHA purity, the proteins were subjected to Sodium dodecyl-sulfate polyacrylamide gel electrophoresis (SDS-PAGE), allowing the samples to run for 30 minutes with 200V. During the run, protein separation was monitored and any contaminates were visualized with Coomassie blue (Thermo Fisher, Waltham, MA, USA).

Vaccinations

DBA/2J female mice (n=140; 6 to 8 weeks in age) were purchased from Jackson Laboratory (Bar Harbor, ME, USA). All of the mice were contained in microisolator cages and had access to drinking water and food. USDA guidelines for laboratory animals were followed for caring for the mice and all of the procedures performed on the mice were reviewed and approved by the University of Georgia Institutional Animal Care and Use Committee (IACUC) (no. A2020 03-007-Y2-A7). Vaccinations and mouse bleeds were carried out as previously described [10]. Prior to starting the study, all of the mice were randomized and separated into different experimental groups with an n=20 per group

(Figure 5. 1a). 3 naïve mice were used as comparers for lung pathology only (no challenge). Prior to vaccination (day 0), serum samples were collected to verify that each mouse was seronegative, having no antibodies against A/California/07/2009 (Cal/09) and A/Brisbane/02/2018 (Bris/18) H1N1 influenza viruses. Red blood cells were isolated from sera by centrifugation at a speed of ten thousand rpm for ten minutes and the sera samples were then stored at -20°C ± 5°C. Some of the mice were vaccinated intramuscularly (IM) with 1.5 μg of Y2 COBRA HA antigen, and adjuvanted with 1μg of INI-2002 (TLR 4) or 10 μg of INI-4001 (TLR 7/8) in aqueous, liposome, or emulsions formulations. Other mice were vaccinated with COBRA HA antigens without adjuvant or the mice pertaining to the control groups were mock vaccinated (no vaccine or adjuvant). (Figure 5. 1b). After the first vaccinations, (Days 14 and 27), all of the mice were bled as before. For boost vaccinations, all of the mice were intramuscularly vaccinated at the 4^{th} week (Day 28), as before. At day 34, 4 mice from each group were humanely euthanized via carbon dioxide asphyxiation followed by secondarily cervical dislocation, and spleens were harvested. After the boost, each mouse was bled on days 53 and 60 and the sera was processed via centrifugation and pooled, prior to storing at -20°C ± 5°C. For challenge (Day 67), the mice were anesthetized and intranasally infected with 3.6 $x10^6$ PFU/50 μL of Bris/18 (H1N1) influenza A virus. Once the mice recovered from anesthesia, they were placed back into their cages and monitored for morbidity, mortality, and clinical signs (0-3; 0=no clinical signs; 1=weight loss 15-<20%; 2=dyspnea; 3=weight loss >20%/failure to respond to external stimulus/severe respiratory distress/neurological signs), for 14 days after. A mean clinical score 3 was considered the endpoint and the animal was humanely euthanized via carbon dioxide asphyxiation followed by secondarily cervical dislocation. At days 70 and

73, vaccinated mice were euthanized as before and lungs were harvested from 4 mice in each group. The right lobes were snap-frozen on dry ice and stored at -80°C for determining viral lung titers and the left lobe for histopathology.

Viral Lung Titers

The protocol used for this plaque assay was followed as previously described [9]. To determine viral lung titers, $1x10^6$ per 10 cm^2 MDCK cells were added to tissue culture plates (Fisher Scientific, Pittsburgh, PA, USA) and placed in a static incubator for twenty-four hours at 37 °C + 5% CO_2 until a monolayer of about ninety-five percent confluency was attained. The weights of each mouse lung was weighed and subjected to homogenizing in DMEM media containing 1 percent penicillin-streptomycin (P/S), in volumes of 10 times the weights of the lungs. Homogenized samples were subsequently centrifuged at one thousand five hundred rpm for ten minutes and serially diluted at 10-folds. For a positive control, Bris/18 virus was also serially diluted at 10-folds. 100 μL of the diluted homogenates or Bris/18 positive control were added to monolayers of MDCK cells to infect them for 60 minutes at RT, with fifteen-minute shaking intervals. Some wells served as negative controls and 100μL of DMEM P/S only was added to them. Following the 60-minute incubation, the supernatants were removed from each well, laved one time with DMEM P/S media, and overlayed with 2mL of a 1:1 solution of 1.6% agarose in 2x cMEM media + TPCK-Trypsin at 1 μg/mL. The plates were then placed in a static incubator for two to five days at 37 °C + 5% CO_2. Upon confirmation of visible cytopathic effects, the agarose was detached and the monolayer of cells were fixed with ten percent formalin for ten minutes at room temperature. Subsequently, the formalin was discarded from each well

and the monolayers were stained for ten to fifteen minutes at RT with one percent Crystal Violet (Fisher Science Education, Waltham, MA, USA). Lastly, following the incubation period, the Crystal Violet was discarded from each well and the monolayers were rinsed with water. The plates were allowed to air-dry and the plaque forming units (PFUs) were determined and calculated as PFU/g of tissue.

Histopathology

At day 70, lungs were harvested from 4 mice in each group. The left lobes of each lung were inflated with 10% neutral formalin to fix the tissues for histopathology and subjected to staining with Hematoxylin and Eosin (H&E) staining on lung slices measuring 5 μm to visualize pathology in the lungs of vaccinated mice versus non-vaccinated mice.

Enzyme-linked Immunosorbent Assay (ELISA)

The ELISA assays were performed as previously described [78]. Total IgG in mice sera and associated binding to COBRA Y2 HA was assessed using in Immulon 4HBX 96-well flat bottom plates (Thermo Fisher Scientific, Waltham, MA, USA). 100μL of COBRA Y2 HA, at 1 μg/mL in carbonate coating buffer (pH 9.4) solution was added to the well of each plate and incubated at 4°C overnight in a humidified chamber. After the incubation, the coating solutions were removed and the wells were blocked for 1.5 hours at 37°C with 200 μL of blocking buffer (BB) containing 4% FBS + 0.05% Tween. The serum samples were made at 1:100 ratio followed by serially diluting (1:3) from an initial 1:500 dilution. After blocking, 100 μL of diluted sera was added to the Y2 HA coated plates and incubated for 1.5 hours at 37°C. After the incubation, the plates were thoroughly

laved, one hundred microliters of secondary goat anti-mouse IgG HRP (Southern Biotech, Birmingham, AL, USA) antibody, diluted 1:4000 in blocking buffer added to each well, followed by statically incubating the plates for 1.5 hours at 37°C. Subsequently, the antibody solution was discarded, each well was thoroughly laved and received one hundred microliters of 1x ABTS (VWR Corporation, Radnor, PA, USA) with static incubation for thirteen minutes at 37°C. Succeeding incubation, fifty microliters of one percent SDS was added to halt the reaction of each well. IgG titers were measured as the optical density (O.D.) of each sample at 414nm with a spectrophotometer (PowerWave XS, BioTek, Santa Clara, CA, USA) utilizing the Gen05 software (version 3.14, https://www.agilent.com/en/support/biotek-software-releases). IgG was compared to positive and negative controls within each plate. To determine the isotypes against Y2 HA, the samples were initially handled as before with subsequent static incubated with secondary goat anti-mouse IgG1, IgG2a or IgG2b antibodies and the O.D. measured as before. For these sets, sera were made at 1:100 ratio and serially diluted (1:3) from a starting 1:500 dilution for isotype determination.

Hemagglutination Inhibition Assay (HAI)

Anti-HA antibodies that are able to block viruses from agglutinating red blood cells (RBC) were assessed from collected sera. The protocol followed the manual for laboratory diagnosis and virological surveillance of influenza published by the World Health Organization (WHO) [211]. HAI activity was tested against Cal/09 and Bris/18 H1N1 influenza viruses. Specific details on how the HAI assay was completed has been described [212]. Concisely, sera from individual mice were mixed with receptor destroying enzyme

(RDE) (Denka Seiken, Co., Tokyo, Japan) and diluted 10-fold by reconstituting one hundred microliters of serum with three volumes of RDE in 1x PBS. The reconstituted samples where then incubated at 37°C overnight. After overnight incubation, the treated sera were heat inactivated in a water bath at 56°C for forty-five minutes, allowed to cooled to RT, followed by adding 6 volumes of 1x PBS. 96-well plates (v-bottoms) containing 25 μL of PBS was used to serially diluted the RDE-treated sera samples, in duplicates. 1:8 solutions of each virus to be tested was added to the plates with serially diluted sera samples and incubated at RT for twenty minutes. After the incubation, samples received 0.8% turkey RBC (TRBCs), were manually agitated, followed by incubated at RT for thirty minutes. Subsequently, the reciprocal dilutions of the last wells that ran (no agglutination) were reported as the titers. A 1:40 titer was the measurement of seroprotection as per the European Medicines Agency Guidelines on Influenza Vaccines [213].

FluoroSpot Assay

The FluoroSpot assays were performed as previously described [78]. On day 34, spleens were collected (n=4) per study arm. Following homogenization, splenocytes were washed twice with RPMI 1640 BCM Medium (Gibco™, Grand Island, New York, USA) and centrifuged at 400G for 10 min at 4°C. After the second wash, the BCM media was discarded and the cell pellets were resuspended in 4 mL of 90% FBS/10%DMSO freezing media and aliquoted into cryotubes for storage at -80°C overnight, and then transferred to LN_2 for future use. To assess antigen-specific antibody secreting cells (ASCs), the three Color Immunospot® kit (CTL, Shaker Heights, OH, USA) was employed. Following the manufacturer's instructions, *in vivo* pre-stimulated splenocytes were washed with BCM

and filtered through 70 μm MACS® SmartStrainers to removed debris. In v-bottom, 96-well plates, splenocytes were serially diluted 3-fold, in duplicates, starting at 3 x 10^5 live cells per well and transferred to pre-treated (with 70% ethanol) PVDF plates, coated with Y2 or BSA at 25 μg/mL, or 1 x 10^5 live cells per well for anti-Igκ/λ capture antibody coated plates, in Diluent A. The diluent A solution was provided in the Immunospot kit. Following the addition of splenocytes to the wells, the plates were incubated in a humidified chamber with 5% CO_2 for 16-18 hours at 37°C, as per the manufacturer's instructions. Following incubation, the ASCs were removed and the plates were washed twice with 1x PBS. An anti-mouse detection solution containing IgG1/IgG2a/IgG2b was prepared and added to each well, followed by a 2h incubation in the dark, at room temperature (RT). After the incubation period, the plates were washed twice with PBS-T, follow by the addition of a prepared tertiary solution and incubated for 1h in the dark, at RT. After incubation, the plates were decanted, washed twice with distilled water, and allowed to dry overnight in a dark, running laminar flow hood, face down on paper. FluoroSpot detection was achieved upon reading the plates on the ImmunoSpot® S6 Ultimate Analyzer. Spot-forming-units (SFUs) were enumerated using the Basic Count mode of the CTL ImmunoSpot SC Studio (Version 1.6.2, Shaker Heights, OH, USA).

Results

TLR4 or TLR7/8 agonists with COBRA HA vaccines protect mice against influenza virus challenge

DBA/2J mice were divided into eight study arms and vaccinated intramuscularly following prime-boost regimens. Each mouse was challenge intranasally with 3.6 x 10^6

PFU of Bris/18 H1N1 after boost (Figure 5. 1a-b). Control mice mock-immunized mice lost an average of 24% of their original body weight by day 6 post-infection, with a mean clinical score of 3 and all succumbing to infection by day 6 post-infection. All of the mice vaccinated with COBRA HA proteins formulated with INI 2002 in the aqueous formulation and challenged with Bris/18 lost an average of 2.75% of their original body weight by day 3, had no clinical signs, and all survived viral challenge. All of the mice vaccinated with COBRA HA proteins formulated with INI 2002 in the liposome formulation lost an average of 4.1% of their original body weight by day 3, had no clinical signs, and all survived viral challenge. All of the mice vaccinated with COBRA HA proteins formulated with INI 2002 in the emulsion formulation lost an average of 5.42% of their original body weight by day 4, had an average clinical score of 0.3 by day 6, and ~87% survived challenge (Figure 5. 2a-b). All of the mice vaccinated with COBRA HA proteins formulated with INI 4001 in the aqueous formulation lost an average of 8.87% of their original body weight by day 3, had no clinical signs, and all survived viral challenge. All of the mice vaccinated with COBRA HA proteins formulated with INI 4001 in the liposome formulation lost an average of 9.57% of their original body weight by day 3, had no clinical signs, and all survived viral challenge. All of the mice vaccinated with COBRA HA proteins formulated with INI 4001 in the emulsion formulation lost an average of 4.1% of their original body weight by day 3, had no clinical signs, and all survived viral challenge (Figure 5. 2c-d). Mice vaccinated with COBRA HA alone lost an average of 21.82% of their original weight loss by day 6 post-infection with the survivors in this group slowly returning to their original body weight by day 14 post-infection, with a mean clinical score of 1.8 and only 33% survival (Figure 5. 2a-d).

Three or four mice in each group were sacrificed at day 3 post-infection for assessment of lung virus titers and lung pathology. None of the mice vaccinated with the COBRA HA plus INI 2002 agonist in the aqueous formulation had detectable lung titers, whereas two out of the four mice vaccinated with COBRA HA plus INI 2002 agonist in the liposome formulation had low viral titers (4 x 10^2 pfu/g of tissue) and one mouse vaccinated with COBRA HA plus INI 2002 agonist in the emulsion formulation had a viral titer of 1.6 x 10^3 pfu/g of tissue. Two mice vaccinated with COBRA HA vaccines with INI 4001 agonist in the aqueous formulation had lung viral titers between 2-4 x 10^2 pfu/g of tissue, and mice vaccinated with COBRA HA vaccines with INI 4001 agonist in the liposome formulation had lung viral titers between 1.8 x 10^3–3.7 x 10^5 pfu/g of tissue. None of the mice vaccinated with COBRA HA vaccines with INI 4001 agonist in the emulsion formulation had detectable viral lung titers. In contrast, mice vaccinated with COBRA HA alone had lung viral titer between 1.3 x 10^5–1.56 x 10^6 pfu/g of tissue. Additionally, control mock-vaccinated mice (no vaccine and no adjuvant) had high viral lung titers (1x10^6 pfu/g of tissue) (Figure 5. 3).

TLR4 or TLR7/8 agonists with COBRA HA vaccines protect mice from developing lung pathology following influenza infection

Following challenge with Bris/18 H1N1 influenza virus, lungs from mice were harvested 3 days post-infection for histopathology. The levels of inflammatory cell infiltration were measured as having 0%, <25%, 25-50%, 50-75%, or >75% of affected lung tissue. Mice vaccinated with COBRA HA proteins plus INI 2002 or INI 4001 agonists, regardless of formulation (except for the INI 4001 liposome formulation), were protected

from inflammation of their lungs, having no inflammatory cell infiltration (0%) as observed in the upper or lower lungs, following challenge with Bris/18 (Figure 5. 4a-c and e). This observation was similar to normal lungs of unchallenged and un-vaccinated mice that had no evidence of inflammatory cell infiltration (Figure 5. 4h). In contrast, mice vaccinated with COBRA HA alone (Figure 5. 4d) or with COBRA HA with INI 4001 agonist in the liposome formulation (Figure 5. 4f) had increased lung inflammatory cell infiltration (~50-60%), which was decreased, compared to mock immunized mice that had increased inflammatory cell infiltration (~70-80%).

Serum anti-influenza HA IgG following vaccination with TLR4 or TLR7/8 agonists

To assess the anti-influenza HA binding antibodies elicited by each vaccine formulation, sera was collected from mice following the booster vaccination at week 8 (days 53 and 60) and was pooled according to group for assessment of total anti-Y2 IgG titers (Figure 5. 5a-b). Mice vaccinated with COBRA HA with INI 2002 or INI 4001 agonists, regardless of formulation, had higher total anti-HA IgG titers against Y2 HA than sera collected from mice vaccinated with COBRA HA only with no adjuvant (Figure 5. 5a). Mice vaccinated with COBRA HA with INI 2002 or INI 4001 agonists had enhanced IgG1, IgG2a, and IgG2b subclasses compared to mice that received unadjuvanted COBRA HA (Figure 5. 5b). These mice had low IgG1 and IgG2a antibodies, with no detectable IgG2b against Y2 HA. Mock-vaccinated mice had no detectable serum antibodies.

TLR4 or TLR7/8 agonists enhance serum hemagglutination-inhibition (HAI) titers in vaccinated mice

Vaccinated mice had sera capable of blocking H1N1 influenza viruses from agglutinating RBCs. 88-100% of mice vaccinated with COBRA HA antigens with INI 2002 agonists, regardless of formulation, had ≥1:40 serum HAI titers against the Cal/09 and Bris/18 H1N1 influenza viruses (Figure 5. 6a). 81-100% of mice vaccinated with INI 4001 in the aqueous and emulsion formulations had ≥1:40 HAI titers against Cal/09 and Bris/18 H1N1 influenza viruses, whereas ~50% of the mice vaccinated with COBRA HA antigens with INI 4001 agonists in the liposome formulation had ≥1:40 (Figure 5. 6b). In contrast, only 40-50% of the mice vaccinated with the COBRA HA vaccine alone had HAI responses ≥1:40 against the two H1N1 influenza viruses (Figure 5. 6a-b). None of the mock-vaccinated mice (no vaccine and no adjuvant), developed serum HAI titers against either H1N1 influenza virus.

TLR4 or TLR7/8 agonists drive production of IgG1, IgG2a, and IgG2b antibody-secreting cells

IgG1, IgG2a, and IgG2b antibody secreting cells (ASC) were identified in the spleens of mice harvested 6 days post-boost vaccination with COBRA HA proteins with INI 2002 or INI 4001 agonists in various formulations. ASC of these mice vaccinated with COBRA HA proteins with INI agonists, regardless of formulation, secreted total IgG1, IgG2a, and IgG2b antibodies that bound to anti-Igκ/λ capture antibody (Figure 5. 7a) with specificity to Y2 HA antigens (Figure 5. 7b). ASC from mice vaccinated with COBRA HA proteins with INI 4001 agonists in the aqueous or liposome formulations, secreted primary

total IgG1 and IgG2a, with some IgG2b antibodies (Figure 5. 7c), with some specificity to Y2 HA (Figure 5. 7d). ASC from mice vaccinated with COBRA HA proteins with INI 4001 agonists in the emulsion formulation, secreted primary total IgG1 and some IgG2a, with no IgG2b antibodies (Figure 5. 7c), and specific IgG1, IgG2a, and IgG2b against Y2 HA (**Error! Reference source not found.**d). Mice vaccinated with unadjuvanted COBRA HA vaccines had little to no total or Y2-specific ASCs, and mock-vaccinated control mice had no ASC (Figure 5. 7a-d).

Discussion

The first adjuvanted influenza vaccine using MF59, a squalene oil-in-water adjuvant, was approved in 1997 and now is used in 38 countries for people 65 years and older [125], [221], [222]. Mixing MF59 to the FLUAD influenza virus vaccine broadens the immune responses and allows for increased protection against drifted influenza viruses [115], [223], [224]. Although squalene-oil-in-water adjuvants are effective at recruiting immune cells to the site of vaccination for enhancing vaccine-induced responses, the use of TLR agonists directly activates innate immune cells for bridging and modulating the adaptive immune response [50], [227], [228]. TLRs are activated through pathogen-associated molecular patterns (PAMPs) that can be found inside and outside of many host cells, including APCs. Specifically, TLR4 are located at the surface of cells, whereas TLR7/8 are located within endosome inside of cells, and when activated by PAMPs, induce Th1 biased immune responses [260], [261]. Influenza viruses have single-stranded RNAs that are recognized by TLR7/8, making agonists of these PRRs suitable targets for influenza virus vaccines [147].

Upon stimulation, TLR4 and TLR7/8 induce the MyD88 and TRIF molecular pathways to induce the production of pro-inflammatory cytokines and antiviral IFN [260], [262]. Currently, monophosphosphoryl lipid A (MPLA) TLR4 agonist and TLR7/8 imiquimod (IMQ) agonist are approved by the FDA and have been effective when mixed with vaccines against hepatitis B and human papilloma virus (TLR4 agonist) and when used as a drug-treatment (chemotherapy) for cancer in humans (TLR7/8 agonist) [260], [262]. In this study, a novel synthetic TLR4 agonist, INI 2002 (a synthetic monophosphoryl Lipid A (MPL)), and a novel synthetic TLR7/8 agonist, INI-4001 (an oxoadenine organic molecule lapidated with a palmitoyl lipid tail) [147], [258], [263], that were formulated as aqueous, liposome, or emulsion adjuvants, were used to adjuvant COBRA HA vaccines and intramuscularly administered to mice.

Following two vaccinations of mice with COBRA HA vaccines plus INI 2002, regardless of formulation, these animals had high antibody titers in their serum that blocked Cal/09 and Bris/18 influenza viruses from binding and agglutinating RBCs. Additionally, these mice had enhanced total IgG, IgG1, IgG2a, and IgG2b antibodies that were specific to Y2 HA, with bias to Th1 or Th1/Th2 responses. Moreover, this groups had ASC in their spleens that were also specific to Y2 HA. In terms of protection, all of these vaccinated mice were challenged with Bris/18 H1N1 influenza virus to measure the level of morbidity and mortality after vaccination. The mice that were vaccinated with COBRA HA vaccines with INI 2002 in the aqueous formulation and little to no weight loss, no clinical signs, no lung inflammation, and lead to a 100% survival. Additionally, these mice had no detectable viral lung titers. The mice that were vaccinated with COBRA HA vaccines with INI 2002 in the liposome formulation had little to no weight loss, no clinical signs, no lung

inflammation, and had 100% survival. However, two out of the four mice that were vaccinated with COBRA HA vaccines with INI 2002 in the liposome formulation had detectable viral lung titers, although these were significantly lower than mice vaccinated with un-adjuvanted vaccines. Furthermore, one mouse out of the four that were vaccinated with COBR HA vaccines with INI 2002 in the emulsion formulation had detectable viral lung titers that were still significantly lower than mice vaccinated with un-adjuvanted vaccines, while the other three mice in this group had no detectable viral lung titers. The mice in this group have little to no clinical signs, no lung inflammation, and 87% survival, post-infection. Similarly, mice that were vaccinated with COBRA HA vaccines with INI 4001 in the aqueous or emulsion formulations, also had enhanced HAI activity against Cal/09 and Bris/18 H1N1 influenza viruses, with high total and Y2 HA-specific IgG, IgG1, IgG2a, and IgG2b in their serum. Moreover, about 50% of the mice that were vaccinated with COBRA HA vaccines with INI 4001 in the liposome formulation had protective HAI activity against Cal/09 and Bris/18 while the others had HAI titers below 1:40. Concurrently, these mice still had enhanced serum total IgG, IgG1, IgG2a, and IgG2b Y2 HA-specific antibodies, with a bias to Th1 or Th1/Th2 responses. Moreover, this group had ASC in their spleens that were also specific to Y2 HA, especially those vaccinated with COBRA HA vaccines with INI 4001 in the emulsion formulation. In terms of protection following influenza challenge, the mice that were vaccinated with COBRA HA vaccines with INI 4001 in the emulsion formulation had no detectable viral lung titers, whereas two out of four mice vaccinated with COBRA HA vaccines with INI 4001 in the aqueous formulation had low and significantly reduced viral tiers, while the other two had no detectable viral lung titers. In contrast, mice vaccinated with COBRA HA vaccines with

INI 4001 in the liposome formulation had lung inflammation and all of the mice had increased viral lung titers, although it was still significantly lower than mice vaccinated with un-adjuvanted COBRA HA vaccines. In terms of HAI activity, only about 40-50% of mice that were vaccinated with COBRA HA vaccines alone, had antibodies in their serum that blocked Cal/09 and Bris/18 H1N1 influenza viruses from binding and agglutinating RBCs. This same vaccine group still had total serum Y2-specific IgG and IgG1 and IgG2a, although lower than all the adjuvanted vaccines tested in this study. Additionally, these mice had lower vaccine-induced ASC cells in their spleens. After infecting these mice with Bris/18 H1N1 influenza virus, significant weight loss and clinical scores were observed that peaked around day 6 post-infection, thus some of the mice succumbing to infection with only a 33% survival.

Unfortunately, naturally derived TLR agonists are often difficult to synthesize due to their complexity, bringing forward a challenge in the development of these molecules for use as adjuvants [264]. Liposome and emulsions are vehicles that when combined with immunostimulatory adjuvants, such as TLR agonists, form an adjuvant system that can enhance the overall adjuvanticity of the formulation [264], [265]. The findings in this study demonstrate that the novel and synthetic TLR4 and TLR7/8 agonists used to vaccinate mice enhanced the efficacy of COBRA HA vaccines, regardless of formulation used, possibly due to a constant release of adjuvant from liposome or emulsions, or the readily available aqueous formulated adjuvants, at the site of vaccination. Regardless, these different formulations where able to enhance the immunogenicity of COBRA HA vaccines that translated to protection against influenza infection. These outcomes thus provide multiple options to meet the need of vaccine development where INI 2002 and INI 4001 agonists

can be formulation into liposome or emulsion for protecting them from degradation and providing for longer stability, increased potency, and increased shelf life [266], [267], [268]. Also important were the vaccine-induced antibody responses seen in this study that are in line with what has been previously shown using these adjuvants in mice [146], [149]. Additionally, these adjuvants allow for a dose-sparing effect [146] which was demonstrated in this study involving the use of a low doses of COBRA HA vaccines, while still allowing for enhanced vaccine efficacy.

Herein, the focus of this study was to determine the optimal TLR4 or TLR7/8 adjuvant formulations to administer to mice with COBRA HA vaccines. Liposomes are potent inducers of CTLs in mice. Liposomes that contain encapsulated antigens and the addition of Lipid A induce enhanced antibody and CTL responses [269].

Emulsions enhance antibody responses to the emulsified antigens, but do not induce CTL activity. Additionally, CTL responses can be elicited when an antigen is incorporated into the emulsion, as opposed to just mixing the antigen with the preformed emulsion molecules [269].

Activation of TLR7 in plasmacytoid dendritic cell (pDCs) induces the early antiviral effects associated with IFNα [147]. On the other hand, activation of TLR8 in myeloid dendritic cells (mDCs) induces the pro-inflammatory responses [147]. Previous studies reported that the murine

TLR8 is not readily activated by imidazoquinolines, and that oxoadenines are weak TLR8 agonists [147], [270]. This would indicate that INI 4001 induced the early pDC antiviral responses by activating TLR7 (by oxoadenines) and not TLR8 (for pro-inflammatory response) [270], and instead, the liposome or emulsion components may have induced the

pro-inflammatory (by liposome) or antibody responses (by emulsion) that contributed to the significantly reduced morbidity and mortality of the vaccinated mice shown in this study. On the contrary, this could also explain why the mice that were vaccinated with COBRA HA vaccines with INI 4001 in liposome formulation, and lacking the secondary adjuvanticity effects of an emulsion, still had morbidity (increased weight loss, detectable lung viral titers, and inflammation) after influenza virus challenge. However, this vaccine still induced the early pDC TLR7 antiviral effect (by oxoadenines) and pro-inflammatory responses (by liposome) that may have contributed to the significant reduction of morbidity and no mortality, compared to the unadjuvanted COBRA HA vaccines, as seen for this group.

In comparison, when INI 4001 in the aqueous formulation was delivered with the COBRA HA vaccines, the readily available agonists could have be quickly taken up via endocytosis [270], inducing the early antiviral response by pDC TLR7 activation (by oxoadenines) and not by TLR8, and the pro-inflammatory response by the exposed lipidated tail (Palmitoyl) of INI 4001 [147]. However, this group exhibited some weight loss and some viral lung titers, similar to the COBRA-INI 4001 liposome vaccinated mice, hence also lacking the emulsion molecule. However, both the weight loss and viral lung titers were still significantly lower than mice that were vaccinated with the unadjuvanted COBRA HA vaccines.

INI 2002 alone induces both the TRIF (antiviral response) and the MyD88 (pro-inflammatory) pathways via TLR4 [149]. As a result, INI 2002 was effective at eliminating or significantly reducing morbidity and mortality, regardless of formulation, and may have even been further enhanced by the presence of pro-inflammatory and antibody inducers

(liposome or emulsion). This could have potentially led to increased activation and uptake of the COBRA antigens that lead to higher HAI activity and antigen-specific IgG, IgG1, IgG2a, and IgG2b isotype antibodies in the serum of mice that were vaccinated with these vaccines [269]. Additionally, all of these possibilities, in terms of INI 2002 and INI 4001 formulations and stimulation of the varies pathways, correlates with the levels of ASCs. Specifically, INI 4001 may have only induced the early pDC antiviral responses by activating TLR7 (by oxoadenines) and not TLR8, and required an antibody-inducer (emulsion) in order to elicit antigen-specific IgG1, IgG2a, and IgG2b compared to INI 4001 in the aqueous or liposome formulations that lack the antibody-inducer (emulsion). Moreover, INI 2002, having the capacity to induced enhanced immune responses (TRIF (antiviral response) and MyD88 (pro-inflammatory)) at the surface of immune cells, as opposed to having to enter the cell, another limiting factor of INI 4001, elicited enhanced antigen-specific IgG1, IgG2a, and IgG2b, regardless of formulation, compared to INI 4001.

Altogether, the combination of a monovalent COBRA HA vaccine with INI 2002 or INI 4001 agonists provide for a promising next-generation influenza vaccine that can be effective for various populations that will provide the necessary protection needed for subsequent exposures to influenza viruses.

a.

TLR4

GROUP	VACCINE	DOSE	ADJUVANT	FORMULATION	DOSE	ROUTE	Challenge
1	Y2 rHA	1.5 µg	None	N/A	None	IM	Brisbane/18
2	Y2 rHA	1.5 µg	INI-2002	AQUEOUS	1 µg	IM	Brisbane/18
3	Y2 rHA	1.5 µg	INI-2002	LIPOSOME	1 µg	IM	Brisbane/18
4	Y2 rHA	1.5 µg	INI-2002	EMULSION	1 µg	IM	Brisbane/18

TLR7/8

GROUP	VACCINE	DOSE	ADJUVANT	FORMULATION	DOSE	ROUTE	Challenge
5	Y2 rHA	1.5 µg	INI-4001	AQUEOUS	10 µg	IM	Brisbane/18
6	Y2 rHA	1.5 µg	INI-4001	LIPOSOME	10 µg	IM	Brisbane/18
7	Y2 rHA	1.5 µg	INI-4001	EMULSION	10 µg	IM	Brisbane/18
8	None	N/A	None	N/A	N/A	IM	Brisbane/18

b.

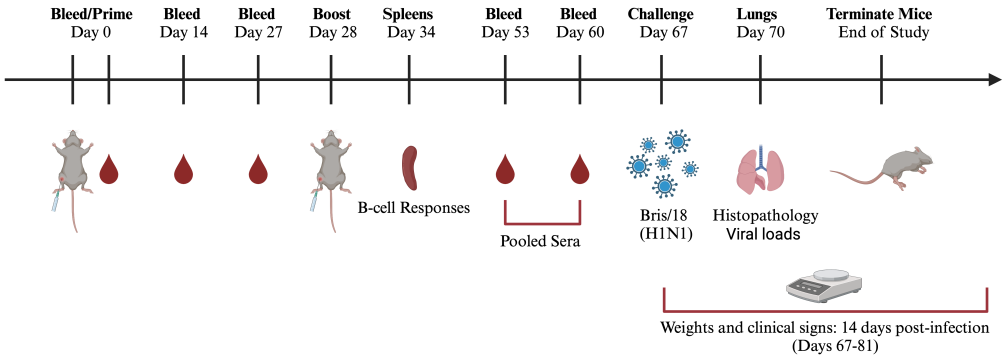

Figure 5. 1 Vaccine regimens and schematic of the study timeline.

Mice were randomly divided into four groups, with n=20 mice in each group, and immunized intramuscularly (IM) with 1.5 µg COBRA Y2 HA protein with (a) 1 µg of INI 2002 or 10 µg of INI 4001 adjuvants in aqueous, liposome or emulsion formulations. As controls, some mice were vaccinated with 1.5 µg COBRA Y2 HA protein alone or with saline only (no vaccine). (b) Schematic of the study timeline. Mice were bled and prime-vaccinated on day 0. On days 14 and 27 the mice were bled, followed by boost-vaccinated on day 28. On day 34, four mice from each group were sacrificed and spleens harvested for B cell FluoroSpot assays. On days 53 and 60 post boost-vaccinations, all of the mice were bled and the serum of each mouse was pooled. Intranasal virus challenge was

performed on day 67 with A/Brisbane/02/2018 (3.6×10^6 PFU/50 μL) influenza virus. Three days post-infection (day 70), lungs were harvested from four mice per group for lung viral titers and pathology, and the remaining mice were monitored for weight loss, clinical signs, and mortality for 14 days post infection.

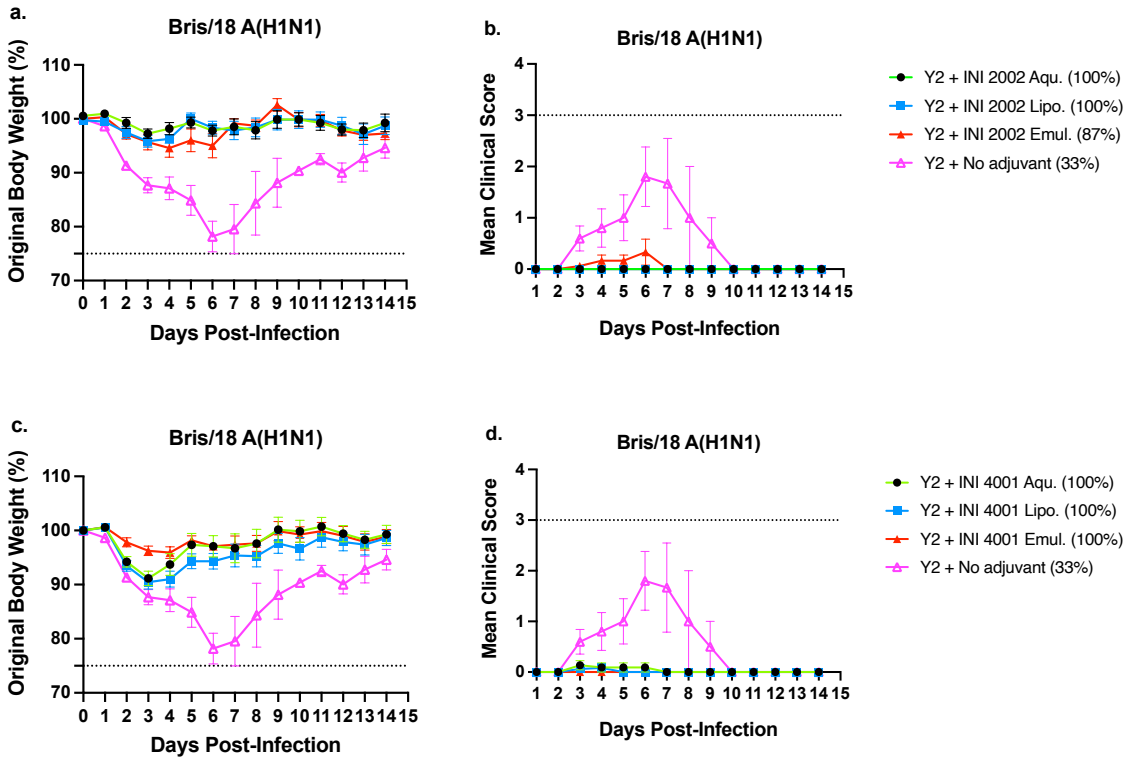

Figure 5. 2 Post-challenge weight loss, clinical signs, and survival of vaccinated mice. Mice were all challenged intranasally (IN) with the H1N1 strain, A/Brisbane/02/2018 (3.6 x 10^6 PFU/50 µL) and observed for 14 days post-infection. (a) Percent of original body weight loss, of INI 2002 groups (b) clinical scores of INI 2002 groups, (c) percent of original body weight loss of INI 4001 groups, and (d) clinical scores of INI 4001 groups. The dotted line in (a and c) represents the 25% weight loss endpoint cutoff. The dotted line in (b and d) represents a mean clinical score of 3. Each line (a-c) is conveyed as the average +/- standard error of the mean (SEM).

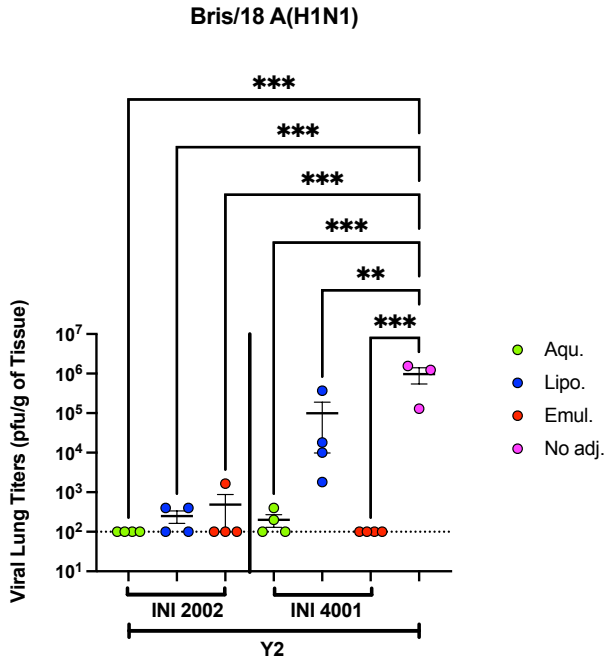

Figure 5. 3 Post-challenge viral lung titers in vaccinated mice.

Lung viral titers of mice 3 days following challenge with A/Brisbane/02/2018. The Y-axis represents the day 3 post-challenge lung viral titers (PFU/g of tissue) and the X-axis represents the vaccine groups. The dotted line represents the limit of detection (LOD). Each column represents dots of 4 or 3 mice per vaccine group and are expressed as the average +/- standard error of the mean (SEM). Viral lung titers were statistically analyzed using nonparametric one-way analysis of variance (ANOVA) by Prism 9 software (GraphPad Software, Inc., San Diego, CA, version 9.4.0, https://www.graphpad.com). A *P* value of less than 0.05 was defined as statistically significant (**, P<0.01; ***).

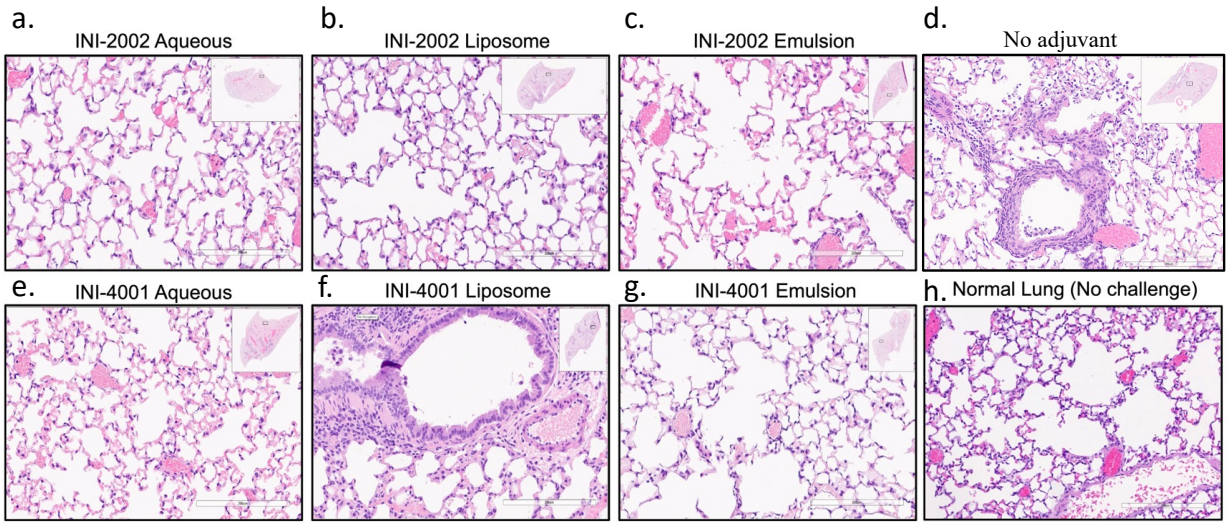

Figure 5. 4 Post-challenge lung pathology of vaccinated mice.

Histopathology of mice lung tissue harvested at 3 days post-infection with H1N1 Brisbane/02/18 influenza virus. The mice were humanely euthanized and their left lungs were infused with 10% formalin for fixing the tissue. Hematoxylin and Eosin (H&E) staining on lung slices measuring 5 µm was used to visualize pathology in the lungs. The lungs are represented at 20x magnification and the lower bar represents 200 um scale. (a-c) COBRA Y2 HA plus various formulations of INI 2002, (d) COBRA Y2 HA with no adjuvant, (e-g) COBRA Y2 HA plus various formulations of INI 4001, and (h) normal, un-vaccinated, no challenge mouse lung.

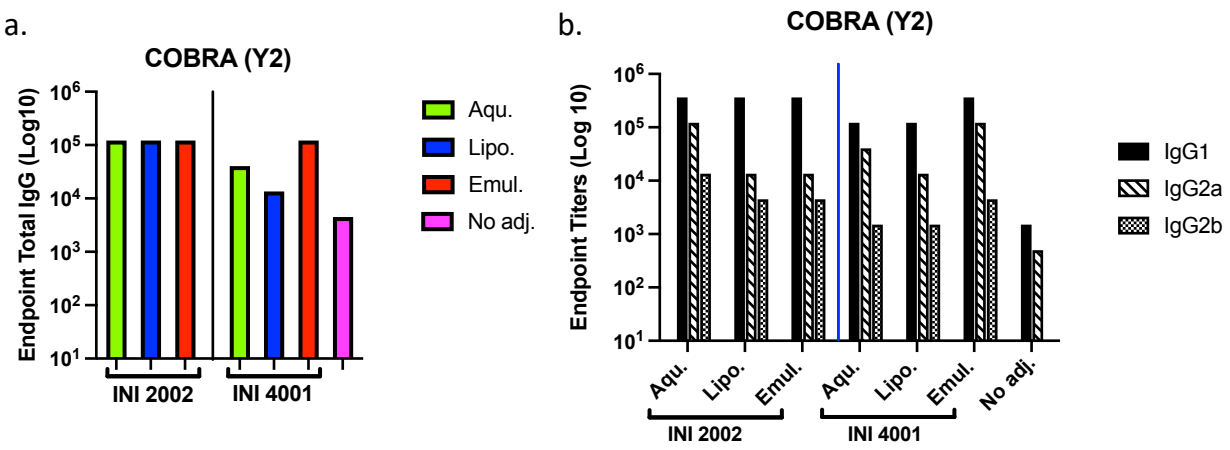

Figure 5. 5 Serum anti-Y2 rHA total IgG, and IgG1, IgG2a, and IgG2b in vaccinated mice. (a) serum total endpoint IgG titers or (b) serum endpoint IgG1, IgG2a, and IgG2b titers against Y2 rHA Represented on the Y-axis are the endpoint titers on a Log_{10} scale. Represented on the X-axis are the different vaccine formulations. Each bar corresponds to day 53/60 pooled serum per each corresponding group collected after boost-vaccinations.

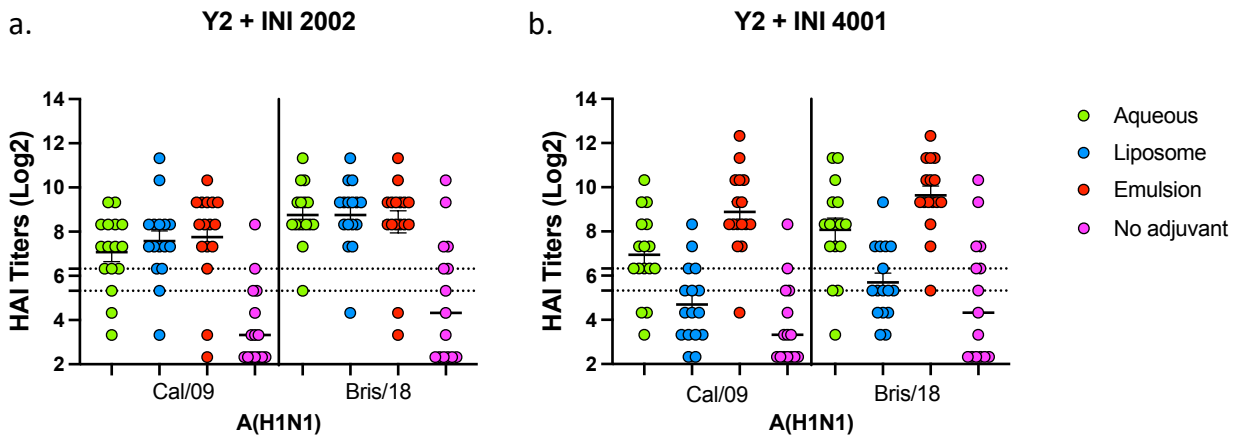

Figure 5. 6 Hemagglutination inhibition activity in mice vaccinated with COBRA HA vaccines (Y2).

Sera collected from immunized mice at days Represented on the Y-axis are the HAI titers on a Log_2 scale. Represented on the X-axis is the panel of H1N1 influenza viruses. The top dotted line indicates a 1:80 HAI titer and the bottom dotted line indicates a 1:40 HAI titer. Each column represents 16 individual mice pertaining to each vaccine regimen and are conveyed as the average +/- standard error of the mean (SEM).

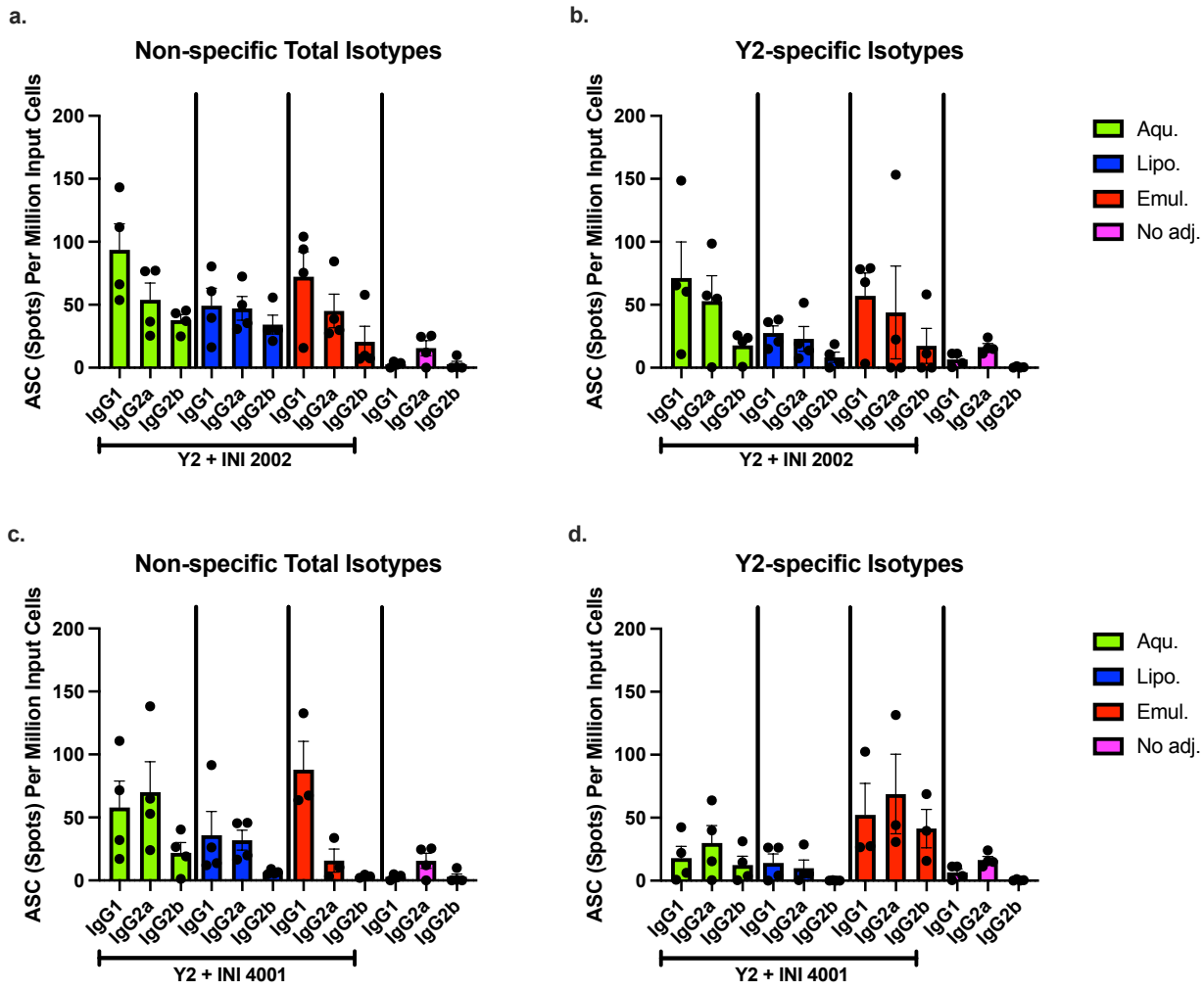

Figure 5. 7 Quantification of total IgG and antigen-specific IgG1, IgG2a, and IgG2b isotypes from antibody secreting cells (ASCs).

Spleens from DBA/2J female mice (6-8 weeks old) were harvested 6 days following boost-vaccinations with COBRA Y2 HA with (a and b) various formulations of INI 2002 or (c and d) various formulations of INI 4001). Plates coated with anti-Igκ/λ (a and c) or Y2 rHA (b and d) were used to detect IgG1, IgG2a, or IgG2b antibodies secreted by ASCs. The Y-axis represents the number of ASCs (spots) per million input cells. The IgG isotypes from ASCs from immunized mice are represented on the X-axis. Represented is an n=4 or

3 of mice per the indicated vaccine regimens and expressed as the average +/- standard error of the mean (SEM).

CHAPTER 6

COBRA (H1/H3/N1/N2) HEMAGGLUTININ AND NEURAMINIDASE INFLUENZA VACCINES ADJUVANTED WITH TLR9 AGONIST[1]

[1]Sanchez, Pedro L. and Ross, Ted M. "COBRA (H1/H3/N1/N2) Hemagglutinin and Neuraminidase Influenza Vaccines Adjuvanted with TLR9 Agonist". To be submitted to a peer-reviewed journal.

Abstract

There is a need for the development of an effective seasonal influenza vaccine that provides broad and long-lasting protection against influenza virus infections. Currently, FLUAD is the only licensed influenza vaccine that is formulated with an adjuvant, which one, and recommended for people 65 years and older. In this study, next generation influenza hemagglutinin (HA) and neuraminidase (NA) vaccine candidates were designed using the Computationally Optimized Broadly Reactive Antigen (COBRA) methodology and formulated with the TLR9 agonist, CpG 1018. These adjuvanted COBRA HA/NA vaccines were administered intramuscularly (IM) or intranasally (IN) to mice with pre-existing anti-influenza immunity or immunologically naive mice. Pre-immune mice that were vaccinated IN with COBRA HA/NA vaccines with CpG 1018 had enhanced IgG titers in their bronchoalveolar lavages (BALF) compared to unadjuvanted vaccines and although this vaccine was administered IN, these mice also had increased IgG titers in their serum, similar to the pre-immune mice that were vaccinated IM. Pre-immune mice that were IN vaccinated with this adjuvanted vaccine also had significantly higher hemagglutination-inhibition activity against a broad range of H1N1 and H3N2 influenza viruses and more antibody secreting cells in their spleens that were specific to WT influenza viruses. Following H1N1 influenza virus infection, pre-immune mice that were vaccinated with COBRA HA/NA vaccine with CpG 1018 were protected from morbidity and mortality and there were no detectable viral lung titers. Overall, CpG 1018 elicited enhanced COBRA HA/NA protective antibodies against several drifted H1N1 and H3N2 influenza viruses in pre-immune mice that were either intramuscularly or intranasally vaccinated, with balanced Th1/Th2 immune responses.

Introduction

Influenza A viruses belong to the family *Orthomyxoviridae* and cause viral respiratory infections. In the United States, it is estimated that 5 to 20% of individuals developed seasonal influenza infections that may cause mild to severe symptoms, including death, and results in approximately 290,000 to 650,000 mortalities around the world [271],[272]. Influenza viruses have several mechanisms to evade the host immune response, including antigenic drift and shift, where the virus particles undergo changes of their surface glycoproteins hemagglutinin (HA) and neuraminidase (NA), thus making these proteins targets for the development of influenza vaccines directed towards these viral components [6]. However, due to the ever-changing strategies of influenza viruses, vaccine development remains a challenge, since yearly vaccines are not always well-matched to circulating virus strains during a given season [273]. Current commercial vaccines include split-inactivated viruses, purified subunit proteins, or live-attenuated virus vaccines [272], [274]. To enhance the effectiveness of licensed vaccines, adjuvants, such as oil-in-water emulsion MF59, have been formulated with vaccines to induce protective immune responses in high-risk populations, including the elderly [275], [276].

Adjuvants are vaccine ingredients that have been used since the 1920s for improving the immunogenicity of vaccine components [83]. Aluminum salt (Alum) precipitates were the first adjuvant used in human Diphtheria Toxoid vaccines and remains effective at inducing protective immune responses [95]. However, overtime, vaccines and classic adjuvants like Alum, have become less efficient as a result of the mutation of viruses, making it possible to evade the host immune systems [81]. Concurrently, there has been an increase in the understanding about the mechanisms of host responses, vaccines,

and adjuvants. Therefore, novel adjuvants that may be more effective than Alum have evolved, including toll-like-receptor (TLR) agonists, such as GLA (glucopyranosyl lipid A) (TLR4) and CpG oligodeoxynucleotides (TLR 9) or saponins (Iscomatrix), all of which have been extensively used with influenza virus vaccines [227]. Additionally, in 1960, the concept of antigenic sin suggested that the immune responses of individuals who were previously infected with native pathogens, are capable of recognizing subsequent infections associated with the same pathogen, or if the pathogen has changed, the initial memory that was developed to a primary infection could potentially contribute to protection against a new variant of the initial pathogen [277]. Thus, this concept is taken into account in terms of how this phenomenon contributes to how yearly influenza vaccines are developed [277]. To date, most influenza vaccines are administered by parenteral injections [247]. However, an intranasal route of vaccination may induce mucosal and systemic immune responses in order to enhance protective immunity in individuals with weak immune systems [248]. Another benefit of intranasal vaccines is they are not associated with pain and are easier to administer compared to the invasive methods used with injectable vaccines, thus likely improving vaccine uptake worldwide [248]. Considering the need for novel effective adjuvants, the concept of the 'original antigenic sin", and exploring the effect of intramuscular or intranasally administered influenza vaccines, the present study involved the use of a TLR 9 agonist (CpG 1018) adjuvant, formulated with hemagglutinin and neuraminidase proteins and compared to unadjuvanted hemagglutinin and neuraminidase proteins in naïve and pre-immune mice via intramuscular or intranasal routes of administration. The novel TLR9 agonists, CpG 1018, is a short 22-mer oligonucleotide sequence containing CpG motifs in rodent, non-human

primates, and humans [178], and has been licensed for use in a hepatitis B virus vaccine HEPLISAV-B® [182]. TLR9 agonists, such as microbial DNA or synthetic CpG oligonucleotides, act via the activation of TLR9 pattern recognition receptors (PRRs), that are located intracellularly within endosomes inside of immune cells, including dendritic cells, B cells, and macrophages [179], [178]. In turn, the activation of TLR9 by CpG 1018 induces the production of pro-inflammatory cytokines, including IFN-γ, that are Th1-biased [178]. However, it is not uncommon for certain classes of CpGs to induce Th2 immune responses [278].

In effort to overcome the annual challenge of influenza vaccination, a computationally optimized broadly reactive antigen (COBRA) design methodology has been used to develop HA and NA molecules that induce the generation of protective broadly-reactive antibodies against drifted influenza virus strains [210], [77], [279]. In previous studies H1, H3, H5, B, and N1 COBRA HA and NA vaccines elicited antibodies with HAI and NAI activity against historical and contemporary influenza A and B viruses in several animal models [10], [279], [11], [12], [13], [14]. To determine the efficacy of COBRA H1, H3, N1, and N2 vaccines adjuvanted with CpG 1018, naïve and pre-immune mice were administered the vaccines intramuscularly or intranasally. The intramuscular or intranasal delivery of COBRA HA and NA proteins with a mixture of CpG enhanced broadly-reactive serum and mucosal antibodies and protected mice against lethal influenza virus infection.

Materials and Methods

Antigen Construction and Synthesis

COBRA hemagglutinin (HA) and neuraminidase (NA) proteins corresponding to H1N1 and H3N2 seasonal influenza viruses (IAVs) were design based on the next-generation COBRA methodology as previously described [14], [77]. Briefly, Y2 (H1) COBRA HA was derived from 6232 full length wild-type influenza A(H1N1) HA protein amino acid sequences, residues 1-566 (starting with methionine as the first amino acid), from human H1N1 virus infections collected from January 1, 2014 to December 31, 2016 were downloaded from the EpiFlu online database and organized by their date of collection [9].

H3 COBRA HA, NG2, was developed using 22,144 full length HA sequences obtained from human wild-type influenza A(H3N2) viruses isolated between January 1, 2016 to December 31, 2018. These sequences represented the HA residues 1-566 (methionine as the first amino acid) from online databases and organized in order of collection [10].

N1-I COBRA NA, N1, originated by extracting full length NA sequences pertaining to 4,891 avian influenza virus isolates ranging between 2000-2015, 3,515 swine influenza virus isolates ranging between 1990-2015, and 9,976 human influenza virus isolates ranging between 2001-2015 [14].

N2-B COBRA NA, N2, was originated by extracting full length NA sequences pertaining to 8,960 human influenza virus isolates ranging between 2000-2019.

COBRA HAs and NAs were purified from cells transfected with pcDNA3.1 plasmids expressing a truncated HA gene that was made by substituting the transmembrane domain with a T4 fold-on domain, an Avitag, and a 6× His-tag [210]. Concentrations of the soluble HA molecules were measured via the bicinchoninic acid assay (BCA).

Using amino acids 1 to 521, the HA nucleotide sequence was cloned into a T4 fibritin fold-on domain sequence. Towards the C-terminus of the truncated HA sequence, an Avitag (Avidity LLC, Orlando, FL, USA) and a 6X histidine (HIS) were inserted. Using the ExpiFectamine 293 Transfection Kit (Thermo Fisher Scientific, Waltham, MA, USA), EXPI239T cells (3 x 10^6 cells/mL) were transfected with purified plasmids. Following the transfections (48-72 hours after), the expressed rHA was confirmed in supernatants and collected 7 days later. The collected rHA containing the HIS-tagged proteins were captured via purification through an immobilized Ni affinity chromatography. The samples were washed with ta buffer (containing 25 mM imidazole, 20 mM $NaPO_4$, 0.5 M NaCl) and then eluted off then column with 5x volumes of buffer containing 250 mM imidazole, 20 mM $NaPO_4$, 0.5 M NaCl. To measure the concentrations of the purified rHA proteins, a bicinchoninic acid assay (BCA) (Thermo Fisher, Waltham, MA, USA) was employed. Additionally, bovine serum albumin (BSA) (Thermo Fisher, Waltham, MA, USA) was used as a standard. To confirm the rHA purity, the proteins were subjected to Sodium dodecyl-sulfate polyacrylamide gel electrophoresis (SDS-PAGE), allowing the samples to run for 30 minutes with 200V. During the run, protein separation was monitored and any contaminates were visualized with Coomassie blue (Thermo Fisher, Waltham, MA, USA).

Vaccination and Infection

DBA/2J female mice (n=128; 6-8 weeks old) were purchased from Jackson Laboratory (Bar Harbor, ME, USA) and housed in microisolator cages with access to food and water. The mice were cared for by USDA guidelines for laboratory animals and all procedures were reviewed and approved by the Institutional Animal Care and Use Committee (IACUC) (no. A2020 03-007-Y1-A0 and LRI2935). Vaccinations, infections, and mouse bleeds were carried out as previously described [10]. Mice were randomly divided into subsets according to routes of administration. Intramuscular (I.M) (Figure 6. 1a-b) or intranasal (I.N.) (Figure 6. 1c), and profile (naïve or pre-immune): three groups (I.M. naïve) with an n=18 per group, three groups (I.M. pre-immune) with an n=18 per group, or two groups (I.N. pre-immune) with an n=10 per group. Prior to vaccination (day 0), all of the mice were bled via the submandibular to confirm seronegative status against seasonal H1N1 influenza viruses, including: A/Singapore/06/1986 (Sing/86), A/Brisbane/59/2007 (Bris/07), A/California/07/2009 (Cal/09), A/Brisbane/02/2018 (Bris/18), A/Guangdong/SWL1536/2019 (GD/19) and H3N2 viruses: A/Panama/2007/1999 (Pan/99), A/Switzerland/9715293/2013 (Swit/13), A/HongKong/4801/2014 (HK/14), A/Singapore/IFNIMH/2016 (Sing/16), A/Kansas/14/2017 (KS/17), A/HongKong/2671/2019 (HK/19), and A/South Astralia/34/2019 (SA/19). On day -28, mice predestined for pre-immunity (Figure 6. 1b-c) were anesthetized with 2-3% isoflurane and received I.N. distillation with 50 μL of $2.5x10^5$ PFU of Sing/86 H1N1 and $2.5x10^5$ PFU of Pan/99 H3N2 influenza A viruses (IAVs). Upon recovery, the mice were returned to their cages and monitored daily for up to 14 days post infection for weight loss, clinical signs, and survival. On day -7 day, some of the mice were

bled and the rest were allowed to rest for 28 days (Figure 6. 1c). After 28 days (Day 0; I.M. and I.N. pre-immune mice) or at day 0 (I.M. naïve mice), some of the mice were bled as before, and all of the mice were either I.M. or I.N. prime-vaccinated (Figure 6. 1a-c) with 50 μL of vaccine formulations containing 3 μg of each of the COBRA rHA and rNA proteins, Y2, NG2, N1, and N2 (COBRA HA/NA), in cold tris buffer solution, and adjuvanted with 10 μg of CpG 1018. As controls, some mice were vaccinated with 50 μL of COBRA HA/NA vaccines without adjuvant (tris buffer only), mock vaccinated with 50 μL of tris buffer only (No vaccine or adjuvant; pre-immunity only), or CpG 1018 alone (tris buffer plus CpG 1018; naïve mice only). Following prime-vaccination, all of the mice were placed back into their cages and monitored. On day fourteen post prime-vaccination, all of the naïve mice were bled (Figure 6. 1a) and sera were separated from blood cells via centrifugation and then stored at -20°C ± 5°C. On day 28 (I.M. naïve and I.N. pre-immune) (Figure 6. 1a,c) or day 62 (I.M. pre-immune) (Figure 6. 1a), all of the mice were boosted as before following the same vaccination regimens and routes of administration. 6 days (I.M. pre-immune mice) or 20 days (I.M. naïve mice) post boost (Figure 6. 1a-b), some of the mice from each group were euthanized and spleens were harvested, homogenized, and stored in 90% fetal bovine serum (FBS) plus 10% dimethyl sulfoxide (DMSO) solution at -80°C for 24 hours and then moved to liquid nitrogen (LN). Concurrently at 7 days (I.N. pre-immune mice) post boost (Figure 6. 1c), some of the mice were euthanized and spleens harvested and processed as before, as well as harvest of lung bronchoalveolar lavage fluids (BALFs). Briefly, the lungs were flushed via the trachea with 450 μL of cold 1x PBS using 23G needles with 22X1 G polyethylene catheters, attached to 1 mL syringes. The samples were placed in sterile microcentrifuge tubes, on ice, followed by centrifugation at 3000 x

g for 5 minutes. After centrifugation, the supernatants were transferred into fresh sterile centrifuge tubes and stored at -20°C ±5°C. Following the boost vaccinations (after 14 and 21 days), all of the DBA/2J mice were bled on days 42 and 48 (I.M. naïve mice), 42 and 49 (I.N. pre-immune mice) or 76 and 83 (I.M. pre-immune mice), as before (Figure 6. 1a-b), and the collected sera was separated by centrifugation in microcentrifuge tubes at 10,000 rpm for 10 min, and both corresponding serum timepoints pooled together equally and then stored at -20°C ±5°C. At day 56 (I.M. naïve and I.N. pre-immune) or day 90 (I.M. pre-immune), all of the mice were anesthetized with 2-3% isoflurane and received I.N. distillation with 50 μL of $8x10^6$ PFU of Bris/18 (H1N1) influenza A virus (Figure 6. 1a-c). Upon recovery, the mice were returned to their cages and monitored daily for 14 days post infection for both morbidity and mortality. At day 59 (I.M. naïve and I.N. pre-immune) or day 93 (I.M. pre-immune), lungs were harvested from some of the mice in each group, snap-frozen on dry ice, and stored at -80°C for determining viral lung titers (Figure 6. 1a-c).

Enzyme-linked Immunosorbant Assay (ELISA)

The ELISA assays were performed as previously described [78]. To assess total IgG antibody reactivity in serum or BALFs from each vaccine group, and its specificity to WT IAV HAs and NAs, Immulon 4HBX 96-well flat bottom plates (Thermo Fisher Scientific, Waltham, MA, USA) were coated with 100 μL of WT Bris/18 (rHA), Bris/18 (rNA), Sing/16 (rHA), or Swit/13 (rNA) at 1 μg/mL in carbonate coating buffer (pH 9.4) and incubated overnight in a humidified chamber at 4°C. Following the incubation, the plates were decanted and blocked with 200 μL, per well, of 4% FBS + 0.05% Tween 20

blocking buffer (BB) in 1x PBS, for 90 minutes at 37°C. During the blocking incubation, serum samples for measuring IgG were prepared at 1:100 ratio and serially diluted (1:3) from an initial 1:500 dilution, or prepared at 1:10 ratio and serially diluted (1:2) from the initial 1:10 for lung lavage. Following blocking completion, 100 µL of each sera diluted sample from individual mice or 50 µL of each lung lavage diluted sample from individual mice, was added to WT Bris/18 HA or NA, Sing/16 HA, or Swit/13 NA coated plates and incubated for 90 min at 37°C. Plates were washed and 100 µL of prepared secondary goat anti-mouse IgG HRP (Southern Biotech, Birmingham, AL, USA), diluted 1:4000 in BB, added to each well, followed by incubation for 90 min at 37°C. After incubation with secondary antibody, the plates were washed and received 100 µL of 1x ABTS (VWR Corporation) solution and incubated for about 13 min at 37°C. After complete colorimetric development, 50 µL 1% SDS solution was added to each well to stop the colorimetric reaction. The optical density (O.D.) of the samples were immediately read at 414nm in a spectrophotometer (PowerWave XS, BioTek) using the Gene05 software (version 3.14, https://www.agilent.com/en/support/biotek-software-releases (accessed on 4 April 2024)) to measure the antibody end-point titers, and compared to positive and negative controls. To further assess specific IgA, IgG1, IgG2a, and IgG2b isotype binding antibodies, samples were processed as before on WT Bris/18 HA or NA, Sing/16 HA, or Swit/13 NA (for sera and lung lavages of individual mice) and incubated with secondary goat anti-mouse IgA, IgG1, IgG2a or IgG2b antibody solutions and measured as before. Lung lavages were prepared at an initial 1:10 and serially diluted (1:2) for detection of IgA, IgG1, IgG2a, and IgG2b.

Hemagglutination Inhibition Assay (HAI)

The HAI assay was performed for the detection of sera antibodies that inhibit binding of influenza viruses from agglutinating red blood cells (RBCs) by preventing binding of viral surface HA to sialic acid residues on RBCs. This protocol was based on the WHO manual for laboratory diagnosis and virological surveillance of influenza [211]. This HAI assay was performed against a panel of H1N1 viruses, including: Sing/86, Bris/07, Cal/09, Bris/18, GD/19 and H3N2 viruses: Pan/99, Swit/13, HK/14, Sing/16, KS/17, HK/19, SA/19. The HAI assay was performed as previously decribed [212]. Sera from each mouse was initially treated with receptor destroying enzyme (RDE) (Denka Seiken, Co., Tokyo Japan) for eliminating non-specific inhibitors. In a deep-well, 96-well block, sera was diluted to $1/10^{th}$ final solutions by reconsituting 100 μL of serum with 3 volumes of RDE in 1x PBS, followed by overnight incubation at 37°C. The following day, the RDE-treated sera was heat inactivated in a water bath at 56°C for 45 minutes, followed by cooling to room temperature (RT) , and the addition of 6 volumes of 1x PBS. In a v-bottom 96-well plate, 25 μL of PBS was added into each well. RDE treated sera was added in duplicates and serially diluted across the plate. Following serial dilutions, each virus was prepared and tested at a 1:8 solution. The plates were incubated at RT for 20 min for H1N1 influenza viruses or 30 min for H3N2 influenza viruses. Following incubation, 0.8% turkey red blood cells (TRBCs) for H1N1 viruses or guinea pig red blood cell (GPRBCs) for H3N2 influenza viruses were added to all of the corresponding wells, mixed by agiation, and then incubated at RT for 30 min (H1N1) or 1 h (H3N2). After incubation, the titer of each serum sample was reported as the reciprocal dilution of the last well without

agglutination. An HAI titer of 1:40 was considered seroprotective as recommeded by the European Medicines Agency Guidelines on Influenza Vaccines [213].

Enzyme-linked Lectin Assay (ELLA)

The ELLA assay was performed as previously described [14]. To assess the ability of vaccinated mice serum to inhibit influenza-specific NA enzymatic activity, flat-bottom 96-well microtiter plates with MaxiSorp surfaces were coated overnight with 100 µL of a 25 µg/mL fetuin (Sigma-Aldrich, St. Louis, MO, USA) in KPL coating buffer (Seracare Life Sciences Inc, Milford, MA, USA) and stored at 4°C until ready for use. Mouse sera samples were serially diluted 2-fold from an initial 1:10 dilution in sample diluent (Dulbecco's phosphate-buffered saline containing 0.133 g/liter CaCl2 and 0.1 g/liter MgCl2 [DPBS], 1% BSA, 0.5% Tween 20). Before adding rNAs, the fetuin-coated plates were washed three times in PBS-T (PBS + 0.05% Tween 20). 50 µL of 2-fold serial dilutions of rNAs and 50 µL of the serially diluted serum samples were added into the fetuin-coated plate containing 50 µL of sample diluent, in duplicates. A negative-control column containing 100 µL of sample diluent only and a positive-control column containing 100 µL of rNAs only, were included. Plates were sealed and incubated for 18 h at 37°C. After incubation, the plates were washed six times with PBS-T, and 100 µL of peanut agglutinin-HRPO (Sigma-Aldrich, St. Louis, MO) diluted 1,000-fold in conjugate diluent (DPBS, 1% BSA) was added to each well, followed by 2 h incubation at RT. After the incubation, the plates were washed three times with PBS-T, and 100 µL (500 µg/mL) of o-phenylenediamine dihydrochloride (OPD); Sigma-Aldrich, St. Louis, MO) in 0.05 M phosphate-citrate buffer with 0.03% sodium perborate pH 5.0 (Sigma-Aldrich, St. Louis,

MO) solution, was added to each well and incubated in the dark for 10 min at RT. The colorimetric reaction was stopped by adding 100 µL of 1 N sulfuric acid per well. The absorbance was read at 490 nm using a spectrophotometer (PowerWave XS, BioTek, Santa Clara, CA, USA) utilizing the Gen05 software (version 3.14, https://www.agilent.com/en/support/biotek-software-releases (accessed on 4 April 2024)). The NA activity was determined after subtracting the mean background absorbance of the negative-control wells and divided by the mean of the positive-control wells. Linear regression analysis was used to determine the dilutions of the Swit/13 and Bris/18 rNAs used in the assay necessary to achieve 90 to 95% NA activity and was used for determining the Log_2 50% titer of the NA inhibition enzyme-linked lectin assays (ELLAs).

Lung Viral Titers

The protocol used for this plaque assay was followed as previously described [9]. MDCK cells were seeded at $1x10^6$ cells per $10cm^2$ and incubated for 24h and grown to ~95% confluency. Day 59 (I.M. naïve), 93 (I.M. pre-immune), or 56 (I.N. pre-immune) lungs from each DBA/2J mouse were weighed and homogenized in DMEM supplemented with 1% penicillin-streptomycin (P/S), 10 times their weights. The lung homogenates where then centrifuged at 1500 rpm for 10 min to remove debris and serially diluted, 10-fold. Additionally, a 10-fold serial dilution of Bris/18 was used as a positive control. The diluted samples were then added to the MDCK monolayers at 100 µL per well, and allowed to infect for one hour, with 15-minute shaking intervals, at RT. Moreover, negative control wells received 100 µL of DMEM P/S only. After one hour of infection, the supernatant from each well was aspirated and the wells were washed once with DMEM P/S, with

removal of media after the wash. Next, 2mL of a 1:1 solution of 1.6% agarose in 2x cMEM media containing TPCK-Trypsin at 1 μg/mL was added to each well and allowed to solidify, followed by incubation for 2-5 days at 37 °C with 5% CO_2. Once cytopathic effects were confirmed, the agarose layers were removed from each well and the cells were fixed with 10% formalin solution for 10 minutes at RT. After the 10 minutes, the formalin was removed and the cells were stained with 1% Crystal Violet (Fisher Science Education, Waltham, MA, USA) at RT, for 10-15 minutes. Following completion of staining, the Crystal Violet was removed and the wells were rinsed in water. The plates were allowed to dry and the plaque forming units (PFUs) were counted, followed by calculation of the lung viral titers as PFU/g of tissue.

FluoroSpot Assay

The FluoroSpot assays were performed as previously described [78]. On day 48 (I.M. naïve), 6 (I.M. pre-immune), or 35 (I.N. pre-immune), spleens were collected (n=3 for I.M. naive and I.M pre-immune) or (n=2 for I.N. pre-immune) per study arm. Following homogenization, splenocytes were washed twice with RPMI 1640 BCM Medium (Gibco™, Grand Island, New York, USA) and centrifuged at 400G for 10 minutes, at 4°C. After the second wash, the BCM media was discarded and the cell pellets were resuspended in 4 mL of 90% FBS/10%DMSO freezing media and aliquoted into cryotubes for storage at -80°C overnight, and then transferred to LN_2 for future use. To assess antigen-specific antibody secreting cells (ASCs), the two Color Immunospot® kit (CTL, Shaker Heights, OH, USA) was employed. Following the manufacturer's instructions, day 48 (I.M. naïve) resting splenocytes were washed with BCM and filtered through 70 μm MACS®

SmartStrainers to removed debris and resuspended in BCM media containing Poly-S for 5-day stimulation. *in vivo* pre-stimulated splenocytes (day 6 and 35 spleens) were washed with BCM and filtered through 70 μm MACS® SmartStrainers to removed debris. In v-bottom, 96-well plates, splenocytes were serially diluted 3-fold, in duplicates, starting at 1 x 10^5 or 3 x 10^5 live cells per well and transferred to pre-treated (with 70% ethanol) PVDF plates, coated with anti-Igκ/λ capture antibody or Bris/18 HA at 25 μg/mL in Diluent A, provided in the Immunospot kit. Following the addition of splenocytes to the wells, the plates were incubated in a humidified chamber with 5% CO_2 for 16-18 hours at 37°C, as per the manufacturer's instructions. Following incubation, the ASCs were removed and the plates were washed twice with 1x PBS. An anti-mouse detection solution containing IgG/IgA was prepared in Diluent B and added to each well, followed by a 2h incubation in the dark, at room temperature (RT). After the incubation period, the plates were washed twice with PBS-T, follow by the addition of a prepared tertiary solution in Diluent C and incubated for 1h in the dark, at RT. After incubation, the plates were decanted, washed twice with distilled water, and allowed to dry overnight in a dark, running laminar flow hood, face down on paper. FluoroSpot detection was achieved upon reading the plates on the ImmunoSpot® S6 Ultimate Analyzer. Spot-forming-units (SFUs) were enumerated using the Basic Count mode of the CTL ImmunoSpot SC Studio (Version 1.6.2, Shaker Heights, OH, USA).

Results

CpG 1018 adjuvant enhances serum and BALF anti-HA/NA antibodies

Serum was collected at 14 weeks and BALF was collected at 5 weeks after the vaccine boost and assessed for anti-HA and anti-NA antibodies. Naïve mice vaccinated with COBRA HA/NA vaccine plus CpG 1018 had sera with endpoint dilution IgG titers between 5×10^2–4.1×10^4 that were similar to naïve mice vaccinated with COBRA HA/NA with no adjuvant (Figure 6. 2a). Pre-immune mice vaccinated intramuscularly with COBRA HA/NA vaccines with CpG 1018 had on average a total IgG endpoint titer against wild-type HA proteins between 1.4×10^4–3.7×10^5 against, which were significantly higher than the titers in intramuscularly vaccinated naïve mice with the same adjuvanted vaccine. These results were similar to pre-immune mice vaccinated IM with COBRA HA/NA vaccine alone (Figure 6. 2a). In addition, pre-immune mice that were vaccinated IN with COBRA HA/NA vaccines formulated with CpG 1018 had detectable anti-HA IgG titers in their serum, ranging between 5×10^2–1.4×10^4 against the WT rHAs and rNAs tested, which were similar to mice vaccinated IN with COBRA HA/NA vaccines alone (Figure 6. 2a). Pre-immune mice that were mock vaccinated (no vaccine or adjuvant) had little to no detectable anti-HA or anti-NA IgG antibodies, except for the Switz/13 N2 NA protein (Figure 6. 2a). Moreover, in IM vaccinated naïve mice, none of the vaccine regimens induced serum IgA antibodies against any of the WT rHAs or rNAs. Pre-immune mice vaccinated IM with COBRA HA/NA vaccines plus CpG 1018 had detectable IgA antibodies in their serum against all WT rHAs and NAs with higher titers than pre-immune mice vaccinated IM with COBRA HA/NA with no adjuvant (Figure 6. 2b). Furthermore,

pre-immune mice that were IN vaccinated with COBRA HA/NA vaccines plus CpG 1018 or COBRA HA/NA antigens alone with no adjuvant did not have detectable IgA titers in their BALFs (Figure 6. 2b).

Additionally, pre-immune mice that were IN vaccinated with COBRA HA/NA vaccines formulated with CpG 1018 also had enhanced IgG titers in their BALFs, whereas when vaccinated without adjuvant, these mice had low to undetectable IgG titers in their BALFs (Figure 6. 3).

The same sera were used to test for antibodies specific to WT IAV Sing/16 and Bris/18 rHAs and Switz/13 and Bris/18 rNAs (Figure 6. 4a-d). Naïve mice vaccinated IM with COBRA HA/NA vaccines with CpG 1018 adjuvant had serum IgG1 titers between 5 x 10^2–4 x 10^4 against all of the rHAs and rNAs tested. They also had IgG2a titers between 5 x 10^2–1.4 x 10^4, and IgG2b titers between 5 x 10^2–1.4 x 10^4 (Figure 6. 4a-d). Naïve mice vaccinated IM with COBRA HA/NA vaccines with no adjuvant had serum IgG1 titers between 1.5 x 10^3–3.6 x 10^5, IgG2a titers between 0–1.4 x 10^4, and IgG2b titers between 0–4 x 10^4. Pre-immune mice that were IM vaccinated with COBRA HA/NA vaccines with CpG 1018 adjuvant had serum IgG1 titers between 4.5 x 10^3–1.3 x 10^5, IgG2a titers between 4.5 x 10^3–3.6 x 10^5, and IgG2b titers between 1.5 x 10^3–4 x10^4 (Figure 6. 4a-d). Pre-immune mice that were vaccinated IM with COBRA HA/NA with no adjuvant had serum IgG1 titers between 4 x 10^4–3.6 x 10^5, IgG2a titers between 4.5 x 10^3–4 x 10^4, and IgG2b titers between 4.5 x 10^3–3.6 x10^5 (Figure 6. 4a-d). Naïve mice vaccinated IM with COBRA HA/NA vaccines with CpG 1018 had balanced IgG1:IgG2a ratio/Th0 immune responses against all of the influenza-specific rHAs and rNAs with an equal distribution of IgG1, IgG2a, and IgG2b (Figure 6. 5a). In contrast, naïve mice vaccinated IM with COBRA

HA/NA vaccines with no adjuvant had a bias to Th2 immune responses against all of the influenza-specific rHAs and rNAs with dominating IgG1 titers (Figure 6. 5a). Pre-immune mice that were vaccinated IM with COBRA HA/NA vaccines with CpG 1018 had balanced Th0 immune responses against all of the influenza-specific rHAs and rNAs with equal distribution of IgG1, IgG2a, and IgG2b (Figure 6. 5b). In contrast, pre-immune mice that were vaccinated IM with COBRA HA/NA vaccines with no adjuvant had a bias to Th2 immune responses against all of the influenza-specific rHAs and rNAs with a dominating IgG1 proportion (Figure 6. 5b).

CpG 1018 adjuvant administered via different routes enhances serum hemagglutination-inhibition (HAI) titers in naïve and pre-immune vaccinated mice

Anti-HA antibodies can block viruses from agglutinating red blood cells (RBC). To determine the HAI activity in the sera of vaccinated mice, the HAI assay was used. Naïve mice were vaccinated IM with COBRA HA/NA vaccines with CpG 1018, with no adjuvant, or with CpG 1018 only. At week 6 and 7, collected sera from several naïve mice that were vaccinated IM with COBRA HA/NA proteins with CpG 1018 or with no adjuvant had titers >1:40 against all three H1N1 influenza viruses tested (Figure 6. 6a). The sera of these same mice did not have HAI activity against the H3N2 influenza virus panel. (Figure 6. 6b). On average, the sera from the majority of pre-immune mice that were vaccinated IM with COBRA HA/NA proteins plus CpG 1018 had HAI titers of $\geq$1:40 against all three H1N1 influenza viruses, while fewer of the pre-immune mice that were vaccinated IM with COBRA HA/NA proteins with no adjuvant had HAI titers of >1:40 against the H1N1 influenza viruses. A similar trend was observed against the H3N2 influenza viruses where

~50% of the pre-immune mice that were vaccinated IM with COBRA HA/NA proteins plus CpG 1018 had HAI titers of ≥1:40 against and to a lesser extent mice vaccinated with un-adjuvanted vaccines. In contrast, all of the pre-immune mice that were vaccinated IN with COBRA HA/NA proteins formulated with CpG 1018 had HAI titers of ≥1:80 against all of the three H1N1 influenza viruses and ≥1:80 against the H3N2 influenza viruses (except HK/19) (Figure 6. 6b).

CpG 1018 adjuvant administered via different routes does not enhance serum neuraminidase-inhibition (NAI) titers in naïve or pre-immune vaccinated mice

The enzymatic activity of NA to cleave sialic acid allows the release of influenza virions. To determine the NA inhibition activity by anti-NA antibodies in vaccinated mice serum, the ELLA assay was employed. Naïve mice were vaccinated IM with COBRA HA/NA proteins with CpG 1018 had detectable NAI titers against Bris/18 rNA, but not against Switz/13 rNA, which had lower NAI activity than mice vaccinated with COBRA HA/NA proteins with no adjuvant (Figure 6. 7). Mice with pre-existing anti-influenza immunity that were vaccinated via either IM or IN routes with the same COBRA vaccines with CpG 1018 had enhanced NAI activity against Switz/13 and Bris/18 rNAs, but had similar NAI activity against the pre-immune mice vaccinated IM or IN with COBRA vaccines with no adjuvant (Figure 6. 7).

COBRA HA/NA vaccines formulated with CpG 1018 protect mice against influenza A virus challenge

Following infection of vaccinated mice, animals were recorded for weight loss, clinical scores, survival, and viral lung titers were assessed. Naïve mice vaccinated IM with COBRA HA/NA vaccines with CpG 1018 lost an average of ~20% of their original body weights by day 4 post-infection with mean clinical scores between 1.8–3, with 50% survival (Figure 6. 8a). Naive mice IM vaccinated with COBRA HA/NA vaccines with no adjuvant lost an average ~14% of their original body weight by day 4 post-infection and had a mean clinical score of 1 by day 6 post-infection, with 50% survival. Naïve mice mock-vaccinated IM with CpG 1018 lost an average ~25% of their original body weight, with a mean clinical score of 3 and reached their endpoint by day 6 post-infection, with 0% survival (Figure 6. 8a).

Pre-immune mice vaccinated IM with COBRA HA/NA vaccines with CpG 1018 lost an average of ~10% of their original body weight by day 3 post-infection with clinical scores of 0 and 100% survival (Figure 6. 8b). Pre-immune mice vaccinated IM with COBRA HA/NA vaccines with no adjuvant lost an average of ~9% of their original body weight by day 3 post-infection with clinical scores of 0 and 100% survival. In comparison, pre-immune, IM mock-vaccinated mice, lost an average ~22% of their original body weight with a mean clinical score of 1.8 by day 6 post-infection, with ~38% survival (Figure 6. 8b).

Pre-immune mice vaccinated IN with COBRA HA/NA vaccines with CpG 1018 only lost an average ~4% of their original body weights by day 7 post-infection with no clinical scores, and had 100% survival. Pre-immune mice vaccinated IN with COBRA

HA/NA vaccines with no adjuvant lost an average ~9.5% of their original body weight with a mean clinical score of 0.25 by day 10 post-infection and had 100% survival. Pre-immune, IN mock-vaccinated mice, lost an average ~22% of their original body weight with a mean clinical score of 1.8 by day 6 post-infection and had ~38% survival (Figure 6. 8c).

At 3 days post-infection following Bris/18 influenza virus challenge, naive mice vaccinated IM with COBRA HA/NA vaccines with CpG 1018 had reduced viral lung titers between 6.0×10^2 to 5.0×10^3 pfu/g of tissue compared to naive mice vaccinated IM with COBRA HA/NA vaccines with no adjuvant had viral lung titers between 5.0×10^3 to 5.0×10^4 pfu/g of tissue (Figure 6. 9). One mouse vaccinated IM with COBRA HA/NA vaccines with CpG 1018 and one mouse vaccinated with IM with COBRA HA/NA vaccines with no adjuvant, had no detectable viral lung titers. In contrast, naïve mice mock (no vaccine)-vaccinated IM with CpG 1018 alone had viral lung titers between 5.0×10^4 to 1.0×10^5 pfu/g of tissue (Figure 6. 9).

At 3 days post-infection with Bris/18 influenza virus, pre-immune mice vaccinated IM with COBRA HA/NA vaccines with CpG 1018 had no detectable viral titers in their lungs. In comparison, only two mice IM vaccinated with COBRA HA/NA vaccines with no adjuvant had no detectable viral lung titers, while the other mouse in this group had a viral lung titer of 6.5×10^3 pfu/g of tissue. Pre-immune mock (no vaccine) vaccinated IM mice had viral lung titers of 5.0×10^4 to 5.0×10^5 pfu/g of tissue (Figure 6. 9).

At 3 days post-infection with Bris/18 influenza virus, pre-immune mice IN vaccinated with COBRA HA/NA vaccines CpG 1018 had no detectable viral lung titers

whereas 1 out of the 3 pre-immune mice that were vaccinated IN with COBRA HA/NA vaccines with no adjuvant had viral lung titers of 3.0 x 10^4 pfu/g of tissue (Figure 6. 9).

CpG 1018 adjuvant drives production of IgG and IgA antibody-secreting cells following vaccination

Spleens were harvested 20 days (D:48) post-boost (Naïve mice), 6 days following one vaccination (I.M. pre-immune mice), or 7 days following two vaccinations (I.N. pre-immune mice), to determine the number of ASCs (**Error! Reference source not found.**). Spleens of naïve mice vaccinated IM with COBRA HA/NA vaccines with CpG 1018 or with no adjuvant had little to no total IgG or IgA ASCs (Figure 6. 10a) and had no IgG or IgA ASCs that were specific to WT Bris/18 rHA (Figure 6. 10b). Spleens of pre-immune mice IM vaccinated with COBRA HA/NA vaccines with CpG 1018 or with no adjuvant had total non-specific IgG and IgA ASCs, but low to no specificity to WT Bris/18 rHA or Bris/18 rHA (Figure 6. 10a-b). In contrast, spleens collected from pre-immune mice vaccinated IN with COBRA HA/NA vaccines with CpG 1018 had enhanced numbers of IgG and IgA ASCs that were highly-specific to WT Bris/18 rHA, compared to ASCs collected from mice vaccinated with unadjuvanted vaccines (Figure 6. 10a-b).

Discussion

Infections with influenza viruses leads to significant morbidity and mortality in humans [280]. Currently, The FLUAD is the only licensed adjuvanted influenza vaccine for older adults 64 years or older in USA [281]. A main goal in the field of influenza is to develop vaccines that stimulate broadly-reactive and long-lasting immune responses in all

age groups. Since unadjuvanted vaccines fail to induced adequate immune responses, adjuvants can be added to the formulations [276]. Several novel adjuvant systems are approved for use with vaccines in clinical trials, including CpG 1018 and Alum [178], [225]. The oil-in-water emulsion (MF59) adjuvant formulated in the FLUAD vaccine (Seqirus Inc., Holly Springs, NC, USA) is administered intramuscularly and induces protective antibodies in the sera of vaccinated elderly patients [281], [282]. However, parentally administered vaccines mainly induce systemic immune responses, whereas intranasally administered vaccines have the potential to induce both systemic and mucosal immune responses [283]. This is a characteristic that is effective against pathogens, such as influenza viruses, that naturally infect via mucosal compartments of the respiratory tract [284]. CpG 1018 is a short 22-mer oligonucleotide sequence containing CpG motifs in rodents, non-human primates, and humans, that activates TLR 9 within host immune cells, including dendritic cell, natural killer cells, macrophages, and B-cells [285]. Additionally, this adjuvant induces Th1 biased pro-inflammatory immune responses associated with IFN-γ via the MyD88 pathway [286], [287]. However, it is not uncommon for certain classes of CpG oligonucleotides to induce Th2 immune responses [278]. In this study, the Th1 polarizing immunopotentiator, CpG 1018, was tested in combination with COBRA HA and NA vaccines that were administered intramuscularly or intranasally in mice with different immune backgrounds.

CpG induces Th1-biased immune responses that are associated with cytotoxic T-lymphocytes (CTLs) that kill infected cells during clearance of established infections, when neutralizing antibodies are not present [288]. However, Th1 responses also induce the activation of B -cells that secret opsonizing antibodies that are able to mark infected

cells for killing, during an active infection [289]. This could explain why in naïve models used in the study, adding CpG 1018 alone to these vaccines did not induce sufficient levels of HAI and NAI activities in the sera following vaccination, but still had detectable total IgG antibodies. Additionally, the effect of low HAI and NAI activities by vaccination with this regimen resulted in little protection against challenge following influenza virus infection naïve mice. However, vaccinating naïve mice IM with COBRA HA/NA antigens with CpG 1018 induced rHA and NA-specific total serum IgG titers and a balanced (Th0) of IgG1 (23.9-51.1%), IgG2a (24.6-45.2%), and IgG2b (21.3-36%) profile. The serum antibody production was not in line with having no detectable IgG or IgA ASCs in the spleens of these mice. Similarly, naïve mice vaccinated IM with COBRA HA/NA vaccines with no adjuvant induced low to no serum HAI titers against H1N1 and H3N2 influenza viruses, but there was some detectable NAI activity. This NAI activity was not sufficient to protect mice from influenza virus infection, but still induced rHA and NA-specific total serum IgG titers with a less balance (Th2 polarized) IgG1 (86.9-97.7%), IgG2a (1.1-3.1%), and IgG2b (1.2-10%) profile. The production of low serum antibody titers are in line with the number of IgG ASCs in the spleens of these mice. In the case of naive mice that were vaccinated IM with COBRA HA/NA vaccines with CpG or no adjuvant, having little to no antibodies present could neutralize the influenza viruses. This may have allowed the host cells to be infected and may have resulted in a CpG-dependent CTL response [7] that was directed towards the infected cells or the production of opsonizing antibodies that were not sufficient to eliminate, but only reduce the progression of the infection, hence only a 50% survival rate. Moreover, COBRA NA-induced antibodies, although low in these mice, may have also contributed to some level of reduction of the progression of influenza virus

infection by targeting infected cells for killing or blocking the NA enzyme activity from cleaving progeny virions.

Mice that were pre-immunized with the historical H1N1 and H3N2 influenza viruses and then vaccinated with COBRA HA/NA vaccines with or without adjuvant, all had enhanced HAI activity and NAI titers (especially the pre-immune IN vaccinated mice). These mice also had WT influenza virus rHA and NA-specific total IgG and isotypes in their serum. This not surprising since the extent of vaccine-induce IgG is determined by pre-existing immunity to influenza exposures via follicular $CD4^+$ T-cells [28]. Enhanced levels of rHA and NA-specific total IgG were also observed in the BALFs of the IN vaccinated groups, as well detectable serum IgG titers, although they were not significantly different than unadjuvanted IN vaccines. Notably, the proportions of IgG1, IgG2a, and IgG2b in the pre-immune model, where mice were vaccinated IM, followed a similar trend as the naïve IM vaccinated mice, in terms of Th1 or Th2 polarity, suggesting the CpG 1018 does indeed induce balanced immune responses compared to unadjuvanted vaccines. Furthermore, and unlike the IM vaccinated naïve or pre-immune IN vaccinated mice, the pre-immune mice vaccinated IM with COBRA HA/NA vaccines with CpG 1018 induced the production of enhanced serum IgA antibodies, suggesting that CpG 1018 induces additional immune mediators by various routes of administration, such as mucosal IgA secreting B cells that maintain the integrity of the mucosal barriers [290]. Additional beneficial outcomes by formulating with CpG 1018 was observed in pre-immune mice that were vaccinated IM with COBRA HA/NA vaccines with CpG, having a more balanced Th0 profile with ranges of IgG1 (21-43.20%), IgG2a (44.60-70.50%), and IgG2b (8.50-22.19-36%), whereas pre-immune mice that were vaccinated IM with COBRA HA/NA

vaccines without adjuvant had a more limiting profile that was biased to Th2 immune responses alone. As shown here, IM and IN vaccinated pre-immune mice also exhibited enhanced total IgG, IgA ASCs, and rHA specific ASCs in the spleens of IN vaccinated pre-immune mice, further confirming the correlations and outcomes of vaccinating with COBRA HA/NA vaccines with CpG 1018 in pre-immune models. The presence pre-existing immunity could explain why these COBRA HA/NA vaccine with CpG 1018 further enhanced the immune responses, since these pre-existing antibodies may have also contributed to neutralizing the influenza viruses before they could infect healthy host cells. Based on this speculation, all of the vaccinated pre-immune mice survived lethal influenza virus infection, as well as ~38% of the unvaccinated pre-immune mice, as a result of pre-existing immunity to historical influenza viruses [291]. This confirms that a pre-immune background shapes the outcomes of vaccinations, possibly through the overall memory response of previous exposure to influenza viruses and translated to the protection against infection with an H1N1 influenza virus. Naïve mice antibody responses are generally short-lived since they fail to maintain an optimal plasma-cell pool in the bone marrow during early life [292]. Specifically, post-germinal plasma blast home into the bone marrow but since these naïve mice have little to no differentiation survival signals, they remain incompetent [292]. On the contrary, having experienced multiple exposures to various antigens throughout life, as elderly individuals have, results in an overexpression of different classes of antibodies derived from B-cell clones, and an increased pool of organ-specific and organ-non-specific autoantibodies [292]. In terms of administering adjuvants to individuals with trained immune responses (pre-exciting immunity), CpG ODNs have been shown to take advantage of this pre-exciting immunity to drive the induction of adult-

like DC and T-cell activation patterns, as well as the activation of pre-exiting memory B cells [292], [293]. Although the extent to whether Th1- versus Th2-biased responses contributes to protection against influenza virus infection has not been clearly defined [294], these findings indicated that in a naïve setting, the combination of low HAI and NAI activity and a balanced, but low proportions of IgG1, IgG2a, and IgG2b were not sufficient to protect mice from morbidity or mortality. However, vaccinating pre-immune mice by different routes with CpG 1018 adjuvant did induced a more diverse adjuvant profile, having elicited IgG, IgA, and a broader range of isotypes (IgG1, IgG2a, IgG2a) as shown in this study, and possibly the elicitation of CTL immune responses [288].

Overall, these finding suggest that adjuvating COBRA HA/NA vaccines with CpG 1018 enhanced the efficacy of the vaccines in pre-immune models that resembles the trained immune system of an adult, but not in a naïve model that resembles the untrained immune system of a child. In both scenarios, broadly reactive HAI and NAI activity against several drifted H1N1 and H3N2 influenza viruses were elicited compared to unadjuvanted COBRAHA/NA vaccines, however these results were not always statistically different. Furthermore, vaccinating pre-immune mice IN with COBRA HA/NA vaccines adjuvanted with CpG 1018 led to a greater potential at inducing effective influenza virus specific mucosal and systemic responses and protection from influenza virus infection. Specifically, since the nasal mucosa has a wider vesiculated surface area, CpG 1018 and vaccine antigens could have been better absorbed through local mucosal lymphoid follicles referred to as nasal-associated lymphoid (NALT). This area of vaccination is beneficial since this is the site where CpG1018 and COBRA HA/NA antigens first reached the respiratory tract [295]. This may also suggest that IN administration of CpG 1018 in these

pre-immune models could also be superior at recalling resident mucosal CTLs that were initially induced by prior influenza exposure, hence the IN pre-immunization of mice, newly induced local CTLs by CpG [296], or even locally distinct CPG-NALT-associated responses that could only be achieved by IN vaccination [297]. In turn, these findings offer an option for the development of COBRA HA/NA vaccines that can potentially be tailored with CpG 1018 adjuvant for inducing distinct adjuvant profiles that could be relevant for pre-immune populations where the majority of individuals have already been exposed to several influenza viruses, but this adjuvant may not be as effective for naïve populations.

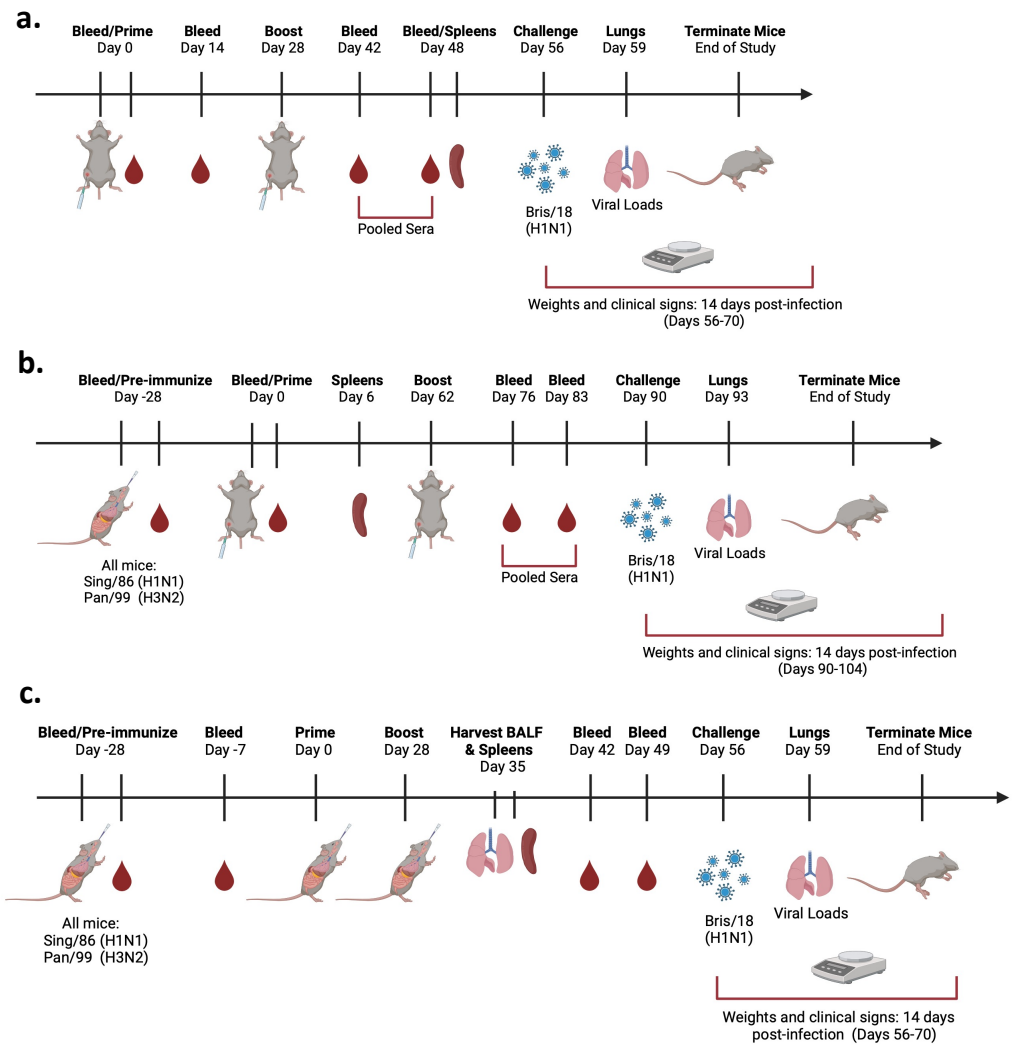

Figure 6. 1 Schematic of the study timelines.

DBA/2J (6-8 weeks old) female mice were randomly divided into 8 groups. (a) 3 naive groups with n=18 mice were vaccinated intramuscularly (IM) with 12 µg COBRA HA and NA proteins (Y2, NG2, N1-I, and N2-B) plus the addition of 10 µg of CpG 1018 or with no adjuvant. As controls, some mice were vaccinated with no CpG 1018 only in tris buffer. All of the naïve mice were bled and prime vaccinated on day 0 follow by blood collection on day 14 and boost-vaccinated on day 28. On days 42 and 48, the mice were bled and spleens were harvested from 4 mice from each group. On day 56, all of the mice were intranasal challenged with A/Bris/02/2018. Three days post-infections, lungs were

harvested from 4 mice from each group and the remainder mice were monitored for 14 days post infection. (b) 3 pre-immune groups with n=18 or (c) 2 pre-immune groups with n=10, were intranasally (IN) pre-immunized with historical H1N1 Sing/86 and H3N2 Pan/99 at 2.5×10^5 PFU/25 μL of each virus for a total 50 μL dose per mouse. All of the mice were vaccinated IM (b) or IN (c) with COBRA HA and NA proteins (Y2, NG2, N1-I, and N2-B) plus the addition of 10 μg of CpG 1018, or no adjuvant. As controls, some of the pre-immune mice were mock-vaccinated (tris buffer only). All of the pre-immune mice were bled at day –28, at day –7 (IN groups), or at day 0 (IM groups), and prime vaccinated on day 0 , followed by a boost on day 62 (IM groups) or day 28 (IN groups). BALFs and spleens (IN groups) were harvested from 2 mice from each group 7 days post-boost (day 35), and 4 spleens were harvested from 4 mice (IM groups) at day 6 post-prime-vaccination. On days 76 and 83 (IM groups) or 42 and 49 (IN groups), all of the mice were bled followed by intranasal challenge (Day 90 or 56) with A/Bris/02/2018. Three days post-infections, lungs were harvested from 3 mice from each group and the remainder mice were monitored for 14 days post infection. Created with BioRender.com.

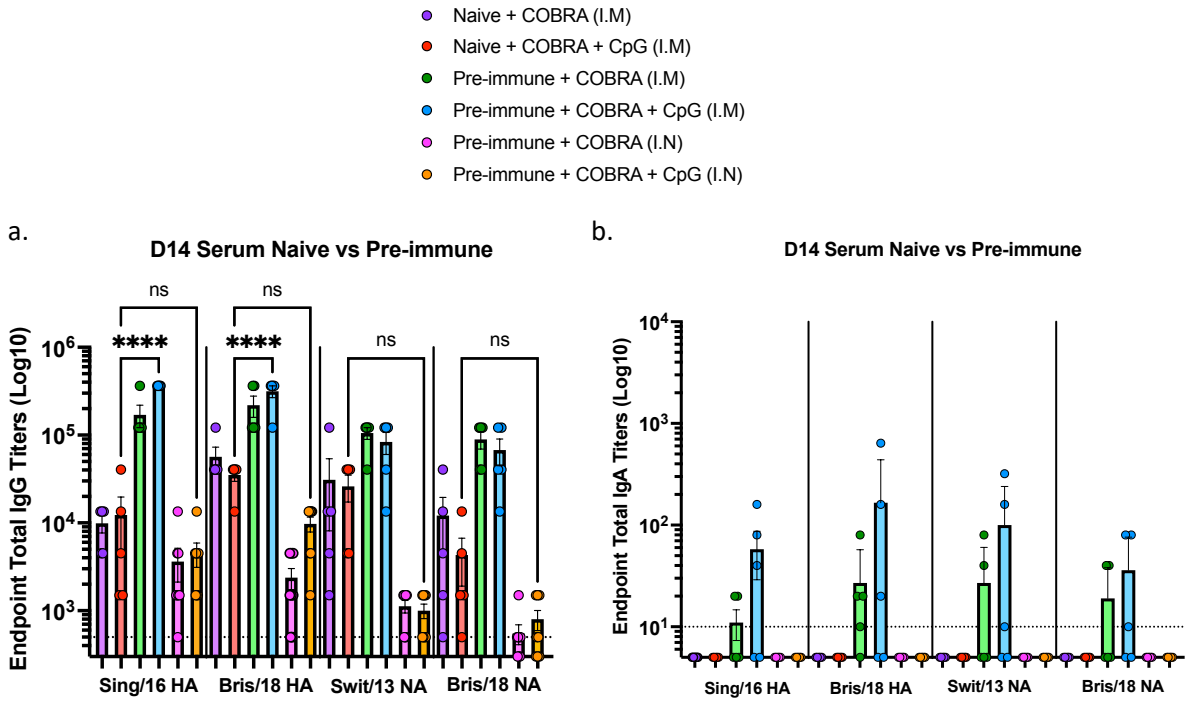

Figure 6. 2 Serum anti-influenza total IgG and IgA in vaccinated naïve and pre-immune mice.

Mice were vaccinated with 12 µg of COBRA HA and NA vaccines (Y2, NG2, N1-I, and N2-B) with CpG 1018 or with no adjuvant. Sera collected 14 days post-boost vaccinations (Days 42/48 for IM naïve mice), (76/83 for IM pre-immune mice), and (Days 42/49 for IN pre-immune mice) from each mouse was pooled. (a) serum anti-influenza total IgG against Sing/16 and Bris/18 rHA, or Swit/13 and Bris/18 rNA. (b) serum anti-influenza total IgA against Sing/16 and Bris/18 rHA, or Swit/13 and Bris/18 rNA. Represented on the Y-axis are the endpoint titers. Represented on the X-axis are the WT rHAs and rNAs (a,b). Each bar corresponds to 5 individual mice according to vaccine regimens and are conveyed as the average +/− standard error of the mean (SEM)/ IgG titers were statistically analyzed using nonparametric one-way analysis of variance (ANOVA) by Prism 9 software (GraphPad Software, Inc., San Diego, CA, version 9.4.0, https://www.graphpad.com). A *P* value of less than 0.05 was defined as statistically significant. $p < 0.0001$ ****.

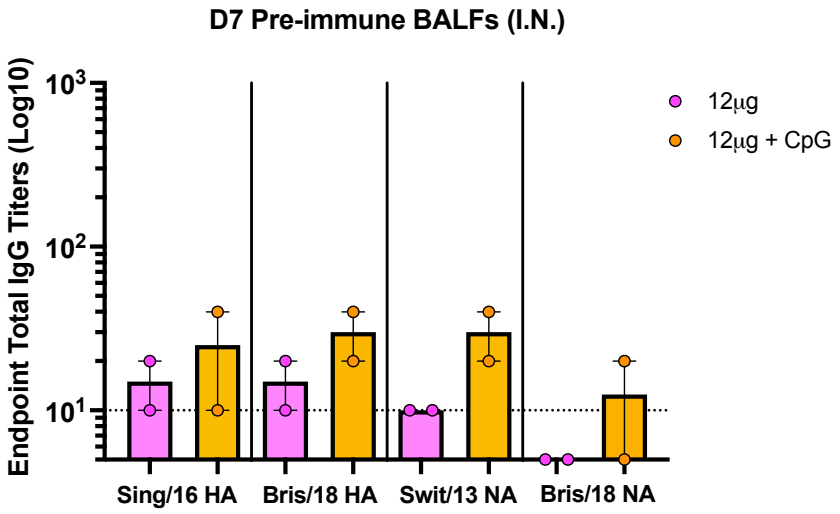

Figure 6. 3 BALF total IgG in intranasally vaccinated pre-immune mice.

Mice were vaccinated with 12 μg of COBRA HA and NA vaccines (Y2, NG2, N1-I, and N2-B) with CpG 1018 or with no adjuvant. BALFs were collected 7 days post-boost (Day 35) and tested for anti-influenza total IgG against and Sing/16 and Bris/18 rHA, or Swit/13 and Bris/18 rNA. Represented on the Y-axis are the endpoint titers. Represented on the X-axis are the WT rHAs and rNAs. Each bar corresponds to 2 individual mice according to vaccine regimens and are conveyed as the average +/− standard error of the mean (SEM).

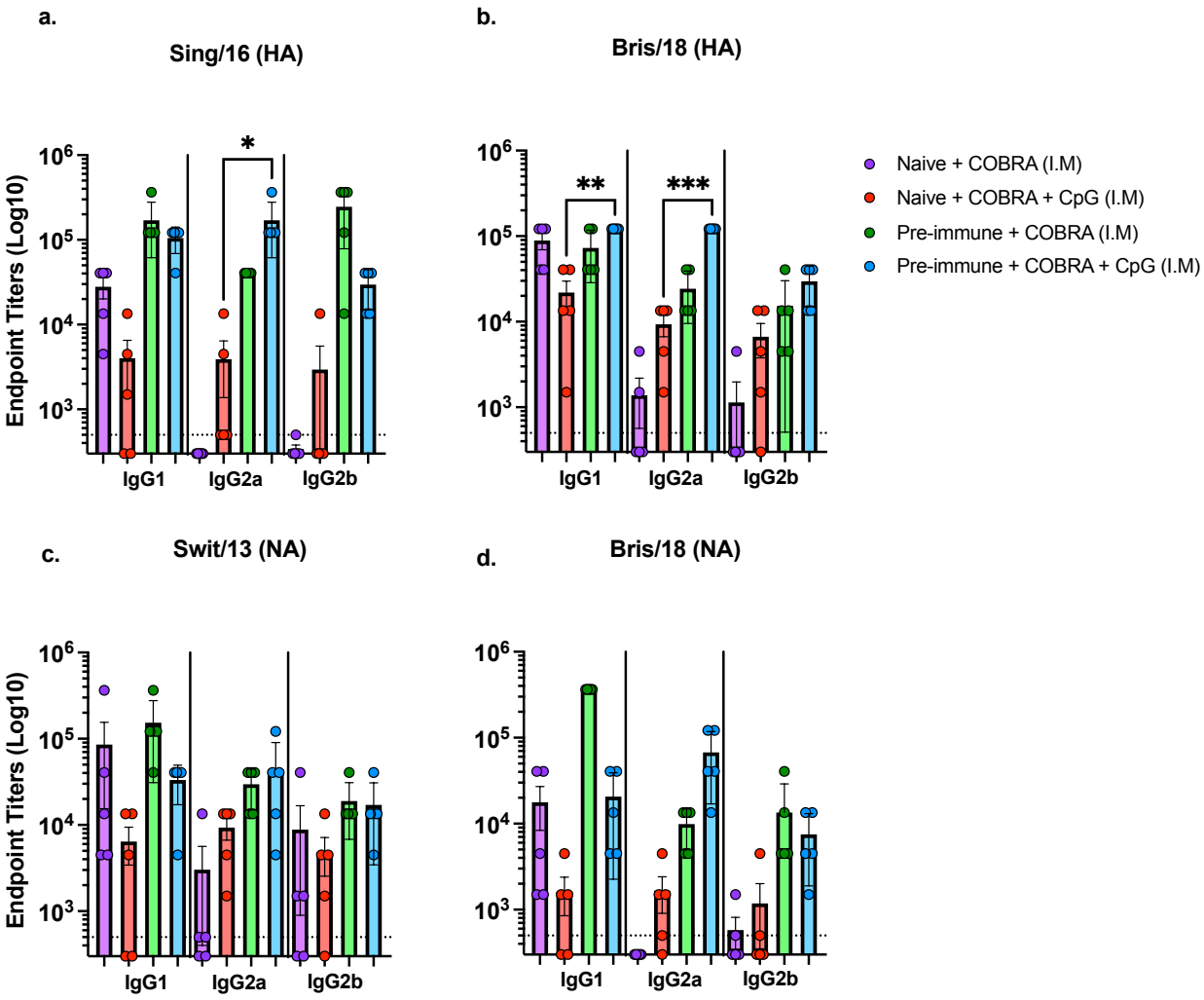

Figure 6. 4 Serum anti-influenza Ig isotypes in intramuscularly vaccinated naïve mice or pre-immune mice.

Mice were vaccinated with 12 μg of COBRA HA and NA vaccines (Y2, NG2, N1-I, and N2-B) with CpG 1018 or with no adjuvant. Sera collected 14 days post-boost vaccinations (Days 42/48. For naïve mice) or (76/83 for IM pre-immune mice) from each mouse was pooled. Serum was tested for IgG1, IgG2a, and IgG2b against WT influenza virus (a) Sing/16 rHA, (b) Bris/18 rHA, (c) Swit/13 rNA, or (d) Bris/18 rNA. (e). Represented on the Y-axis are the isotype titers on a Log10 scale and represented on the X-axis are the different antibody isotypes. Each bar corresponds to 5 individual mice according to vaccine

regimens and are conveyed as the average +/− standard error of the mean (SEM).) Isotype titers were statistically analyzed using nonparametric one-way analysis of variance (ANOVA) by Prism 9 software (GraphPad Software, Inc., San Diego, CA, version 9.4.0, https://www.graphpad.com). A *P* value of less than 0.05 was defined as statistically significant. $p < 0.05$ *, $p < 0.01$ **, $p < 0.001$ ***.

a.

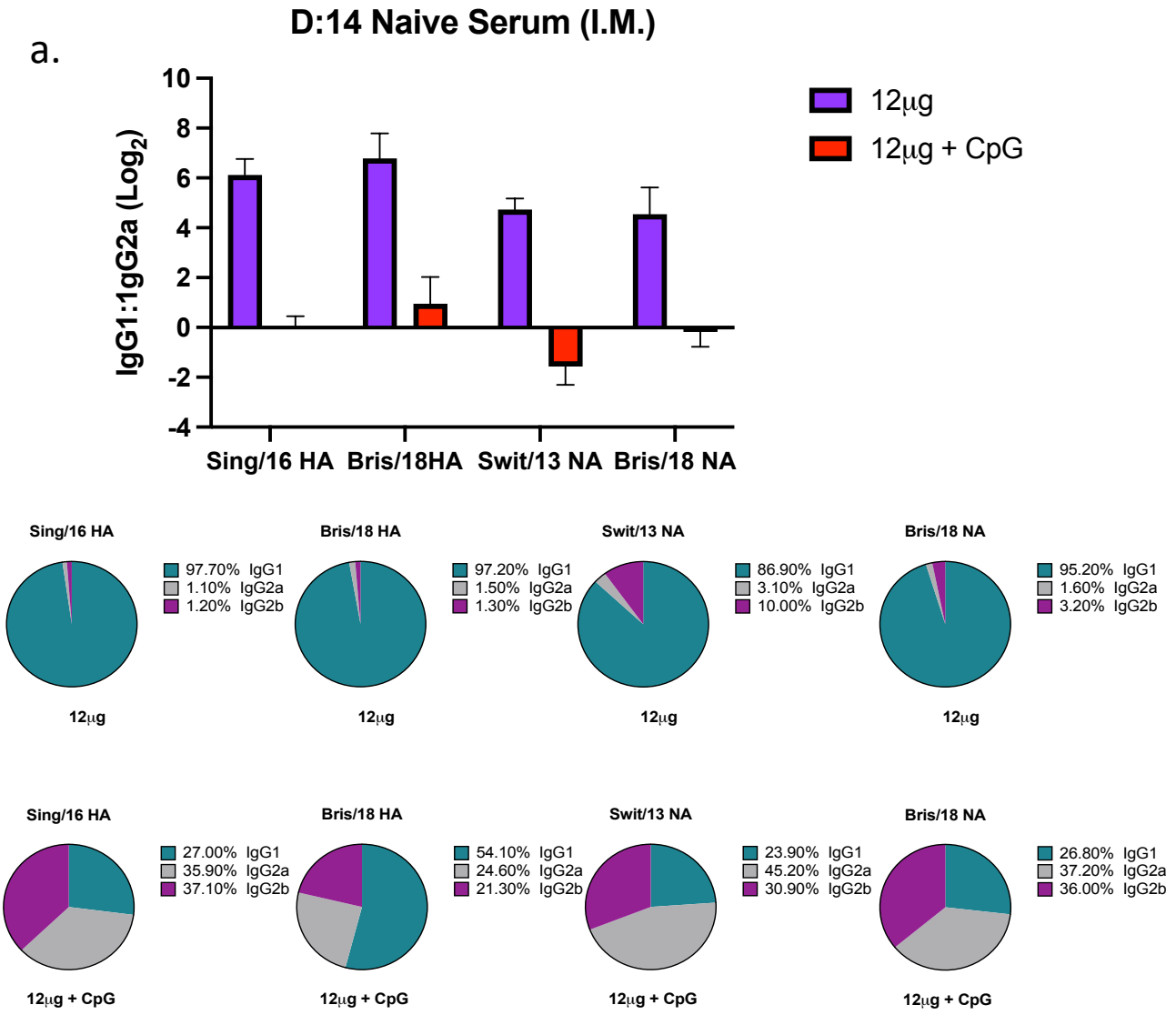
D:14 Naive Serum (I.M.)
IgG1:1gG2a (Log2)
10
8
6
4
2
0
-2
-4
Sing/16 HA
Bris/18HA
Swit/13 NA
Bris/18 NA
12μg
12μg + CpG
Sing/16 HA
97.70% IgG1
1.10% IgG2a
1.20% IgG2b
12μg
Bris/18 HA
97.20% IgG1
1.50% IgG2a
1.30% IgG2b
12μg
Swit/13 NA
86.90% IgG1
3.10% IgG2a
10.00% IgG2b
12μg
Bris/18 NA
95.20% IgG1
1.60% IgG2a
3.20% IgG2b
12μg
Sing/16 HA
27.00% IgG1
35.90% IgG2a
37.10% IgG2b
12μg + CpG
Bris/18 HA
54.10% IgG1
24.60% IgG2a
21.30% IgG2b
12μg + CpG
Swit/13 NA
23.90% IgG1
45.20% IgG2a
30.90% IgG2b
12μg + CpG
Bris/18 NA
26.80% IgG1
37.20% IgG2a
36.00% IgG2b
12μg + CpG

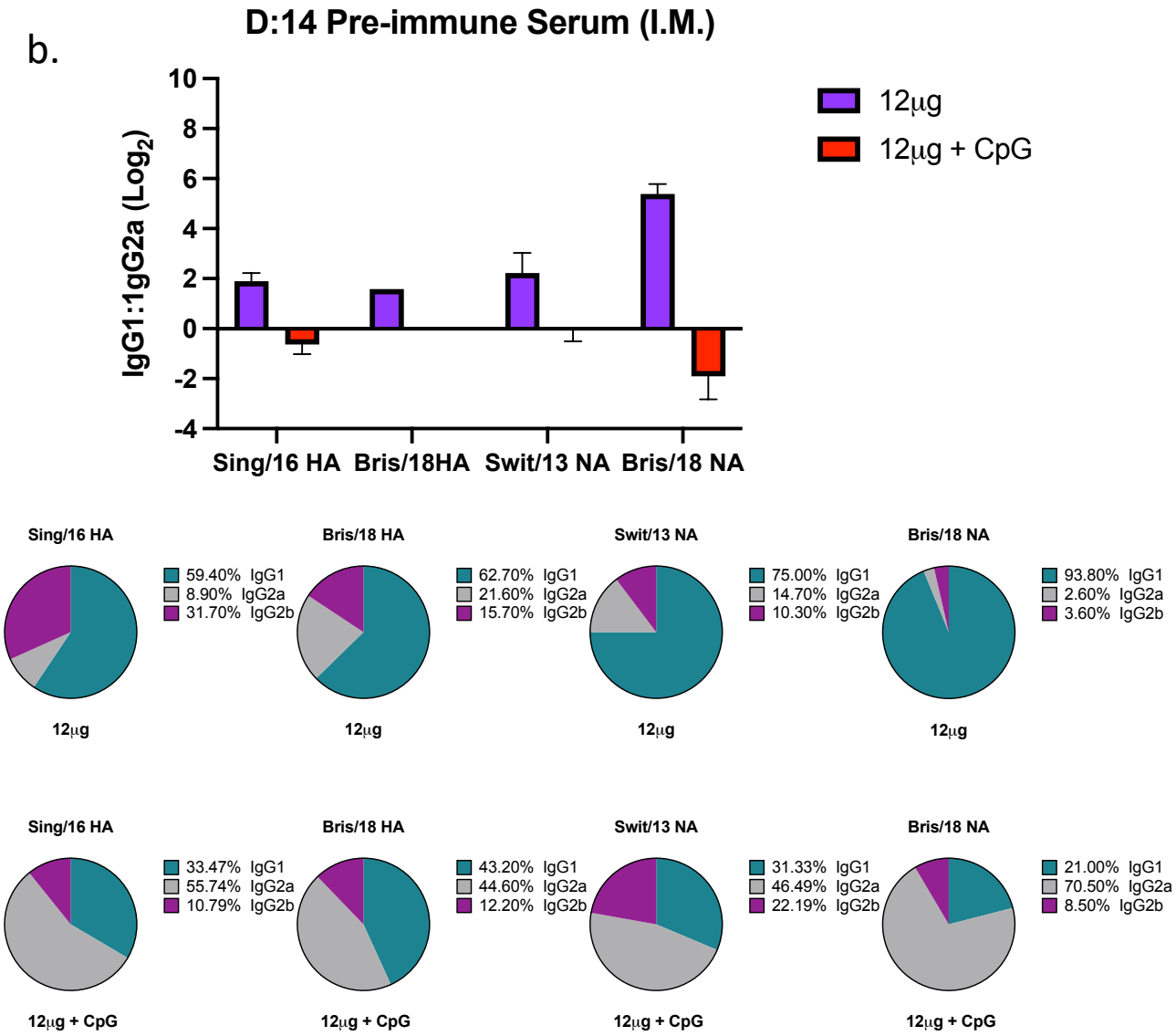

Figure 6. 5 Ratios and proportions of serum anti-influenza IgG isotypes in intramuscularly vaccinated naïve and pre-immune mice.

Mice were vaccinated with 12 μg of COBRA HA and NA vaccines (Y2, NG2, N1-I, and N2-B) with CpG 1018 or with no adjuvant. Sera collected 14 days post-boost (Days 42/48 for IM naïve mice) or (76/83 for IM pre-immune mice) from each mouse was pooled. Serum of IM vaccinated naïve mice (a) or IM pre-immune mice (b) was tested for IgG1, IgG2a, and IgG2b against Sing/16 rHA, Bris/18 rHA, Swit/13 rNA, or Bris/18 rNA. The top panels convey the IgG1 to IgG2a ratios and the bottom panels convey the proportion

of IgG1, IgG2a, and IgG2b. Represented on the Y-axis of the top panels are the isotype ratios on a Log2 scale. Represented on the X-axis of the top panels are the different WT influenza rHAs and NAs tested. The bottom panels represent the WT rHAs or rNAs tested (above pie charts) or the vaccine formulations (below pie charts). Each bar (panels a and b) corresponds to 5 individual mice according to vaccine regimens and are conveyed as the average +/− standard error of the mean (SEM).

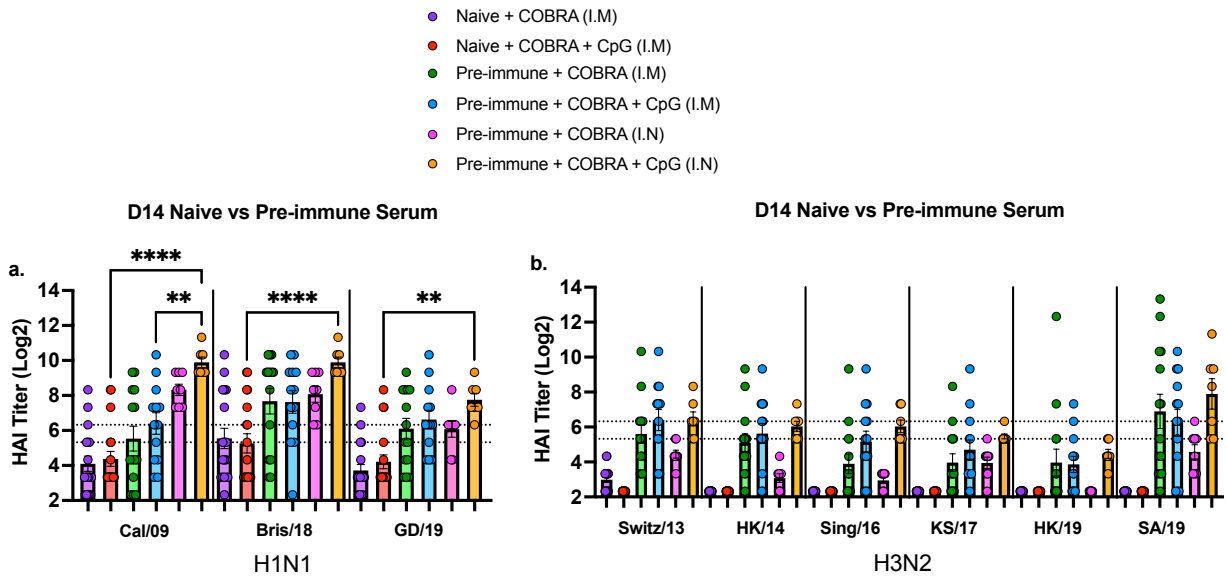

Figure 6. 6 Hemagglutination inhibition activity in the serum naïve and pre-immune mice vaccinated.

Mice were vaccinated with 12 μg of COBRA HA and NA vaccines (Y2, NG2, N1-I, and N2-B) with CpG 1018 or with no adjuvant. Sera collected 14 days post-boost vaccinations (Days 42/48 for IM naïve mice), (76/83 for IM pre-immune mice), (Days 42/49 for IN pre-immune mice) from each mouse was pooled and tested for HAI activity against (a) three H1N1 viruses, Cal/09, Bris/18, and GD/19 or (b) six H3N2 influenza viruses, Swit/13, HK/14, Sing/16, KS/17, HK/19, and SA/19. Represented on the Y-axis are the HAI titers on a log 2 scale. Represented on the X-axis are the panels of H1N1 and H3N2 influenza viruses. The top dotted line indicates a 1:80 HAI titer and the bottom dotted line indicates a 1:40 HAI titer. Each column represents 18 (IM naïve), 14 (IM pre-immune), or 10 (IN pre-immune) individual mice pertaining to each vaccine regimen and are conveyed as the average +/− standard error of the mean (SEM). HAI titers were statistically analyzed using nonparametric one-way analysis of variance (ANOVA) by Prism 9 software (GraphPad Software, Inc., San Diego, CA, version 9.4.0, https://www.graphpad.com). A *P* value of less than 0.05 was defined as statistically significant. $p < 0.01$ **, $p < 0.0001$ ****.

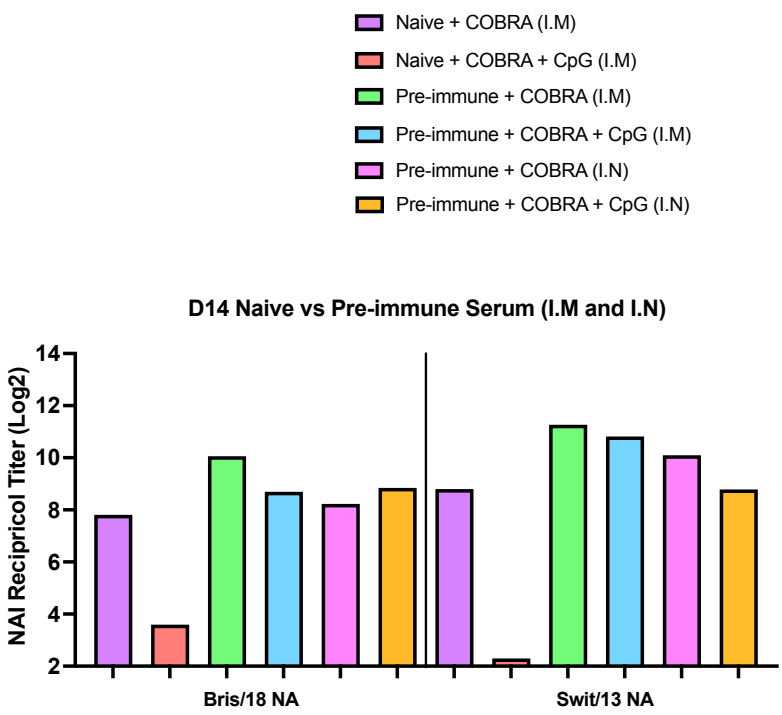

Figure 6. 7 The NAI titers of influenza NA-specific anti-serum antibodies in vaccinated mice.

Mice were vaccinated with 12 μg of COBRA HA and NA vaccines (Y2, NG2, N1-I, and N2-B) with CpG 1018 or with no adjuvant. Sera collected from each immunized mice were pooled according to vaccine groups. The NAI activity in the sera of mice collected 14 days post-boost vaccinations (Days 42/48 for IM naïve mice), (76/83 for IM pre-immune mice), (Days 42/49 for IN pre-immune mice) was tested against WT Bris/18 or Swit/13 rNAs. Represented on the Y-axis are the NAI reciprocal titers on a Log2 scale that inhibited 50% of the NA activity with 95% confidence on a non-linear regression curve. Represented on the X-axis are the WT influenza virus-specific rNAs tested. Each column represents total pooled mice serum pertaining to each vaccine regimen.

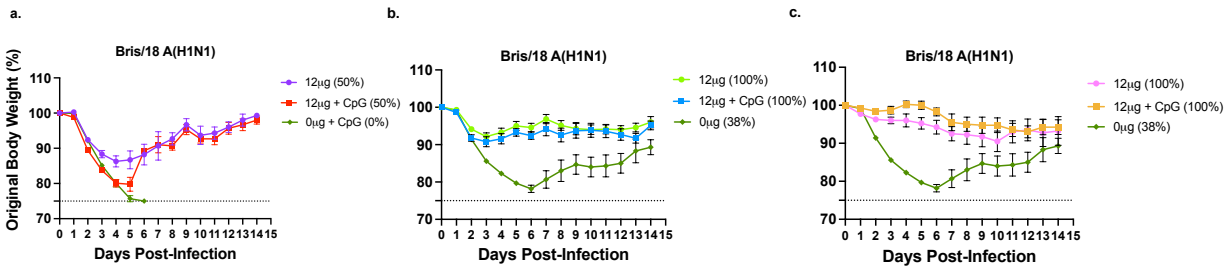

Figure 6. 8 Post-challenge weight loss and survival of vaccinated mice.

Mice were vaccinated with 12 μg of COBRA HA and NA vaccines (Y2, NG2, N1-I, and N2-B) with CpG 1018 or with no adjuvant. All of the vaccinated mice were challenged intranasally with the H1N1 strain, A/Brisbane/02/2018 (8×10^6 PFU/50 μL), and observed for 14 days post-infection. (a) Percent of original body weight loss and survival of naïve mice IM vaccinated. (b) percent of original body weight loss and survival of pre-immune mice IM vaccinated, and (c) percent of original body weight loss and survival of pre-immune mice IN vaccinated. The dotted line in (a-c) represents the 25% weight loss endpoint cutoff. Each line (a-c) is conveyed as the average +/− standard error of the mean (SEM).

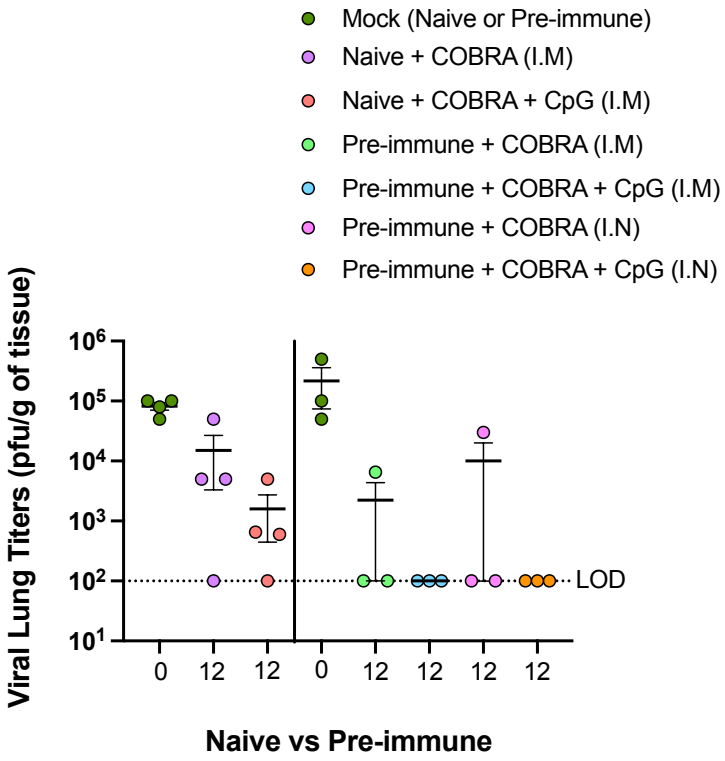

Figure 6. 9 Post-challenge viral lung titers of vaccinated mice.

Mice were vaccinated with 12 μg of COBRA HA and NA vaccines (Y2, NG2, N1-I, and N2-B) with CpG 1018 or with no adjuvant Lung viral titers of mice three days following challenge with A/Brisbane/02/2018 in naïve, IM vaccinated mice, pre-immune, IM vaccinated mice, or pre-immune IN vaccinated mice. The Y-axis represents the day 3 post-challenge lung viral titers (PFU/g of tissue) and the X-axis represents the vaccine doses. The dotted line represents the limit of detection (LOD).

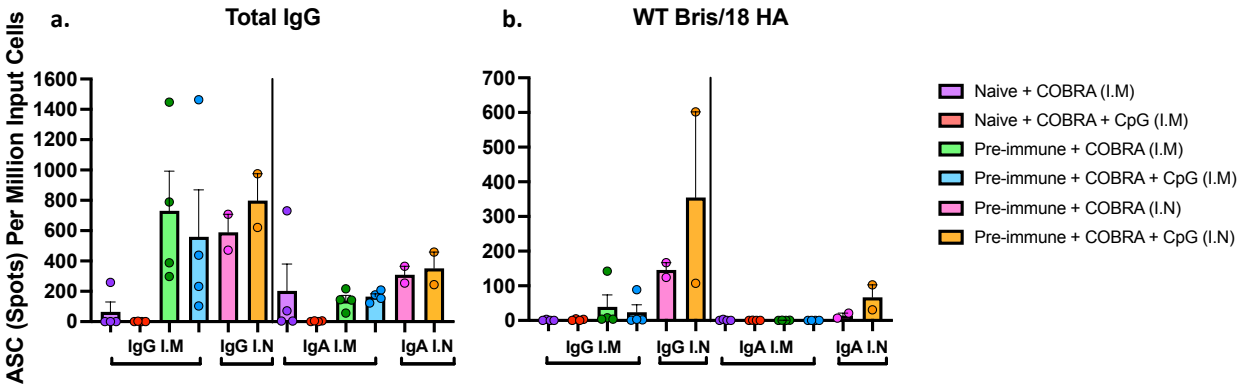

Figure 6. 10 Quantification of total and antigen-specific IgG and IgA from antibody secreting cells (ASCs) in vaccinated mice.

Mice were vaccinated with 12 μg of COBRA HA and NA vaccines (Y2, NG2, N1-I, and N2-B) with CpG 1018 or with no adjuvant. Spleens were harvested from naïve, IM vaccinated mice (day 48), pre-immune, IM vaccinated (day 6) mice, and pre-immune, IN vaccinated (day 35) mice. Plates were coated with anti-Igκ/λ for measuring (a) total IgG or IgA ASCs in spleens, or coated with (b) WT Bris/18 rHA for measuring influenza virus-specific IgG or IgA ASCs in spleens. The Y-axis represents the number of ASCs per 1M input cells for individual mice and the X-axis represents the secreted antibodies from ASCs.

CHAPTER 7

CONCLUSIONS

The goal of this project was to identify effective adjuvants that are capable of enhancing the immunogenicity of COBRA HA and NA vaccine in naïve and mice with pre-exciting immunity to influenza viruses. To do this, specific adjuvants that directly activate cells of the innate immune response for enhancing the uptake of vaccine antigens for bridging and modulating the adaptive immune response were used. Additionally, these adjuvants were tested on the basis that an influx of immune-cell recruitment to the site would further enhance the efficacy of the vaccines, and in turn, stimulate both cellular and humoral immune responses and lead to the production of antibodies that are able to recognize broad panels of drifted H1N1 and H3N2 influenza viruses. Moreover, the adjuvanticity of each adjuvant tested should promote efficient immune responses to COBRA HA and NA antigens that further protect mice from morbidity and mortality, following lethal infection with influenza viruses. According to the results shown in this project, different formulations (aqueous, liposome, or emulsion) of the novel TLR4, and TLR7/8 agonists (INI 2002 and INI 4001) were tested with COBRA HA vaccine in naïve mice. This part of the project offers insight on the outcomes of these adjuvanted vaccines in individual with no pre-existing immunity to influenza viruses, thus offering potential 3 options for vaccinating children and inducing enhance immune responses that will protect them from subsequent influenza virus exposures. The studies involving the administration

of a novel TLR9 agonist (CpG 1018) with COBRA HA/NA vaccines, offer some interesting findings that demonstrated that the novel TLR9 agonists' ability to induce immune responses was ideal the presence of pre-existing immunity to influenza viruses, but not in immunologically naïve subjects that had no pre-existing immunity. This translates to a true-reflection of the majority of people in all populations across the world, which have already been exposed to several influenza viruses from early age. Although enhance vaccine-induced and protective immune responses to influenza virus infection were observed with either intramuscularly or intranasally administered COBRA HA/NA vaccines with the novel TLR9 agonist (CpG 1018) studied here, vaccinating mice via the intranasal route led to promising outcomes. Although comparable responses were demonstrated between intramuscularly or intranasally vaccinations in pre-immune mice, it is ideal that enhanced systemic and mucosal immune responses could be achieved via the intranasal route, suggesting that parental injection could potentially be eliminated using this regimen, thus encouraging more easily administered vaccinations to the population. On the contrary, the study involving the administration of a combination of inulin and CpG 55.2 (Advax-SM™) in naïve mice that had no pre-existing immunity was effective compared to the studies involving CpG 1018 in mice with the same immunological background. This further confirms the importance of tailoring vaccine antigens with the right adjuvant. Although both are CpG ODN, different classes of CpG's have been shown to induce unique responses. But in order to achieve the desirable vaccine-induced responses and protection as shown in this study, 3 vaccinations were required. Regardless, further options can be explored to optimize this vaccine since it was still very effective. In another study, naïve mice with the same immunological background were intranasally vaccinated

with COBRA HA vaccines with the M7 peptide and effective systemic and mucosal immune responses were observed different two distinct mouse strains. Put together, this vaccine could potentially provide a possibility for vaccinated individuals with diverse racial backgrounds and even children who do not have pre-existing immunity to influenza viruses.

In terms of formulations, three adjuvant formulations provide unique beneficial characteristics for manufacturing for influenza vaccine: 1). Aqueous formulations can be formulated easily, faster, and antigen or adjuvant molecules are readily available in solution. However, a vehicle adjuvant system may be required for effectively delivering and protecting the vaccine antigens and adjuvant molecules from degradation during storage and upon vaccination [86]. 2.) liposome are safe, biocompatible, and biodegradable and can be delivered by various routes of administration (including intranasally), which is a plus when aiming to avoiding parental injections where individuals are afraid of needles. Liposomes also protect molecules, such as antigens or adjuvant molecules, from enzymatic degradation. Moreover, liposomes are not associated with toxicity and are easy to scale up in the event that they are needed to adjuvant influenza vaccines against future pandemic [298]. 3). Emulsion (oil-in-water) are safe, highly tolerable, offer additional adjuvant activity effect by the encapsulated oils, provide a dose-sparing effect by allowing slow-release of vaccine antigens (depot effect) at the site of vaccination, and have a good stability for storge, even after being autoclaved [299], in the event that they are immediately needed during sudden pandemics associated with influenza viruses [300]. Moreover, emulsions are effective at adsorbing vaccine antigens via electrostatic interactions to their surfaces and retaining the vaccine antigens stability for up to 3 months [299], making this option

more effective, precise, and potent at delivering vaccine antigens for individuals with no pre-existing influenza virus immunities, but especially for high-risk populations [300]. However, oil-in-water emulsions are usually safely administered intramuscularly, still requiring needles.

Compared to conventional vaccines, new-generation vaccines, especially recombinant protein or synthetic peptide vaccines, are safer but less immunogenic than crude inactivated microbial vaccines [300]. For example, compared to COBRA rHA vaccines, live-attenuated viral (LAV) vaccines are highly unstable in aqueous formulation [301]. Additionally, mRNA vaccines are susceptible to degradation by RNA enzymes in extracellular serum [86]. Novel adjuvants, like the ones tested here, are being explored for adjuvanting influenza rHA vaccines to enhance their immunogenicity. Influenza viruses have single-stranded RNAs that are recognized by TLR7/8, making agonists of these PRRs suitable targets for influenza virus vaccines [147]. Through extensive testing, as shown in these studies, potential adjuvant candidates were identified that may be effective in humans with diverse immune background. Ideally, mimicking the immune responses as close as possible by vaccination, to match pathogen-associated responses in a live host could set the stage for subsequent exposure to influenza viruses. Employing the right tools to achieve the desired and effective outcomes from a next-generation influenza vaccine would include: Reduced doses of COBRA rHA/NAs that induce broadly-reactive antibodies that recognized many influenza virus strains, adjuvanted with a novel TLR7/8 agonists to elicit the influenza virus-associated immune-mediators, incorporating both the antigens and agonists into an oil-in-water emulsion for protecting the vaccine antigens and releasing at

the site of vaccination via a depot effect, and taking advantage of the increased antibody responses induced by the emulsion themselves [259].

Overall, it was hypothesized that adjuvating COBRA HA and NA vaccines with TLR4, TLR7/8 or TLR9 agonists, M7-NH_2, or Advax-SM^{TM}, would lead to enhanced levels of broadly-reactive antibodies in naïve and pre-immune mice that would protect them from the outcomes of influenza virus infection. To test this hypothesis, the following specific aims were addressed:

Specific Aim 1: Determine the breadth of protective antibodies elicited by COBRA HA and NA vaccines using different adjuvants in naïve mice vaccinated via different routes of administration. The working hypothesis was that the addition of adjuvants will enhance COBRA HA and NA vaccine-induced systemic and mucosal immune responses and protect naïve mice from IAV challenge compared to unadjuvanted vaccines. Naïve vaccinated IM with COBRA HA vaccines with INI 2002 or INI 4001 had enhanced serum antibodies capable of blocking H1N1 influenza viruses from agglutinating RBCs. Specifically, vaccinated with COBRA HA antigens with INI 2002 agonists, regardless of formulation, had high serum HAI titers against the Cal/09 and Bris/18 H1N1 influenza viruses. Naïve mice vaccinated IM with INI 4001 in the aqueous and emulsion formulations had high HAI titers against Cal/09 and Bris/18 H1N1 influenza viruses, whereas ~50% of the mice vaccinated with COBRA HA antigens with INI 4001 agonists in the liposome formulation had HAI titers ≥1:40. Additionally, the mice had enhanced serum total IgG, IgG1, IgG2a, and IgG2b Y2 HA-specific antibodies, with a bias to Th1 or balanced Th1/Th2 responses. Furthermore, vaccinating these naïve mice with COBRA HA

vaccines with INI 2002 or INI 4001 adjuvants, regardless of formulation, protected the mice from morbidity and mortality following infection with an H1N1 influenza virus, with little to no weight loss, no clinical signs, no lung inflammation, and lead to a 100% survival. Additionally, these mice had significantly reduced or no detectable viral lung titers. Naïve mice that were intramuscularly vaccinated with Advax-SM™ -adjuvanted COBRA HA vaccines had elevated functional antibodies in their serum that were able to block a range of H1N1 and H3N2 influenza viruses from binding and agglutinating RBCs. These mice also had increased serum IgG, IgA, IgG1, IgG2a, IgG2b directed against H1 and H3 HAs. Mice immunized with COBRA HA plus Advax-SM™ adjuvant had both Th1 and Th2 anti-influenza immune responses and were fully protected from morbidity and mortality with less than 5% weight loss, no clinical signs, and 100% survival following infection with a lethal H1N1 influenza virus. Advax-SM™ adjuvant has a unique ability to induce responses independent of inflammation to the lungs and the ability to activate complement which, in part, may contribute to its beneficial adjuvant effects on the COBRA HA vaccines. Naïve mice intranasally vaccinated with M7-NH_2 adjuvanted COBRA HA vaccines had elevated functional antibodies in their serum that were able to block a range of H1N1 and H3N2 influenza viruses from binding and agglutinating RBCs. These mice also had enhanced levels of influenza-specific IgG, IgG1, IgG2a, and IgG2b both in their serum and in the BALFs, with a bias to Th2 immune responses. Following infection with lethal H1N1 or H3N2 influenza viruses, mice vaccinated with this regimen only lost an average of ~5% (H3N2 infection) ~8% (H1N1) of their original body weights post-infection with little to no clinical scores, they had 100% survival, and no detectable viral lung titers. M7-NH_2 peptides have potential as an intranasal adjuvant that induces mucosal

and systemic immune responses to enhance protective immunity in individuals with weak immune systems, such as young kids and older adults, and provide for easier administration compared to injectable vaccines. Naïve mice that were vaccinated intramuscularly with COBRA HA and NA proteins formulated with CpG 1018 only elicited low functional antibodies in their serum that were able to block a range of H1N1 influenza viruses from binding and agglutinating RBCs. The serum of these mice also had low to no NAI activity. However, these mice still induced the production of serum IgG, IgG1, IgG2a, and IgG2b antibodies titers that were specific to WT influenza virus rHAs and rNAs. IgG1 to IgG2a ratios and IgG1, IgG2a, and IgG2b proportions by CpG 1018 induced immune responses were balanced compared to unadjuvanted vaccines. Following infection with a lethal H1N1 influenza virus, mice vaccinated with this regimen lost an average of ~20% of their original body weights with mean clinical scores between 1.8–3, and 50% survival. Although these mice still exhibited detectable viral lung titers, they were still reduced compared to unadjuvanted vaccines. In this study, the adjuvanticity of CpG 1018 was not sufficient at enhancing the efficacy of COBRA HA/NA vaccines in naïve mice, thus did not demonstrate a promising platform for tailoring this adjuvant to influenza vaccines for the younger, naïve population.

Specific Aim 2: Assess the effectiveness of COBRA HA and NA vaccines formulated with different adjuvants and administered via different routes in mice that are pre-immune to historical influenza viruses. The working hypothesis is that the pre-immune status in mice will shape the response to vaccination and further enhanced vaccine-induced systemic and mucosal immune responses to adjuvanted COBRA HA and NA vaccines and protect mice

from IAV challenge. Mice that were pre-immunized with pre-historical H1N1 and H3N2 influenza viruses and intramuscularly or intranasally vaccinated with COBRA HA and NA vaccines with CpG had elevated functional antibodies in their serum that were able to block a range of H1N1 and H3N2 influenza viruses from binding and agglutinating RBCs. They also had elevated NAI titers and induced rHA and rNA-specific total IgG, IgA or IgG1, IgG2a, and IgG2b isotypes in their serum and in their BALFs. Based on a IgG1:IgG2a ratio and IgG1, IgG2a, and IgG2b proportions by CpG1018, this adjuvant formulation induced balanced Th0 responses compared to un-adjuvated vaccines. Pre-immune mice vaccinated IM with COBRA HA/NA vaccines with CpG 1018 lost an average of ~10% of their original body weight with no clinical signs, and 100% survival. Pre-immune mice vaccinated IN with COBRA HA/NA vaccines with CpG 1018 only lost an average ~4% of their original body weight with no clinical signs, and 100% survival. Regardless of route of administration, these mice had no detectable viral lung titers following infection with an H1N1 influenza virus. The adjuvanticity of CpG 1018 in inducing protective immune responses in pre-immune models demonstrate a promising platform for influenza vaccines that target populations that closely resemble the majority of people today who already have pre-existing immunity to influenza viruses from previous exposures. Additionally, ideal immune responses were achieved by intramuscularly and intranasal routes of vaccinations, thus provided the opportunity for painless vaccination that are easily administered to the population.

Specific Aim 3: Determine the elicitation of B-cell responses by adjuvants formulated with COBRA HA and NA antigens. The working hypothesis is that naïve or pre-immune mice

vaccinated with adjuvanted COBRA HA and NA vaccines will have more antibody-secreting cells in their spleens that secret a variety of antibody isotypes that are Th1 biased, Th2 biased, or balanced Th0 profiles. Naive mice IM vaccinated with COBRA Y2 HA proteins with INI 2002 or INI 4001 agonists, regardless of formulation, secreted, for the most part, balanced total IgG1, IgG2a, and IgG2b antibodies that bound to anti-Igκ/λ capture antibodies, with specificity to Y2 HA antigens. Specifically, ASCs from naïve mice IM vaccinated with COBRA HA proteins with INI 4001 agonists in the aqueous or liposome formulations, secreted primary total IgG1 and IgG2a, with some IgG2b antibodies, with some specificity to Y2 HA. ASCs from naïve mice IM vaccinated with COBRA HA proteins with INI 4001 agonists in the emulsion formulation, secreted primary total IgG1 and some IgG2a, with no IgG2b antibodies, and specific IgG1, IgG2a, and IgG2b against Y2 HA. Naïve mice that were IM vaccinated with Advax-SM^{TM} -adjuvanted COBRA HA vaccines also had increased numbers of IgG1, IgG2a, and IgG2b ASCs in their spleens that bound the Y2 and NG2 COBRA HA antigens. On the contrary, naïve mice that were vaccinated IM with COBRA HA and NA vaccines with CpG 1018 had little to no total IgG or IgA ASCs that were not specific to WT Bris/18 rHA. Spleens of pre-immune mice IM vaccinated with COBRA HA/NA vaccines with CpG 1018 had enhanced total IgG and IgA ASCs, with low specificity to WT Bris/18 rHA. In comparison, spleens of pre-immune mice IN vaccinated with COBRA HA/NA vaccines with CpG 1018 had enhanced total IgG and IgA ASCs, that were highly-specific to WT Bris/18 rHA. These finding show that vaccinating with COBRA HA and NA vaccines adjuvanted with different classes of adjuvants induced efficient isotype switching that confers a broad pool of

isotypes necessary for protecting against subsequent infection infections as compared to un-adjuvanted COBRA HA and NA vaccines.

All together, these results demonstrate the identification of promising novel adjuvants that function in distinct ways to mount a mimicry of immune responses necessary to set the stage for future influenza virus encounters. Through this project, several novel adjuvants were tailored to next-generation COBRA HA and NA influenzas vaccines that can be used in naïve and pre-immune models, thus providing several options to induce COBRA's full potential via different routes of administrations.

References

[1] A. M. Smith, “Host-pathogen kinetics during influenza infection and coinfection: insights from predictive modeling,” *Immunological Reviews*, vol. 285, no. 1, pp. 97–112, Sep. 2018, doi: 10.1111/imr.12692.

[2] A. S. Monto, S. Gravenstein, M. Elliott, M. Colopy, and J. Schweinle, “Clinical Signs and Symptoms Predicting Influenza Infection,” *Arch Intern Med*, vol. 160, no. 21, p. 3243, Nov. 2000, doi: 10.1001/archinte.160.21.3243.

[3] J. K. Taubenberger and D. M. Morens, “The Pathology of Influenza Virus Infections,” *Annual Review of Pathology: Mechanisms of Disease*, vol. 3, no. 1, pp. 499–522, 2008, doi: 10.1146/annurev.pathmechdis.3.121806.154316.

[4] D. Raoult and M. Drancourt, Eds., *Paleomicrobiology: past human infections*. Berlin Heidelberg: Springer, 2008.

[5] S. Al Hajjar and K. McIntosh, “The first influenza pandemic of the 21st century,” *Ann Saudi Med*, vol. 30, no. 1, pp. 1–10, 2010, doi: 10.4103/0256-4947.59365.

[6] H. Kim, R. G. Webster, and R. J. Webby, “Influenza Virus: Dealing with a Drifting and Shifting Pathogen,” *Viral Immunology*, vol. 31, no. 2, pp. 174–183, 2018, doi: 10.1089/vim.2017.0141.

[7] C. E. Van De Sandt, J. H. C. M. Kreijtz, and G. F. Rimmelzwaan, “Evasion of Influenza A Viruses from Innate and Adaptive Immune Responses,” *Viruses*, vol. 4, no. 9, pp. 1438–1476, Sep. 2012, doi: 10.3390/v4091438.

[8] M. Alfelali, G. Khandaker, R. Booy, and H. Rashid, "Mismatching between circulating strains and vaccine strains of influenza: Effect on Hajj pilgrims from both hemispheres," *Human Vaccines & Immunotherapeutics*, vol. 12, no. 3, pp. 709–715, Mar. 2016, doi: 10.1080/21645515.2015.1085144.

[9] Y. Huang, M. S. França, J. D. Allen, H. Shi, and T. M. Ross, "Next Generation of computationally optimized broadly reactive ha vaccines elicited cross-reactive immune responses and provided protection against H1N1 virus infection," *Vaccines*, vol. 9, no. 7, p. 793, 2021.

[10] J. D. Allen and T. M. Ross, "Bivalent H1 and H3 COBRA Recombinant Hemagglutinin Vaccines Elicit Seroprotective Antibodies against H1N1 and H3N2 Influenza Viruses from 2009 to 2019," *Journal of Virology*, vol. 96, no. 7, pp. e01652-21, 2022.

[11] B. M. Giles *et al.*, "A Computationally Optimized Hemagglutinin Virus-Like Particle Vaccine Elicits Broadly Reactive Antibodies that Protect Nonhuman Primates from H5N1 Infection," *The Journal of Infectious Diseases*, vol. 205, no. 10, pp. 1562–1570, May 2012, doi: 10.1093/infdis/jis232.

[12] N. Uno and T. M. Ross, "Multivalent next generation influenza virus vaccines protect against seasonal and pre-pandemic viruses," *Scientific Reports*, vol. 14, no. 1, p. 1440, 2024.

[13] M. A. Carlock and T. M. Ross, "A computationally optimized broadly reactive hemagglutinin vaccine elicits neutralizing antibodies against influenza B viruses from both lineages," *Scientific Reports*, vol. 13, no. 1, p. 15911, 2023.

[14] A. L. Skarlupka, A.-G. Bebin-Blackwell, S. F. Sumner, and T. M. Ross, "Universal Influenza Virus Neuraminidase Vaccine Elicits Protective Immune Responses against Human Seasonal and Pre-pandemic Strains," *J Virol*, vol. 95, no. 17, pp. e00759-21, Aug. 2021, doi: 10.1128/JVI.00759-21.

[15] R. M. Pielak and J. J. Chou, "Influenza M2 proton channels," *Biochimica et Biophysica Acta (BBA) - Biomembranes*, vol. 1808, no. 2, pp. 522–529, Feb. 2011, doi: 10.1016/j.bbamem.2010.04.015.

[16] M. Javanian, M. Barary, S. Ghebrehewet, V. Koppolu, V. Vasigala, and S. Ebrahimpour, "A brief review of influenza virus infection," *Journal of Medical Virology*, vol. 93, no. 8, pp. 4638–4646, Aug. 2021, doi: 10.1002/jmv.26990.

[17] M. Huarte, J. J. Sanz-Ezquerro, F. Roncal, J. Ortín, and A. Nieto, "PA Subunit from Influenza Virus Polymerase Complex Interacts with a Cellular Protein with Homology to a Family of Transcriptional Activators," *J Virol*, vol. 75, no. 18, pp. 8597–8604, Sep. 2001, doi: 10.1128/JVI.75.18.8597-8604.2001.

[18] S. González and J. Ortín, "Characterization of Influenza Virus PB1 Protein Binding to Viral RNA: Two Separate Regions of the Protein Contribute to the Interaction Domain," *J Virol*, vol. 73, no. 1, pp. 631–637, Jan. 1999, doi: 10.1128/JVI.73.1.631-637.1999.

[19] J. C. D. Long and E. Fodor, "The PB2 Subunit of the Influenza A Virus RNA Polymerase Is Imported into the Mitochondrial Matrix," *J Virol*, vol. 90, no. 19, pp. 8729–8738, Oct. 2016, doi: 10.1128/JVI.01384-16.

[20] S. K. Biswas, P. L. Boutz, and D. P. Nayak, “Influenza Virus Nucleoprotein Interacts with Influenza Virus Polymerase Proteins,” *J Virol*, vol. 72, no. 7, pp. 5493–5501, Jul. 1998, doi: 10.1128/JVI.72.7.5493-5501.1998.

[21] K. Haye, S. Burmakina, T. Moran, A. García-Sastre, and A. Fernandez-Sesma, “The NS1 Protein of a Human Influenza Virus Inhibits Type I Interferon Production and the Induction of Antiviral Responses in Primary Human Dendritic and Respiratory Epithelial Cells,” *J Virol*, vol. 83, no. 13, pp. 6849–6862, Jul. 2009, doi: 10.1128/JVI.02323-08.

[22] L. Brunotte, J. Flies, H. Bolte, P. Reuther, F. Vreede, and M. Schwemmle, “The Nuclear Export Protein of H5N1 Influenza A Viruses Recruits Matrix 1 (M1) Protein to the Viral Ribonucleoprotein to Mediate Nuclear Export,” *Journal of Biological Chemistry*, vol. 289, no. 29, pp. 20067–20077, Jul. 2014, doi: 10.1074/jbc.M114.569178.

[23] M. C. Zambon, “Epidemiology and pathogenesis of influenza,” *Journal of Antimicrobial Chemotherapy*, vol. 44, no. suppl_2, pp. 3–9, Nov. 1999, doi: 10.1093/jac/44.suppl_2.3.

[24] N. Nikitin, E. Petrova, E. Trifonova, and O. Karpova, “Influenza Virus Aerosols in the Air and Their Infectiousness,” *Advances in Virology*, vol. 2014, pp. 1–6, 2014, doi: 10.1155/2014/859090.

[25] S. S. Y. Wong and K. Yuen, “Avian Influenza Virus Infections in Humans,” *Chest*, vol. 129, no. 1, pp. 156–168, Jan. 2006, doi: 10.1378/chest.129.1.156.

[26] W.-S. Ryu, “Influenza Viruses,” in *Molecular Virology of Human Pathogenic Viruses*, Elsevier, 2017, pp. 195–211. doi: 10.1016/B978-0-12-800838-6.00015-1.

[27] X. Chen, S. Liu, M. U. Goraya, M. Maarouf, S. Huang, and J.-L. Chen, "Host Immune Response to Influenza A Virus Infection," *Front. Immunol.*, vol. 9, p. 320, Mar. 2018, doi: 10.3389/fimmu.2018.00320.

[28] Y. Janssens, J. Joye, G. Waerlop, F. Clement, G. Leroux-Roels, and I. Leroux-Roels, "The role of cell-mediated immunity against influenza and its implications for vaccine evaluation," *Front. Immunol.*, vol. 13, p. 959379, Aug. 2022, doi: 10.3389/fimmu.2022.959379.

[29] M. Honigsbaum, "Revisiting the 1957 and 1968 influenza pandemics," *The Lancet*, vol. 395, no. 10240, pp. 1824–1826, Jun. 2020, doi: 10.1016/S0140-6736(20)31201-0.

[30] H. Pott *et al.*, "Vaccine Effectiveness of non-adjuvanted and adjuvanted trivalent inactivated influenza vaccines in the prevention of influenza-related hospitalization in older adults: A pooled analysis from the Serious Outcomes Surveillance (SOS) Network of the Canadian Immunization Research Network (CIRN)," *Vaccine*, vol. 41, no. 42, pp. 6359–6365, Oct. 2023, doi: 10.1016/j.vaccine.2023.08.070.

[31] T. G. Boyce *et al.*, "Safety and immunogenicity of adjuvanted and unadjuvanted subunit influenza vaccines administered intranasally to healthy adults," *Vaccine*, vol. 19, no. 2–3, pp. 217–226, Sep. 2000, doi: 10.1016/S0264-410X(00)00171-7.

[32] T. Samji, "Influenza A: understanding the viral life cycle," *Yale J Biol Med*, vol. 82, no. 4, pp. 153–159, Dec. 2009.

[33] C. Zhao and J. Pu, "Influence of Host Sialic Acid Receptors Structure on the Host Specificity of Influenza Viruses," *Viruses*, vol. 14, no. 10, p. 2141, Sep. 2022, doi: 10.3390/v14102141.

[34] R. Trebbien, L. E. Larsen, and B. M. Viuff, "Distribution of sialic acid receptors and influenza A virus of avian and swine origin in experimentally infected pigs," *Virol J*, vol. 8, no. 1, p. 434, Dec. 2011, doi: 10.1186/1743-422X-8-434.

[35] H. Shelton *et al.*, "Receptor Binding Profiles of Avian Influenza Virus Hemagglutinin Subtypes on Human Cells as a Predictor of Pandemic Potential," *J Virol*, vol. 85, no. 4, pp. 1875–1880, Feb. 2011, doi: 10.1128/JVI.01822-10.

[36] W. Ma *et al.*, "Viral reassortment and transmission after co-infection of pigs with classical H1N1 and triple-reassortant H3N2 swine influenza viruses," *Journal of General Virology*, vol. 91, no. 9, pp. 2314–2321, Sep. 2010, doi: 10.1099/vir.0.021402-0.

[37] C. Sieben, E. Sezgin, C. Eggeling, and S. Manley, "Influenza A viruses use multivalent sialic acid clusters for cell binding and receptor activation," *PLoS Pathog*, vol. 16, no. 7, p. e1008656, Jul. 2020, doi: 10.1371/journal.ppat.1008656.

[38] Z. Zhu, H. Fan, and E. Fodor, "Defining the minimal components of the influenza A virus replication machinery via an in vitro reconstitution system," *PLoS Biol*, vol. 21, no. 11, p. e3002370, Nov. 2023, doi: 10.1371/journal.pbio.3002370.

[39] D. Dou, R. Revol, H. Östbye, H. Wang, and R. Daniels, "Influenza A Virus Cell Entry, Replication, Virion Assembly and Movement," *Front. Immunol.*, vol. 9, p. 1581, Jul. 2018, doi: 10.3389/fimmu.2018.01581.

[40] Y. Matsuoka *et al.*, "A comprehensive map of the influenza A virus replication cycle," *BMC Syst Biol*, vol. 7, no. 1, p. 97, Dec. 2013, doi: 10.1186/1752-0509-7-97.

[41] W. Zheng and Y. J. Tao, “Structure and assembly of the influenza A virus ribonucleoprotein complex,” *FEBS Letters*, vol. 587, no. 8, pp. 1206–1214, Apr. 2013, doi: 10.1016/j.febslet.2013.02.048.

[42] A. J. Eisfeld, G. Neumann, and Y. Kawaoka, “At the centre: influenza A virus ribonucleoproteins,” *Nat Rev Microbiol*, vol. 13, no. 1, pp. 28–41, Jan. 2015, doi: 10.1038/nrmicro3367.

[43] K. L. Roberts, B. Manicassamy, and R. A. Lamb, “Influenza A Virus Uses Intercellular Connections To Spread to Neighboring Cells,” *J Virol*, vol. 89, no. 3, pp. 1537–1549, Feb. 2015, doi: 10.1128/JVI.03306-14.

[44] M. N. Matrosovich, T. Y. Matrosovich, T. Gray, N. A. Roberts, and H.-D. Klenk, “Neuraminidase Is Important for the Initiation of Influenza Virus Infection in Human Airway Epithelium,” *J Virol*, vol. 78, no. 22, pp. 12665–12667, Nov. 2004, doi: 10.1128/JVI.78.22.12665-12667.2004.

[45] G. S. Getz, “Bridging the innate and adaptive immune systems,” *Journal of Lipid Research*, vol. 46, no. 4, pp. 619–622, Apr. 2005, doi: 10.1194/jlr.E500002-JLR200.

[46] G. Malik and Y. Zhou, “Innate Immune Sensing of Influenza A Virus,” *Viruses*, vol. 12, no. 7, p. 755, Jul. 2020, doi: 10.3390/v12070755.

[47] L. K. Campbell and K. E. Magor, “Pattern Recognition Receptor Signaling and Innate Responses to Influenza A Viruses in the Mallard Duck, Compared to Humans and Chickens,” *Front. Cell. Infect. Microbiol.*, vol. 10, p. 209, May 2020, doi: 10.3389/fcimb.2020.00209.

[48] W. Wu and J. P. Metcalf, “The Role of Type I IFNs in Influenza: Antiviral Superheroes or Immunopathogenic Villains?,” *J Innate Immun*, vol. 12, no. 6, pp. 437–447, 2020, doi: 10.1159/000508379.

[49] T. Uehata and O. Takeuchi, “RNA Recognition and Immunity—Innate Immune Sensing and Its Posttranscriptional Regulation Mechanisms,” *Cells*, vol. 9, no. 7, p. 1701, Jul. 2020, doi: 10.3390/cells9071701.

[50] M. D. Tate and A. Mansell, “An update on the NLRP3 inflammasome and influenza: the road to redemption or perdition?,” *Current Opinion in Immunology*, vol. 54, pp. 80–85, Oct. 2018, doi: 10.1016/j.coi.2018.06.005.

[51] K. B. Gorden *et al.*, “Synthetic TLR Agonists Reveal Functional Differences between Human TLR7 and TLR8,” *The Journal of Immunology*, vol. 174, no. 3, pp. 1259–1268, Feb. 2005, doi: 10.4049/jimmunol.174.3.1259.

[52] A. Iwasaki and P. S. Pillai, “Innate immunity to influenza virus infection,” *Nat Rev Immunol*, vol. 14, no. 5, pp. 315–328, May 2014, doi: 10.1038/nri3665.

[53] Z. Guo *et al.*, “Use of Biolayer Interferometry to Identify Dominant Binding Epitopes of Influenza Hemagglutinin Protein of A(H1N1)pdm09 in the Antibody Response to 2010–2011 Influenza Seasonal Vaccine,” *Vaccines*, vol. 11, no. 8, p. 1307, Jul. 2023, doi: 10.3390/vaccines11081307.

[54] S. T. H. Liu *et al.*, “Antigenic sites in influenza H1 hemagglutinin display species-specific immunodominance,” *Journal of Clinical Investigation*, vol. 128, no. 11, pp. 4992–4996, Oct. 2018, doi: 10.1172/JCI122895.

[55] L. Popova *et al.*, “Immunodominance of Antigenic Site B over Site A of Hemagglutinin of Recent H3N2 Influenza Viruses,” *PLoS ONE*, vol. 7, no. 7, p. e41895, Jul. 2012, doi: 10.1371/journal.pone.0041895.

[56] N. Abbadi and J. J. Mousa, “Broadly Protective Neuraminidase-Based Influenza Vaccines and Monoclonal Antibodies: Target Epitopes and Mechanisms of Action,” *Viruses*, vol. 15, no. 1, p. 200, Jan. 2023, doi: 10.3390/v15010200.

[57] J. A. McMurry, B. E. Johansson, and A. S. De Groot, “A call to cellular & humoral arms: Enlisting cognate T cell help to develop broad-spectrum vaccines against influenza A,” *Human Vaccines*, vol. 4, no. 2, pp. 148–157, Mar. 2008, doi: 10.4161/hv.4.2.5169.

[58] H. Wan *et al.*, “Molecular Basis for Broad Neuraminidase Immunity: Conserved Epitopes in Seasonal and Pandemic H1N1 as Well as H5N1 Influenza Viruses,” *J Virol*, vol. 87, no. 16, pp. 9290–9300, Aug. 2013, doi: 10.1128/JVI.01203-13.

[59] R. F. Nuwarda, A. A. Alharbi, and V. Kayser, “An Overview of Influenza Viruses and Vaccines,” *Vaccines*, vol. 9, no. 9, p. 1032, Sep. 2021, doi: 10.3390/vaccines9091032.

[60] S.-S. Wong and R. J. Webby, “Traditional and New Influenza Vaccines,” *Clin Microbiol Rev*, vol. 26, no. 3, pp. 476–492, Jul. 2013, doi: 10.1128/CMR.00097-12.

[61] K. G.-I. Mohn, I. Smith, H. Sjursen, and R. J. Cox, “Immune responses after live attenuated influenza vaccination,” *Hum Vaccin Immunother*, vol. 14, no. 3, pp. 571–578, Mar. 2018, doi: 10.1080/21645515.2017.1377376.

[62] X. Dai, Y. Xiong, N. Li, and C. Jian, “Vaccine Types,” in *Vaccines - the History and Future*, V. Kumar, Ed., IntechOpen, 2019. doi: 10.5772/intechopen.84626.

[63] D. Gupta and S. Mohan, “Influenza vaccine: a review on current scenario and future prospects,” *Journal of Genetic Engineering and Biotechnology*, vol. 21, no. 1, p. 154, Dec. 2023, doi: 10.1186/s43141-023-00581-y.

[64] P. G. Van Buynder *et al.*, “The comparative effectiveness of adjuvanted and unadjuvanted trivalent inactivated influenza vaccine (TIV) in the elderly,” *Vaccine*, vol. 31, no. 51, pp. 6122–6128, Dec. 2013, doi: 10.1016/j.vaccine.2013.07.059.

[65] W.-C. Wang, E. E. Sayedahmed, S. Sambhara, and S. K. Mittal, “Progress towards the Development of a Universal Influenza Vaccine,” *Viruses*, vol. 14, no. 8, p. 1684, Jul. 2022, doi: 10.3390/v14081684.

[66] B. L. Bullard and E. A. Weaver, “Strategies Targeting Hemagglutinin as a Universal Influenza Vaccine,” *Vaccines*, vol. 9, no. 3, p. 257, Mar. 2021, doi: 10.3390/vaccines9030257.

[67] D. Stadlbauer *et al.*, “Broadly protective human antibodies that target the active site of influenza virus neuraminidase,” *Science*, vol. 366, no. 6464, pp. 499–504, Oct. 2019, doi: 10.1126/science.aay0678.

[68] E. Hansen, T. Day, J. Arino, J. Wu, and S. M. Moghadas, “Strategies for the Use of Oseltamivir and Zanamivir during Pandemic Outbreaks,” *Canadian Journal of Infectious Diseases and Medical Microbiology*, vol. 21, no. 1, pp. e28–e63, 2010, doi: 10.1155/2010/690654.

[69] R. Trebbien, S. S. Pedersen, K. Vorborg, K. T. Franck, and T. K. Fischer, “Development of oseltamivir and zanamivir resistance in influenza A(H1N1)pdm09 virus, Denmark, 2014,” *Eurosurveillance*, vol. 22, no. 3, Jan. 2017, doi: 10.2807/1560-7917.ES.2017.22.3.30445.

[70] R. Kavishna *et al.*, "A single-shot vaccine approach for the universal influenza A vaccine candidate M2e," *Proc. Natl. Acad. Sci. U.S.A.*, vol. 119, no. 13, p. e2025607119, Mar. 2022, doi: 10.1073/pnas.2025607119.

[71] E. E. Sayedahmed, N. O. Elshafie, A. P. Dos Santos, C. Jagannath, S. Sambhara, and S. K. Mittal, "Development of NP-Based Universal Vaccine for Influenza A Viruses," *Vaccines*, vol. 12, no. 2, p. 157, Feb. 2024, doi: 10.3390/vaccines12020157.

[72] X. Xie *et al.*, "Influenza Vaccine With Consensus Internal Antigens as Immunogens Provides Cross-Group Protection Against Influenza A Viruses," *Front. Microbiol.*, vol. 10, p. 1630, Jul. 2019, doi: 10.3389/fmicb.2019.01630.

[73] H. Miwa *et al.*, "Improved Humoral Immunity and Protection against Influenza Virus Infection with a 3d Porous Biomaterial Vaccine," *Advanced Science*, vol. 10, no. 31, p. 2302248, Nov. 2023, doi: 10.1002/advs.202302248.

[74] D. J. Laddy *et al.*, "Heterosubtypic Protection against Pathogenic Human and Avian Influenza Viruses via In Vivo Electroporation of Synthetic Consensus DNA Antigens," *PLoS ONE*, vol. 3, no. 6, p. e2517, Jun. 2008, doi: 10.1371/journal.pone.0002517.

[75] S. T. C. Elliott *et al.*, "A Synthetic Micro-Consensus DNA Vaccine Generates Comprehensive Influenza A H3N2 Immunity and Protects Mice Against Lethal Challenge by Multiple H3N2 Viruses," *Human Gene Therapy*, vol. 29, no. 9, pp. 1044–1055, Sep. 2018, doi: 10.1089/hum.2018.102.

[76] E. A. Weaver, A. M. Rubrum, R. J. Webby, and M. A. Barry, "Protection against Divergent Influenza H1N1 Virus by a Centralized Influenza Hemagglutinin," *PLoS ONE*, vol. 6, no. 3, p. e18314, Mar. 2011, doi: 10.1371/journal.pone.0018314.

[77] J. D. Allen and T. M. Ross, “Next generation methodology for updating HA vaccines against emerging human seasonal influenza A(H3N2) viruses,” *Scientific Reports*, vol. 11, no. 1, p. 4554, Mar. 2021, doi: 10.1038/s41598-020-79590-7.

[78] P. L. Sanchez, G. Andre, A. Antipov, N. Petrovsky, and T. M. Ross, “Advax-SM™-Adjuvanted COBRA (H1/H3) Hemagglutinin Influenza Vaccines,” *Vaccines*, vol. 12, no. 5, p. 455, Apr. 2024, doi: 10.3390/vaccines12050455.

[79] C. J. Crevar, D. M. Carter, K. Y. J. Lee, and T. M. Ross, “Cocktail of H5N1 COBRA HA vaccines elicit protective antibodies against H5N1 viruses from multiple clades,” *Human Vaccines & Immunotherapeutics*, vol. 11, no. 3, pp. 572–583, Mar. 2015, doi: 10.1080/21645515.2015.1012013.

[80] M. Kwissa, S. Pai Kasturi, and B. Pulendran, “The science of adjuvants,” *Expert Review of Vaccines*, vol. 6, no. 5, pp. 673–684, Oct. 2007, doi: 10.1586/14760584.6.5.673.

[81] N. Garçon and A. Di Pasquale, “From discovery to licensure, the Adjuvant System story,” *Human Vaccines & Immunotherapeutics*, vol. 13, no. 1, pp. 19–33, Jan. 2017, doi: 10.1080/21645515.2016.1225635.

[82] H. HogenEsch, “Mechanisms of stimulation of the immune response by aluminum adjuvants,” *Vaccine*, vol. 20, pp. S34–S39, May 2002, doi: 10.1016/S0264-410X(02)00169-X.

[83] A. S. McKee and P. Marrack, “Old and new adjuvants,” *Current Opinion in Immunology*, vol. 47, pp. 44–51, Aug. 2017, doi: 10.1016/j.coi.2017.06.005.

[84] A. J. M. Van Oosterhout, “Th1/Th2 paradigm: not seeing the forest for the trees?,” *European Respiratory Journal*, vol. 25, no. 4, pp. 591–593, Apr. 2005, doi: 10.1183/09031936.05.00014105.

[85] S. Romagnani, “Th1/Th2 Cells:,” *Inflammatory Bowel Diseases*, vol. 5, no. 4, pp. 285–294, Nov. 1999, doi: 10.1097/00054725-199911000-00009.

[86] T. Zhao *et al.*, “Vaccine adjuvants: mechanisms and platforms,” *Sig Transduct Target Ther*, vol. 8, no. 1, p. 283, Jul. 2023, doi: 10.1038/s41392-023-01557-7.

[87] M. Luchner, S. Reinke, and A. Milicic, “TLR Agonists as Vaccine Adjuvants Targeting Cancer and Infectious Diseases,” *Pharmaceutics*, vol. 13, no. 2, p. 142, Jan. 2021, doi: 10.3390/pharmaceutics13020142.

[88] D. T. O’Hagan and N. M. Valiante, “Recent advances in the discovery and delivery of vaccine adjuvants,” *Nat Rev Drug Discov*, vol. 2, no. 9, pp. 727–735, Sep. 2003, doi: 10.1038/nrd1176.

[89] B. Levast, S. Awate, L. Babiuk, G. Mutwiri, V. Gerdts, and S. Van Drunen Littel-van Den Hurk, “Vaccine Potentiation by Combination Adjuvants,” *Vaccines*, vol. 2, no. 2, pp. 297–322, Apr. 2014, doi: 10.3390/vaccines2020297.

[90] M. Coccia *et al.*, “Cellular and molecular synergy in AS01-adjuvanted vaccines results in an early IFNγ response promoting vaccine immunogenicity,” *npj Vaccines*, vol. 2, no. 1, p. 25, Sep. 2017, doi: 10.1038/s41541-017-0027-3.

[91] A. M. Didierlaurent *et al.*, “AS04, an Aluminum Salt- and TLR4 Agonist-Based Adjuvant System, Induces a Transient Localized Innate Immune Response Leading to Enhanced Adaptive Immunity,” *The Journal of Immunology*, vol. 183, no. 10, pp. 6186–6197, Nov. 2009, doi: 10.4049/jimmunol.0901474.

[92] D. Laera, H. HogenEsch, and D. T. O'Hagan, "Aluminum Adjuvants—'Back to the Future,'" *Pharmaceutics*, vol. 15, no. 7, p. 1884, Jul. 2023, doi: 10.3390/pharmaceutics15071884.

[93] B. Pulendran, P. S. Arunachalam, and D. T. O'Hagan, "Emerging concepts in the science of vaccine adjuvants," *Nature Reviews Drug Discovery*, vol. 20, no. 6, pp. 454–475, Jun. 2021, doi: 10.1038/s41573-021-00163-y.

[94] B. N. Lambrecht, M. Kool, M. A. Willart, and H. Hammad, "Mechanism of action of clinically approved adjuvants," *Current Opinion in Immunology*, vol. 21, no. 1, pp. 23–29, Feb. 2009, doi: 10.1016/j.coi.2009.01.004.

[95] T. R. Ghimire, "The mechanisms of action of vaccines containing aluminum adjuvants: an in vitro vs in vivo paradigm," *SpringerPlus*, vol. 4, no. 1, p. 181, Dec. 2015, doi: 10.1186/s40064-015-0972-0.

[96] M. Kool *et al.*, "Alum adjuvant boosts adaptive immunity by inducing uric acid and activating inflammatory dendritic cells," *The Journal of Experimental Medicine*, vol. 205, no. 4, pp. 869–882, Apr. 2008, doi: 10.1084/jem.20071087.

[97] S. F. Little, B. E. Ivins, W. M. Webster, S. L. W. Norris, and G. P. Andrews, "Effect of aluminum hydroxide adjuvant and formaldehyde in the formulation of rPA anthrax vaccine," *Vaccine*, vol. 25, no. 15, pp. 2771–2777, Apr. 2007, doi: 10.1016/j.vaccine.2006.12.043.

[98] R. T. Kenney, D. L. Sacks, J. P. Sypek, L. Vilela, A. A. Gam, and K. Evans-Davis, "Protective Immunity Using Recombinant Human IL-12 and Alum as Adjuvants in a Primate Model of Cutaneous Leishmaniasis," *The Journal of Immunology*, vol. 163, no. 8, pp. 4481–4488, Oct. 1999, doi: 10.4049/jimmunol.163.8.4481.

[99] E. Sasaki, H. Asanuma, H. Momose, K. Furuhata, T. Mizukami, and I. Hamaguchi, "Nasal alum-adjuvanted vaccine promotes IL-33 release from alveolar epithelial cells that elicits IgA production via type 2 immune responses," *PLoS Pathog*, vol. 17, no. 8, p. e1009890, Aug. 2021, doi: 10.1371/journal.ppat.1009890.

[100] S. Hutchison, R. A. Benson, V. B. Gibson, A. H. Pollock, P. Garside, and J. M. Brewer, "Antigen depot is not required for alum adjuvanticity," *FASEB J*, vol. 26, no. 3, pp. 1272–1279, Mar. 2012, doi: 10.1096/fj.11-184556.

[101] C. J. Clements and E. Griffiths, "The global impact of vaccines containing aluminium adjuvants," *Vaccine*, vol. 20 Suppl 3, pp. S24-33, May 2002, doi: 10.1016/s0264-410x(02)00168-8.

[102] A. L. Gavin *et al.*, "Adjuvant-enhanced antibody responses in the absence of toll-like receptor signaling," *Science*, vol. 314, no. 5807, pp. 1936–1938, Dec. 2006, doi: 10.1126/science.1135299.

[103] P. Marrack, A. S. McKee, and M. W. Munks, "Towards an understanding of the adjuvant action of aluminium," *Nat Rev Immunol*, vol. 9, no. 4, pp. 287–293, Apr. 2009, doi: 10.1038/nri2510.

[104] E.-J. Ko and S.-M. Kang, "Immunology and efficacy of MF59-adjuvanted vaccines," *Human Vaccines & Immunotherapeutics*, vol. 14, no. 12, pp. 3041–3045, Dec. 2018, doi: 10.1080/21645515.2018.1495301.

[105] I. R. Tizard, "Adjuvants and adjuvanticity," *Vaccines for Veterinarians*, pp. 75-86.e1, 2021, doi: 10.1016/B978-0-323-68299-2.00016-2.

[106] G.-E. Chae, D. W. Kim, and H.-E. Jin, "Development of Squalene-Based Oil-in-Water Emulsion Adjuvants Using a Self-Emulsifying Drug Delivery System for

Enhanced Antigen-Specific Antibody Titers," *IJN*, vol. Volume 17, pp. 6221–6231, Dec. 2022, doi: 10.2147/IJN.S379950.

[107] G. K. Pedersen, K. Wørzner, P. Andersen, and D. Christensen, "Vaccine Adjuvants Differentially Affect Kinetics of Antibody and Germinal Center Responses," *Front. Immunol.*, vol. 11, p. 579761, Sep. 2020, doi: 10.3389/fimmu.2020.579761.

[108] P. Nguyen-Contant, M. Y. Sangster, and D. J. Topham, "Squalene-Based Influenza Vaccine Adjuvants and Their Impact on the Hemagglutinin-Specific B Cell Response," *Pathogens*, vol. 10, no. 3, p. 355, Mar. 2021, doi: 10.3390/pathogens10030355.

[109] Z. Wu and K. Liu, "Overview of vaccine adjuvants," *Medicine in Drug Discovery*, vol. 11, p. 100103, Sep. 2021, doi: 10.1016/j.medidd.2021.100103.

[110] F. M. Audibert and L. D. Lise, "Adjuvants: current status, clinical perspectives and future prospects," *Trends Pharmacol Sci*, vol. 14, no. 5, pp. 174–178, May 1993, doi: 10.1016/0165-6147(93)90204-w.

[111] J. C. Cox and A. R. Coulter, "Adjuvants--a classification and review of their modes of action," *Vaccine*, vol. 15, no. 3, pp. 248–256, Feb. 1997, doi: 10.1016/s0264-410x(96)00183-1.

[112] A. Sepasi, M. Ghafourian, M. Taghizadeh, and M. Mahdavi, "Formulation of Recombinant H1N1 Hemagglutinin in MF59 and Alum Adjuvants: A Comparison of the Vaccines Potency and Efficacy in BALB/C Mice," *Viral Immunology*, vol. 36, no. 6, pp. 401–408, Aug. 2023, doi: 10.1089/vim.2023.0003.

[113] H. Chang *et al.*, "Single immunization with MF59-adjuvanted inactivated whole-virion H7N9 influenza vaccine provides early protection against H7N9 virus challenge

in mice," *Microbes and Infection*, vol. 19, no. 12, pp. 616–625, Dec. 2017, doi: 10.1016/j.micinf.2017.08.012.

[114] T. W. Clark *et al.*, "Trial of 2009 influenza A (H1N1) monovalent MF59-adjuvanted vaccine," *N Engl J Med*, vol. 361, no. 25, pp. 2424–2435, Dec. 2009, doi: 10.1056/NEJMoa0907650.

[115] A. Podda, "The adjuvanted influenza vaccines with novel adjuvants: experience with the MF59-adjuvanted vaccine," *Vaccine*, vol. 19, no. 17, pp. 2673–2680, Mar. 2001, doi: 10.1016/S0264-410X(00)00499-0.

[116] G. Galli *et al.*, "Fast rise of broadly cross-reactive antibodies after boosting long-lived human memory B cells primed by an MF59 adjuvanted prepandemic vaccine," *Proc Natl Acad Sci U S A*, vol. 106, no. 19, pp. 7962–7967, May 2009, doi: 10.1073/pnas.0903181106.

[117] C. R. Kensil, S. Soltysik, D. A. Wheeler, and J. Y. Wu, "Structure/function studies on QS-21, a unique immunological adjuvant from Quillaja saponaria," *Adv Exp Med Biol*, vol. 404, pp. 165–172, 1996, doi: 10.1007/978-1-4899-1367-8_15.

[118] A. M. Didierlaurent, B. Laupèze, A. Di Pasquale, N. Hergli, C. Collignon, and N. Garçon, "Adjuvant system AS01: helping to overcome the challenges of modern vaccines," *Expert Rev Vaccines*, vol. 16, no. 1, pp. 55–63, Jan. 2017, doi: 10.1080/14760584.2016.1213632.

[119] D. Zhu and W. Tuo, "QS-21: A Potent Vaccine Adjuvant," *Nat Prod Chem Res*, vol. 3, no. 4, p. e113, Apr. 2016, doi: 10.4172/2329-6836.1000e113.

[120] C. Pifferi, R. Fuentes, and A. Fernández-Tejada, "Natural and synthetic carbohydrate-based vaccine adjuvants and their mechanisms of action," *Nat Rev Chem*, vol. 5, no. 3, pp. 197–216, 2021, doi: 10.1038/s41570-020-00244-3.

[121] A. Iwasaki and S. B. Omer, "Why and How Vaccines Work," *Cell*, vol. 183, no. 2, pp. 290–295, Oct. 2020, doi: 10.1016/j.cell.2020.09.040.

[122] D. R. Tait *et al.*, "Final Analysis of a Trial of M72/AS01E Vaccine to Prevent Tuberculosis," *N Engl J Med*, vol. 381, no. 25, pp. 2429–2439, Dec. 2019, doi: 10.1056/NEJMoa1909953.

[123] Z. Ji *et al.*, "Immunogenicity and Safety of the M72/AS01E Candidate Vaccine Against Tuberculosis: A Meta-Analysis," *Front Immunol*, vol. 10, p. 2089, 2019, doi: 10.3389/fimmu.2019.02089.

[124] O. Van Der Meeren *et al.*, "Phase 2b Controlled Trial of M72/AS01E Vaccine to Prevent Tuberculosis," *N Engl J Med*, vol. 379, no. 17, pp. 1621–1634, Oct. 2018, doi: 10.1056/NEJMoa1803484.

[125] A. L. Wilkins *et al.*, "AS03- and MF59-Adjuvanted Influenza Vaccines in Children," *Front Immunol*, vol. 8, pp. 1760–1760, Dec. 2017, doi: 10.3389/fimmu.2017.01760.

[126] F. Roman, T. Vaman, B. Gerlach, A. Markendorf, P. Gillard, and J.-M. Devaster, "Immunogenicity and safety in adults of one dose of influenza A H1N1v 2009 vaccine formulated with and without AS03A-adjuvant: preliminary report of an observer-blind, randomised trial," *Vaccine*, vol. 28, no. 7, pp. 1740–1745, Feb. 2010, doi: 10.1016/j.vaccine.2009.12.014.

[127] S. Morel *et al.*, “Adjuvant System AS03 containing α-tocopherol modulates innate immune response and leads to improved adaptive immunity,” *Vaccine*, vol. 29, no. 13, pp. 2461–2473, Mar. 2011, doi: 10.1016/j.vaccine.2011.01.011.

[128] P. Moris *et al.*, “H5N1 influenza vaccine formulated with AS03 A induces strong cross-reactive and polyfunctional CD4 T-cell responses,” *J Clin Immunol*, vol. 31, no. 3, pp. 443–454, Jun. 2011, doi: 10.1007/s10875-010-9490-6.

[129] O. Sobolev *et al.*, “Adjuvanted influenza-H1N1 vaccination reveals lymphoid signatures of age-dependent early responses and of clinical adverse events,” *Nat Immunol*, vol. 17, no. 2, pp. 204–213, Feb. 2016, doi: 10.1038/ni.3328.

[130] K. J. Hager *et al.*, “Efficacy and Safety of a Recombinant Plant-Based Adjuvanted Covid-19 Vaccine,” *N Engl J Med*, vol. 386, no. 22, pp. 2084–2096, Jun. 2022, doi: 10.1056/NEJMoa2201300.

[131] S. G. Reed, D. Carter, C. Casper, M. S. Duthie, and C. B. Fox, “Correlates of GLA family adjuvants’ activities,” *Semin Immunol*, vol. 39, pp. 22–29, Oct. 2018, doi: 10.1016/j.smim.2018.10.004.

[132] N. Garçon, S. Morel, A. Didierlaurent, D. Descamps, M. Wettendorff, and M. Van Mechelen, “Development of an AS04-adjuvanted HPV vaccine with the adjuvant system approach,” *BioDrugs*, vol. 25, no. 4, pp. 217–226, Aug. 2011, doi: 10.2165/11591760-000000000-00000.

[133] M. Kundi, “New hepatitis B vaccine formulated with an improved adjuvant system,” *Expert Rev Vaccines*, vol. 6, no. 2, pp. 133–140, Apr. 2007, doi: 10.1586/14760584.6.2.133.

[134] S. R. Skinner *et al.*, "Human papillomavirus (HPV)-16/18 AS04-adjuvanted vaccine for the prevention of cervical cancer and HPV-related diseases," *Expert Rev Vaccines*, vol. 15, no. 3, pp. 367–387, 2016, doi: 10.1586/14760584.2016.1124763.

[135] S. L. Giannini *et al.*, "Enhanced humoral and memory B cellular immunity using HPV16/18 L1 VLP vaccine formulated with the MPL/aluminium salt combination (AS04) compared to aluminium salt only," *Vaccine*, vol. 24, no. 33–34, pp. 5937–5949, Aug. 2006, doi: 10.1016/j.vaccine.2006.06.005.

[136] J. T. Bryan, B. Buckland, J. Hammond, and K. U. Jansen, "Prevention of cervical cancer: journey to develop the first human papillomavirus virus-like particle vaccine and the next generation vaccine," *Curr Opin Chem Biol*, vol. 32, pp. 34–47, Jun. 2016, doi: 10.1016/j.cbpa.2016.03.001.

[137] D. Stein, S. Roth, E. Vogelsang, and C. Nüsslein-Volhard, "The polarity of the dorsoventral axis in the Drosophila embryo is defined by an extracellular signal," *Cell*, vol. 65, no. 5, pp. 725–735, May 1991, doi: 10.1016/0092-8674(91)90381-8.

[138] B. Lemaitre, E. Nicolas, L. Michaut, J. M. Reichhart, and J. A. Hoffmann, "The dorsoventral regulatory gene cassette spätzle/Toll/cactus controls the potent antifungal response in Drosophila adults," *Cell*, vol. 86, no. 6, pp. 973–983, Sep. 1996, doi: 10.1016/s0092-8674(00)80172-5.

[139] J. A. Hoffmann, "The immune response of Drosophila," *Nature*, vol. 426, no. 6962, pp. 33–38, Nov. 2003, doi: 10.1038/nature02021.

[140] S. Akira and K. Takeda, "Toll-like receptor signalling," *Nat Rev Immunol*, vol. 4, no. 7, pp. 499–511, Jul. 2004, doi: 10.1038/nri1391.

[141] P. A. Hopkins and S. Sriskandan, “Mammalian Toll-like receptors: to immunity and beyond,” *Clin Exp Immunol*, vol. 140, no. 3, pp. 395–407, Jun. 2005, doi: 10.1111/j.1365-2249.2005.02801.x.

[142] B. Pulendran, “Modulating vaccine responses with dendritic cells and Toll-like receptors,” *Immunol Rev*, vol. 199, pp. 227–250, Jun. 2004, doi: 10.1111/j.0105-2896.2004.00144.x.

[143] B. S. Park and J.-O. Lee, “Recognition of lipopolysaccharide pattern by TLR4 complexes,” *Exp Mol Med*, vol. 45, no. 12, pp. e66–e66, Dec. 2013, doi: 10.1038/emm.2013.97.

[144] A. Ciesielska, M. Matyjek, and K. Kwiatkowska, “TLR4 and CD14 trafficking and its influence on LPS-induced pro-inflammatory signaling,” *Cell. Mol. Life Sci.*, vol. 78, no. 4, pp. 1233–1261, Feb. 2021, doi: 10.1007/s00018-020-03656-y.

[145] P. H. Goff *et al.*, “Synthetic Toll-Like Receptor 4 (TLR4) and TLR7 Ligands as Influenza Virus Vaccine Adjuvants Induce Rapid, Sustained, and Broadly Protective Responses,” *J Virol*, vol. 89, no. 6, pp. 3221–3235, Mar. 2015, doi: 10.1128/JVI.03337-14.

[146] V. C. Román-Cruz *et al.*, “Adjuvanted Vaccine Induces Functional Antibodies against Pseudomonas aeruginosa Filamentous Bacteriophages,” *Vaccines*, vol. 12, no. 2, p. 115, Jan. 2024, doi: 10.3390/vaccines12020115.

[147] S. M. Miller *et al.*, “Novel Lipidated Imidazoquinoline TLR7/8 Adjuvants Elicit Influenza-Specific Th1 Immune Responses and Protect Against Heterologous H3N2 Influenza Challenge in Mice,” *Front. Immunol.*, vol. 11, p. 406, Mar. 2020, doi: 10.3389/fimmu.2020.00406.

[148] B. Crouse *et al.*, "A TLR7/8 agonist increases efficacy of anti-fentanyl vaccines in rodent and porcine models," *npj Vaccines*, vol. 8, no. 1, p. 107, Jul. 2023, doi: 10.1038/s41541-023-00697-9.

[149] S. M. Miller *et al.*, "A lipidated TLR7/8 adjuvant enhances the efficacy of a vaccine against fentanyl in mice," *npj Vaccines*, vol. 8, no. 1, p. 97, Jul. 2023, doi: 10.1038/s41541-023-00694-y.

[150] H. Hemmi *et al.*, "A Toll-like receptor recognizes bacterial DNA," *Nature*, vol. 408, no. 6813, pp. 740–745, Dec. 2000, doi: 10.1038/35047123.

[151] R. Medzhitov *et al.*, "MyD88 is an adaptor protein in the hToll/IL-1 receptor family signaling pathways," *Mol Cell*, vol. 2, no. 2, pp. 253–258, Aug. 1998, doi: 10.1016/s1097-2765(00)80136-7.

[152] H. Hochrein *et al.*, "Herpes simplex virus type-1 induces IFN-alpha production via Toll-like receptor 9-dependent and -independent pathways," *Proc Natl Acad Sci U S A*, vol. 101, no. 31, pp. 11416–11421, Aug. 2004, doi: 10.1073/pnas.0403555101.

[153] J. Lund, A. Sato, S. Akira, R. Medzhitov, and A. Iwasaki, "Toll-like receptor 9-mediated recognition of Herpes simplex virus-2 by plasmacytoid dendritic cells," *J Exp Med*, vol. 198, no. 3, pp. 513–520, Aug. 2003, doi: 10.1084/jem.20030162.

[154] D. M. Klinman, D. Currie, I. Gursel, and D. Verthelyi, "Use of CpG oligodeoxynucleotides as immune adjuvants," *Immunol Rev*, vol. 199, pp. 201–216, Jun. 2004, doi: 10.1111/j.0105-2896.2004.00148.x.

[155] T. Kawai and S. Akira, "The role of pattern-recognition receptors in innate immunity: update on Toll-like receptors," *Nat Immunol*, vol. 11, no. 5, pp. 373–384, May 2010, doi: 10.1038/ni.1863.

[156] S. Ning, J. S. Pagano, and G. N. Barber, "IRF7: activation, regulation, modification and function," *Genes Immun*, vol. 12, no. 6, pp. 399–414, Sep. 2011, doi: 10.1038/gene.2011.21.

[157] I. G. Sakala, Y. Honda-Okubo, and N. Petrovsky, "Developmental and reproductive safety of Advax-CpG55. 2™ adjuvanted COVID-19 and influenza vaccines in mice," *Vaccine*, vol. 41, no. 41, pp. 6093–6104, 2023.

[158] Y. Honda-Okubo, F. Saade, and N. Petrovsky, "Advax™, a polysaccharide adjuvant derived from delta inulin, provides improved influenza vaccine protection through broad-based enhancement of adaptive immune responses," *Vaccine*, vol. 30, no. 36, pp. 5373–5381, Aug. 2012, doi: 10.1016/j.vaccine.2012.06.021.

[159] H. Bielefeldt-Ohmann *et al.*, "Safety and immunogenicity of a delta inulin-adjuvanted inactivated Japanese encephalitis virus vaccine in pregnant mares and foals," *Veterinary Research*, vol. 45, no. 1, p. 130, Dec. 2014, doi: 10.1186/s13567-014-0130-7.

[160] D. L. Gordon *et al.*, "Human Phase 1 trial of low-dose inactivated seasonal influenza vaccine formulated with Advax™ delta inulin adjuvant," *Vaccine*, vol. 34, no. 33, pp. 3780–3786, Jul. 2016, doi: 10.1016/j.vaccine.2016.05.071.

[161] D. Gordon, P. Kelley, S. Heinzel, P. Cooper, and N. Petrovsky, "Immunogenicity and safety of Advax™, a novel polysaccharide adjuvant based on delta inulin, when formulated with hepatitis B surface antigen: A randomized controlled Phase 1 study," *Vaccine*, vol. 32, no. 48, pp. 6469–6477, Nov. 2014, doi: 10.1016/j.vaccine.2014.09.034.

[162] K. M. Eichinger *et al.*, "Prefusion RSV F Immunization Elicits Th2-Mediated Lung Pathology in Mice When Formulated With a Th2 (but Not a Th1/Th2-Balanced) Adjuvant Despite Complete Viral Protection," *Front. Immunol.*, vol. 11, p. 1673, Jul. 2020, doi: 10.3389/fimmu.2020.01673.

[163] E. L. Stewart *et al.*, "Mucosal immunization with a delta-inulin adjuvanted recombinant spike vaccine elicits lung-resident immune memory and protects mice against SARS-CoV-2," *Mucosal Immunology*, vol. 15, no. 6, pp. 1405–1415, Nov. 2022, doi: 10.1038/s41385-022-00578-9.

[164] L. Li *et al.*, "Immunisation of ferrets and mice with recombinant SARS-CoV-2 spike protein formulated with Advax-SM adjuvant protects against COVID-19 infection," *Vaccine*, vol. 39, no. 40, pp. 5940–5953, Sep. 2021, doi: 10.1016/j.vaccine.2021.07.087.

[165] Y. Honda-Okubo, R. Bowen, M. Barker, H. Bielefeldt-Ohmann, and N. Petrovsky, "Advax-CpG55.2-adjuvanted monovalent or trivalent SARS-CoV-2 recombinant spike protein vaccine protects hamsters against heterologous infection with Beta or Delta variants," *Vaccine*, vol. 41, no. 48, pp. 7116–7128, Nov. 2023, doi: 10.1016/j.vaccine.2023.10.018.

[166] D. I. Jones *et al.*, "Optimized Mucosal MVA Prime/Soluble gp120 Boost Vaccination Regimen Induces Similar Antibody Responses as an Intramuscular Regimen," *Journal of Virology*, 2019, doi: 10.1128/JVI.00475-19.

[167] C. L. Longland, M. Mezna, and F. Michelangeli, "The Mechanism of Inhibition of the Ca2+-ATPase by Mastoparan MASTOPARAN ABOLISHES COOPERATIVE

Ca2+ BINDING," *Journal of Biological Chemistry*, vol. 274, no. 21, pp. 14799–14805, 1999.

[168] L. Ontiveros-Padilla *et al.*, "Development of a broadly active influenza intranasal vaccine adjuvanted with self-assembled particles composed of mastoparan-7 and CpG," *Frontiers in Immunology*, vol. 14, p. 1103765, 2023.

[169] M. Kumar, K. Duraisamy, and B.-K.-C. Chow, "Unlocking the non-IgE-mediated pseudo-allergic reaction puzzle with mas-related G-protein coupled receptor member X2 (MRGPRX2)," *Cells*, vol. 10, no. 5, p. 1033, 2021.

[170] M. Krystel-Whittemore, K. N. Dileepan, and J. G. Wood, "Mast Cell: A Multi-Functional Master Cell," *Front Immunol*, vol. 6, pp. 620–620, Jan. 2016, doi: 10.3389/fimmu.2015.00620.

[171] T. C. Moon, A. D. Befus, and M. Kulka, "Mast Cell Mediators: Their Differential Release and the Secretory Pathways Involved," *Frontiers in Immunology*, vol. 5, p. 569, 2014, doi: 10.3389/fimmu.2014.00569.

[172] B. Johnson-Weaver, H. W. Choi, S. N. Abraham, and H. F. Staats, "Mast cell activators as novel immune regulators," *Current opinion in pharmacology*, vol. 41, pp. 89–95, 2018.

[173] M. S. Wanyonyi, "The Adjuvant Activity and Mechanisms of Action for Mastoparan 7 Peptide After Intranasal Immunization in Mice," 2014.

[174] A. L. St. John *et al.*, "Novel mucosal adjuvant, mastoparan-7, improves cocaine vaccine efficacy," *npj Vaccines*, vol. 5, no. 1, p. 12, 2020.

[175] B. T. Johnson, M. Kulis, S. N. Abraham, A. W. Burks, and H. F. Staats, "Nasal immunization with peanut antigen and the cationic peptide adjuvant mastoparan 7

induces serum humoral immunity that protects peanut allergic mice against systemic anaphylaxis," *Journal of Allergy and Clinical Immunology*, vol. 129, no. 2, p. AB176, 2012.

[176] B. T. Johnson-Weaver *et al.*, "Nasal immunization with small molecule mast cell activators enhance immunity to Co-administered subunit immunogens," *Frontiers in immunology*, vol. 12, p. 730346, 2021.

[177] D. A. Piggott *et al.*, "MyD88-dependent induction of allergic Th2 responses to intranasal antigen," *The Journal of clinical investigation*, vol. 115, no. 2, pp. 459–467, 2005.

[178] Y. Li and X. Chen, "CpG 1018 Is an Effective Adjuvant for Influenza Nucleoprotein," *Vaccines*, vol. 11, no. 3, p. 649, Mar. 2023, doi: 10.3390/vaccines11030649.

[179] C.-Y. Lai, G.-Y. Yu, Y. Luo, R. Xiang, and T.-H. Chuang, "Immunostimulatory Activities of CpG-Oligodeoxynucleotides in Teleosts: Toll-Like Receptors 9 and 21," *Front. Immunol.*, vol. 10, p. 179, Feb. 2019, doi: 10.3389/fimmu.2019.00179.

[180] J. Vollmer and A. M. Krieg, "Immunotherapeutic applications of CpG oligodeoxynucleotide TLR9 agonists," *Advanced drug delivery reviews*, vol. 61, no. 3, pp. 195–204, 2009.

[181] M. Barry and C. Cooper, "Review of hepatitis B surface antigen-1018 ISS adjuvant-containing vaccine safety and efficacy," *Expert Opin Biol Ther*, vol. 7, no. 11, pp. 1731–1737, Nov. 2007, doi: 10.1517/14712598.7.11.1731.

[182] S. Strohmeier, F. Amanat, J. D. Campbell, P. Traquina, R. L. Coffman, and F. Krammer, "A CpG 1018 adjuvanted neuraminidase vaccine provides robust protection

from influenza virus challenge in mice," *npj Vaccines*, vol. 7, no. 1, p. 81, Jul. 2022, doi: 10.1038/s41541-022-00486-w.

[183] C. Cooper and D. Mackie, "Hepatitis B surface antigen-1018 ISS adjuvant-containing vaccine: a review of HEPLISAV^{TM} safety and efficacy," *Expert Rev Vaccines*, vol. 10, no. 4, pp. 417–427, Apr. 2011, doi: 10.1586/erv.10.162.

[184] P. Richmond *et al.*, "Safety and immunogenicity of S-Trimer (SCB-2019), a protein subunit vaccine candidate for COVID-19 in healthy adults: a phase 1, randomised, double-blind, placebo-controlled trial," *Lancet*, vol. 397, no. 10275, pp. 682–694, Feb. 2021, doi: 10.1016/S0140-6736(21)00241-5.

[185] J. Eichberg *et al.*, "Antiviral Potential of Natural Resources against Influenza Virus Infections," *Viruses*, vol. 14, no. 11, p. 2452, Nov. 2022, doi: 10.3390/v14112452.

[186] Z. Hu, Y. Zhang, J. Hu, S. Hu, and X. Liu, "Characterization of antibody response to an epitope spanning the haemagglutinin cleavage site of H7N9 subtype avian influenza virus for the differentiation of infected and vaccinated chickens," *Avian Pathology*, vol. 51, no. 4, pp. 330–338, Jul. 2022, doi: 10.1080/03079457.2022.2054308.

[187] J. M. White and G. R. Whittaker, "Fusion of Enveloped Viruses in Endosomes," *Traffic*, vol. 17, no. 6, pp. 593–614, Jun. 2016, doi: 10.1111/tra.12389.

[188] A. J. W. Te Velthuis and E. Fodor, "Influenza virus RNA polymerase: insights into the mechanisms of viral RNA synthesis," *Nat Rev Microbiol*, vol. 14, no. 8, pp. 479–493, Aug. 2016, doi: 10.1038/nrmicro.2016.87.

[189] G. A. Sautto, G. A. Kirchenbaum, and T. M. Ross, “Towards a universal influenza vaccine: different approaches for one goal,” *Virology journal*, vol. 15, no. 1, pp. 1–12, 2018.

[190] Y. Zhang, Y. Zhang, W. Gu, and B. Sun, “Th1/Th2 Cell Differentiation and Molecular Signals,” in *T Helper Cell Differentiation and Their Function*, vol. 841, B. Sun, Ed., in Advances in Experimental Medicine and Biology, vol. 841. , Dordrecht: Springer Netherlands, 2014, pp. 15–44. doi: 10.1007/978-94-017-9487-9_2.

[191] J. Paget *et al.*, “Global mortality associated with seasonal influenza epidemics: New burden estimates and predictors from the GLaMOR Project,” *Journal of global health*, vol. 9, no. 2, 2019.

[192] L. Simonsen, K. Fukuda, L. B. Schonberger, and N. J. Cox, “The Impact of Influenza Epidemics on Hospitalizations,” *J INFECT DIS*, vol. 181, no. 3, pp. 831–837, Mar. 2000, doi: 10.1086/315320.

[193] J. Chen and Y.-M. Deng, “Influenza virus antigenic variation, host antibody production and new approach to control epidemics,” *Virol J*, vol. 6, no. 1, p. 30, 2009, doi: 10.1186/1743-422X-6-30.

[194] B. P. Blackburne, A. J. Hay, and R. A. Goldstein, “Changing Selective Pressure during Antigenic Changes in Human Influenza H3,” *PLoS Pathog*, vol. 4, no. 5, p. e1000058, May 2008, doi: 10.1371/journal.ppat.1000058.

[195] R. P. Chauhan and M. L. Gordon, “An overview of influenza A virus genes, protein functions, and replication cycle highlighting important updates,” *Virus Genes*, vol. 58, no. 4, pp. 255–269, Aug. 2022, doi: 10.1007/s11262-022-01904-w.

[196] H. Connaris *et al.*, "Prevention of influenza by targeting host receptors using engineered proteins," *Proc. Natl. Acad. Sci. U.S.A.*, vol. 111, no. 17, pp. 6401–6406, Apr. 2014, doi: 10.1073/pnas.1404205111.

[197] A. S. Clem, "Fundamentals of vaccine immunology," *Journal of global infectious diseases*, vol. 3, no. 1, p. 73, 2011.

[198] X. Lu *et al.*, "Cross-protective immunity in mice induced by live-attenuated or inactivated vaccines against highly pathogenic influenza A (H5N1) viruses," *Vaccine*, vol. 24, no. 44–46, pp. 6588–6593, Nov. 2006, doi: 10.1016/j.vaccine.2006.05.039.

[199] "Vaccine adjuvants: mechanisms and platforms | Signal Transduction and Targeted Therapy." Accessed: Dec. 11, 2023. [Online]. Available: https://www.nature.com/articles/s41392-023-01557-7#citeas

[200] Y. Perrie, A. R. Mohammed, D. J. Kirby, S. E. McNeil, and V. W. Bramwell, "Vaccine adjuvant systems: Enhancing the efficacy of sub-unit protein antigens," *International Journal of Pharmaceutics*, vol. 364, no. 2, pp. 272–280, Dec. 2008, doi: 10.1016/j.ijpharm.2008.04.036.

[201] D. T. O'Hagan, R. N. Lodaya, and G. Lofano, "The continued advance of vaccine adjuvants – 'we can work it out,'" *Seminars in Immunology*, vol. 50, p. 101426, Aug. 2020, doi: 10.1016/j.smim.2020.101426.

[202] D. T. O'Hagan, "MF59 is a safe and potent vaccine adjuvant that enhances protection against influenza virus infection," *Expert Review of Vaccines*, vol. 6, no. 5, pp. 699–710, Oct. 2007, doi: 10.1586/14760584.6.5.699.

[203] F. Gao *et al.*, "AddaVax-Adjuvanted H5N8 Inactivated Vaccine Induces Robust Humoral Immune Response against Different Clades of H5 Viruses," *Vaccines*, vol. 10, no. 10, p. 1683, Oct. 2022, doi: 10.3390/vaccines10101683.

[204] P. H. Goff *et al.*, "Adjuvants and Immunization Strategies to Induce Influenza Virus Hemagglutinin Stalk Antibodies," *PLoS ONE*, vol. 8, no. 11, p. e79194, Nov. 2013, doi: 10.1371/journal.pone.0079194.

[205] B. M. Giles and T. M. Ross, "A computationally optimized broadly reactive antigen (COBRA) based H5N1 VLP vaccine elicits broadly reactive antibodies in mice and ferrets," *Vaccine*, vol. 29, no. 16, pp. 3043–3054, Apr. 2011, doi: 10.1016/j.vaccine.2011.01.100.

[206] S. Esposito and N. Principi, "Different influenza vaccine formulations and adjuvants for childhood influenza vaccination," *Vaccine*, vol. 29, no. 43, pp. 7535–7541, Oct. 2011, doi: 10.1016/j.vaccine.2011.08.012.

[207] A. Jegerlehner, P. Maurer, J. Bessa, H. J. Hinton, M. Kopf, and M. F. Bachmann, "TLR9 Signaling in B Cells Determines Class Switch Recombination to IgG2a," *The Journal of Immunology*, vol. 178, no. 4, pp. 2415–2420, Feb. 2007, doi: 10.4049/jimmunol.178.4.2415.

[208] T. Qin *et al.*, "CpG Oligodeoxynucleotides Facilitate Delivery of Whole Inactivated H9N2 Influenza Virus via Transepithelial Dendrites of Dendritic Cells in Nasal Mucosa," *J Virol*, vol. 89, no. 11, pp. 5904–5918, Jun. 2015, doi: 10.1128/JVI.00296-15.

[209] F. Saade, Y. Honda-Okubo, S. Trec, and N. Petrovsky, "A novel hepatitis B vaccine containing Advax^{TM}, a polysaccharide adjuvant derived from delta inulin, induces

robust humoral and cellular immunity with minimal reactogenicity in preclinical testing," *Vaccine*, vol. 31, no. 15, pp. 1999–2007, Apr. 2013, doi: 10.1016/j.vaccine.2012.12.077.

[210] J. W. Ecker *et al.*, "High-yield expression and purification of recombinant influenza virus proteins from stably-transfected mammalian cell lines," *Vaccines*, vol. 8, no. 3, p. 462, 2020.

[211] World Health Organization, "Manual for the laboratory diagnosis and virological surveillance of influenza," *WHO global influenza surveillance network: manual for the laboratory diagnosis and virological surveillance of influenza*, 2011, [Online]. Available: https://apps.who.int/iris/handle/10665/44518

[212] D. M. Carter *et al.*, "Design and characterization of a computationally optimized broadly reactive hemagglutinin vaccine for H1N1 influenza viruses," *Journal of virology*, vol. 90, no. 9, pp. 4720–4734, 2016.

[213] Committee for Medicinal Products for Human Use, "Guideline on Influenza Vaccines—Non-clinical and Clinical Module," *Eur. Med. Agency EMA/CHMP/VWP/457259/2014*, vol. 44, pp. 1–31, 2016.

[214] C. Hannoun, "The evolving history of influenza viruses and influenza vaccines," *Expert Review of Vaccines*, vol. 12, no. 9, pp. 1085–1094, Sep. 2013, doi: 10.1586/14760584.2013.824709.

[215] M. C. Johns *et al.*, "Seasonal Influenza Vaccine and Protection against Pandemic (H1N1) 2009-Associated Illness among US Military Personnel," *PLoS ONE*, vol. 5, no. 5, p. e10722, May 2010, doi: 10.1371/journal.pone.0010722.

[216] E.-P. Tsilibary, S. A. Charonis, and A. P. Georgopoulos, “Vaccines for Influenza,” *Vaccines*, vol. 9, no. 1, p. 47, Jan. 2021, doi: 10.3390/vaccines9010047.

[217] B. C. Buckland, “The development and manufacture of influenza vaccines,” *Human Vaccines & Immunotherapeutics*, vol. 11, no. 6, pp. 1357–1360, Jun. 2015, doi: 10.1080/21645515.2015.1026497.

[218] A. B. Arunachalam, P. Post, and D. Rudin, “Unique features of a recombinant haemagglutinin influenza vaccine that influence vaccine performance,” *npj Vaccines*, vol. 6, no. 1, p. 144, 2021.

[219] L. Rudenko, L. Yeolekar, I. Kiseleva, and I. Isakova-Sivak, “Development and approval of live attenuated influenza vaccines based on Russian master donor viruses: Process challenges and success stories,” *Vaccine*, vol. 34, no. 45, pp. 5436–5441, Oct. 2016, doi: 10.1016/j.vaccine.2016.08.018.

[220] L. M. Dunkle and R. Izikson, “Recombinant hemagglutinin influenza vaccine provides broader spectrum protection,” *Expert Review of Vaccines*, vol. 15, no. 8, pp. 957–966, Aug. 2016, doi: 10.1080/14760584.2016.1203261.

[221] J. S. Tregoning, R. F. Russell, and E. Kinnear, “Adjuvanted influenza vaccines,” *Human Vaccines & Immunotherapeutics*, vol. 14, no. 3, pp. 550–564, Mar. 2018, doi: 10.1080/21645515.2017.1415684.

[222] K. Lindert, B. Leav, E. Heijnen, J. Barrett, and U. Nicolay, “Cumulative clinical experience with MF59-adjuvanted trivalent seasonal influenza vaccine in young children and adults 65 years of age and older,” *International Journal of Infectious Diseases*, vol. 85, pp. S10–S17, Aug. 2019, doi: 10.1016/j.ijid.2019.03.020.

[223] A. Orsi *et al.*, “Cross-protection against drifted influenza viruses: Options offered by adjuvanted and intradermal vaccines,” *Human Vaccines & Immunotherapeutics*, vol. 9, no. 3, pp. 582–590, Mar. 2013, doi: 10.4161/hv.23239.

[224] D. T. O’Hagan, Derek T et al., “MF59 adjuvant: the best insurance against influenza strain diversity,” *Expert review of vaccines.*, vol. 10, no. 4, p. 447, Jan. 2011.

[225] N. Principi and S. Esposito, “Adjuvanted influenza vaccines,” *Human Vaccines & Immunotherapeutics*, vol. 8, no. 1, pp. 59–66, Jan. 2012, doi: 10.4161/hv.8.1.18011.

[226] O. Even-Or, S. Samira, R. Ellis, E. Kedar, and Y. Barenholz, “Adjuvanted influenza vaccines,” *Expert Review of Vaccines*, vol. 12, no. 9, pp. 1095–1108, Sep. 2013, doi: 10.1586/14760584.2013.825445.

[227] P. C. Soema, R. Kompier, J.-P. Amorij, and G. F. A. Kersten, “Current and next generation influenza vaccines: Formulation and production strategies,” *European Journal of Pharmaceutics and Biopharmaceutics*, vol. 94, pp. 251–263, Aug. 2015, doi: 10.1016/j.ejpb.2015.05.023.

[228] M. Rivera-Patron, M. Moreno, M. Baz, P. M. Roehe, S. P. Cibulski, and F. Silveira, “ISCOM-like Nanoparticles Formulated with Quillaja brasiliensis Saponins Are Promising Adjuvants for Seasonal Influenza Vaccines,” *Vaccines*, vol. 9, no. 11, p. 1350, Nov. 2021, doi: 10.3390/vaccines9111350.

[229] J. Ulmer, “Vaccine Adjuvants: Mode of Action,” *Frontiers in Immunology*, vol. 4, p. 214, 2013, doi: 10.3389/fimmu.2013.00214.

[230] A. C. Allison, “Squalene and Squalane Emulsions as Adjuvants,” *Methods*, vol. 19, no. 1, pp. 87–93, Sep. 1999, doi: 10.1006/meth.1999.0832.

[231] S. T. T. Schetters, L. J. W. Kruijssen, M. H. W. Crommentuijn, H. Kalay, J. M. M. Haan, and Y. Kooyk, "Immunological dynamics after subcutaneous immunization with a squalene-based oil-in-water adjuvant," *FASEB j.*, vol. 34, no. 9, pp. 12406–12418, Sep. 2020, doi: 10.1096/fj.202000848R.

[232] F. Afinjuomo, S. Abdella, S. H. Youssef, Y. Song, and S. Garg, "Inulin and Its Application in Drug Delivery," *Pharmaceuticals*, vol. 14, no. 9, 2021, doi: 10.3390/ph14090855.

[233] J. Zhu *et al.*, "The transcription factor T-bet is induced by multiple pathways and prevents an endogenous Th2 cell program during Th1 cell responses," *Immunity*, vol. 37, no. 4, pp. 660–673, 2012.

[234] E. Maier, A. Duschl, and J. Horejs-Hoeck, "STAT6-dependent and -independent mechanisms in Th2 polarization," *Eur J Immunol*, vol. 42, no. 11, pp. 2827–2833, Nov. 2012, doi: 10.1002/eji.201242433.

[235] I. Monteleone *et al.*, "Regulation of the T helper cell type 1 transcription factor T-bet in coeliac disease mucosa," *Gut*, vol. 53, no. 8, pp. 1090–1095, 2004, doi: 10.1136/gut.2003.030551.

[236] V. T. Thieu *et al.*, "Stat4 is required for T-bet to promote IL-12-dependent Th1 fate determination," *Immunity*, vol. 29, no. 5, p. 679, 2008.

[237] E. Severinson, "Identification of the IgG1 induction factor (interleukin 4)," *Frontiers in immunology*, vol. 5, p. 628, 2014.

[238] A. Yalcindag *et al.*, "The complement component C3 plays a critical role in both Th1 and Th2 responses to antigen," *Journal of allergy and clinical immunology*, vol. 117, no. 6, pp. 1455–1461, 2006.

[239] P. Choi and H. Reiser, “IL-4: role in disease and regulation of production,” *Clinical and Experimental Immunology*, vol. 113, no. 3, pp. 317–319, Dec. 2001, doi: 10.1046/j.1365-2249.1998.00690.x.

[240] N. Petrovsky and P. D. Cooper, “Advax^{TM}, a novel microcrystalline polysaccharide particle engineered from delta inulin, provides robust adjuvant potency together with tolerability and safety,” *Vaccine*, vol. 33, no. 44, pp. 5920–5926, 2015.

[241] N. Salehen and C. Stover, “The role of complement in the success of vaccination with conjugated vs. unconjugated polysaccharide antigen,” *Vaccine*, vol. 26, no. 4, pp. 451–459, Jan. 2008, doi: 10.1016/j.vaccine.2007.11.049.

[242] F. R. Toapanta and T. M. Ross, “Complement-Mediated Activation of the Adaptive Immune Responses: Role of C3d in Linking the Innate and Adaptive Immunity,” *IR*, vol. 36, no. 1–3, pp. 197–210, 2006, doi: 10.1385/IR:36:1:197.

[243] E. Aleebrahim-Dehkordi *et al.*, “T helper type (Th1/Th2) responses to SARS-CoV-2 and influenza A (H1N1) virus: From cytokines produced to immune responses,” *Transplant immunology*, vol. 70, p. 101495, 2022.

[244] P. Cao *et al.*, “On the Role of CD8+ T Cells in Determining Recovery Time from Influenza Virus Infection,” *Front. Immunol.*, vol. 7, Dec. 2016, doi: 10.3389/fimmu.2016.00611.

[245] R. Jia, S. Liu, J. Xu, and X. Liang, “IL16 deficiency enhances Th1 and cytotoxic T lymphocyte response against influenza A virus infection,” *BST*, vol. 13, no. 6, pp. 516–522, Dec. 2019, doi: 10.5582/bst.2019.01286.

[246] P. Kidd, “Th1/Th2 balance: the hypothesis, its limitations, and implications for health and disease,” *Alternative medicine review*, vol. 8, no. 3, pp. 223–246, 2003.

[247] A. Coulter *et al.*, "Intranasal vaccination with ISCOMATRIX® adjuvanted influenza vaccine," *Vaccine*, vol. 21, no. 9–10, pp. 946–949, 2003.

[248] M. A. Rose, S. Zielen, and U. Baumann, "Mucosal immunity and nasal influenza vaccination," *Expert Review of Vaccines*, vol. 11, no. 5, pp. 595–607, May 2012, doi: 10.1586/erv.12.31.

[249] E. Méndez-Enríquez *et al.*, "IgE cross-linking induces activation of human and mouse mast cell progenitors," *J Allergy Clin Immunol*, vol. 149, no. 4, pp. 1458–1463, Apr. 2022, doi: 10.1016/j.jaci.2021.08.019.

[250] J. D. Allen and T. M. Ross, "Next generation methodology for updating HA vaccines against emerging human seasonal influenza A(H3N2) viruses," *Scientific Reports*, vol. 11, no. 1, p. 4554, Mar. 2021, doi: 10.1038/s41598-020-79590-7.

[251] A. Podda, "The adjuvanted influenza vaccines with novel adjuvants: experience with the MF59-adjuvanted vaccine," *Vaccine*, vol. 19, no. 17, pp. 2673–2680, Mar. 2001, doi: 10.1016/S0264-410X(00)00499-0.

[252] B. C. Baudner *et al.*, "MF59 Emulsion Is an Effective Delivery System for a Synthetic TLR4 Agonist (E6020)," *Pharmaceutical Research*, vol. 26, no. 6, pp. 1477–1485, Jun. 2009, doi: 10.1007/s11095-009-9859-5.

[253] N. P. H. Knudsen *et al.*, "Different human vaccine adjuvants promote distinct antigen-independent immunological signatures tailored to different pathogens," *Scientific reports*, vol. 6, no. 1, pp. 1–13, 2016.

[254] E. Maier, A. Duschl, and J. Horejs-Hoeck, "STAT6-dependent and-independent mechanisms in T h2 polarization," *European journal of immunology*, vol. 42, no. 11, pp. 2827–2833, 2012.

[255] G. K. Pedersen *et al.*, "Serum IgG titres, but not avidity, correlates with neutralizing antibody response after H5N1 vaccination," *Vaccine*, vol. 32, no. 35, pp. 4550–4557, Jul. 2014, doi: 10.1016/j.vaccine.2014.06.009.

[256] S. Jangra *et al.*, "Multicomponent intranasal adjuvant for mucosal and durable systemic SARS-CoV-2 immunity in young and aged mice," *npj Vaccines*, vol. 8, no. 1, p. 96, 2023.

[257] K. A. Nagashima and J. J. Mousa, "Next-generation influenza HA immunogens and adjuvants in pursuit of a broadly protective vaccine," *Viruses*, vol. 13, no. 4, p. 546, 2021.

[258] C. C. Hanna, J. Kriegesmann, L. J. Dowman, C. F. W. Becker, and R. J. Payne, "Chemical Synthesis and Semisynthesis of Lipidated Proteins," *Angew Chem Int Ed*, vol. 61, no. 15, p. e202111266, Apr. 2022, doi: 10.1002/anie.202111266.

[259] K. K. Short *et al.*, "Using Dual Toll-like Receptor Agonism to Drive Th1-Biased Response in a Squalene- and α-Tocopherol-Containing Emulsion for a More Effective SARS-CoV-2 Vaccine," *Pharmaceutics*, vol. 14, no. 7, p. 1455, Jul. 2022, doi: 10.3390/pharmaceutics14071455.

[260] C. Vaure and Y. Liu, "A Comparative Review of Toll-Like Receptor 4 Expression and Functionality in Different Animal Species," *Front. Immunol.*, vol. 5, Jul. 2014, doi: 10.3389/fimmu.2014.00316.

[261] D. C. McGowan, "Latest Advances in Small Molecule TLR 7/8 Agonist Drug Research," *CTMC*, vol. 19, no. 24, pp. 2228–2238, Nov. 2019, doi: 10.2174/1568026619666191009165418.

[262] H. Sun *et al.*, "Targeting toll-like receptor 7/8 for immunotherapy: recent advances and prospectives," *Biomark Res*, vol. 10, no. 1, p. 89, Dec. 2022, doi: 10.1186/s40364-022-00436-7.

[263] S. M. Miller *et al.*, "A lipidated TLR7/8 adjuvant enhances the efficacy of a vaccine against fentanyl in mice," *npj Vaccines*, vol. 8, no. 1, p. 97, Jul. 2023, doi: 10.1038/s41541-023-00694-y.

[264] R. N. Lodaya *et al.*, "Stable Nanoemulsions for the Delivery of Small Molecule Immune Potentiators," *Journal of Pharmaceutical Sciences*, vol. 107, no. 9, pp. 2310–2314, Sep. 2018, doi: 10.1016/j.xphs.2018.05.012.

[265] K. K. Short *et al.*, "Co-encapsulation of synthetic lipidated TLR4 and TLR7/8 agonists in the liposomal bilayer results in a rapid, synergistic enhancement of vaccine-mediated humoral immunity," *Journal of Controlled Release*, vol. 315, pp. 186–196, Dec. 2019, doi: 10.1016/j.jconrel.2019.10.025.

[266] T. Mohan, P. Verma, and D. N. Rao, "Novel adjuvants & delivery vehicles for vaccines development: a road ahead," *Indian J Med Res*, vol. 138, no. 5, pp. 779–795, Nov. 2013.

[267] V. V. S. N. L. Andra, S. V. N. Pammi, L. V. K. P. Bhatraju, and L. K. Ruddaraju, "A Comprehensive Review on Novel Liposomal Methodologies, Commercial Formulations, Clinical Trials and Patents," *BioNanoSci.*, vol. 12, no. 1, pp. 274–291, Mar. 2022, doi: 10.1007/s12668-022-00941-x.

[268] J. Zhang *et al.*, "Development of a novel oil-in-water emulsion and evaluation of its potential adjuvant function in a swine influenza vaccine in mice," *BMC Vet Res*, vol. 14, no. 1, p. 415, Dec. 2018, doi: 10.1186/s12917-018-1719-2.

[269] R. L. Richards, M. Rao, T. C. Vancott, G. R. Matyas, D. L. Birx, and C. R. Alving, "Liposome-stabilized oil-in-water emulsions as adjuvants: Increased emulsion stability promotes induction of cytotoxic T lymphocytes against an HIV envelope antigen," *Immunol Cell Biol*, vol. 82, no. 5, pp. 531–538, Oct. 2004, doi: 10.1111/j.0818-9641.2004.01282.x.

[270] H. G. Bazin *et al.*, "Optimization of 8-oxoadenines with toll-like-receptor 7 and 8 activity," *Bioorganic & Medicinal Chemistry Letters*, vol. 30, no. 6, p. 126984, Mar. 2020, doi: 10.1016/j.bmcl.2020.126984.

[271] J. I. Tokars, S. J. Olsen, and C. Reed, "Seasonal Incidence of Symptomatic Influenza in the United States," *Clinical Infectious Diseases*, vol. 66, no. 10, pp. 1511–1518, May 2018, doi: 10.1093/cid/cix1060.

[272] J. M. Bartley, A. N. Cadar, and D. E. Martin, "Better, Faster, Stronger: mRNA Vaccines Show Promise for Influenza Vaccination in Older Adults," *Immunological Investigations*, vol. 50, no. 7, pp. 810–820, Oct. 2021, doi: 10.1080/08820139.2021.1909617.

[273] A. C. Tricco *et al.*, "Comparing influenza vaccine efficacy against mismatched and matched strains: a systematic review and meta-analysis," *BMC Med*, vol. 11, no. 1, p. 153, Dec. 2013, doi: 10.1186/1741-7015-11-153.

[274] A. N. Nafziger and D. S. Pratt, "Seasonal influenza vaccination and technologies," *The Journal of Clinical Pharma*, vol. 54, no. 7, pp. 719–731, Jul. 2014, doi: 10.1002/jcph.299.

[275] A. L. Wilkins *et al.*, "AS03- and MF59-Adjuvanted Influenza Vaccines in Children," *Frontiers in Immunology*, vol. 8, p. 1760, 2017, doi: 10.3389/fimmu.2017.01760.

[276] J. S. Tregoning, R. F. Russell, and E. Kinnear, "Adjuvanted influenza vaccines," *Human Vaccines & Immunotherapeutics*, vol. 14, no. 3, pp. 550–564, Mar. 2018, doi: 10.1080/21645515.2017.1415684.

[277] A. Vatti, D. M. Monsalve, Y. Pacheco, C. Chang, J.-M. Anaya, and M. E. Gershwin, "Original antigenic sin: A comprehensive review," *Journal of Autoimmunity*, vol. 83, pp. 12–21, Sep. 2017, doi: 10.1016/j.jaut.2017.04.008.

[278] Y. Wang *et al.*, "A novel CpG ODN compound adjuvant enhances immune response to spike subunit vaccines of porcine epidemic diarrhea virus," *Front. Immunol.*, vol. 15, p. 1336239, Jan. 2024, doi: 10.3389/fimmu.2024.1336239.

[279] Y. Huang, M. S. França, J. D. Allen, H. Shi, and T. M. Ross, "Next Generation of computationally optimized broadly reactive ha vaccines elicited cross-reactive immune responses and provided protection against H1N1 virus infection," *Vaccines*, vol. 9, no. 7, p. 793, 2021.

[280] K. Boonnak *et al.*, "Immune responses to intradermal and intramuscular inactivated influenza vaccine among older age group," *Vaccine*, vol. 35, no. 52, pp. 7339–7346, Dec. 2017, doi: 10.1016/j.vaccine.2017.10.106.

[281] T. F. Tsai, "Fluad®-MF59®-Adjuvanted Influenza Vaccine in Older Adults," *Infect Chemother*, vol. 45, no. 2, p. 159, 2013, doi: 10.3947/ic.2013.45.2.159.

[282] T. Vesikari, N. Groth, A. Karvonen, A. Borkowski, and M. Pellegrini, "MF59®-adjuvanted influenza vaccine (FLUAD®) in children: Safety and immunogenicity

following a second year seasonal vaccination," *Vaccine*, vol. 27, no. 45, pp. 6291–6295, Oct. 2009, doi: 10.1016/j.vaccine.2009.02.004.

[283] Z. Moldoveanu, M. L. Clements, S. J. Prince, B. R. Murphy, and J. Mestecky, "Human immune responses to influenza virus vaccines administered by systemic or mucosal routes," *Vaccine*, vol. 13, no. 11, pp. 1006–1012, 1995, doi: 10.1016/0264-410X(95)00016-T.

[284] B. Killingley and J. Nguyen-Van-Tam, "Routes of influenza transmission," *Influenza Resp Viruses*, vol. 7, no. s2, pp. 42–51, Sep. 2013, doi: 10.1111/irv.12080.

[285] J. P. Wong *et al.*, "Activation of toll-like receptor signaling pathway for protection against influenza virus infection," *Vaccine*, vol. 27, no. 25–26, pp. 3481–3483, May 2009, doi: 10.1016/j.vaccine.2009.01.048.

[286] X. Kang, Y. Li, Y. Zhao, and X. Chen, "Overcoming Aging-Associated Poor Influenza Vaccine Responses with CpG 1018 Adjuvant," *Vaccines*, vol. 10, no. 11, p. 1894, Nov. 2022, doi: 10.3390/vaccines10111894.

[287] M. Schnare, A. C. Holt†, K. Takeda, S. Akira, and R. Medzhitov, "Recognition of CpG DNA is mediated by signaling pathways dependent on the adaptor protein MyD88," *Current Biology*, vol. 10, no. 18, pp. 1139–1142, Sep. 2000, doi: 10.1016/S0960-9822(00)00700-4.

[288] S. Duan and P. G. Thomas, "Balancing Immune Protection and Immune Pathology by CD8+ T-Cell Responses to Influenza Infection," *Front. Immunol.*, vol. 7, Feb. 2016, doi: 10.3389/fimmu.2016.00025.

[289] J. S. Marshall, R. Warrington, W. Watson, and H. L. Kim, “An introduction to immunology and immunopathology,” *Allergy Asthma Clin Immunol*, vol. 14, no. S2, p. 49, Sep. 2018, doi: 10.1186/s13223-018-0278-1.

[290] S. H. Blaas, M. Stieber-Gunckel, W. Falk, F. Obermeier, and G. Rogler, “CpG-oligodeoxynucleotides stimulate immunoglobulin A secretion in intestinal mucosal B cells,” *Clinical and Experimental Immunology*, vol. 155, no. 3, pp. 534–540, Feb. 2009, doi: 10.1111/j.1365-2249.2008.03855.x.

[291] I. Skountzou *et al.*, “Immunity to Pre-1950 H1N1 Influenza Viruses Confers Cross-Protection against the Pandemic Swine-Origin 2009 A (H1N1) Influenza Virus,” *The Journal of Immunology*, vol. 185, no. 3, pp. 1642–1649, Aug. 2010, doi: 10.4049/jimmunol.1000091.

[292] C.-A. Siegrist and R. Aspinall, “B-cell responses to vaccination at the extremes of age,” *Nat Rev Immunol*, vol. 9, no. 3, pp. 185–194, Mar. 2009, doi: 10.1038/nri2508.

[293] A. D. Henn *et al.*, “Functionally Distinct Subpopulations of CpG-Activated Memory B Cells,” *Sci Rep*, vol. 2, no. 1, p. 345, Mar. 2012, doi: 10.1038/srep00345.

[294] D. C. Powers *et al.*, “Humoral and Cellular Immune Responses following Vaccination with Purified Recombinant Hemagglutinin from Influenza A (H3N2) Virus,” *Journal of Infectious Diseases*, vol. 175, no. 2, pp. 342–351, Feb. 1997, doi: 10.1093/infdis/175.2.342.

[295] X. Nian, J. Zhang, S. Huang, K. Duan, X. Li, and X. Yang, “Development of Nasal Vaccines and the Associated Challenges,” *Pharmaceutics*, vol. 14, no. 10, p. 1983, Sep. 2022, doi: 10.3390/pharmaceutics14101983.

[296] W. S. Gallichan, R. N. Woolstencroft, T. Guarasci, M. J. McCluskie, H. L. Davis, and K. L. Rosenthal, “Intranasal Immunization with CpG Oligodeoxynucleotides as an Adjuvant Dramatically Increases IgA and Protection Against Herpes Simplex Virus-2 in the Genital Tract,” *The Journal of Immunology*, vol. 166, no. 5, pp. 3451–3457, Mar. 2001, doi: 10.4049/jimmunol.166.5.3451.

[297] A. N. Aljurayyan *et al.*, “A critical role of T follicular helper cells in human mucosal anti-influenza response that can be enhanced by immunological adjuvant CpG-DNA,” *Antiviral Research*, vol. 132, pp. 122–130, Aug. 2016, doi: 10.1016/j.antiviral.2016.05.021.

[298] V.-A. Duong, T.-T.-L. Nguyen, and H.-J. Maeng, “Recent Advances in Intranasal Liposomes for Drug, Gene, and Vaccine Delivery,” *Pharmaceutics*, vol. 15, no. 1, p. 207, Jan. 2023, doi: 10.3390/pharmaceutics15010207.

[299] J. Deng, W. Cai, and F. Jin, “A novel oil-in-water emulsion as a potential adjuvant for influenza vaccine: Development, characterization, stability and in vivo evaluation,” *International Journal of Pharmaceutics*, vol. 468, no. 1–2, pp. 187–195, Jul. 2014, doi: 10.1016/j.ijpharm.2014.04.003.

[300] Z. Huang, H. Gong, Q. Sun, J. Yang, X. Yan, and F. Xu, “Research progress on emulsion vaccine adjuvants,” *Heliyon*, vol. 10, no. 3, p. e24662, Feb. 2024, doi: 10.1016/j.heliyon.2024.e24662.

[301] N. Dumpa *et al.*, “Stability of Vaccines,” *AAPS PharmSciTech*, vol. 20, no. 2, p. 42, Feb. 2019, doi: 10.1208/s12249-018-1254-2.